

# **Alkali-Metal Alkoxide Mediated Activation of Organozinc and Organomagnesium Reagents for Arene Functionalisation**

Inaugural dissertation  
of the Faculty of Science,  
University of Bern

presented by

Neil R. Judge

From Glasgow, Scotland

Supervisor of the doctoral thesis:

Prof. Dr. Eva Hevia

Universität Bern - Departement für Chemie, Biochemie und  
Pharmazie

**Alkali-Metal Alkoxide Mediated Activation of  
Organozinc and Organomagnesium Reagents for Arene  
Functionalisation**

Inaugural dissertation  
of the Faculty of Science,  
University of Bern

presented by

Neil R. Judge

From Glasgow, Scotland

Supervisor of the doctoral thesis:

Prof. Dr. Eva Hevia

Universität Bern - Departement für Chemie, Biochemie und  
Pharmazie

Accepted by the Faculty of Science.

Bern, 18/01/2024

The Dean

Prof. Dr. Marco Herwegh

*Dedicated to my auntie Phyllis*

*- the embodiment of strength*



This work - Alkali-Metal Alkoxide Activation of Organozinc and Organomagnesium reagents for Arene functionalisation © 2024 by Neil Ronald Judge is licensed under [Creative Commons Attribution-NonCommercial-NoDerivatives 4.0 International](http://creativecommons.org/licenses/by-nc-nd/4.0/). To view a copy of this license, visit <http://creativecommons.org/licenses/by-nc-nd/4.0/> or send a letter to Creative Commons, PO Box 1866, Mountain View, CA 94042, USA.

## Acknowledgements

Leaving Glasgow to begin my PhD studies in Bern was undoubtedly the hardest decision I have ever made in my life but as I sit here putting the finishing touches on my thesis, I don't regret it for a second. The last four years has been a life changing journey for me with surreal highs and some tough lows, but it's all been worth it in the end. Of course, doing a PhD requires a certain amount of self-motivation and perseverance but I really could not have done this without the help of some very special people in my life, so I'd like to take some time to thank them.

There really is no other place to start than with my supervisor and role model ("The Chief"), Prof. Eva Hevia. It's impossible to put into words how grateful I am to you for your unwavering and heartfelt support throughout these last four years. Your passion and enthusiasm for chemistry is contagious, which is something I have learnt on many times during my PhD... whenever I felt like giving up, a quick meeting with you left me feeling 10ft tall and ready to get back to my Schlenk line full of energy and ideas. I need to thank you for constantly pushing me to do the best I can and for picking up the pieces after I have a meltdown (which were frequent!). Although I feel like whenever I look back on my PhD I will think about how many times we have been in fits of laughter over the years; whether it was you trying to get home after the Christmas night out, wee Marina asking if I've ever been in love before(!) or how it always seemed to be us two angling to get a beer on whatever group outing we were on! Jokes aside it has been an absolute honour to be a part of your group and I cannot thank you enough for offering me this opportunity to become part of the Hevia family... I'll never forget it. Speaking of family, I need to thank big Gordo for always being there to talk Celtic with me over the past years!

I need to also thank two other professors who have helped on this journey, Prof. Rab Mulvey and Prof. Martin Albrecht. I probably wouldn't have even studied Chemistry at Strathclyde if it wasn't for Rab letting me do my work experience in his lab when I was just 15 years old! The two summer placements and masters project I did in his lab after that gave me the knowledge and enthusiasm for bimetallic chemistry that led me down the path to a PhD. To Prof. Martin Albrecht, I'd hate to think how hard it would have been to move to the university of Bern without you and your groups help so thank you for making such a big transition so easy and for always being our Swiss mountain guide whenever we went on our joint group trips!

I want to thank the NMR, X-ray services and analytical services for all their help with the characterisation of my compounds over the years. A thanks also to our collaborators at

Ludwig-Maximilians-Universität, München, Department Chemie: Prof. Paul Knochel, and Alexandre Desaintjean. Prof. Paul Knochel is thanked in particular for his contributions and expertise within aspects of this thesis and are acknowledged therein.

To the troops! There are too many names to list, but I want to thank each and every person in the Hevia group, past and present, for making these past four years such a special time in my life and making some of the tough times easier. To my supervisor, flat mate and best pal Dr Boley! Leonie, I can't thank you enough for everything you taught me in the lab and your patience (of which you needed a lot of, dealing with me) coaching me through the first years of my PhD. The first two years moving here were rough for us (COVID n that), but we had some laugh together and memories that'll last a lifetime, like you shaving ma heed, our hours long chats in the flat sorting the world out and dancing to the Bee Gee's, or "here, I could land that". You were basically the big sister I never had, and I hope you know how much I appreciate everything you did for me. To my adopted maw n da and my skiing buddies, Lewis and Rach! Thanks for always being there for me and steering me through life with your wisdom (roughly translated that means thanks for telling me which run we were doing next). I'll never forget Verbier and "are you new here?". To my gym and coffee buddy Andryj, thanks for all your help over the years and always listening to me moan in the middle of sets... lightweight babyyy! To Andreu, my new flatmate and coffee club member, thanks for answering my stupid questions all the time and for helping to fill some pretty big gaps left in the lab when people close to me had to move on.

Someone that deserves their own little paragraph is my wee Italian partner in crime and therapist, Ale! We started our PhD's on the same day, and we are finishing them a week apart and there's no one else I would rather have gone through this journey with. We have been through so much together (with scary similar timing) and you've been there for me in my lowest moments the past 4 years. I feel like I'm going to lose an arm after all this time being joined at the hip... you better not lose that Scottish accent! Thank you so much for everything Ale, I couldn't have done this without you.

Mr Mc Zimma! Keir, my best mate, cheers for three of the best years in Bern. Who would have thought an Englishmen and a Scotsmen could be such good pals eh? Turns out football, beer and warzone is all it takes. Thanks for some of the funniest memories from being on the boats, Karma, FORTLOWANIN, Tuesday nights and countless amounts of things I'm not allowed to write on paper! Been a rock for me these past few years mate, so thanks for that.

Finally, to my family, as without them I wouldn't be in the privileged position I am today. To my Dad, my best mate, thank you for all of the sacrifices you have made over the years and giving me the platform I needed in life to get to this stage. Couple of neds from the scheme didn't end up doing too bad, eh? To my wee mum, thank you for constantly being my moral compass in life and for always being a phone call away when I'm in need of a virtual hug over these last 4 years. Your constant encouragement and belief in me has kept me going during the toughest times of my PhD. Last but by no means least to my step mum Lara (aka smum), thank you for giving me the different perspectives I needed in life to grow and mature whilst always being on the end of the phone for all the rants and breakdowns over the years.

## Abstract

This thesis explores the use of alkali-metal alkoxides as additives for the activation of organomagnesium and organozinc reagents towards arene functionalisation focussing on two cornerstone reaction in organic synthesis, namely metal/halogen exchange and deprotonative metalation. Approaching this area from a more metal-focussed perspective, the work collected in this thesis not only aims at advancing the synthetic applications of these heterobimetallic combinations for regioselective functionalisation of arenes but also to advance the understanding on the constitution of the key organometallic species involved in these transformations, providing valuable mechanistic understanding that can then be used for further rational design. Essential analytical tools to carry out this research have been advanced NMR spectroscopic analysis as well as X-ray crystallographic studies which have help to shed light on the unique activating effects mediated by alkali-metal alkoxides in these main group bimetallic systems.

*Chapter 2* explores the use of mixed alkyl/alkoxy lithium magnesiates for atom economical Mg/Br exchange under mild conditions, displaying remarkable levels of chemo- and regioselective control. Spectroscopic and structural mapping allowed for a deeper understanding of the hidden reaction pathways as well as revealing a novel bimetallic derivative of the Schlenk equilibrium.

*Chapter 3* focuses primarily on how the nature of the alkali-metal and alkoxide ligand used effects the reactivity of these mixed alkyl/alkoxy magnesiates towards bromoarenes. These studies revealed that subtle changes to these parameters had quite drastic consequences on the Mg/Br exchange ability of the bimetallic reagents but also on the constitution of the metalated intermediates formed in the reaction.

Moving from metal/halogen exchange to deprotonative metalation, *Chapter 4* reveals how the addition of two molar equivalents of KO $t$ Bu to Zn(TMP)<sub>2</sub> (TMP = 2,2,6,6-tetramethylpiperidide) transforms this mild zinc *bis*-amide base to a powerful metalating agent able to perform facile regioselective zincation of a wide range of sensitive fluoroarenes. Structural authentication of the intermediates post Zn-H exchange demonstrates activation of both TMP groups to form a range of higher order bis-aryl potassium zincates which are further functionalized in electrophilic interception reactions. While several intermediates have been isolated and structurally characterized, showing a remarkable stability at room temperature, these compounds can still engage into C-C bond forming processes such as Negishi cross-couplings and Cu catalysed allylations. *Chapter 5* extends this methodology to reveal the true metalating power of this bimetallic mixture, able to perform challenging regioselective



zincations of non-activated arenes such as benzene, ferrocene, and naphthalene. Complex redistribution patterns of the metalated intermediates, induced by alkoxide additives, are unveiled through spectroscopic and crystallographic studies. Interestingly for these less activated substrates there is a clear alkali-metal effect, with only KO*t*Bu being able to enhance the metalating power of Zn(TMP)<sub>2</sub>. Finally, a “cleave and capture” decomposition pathway of this strong base in THF has been uncovered, allowing for the isolation of an unusual potassium zincate complex containing a zincated 1,3 butadiene fragment resulting from the synergic cleavage of THF which is used as a solvent in these reactions.

## Publications

1. “Regioselective Bromine/Magnesium Exchange for the Selective Functionalisation of Polyhalogenated Arenes and Heterocycles” Alexandre desaintjean, Tobias Haupt, Leonie J. Bole, Neil R. Judge, Eva Hevia\*, Paul Knochel\*, *Angew. Chem. Int. Ed.*, **2021**, 60, 1513. <https://doi.org/10.1002/anie.202012496>
2. “Untangling the Complexity of Mixed Lithium/Magnesium Alkyl/Alkoxy Combinations Utilised in Br/Mg Exchange Reactions” Leonie J. Bole, Neil R. Judge, Eva Hevia\*, *Angew. Chem. Int. Ed.*, **2021**, 60, 7626. (VIP) <https://doi.org/10.1002/ange.202016422>
3. “Assessing Alkali-Metal Effects in the Structures and Reactivity of Mixed-Ligand Alkyl/Alkoxide Alkali-Metal Magnesiates” Neil R. Judge, Leonie J. Bole, Eva Hevia\*, *Chem. Eur. J.*, **2022**, 28, e202104164. <https://doi.org/10.1002/chem.202104164>
4. “Alkali-Metal Alkoxide Powered Zincations of Fluoroarenes Employing Zinc Bis-Amide  $Zn(TMP)_2$ ” Neil R. Judge, Eva Hevia\*, *Angew. Chem. Int. Ed.*, **2023**, 135, e202303099. <https://doi.org/10.1002/ange.202303099>
5. “Main Group Metal Strategies for C–H and C–F Bond Activation and Functionalisation of Fluoroarenes” Neil R. Judge, A. Logallo, E. Hevia, \* *Chem. Sci.*, **2023**, 11617–11628. <https://doi.org/10.1039/d3sc03548d>.
6. “Combining Two Weak Bases ( $Zn(TMP)_2$  and  $KOtBu$ ) for the Regioselective Metalation of Non-Activated Arenes and Heteroarenes” Neil R. Judge, Eva Hevia\*, *Chem. Sci.*, **2024**, Accepted Manuscript. <https://doi.org/10.1039/D4SC03892D>
7. “Enhancing the Metalating Power of  $ZnEt_2$  via Formation of an Alkyl/Alkoxide Potassium Zincate” Jasmin Kocher, Neil R. Judge, Eva Hevia\*, *Helv. Chim. Acta*, 2024, **107**, e202300237. <https://doi.org/10.1002/hlca.202300237>.

## Conference Presentations

1. *“Shedding light on lithium-alkoxide mediated Mg/Br exchange reactions”* – Poster presentation at Swiss Chemical Society Fall Meeting, **2020** (Virtual Conference).
2. *“Exploring the alkali-metal effect in Mg/Br exchange reactions mediated by group 1 alkoxides”* – Poster presentation at Royal Society of Chemistry, **2021** (Twitter Conference).
3. *“Complexity and structural diversity of mixed alkyl/alkoxide alkali-metal magnesiates and their consequences in Mg-Br exchange applications”* – Poster presentation at Swiss Chemical Society Fall Meeting, **2021** (Virtual Conference).
4. *“Complexity and structural diversity in regioselective lithium-alkoxide mediated Mg/Br exchange Reactions”* – Poster presentation at Swiss Summer School: Catalysis and Sustainable Chemistry in Les Diablerets (Switzerland), **2021**.
5. *“Unlocking the Metalation Potential of ZnTMP<sub>2</sub> via K<sup>t</sup>OBu Mediated Zincations”* – Poster presentation at International Conference on Organometallic Chemistry (ICOMC) in Prague (Czech Republic), **2022**.
6. *“Unlocking the Metalation Potential of ZnTMP<sub>2</sub> via K<sup>t</sup>OBu Mediated Zincations”* – Poster presentation at Swiss Chemical Society Fall Meeting in Zurich (Switzerland), **2022**.
7. *“Unlocking the Metalation Potential of ZnTMP<sub>2</sub> with K<sup>t</sup>OBu”* – Poster presentation at European Conference of Organometallic Chemistry (EuCOMC) in Alcalá de Henares (Spain), **2023**.
8. *“Unlocking the Metalation Potential of ZnTMP<sub>2</sub> with K<sup>t</sup>OBu”* – Poster presentation at Swiss Chemical Society Fall Meeting in Bern (Switzerland), **2023**.

## List of Common Abbreviations

<b><i>AM</i></b>	Alkali-metal
<b><i>AM-OR</i></b>	Alkali-metal alkoxide
<b><i>AMMM</i></b>	Alkali-Metal Mediated Metalation
<b><i>Ar*</i></b>	2,6-Diisopropylphenyl
<b>CCDC</b>	Cambridge Crystallographic Data Centre
<b><math>C_6D_6</math></b>	Deuterated benzene
<b><math>CDCl_3</math></b>	Deuterated chloroform
<b><math>C_6Me_6</math></b>	Hexamethylbenzene
<b>CIP</b>	Contacted Ion-Pair
<b>CIPE</b>	Complex-Induced proximity effect
<b>CSD</b>	Cambridge Structural Database
<b><math>cS_NAr</math></b>	Concerted nucleophilic aromatic substitution
<b><math>d_8</math>-THF</b>	Deuterated THF
<b><math>d_8</math>-Tol</b>	Deuterated toluene
<b><i>D</i></b>	Diffusion coefficient
<b>DABCO</b>	1,4-diazabicyclo[2.2.2]octane
<b>DFT</b>	Density Functional Theory
<b>DG</b>	Directing Group
<b><i>DoM</i></b>	Directed <i>ortho</i> -metalation
<b>DOSY</b>	Diffusion Ordered Spectroscopy
<b><math>e^-</math></b>	Electron
<b><math>E^+</math></b>	Electrophile
<b>ECC</b>	External calibration curve
<b>EPR</b>	Electron Paramagnetic Resonance Spectroscopy
<b><i>E.q</i></b>	Equivalent(s)
<b>Et</b>	Ethyl
<b>FG</b>	Functional Group
<b>GC</b>	Gas chromatography
<b>h</b>	Hour(s)
<b>Hal</b>	Halogen

<b>Het</b>	Heteroatom
<b>HMDS(H)</b>	Hexamethyldisilazane
<b>HMDS</b>	Hexamethyldisilazide
<b><i>i</i>Pr</b>	<i>Iso</i> -propyl
<b>K</b>	Kelvin
<b><math>K_{eq}</math></b>	Equilibrium constant
<b>kcal</b>	Kilocalorie
<b>LG</b>	Leaving Group
<b>M</b>	Molar
<b>min(s)</b>	Minute(s)
<b>mol</b>	moles
<b>MHz</b>	Megahertz
<b>mM</b>	Millimolar
<b>mmoles</b>	Millimoles
<b><math>MW_{calc}</math></b>	Calculated molecular weight
<b><math>MW_{det}</math></b>	Determined molecular weight
<b><i>n</i>Bu</b>	<i>n</i> -Butyl
<b><i>n</i>BuLi</b>	<i>n</i> -Butyllithium
<b>NMR</b>	Nuclear Magnetic Resonance
<b>Nu<sup>-</sup></b>	Nucleophile
<b>Ph</b>	Phenyl
<b>PMDETA</b>	N,N,N',N'',N'''-pentamethyldiethylenetriamine
<b>ppm</b>	Parts Per Million
<b>R</b>	Trimethylsilyl(methyl) or CH <sub>2</sub> SiMe <sub>3</sub>
<b>RLi</b>	Organolithium reagent
<b>RT</b>	Room (ambient) Temperature, <i>ca.</i> 20 °C
<b>s</b>	Second
<b><i>s</i>Bu</b>	<i>sec</i> -Butyl
<b>S<sub>N</sub>Ar</b>	Nucleophilic aromatic substitution
<b>SSIP</b>	Solvent-separated ion pair
<b><i>t</i>Bu</b>	<i>tert</i> -Butyl
<b>THF</b>	Tetrahydrofuran

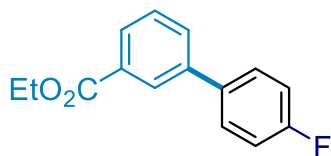
<b>THT</b>	Tetrahydrothiophene
<b>TMEDA</b>	N,N,N',N'-tetramethylethylenediamine
<b>TMP</b>	2,2,6,6-Tetramethylpiperidide
<b>TMP(H)</b>	2,2,6,6-Tetramethylpiperidine
<b>TMS</b>	Tetramethylsilane
<b>vdW</b>	van der Waals
<b>VT</b>	Variable Temperature
<b>°C</b>	Degrees Celsius
<b>Å</b>	Angstrom
<b>°</b>	Degrees
<b><math>\eta</math></b>	Eta (denoting hapticity)
<b><math>\infty</math></b>	Infinity (denoting a long polymeric chain)
<b><math>\sigma</math></b>	Sigma (denoting a sigma bond)
<b><math>\pi</math></b>	Pi (denoting a pi bond)
<b><math>\rho</math></b>	Rho (denoting electron density)
<b><math>^{19}\text{F}\{\text{}^1\text{H}\}</math></b>	Fluorine-19 proton decoupled
<b><math>^7\text{Li}\{\text{}^1\text{H}\}</math></b>	Lithium-7 proton decoupled
<b><math>^1\text{H}</math></b>	Hydrogen-1

# Tables of Numbered Compounds

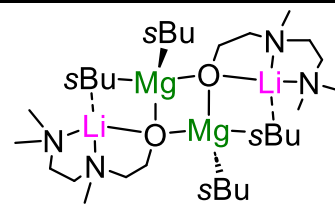
## Chapter 2

Number	Compound	Number	Compound
1a		1b	
1c		2a	
2b		3a	
3b		4a	

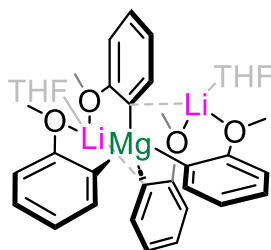
4b



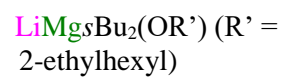
5



6



I



II



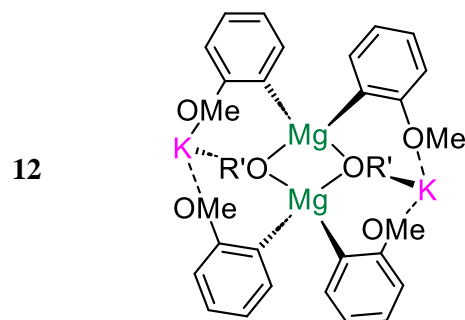
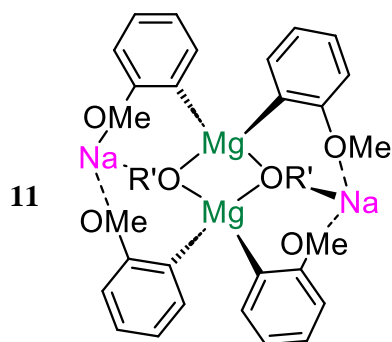
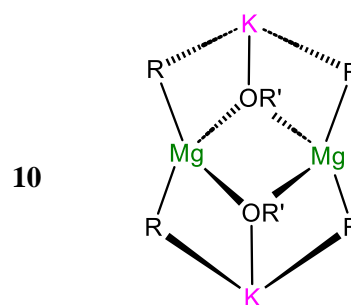
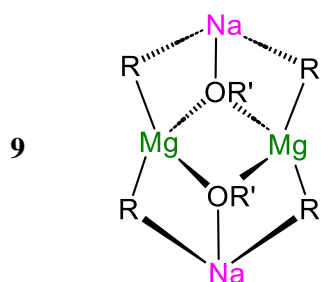
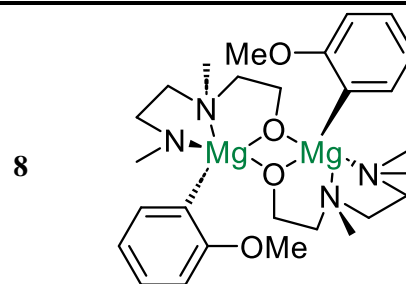
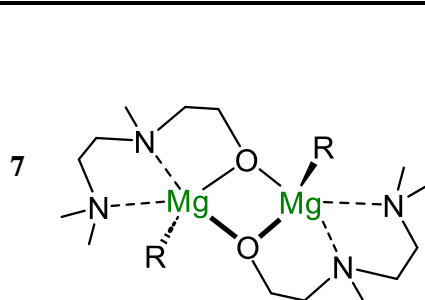
III



### Chapter 3

Number	Compound	Number	Compound
1	$\text{Li}(\text{dmem})$	2	$\text{Na}(\text{dmem})$
3	$\text{K}(\text{dmem})$	4	
5		6	





## Chapter 4

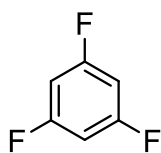
Number

Compound

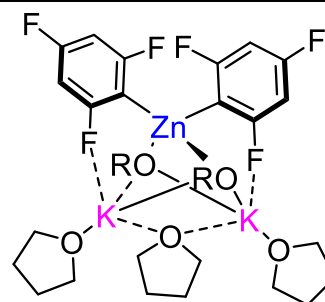
Number

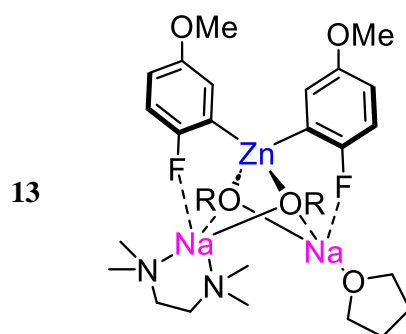
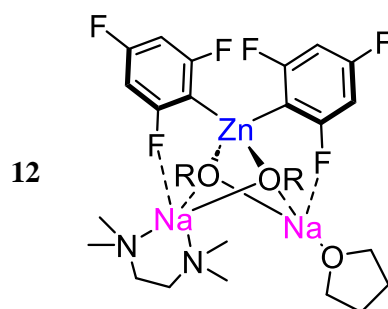
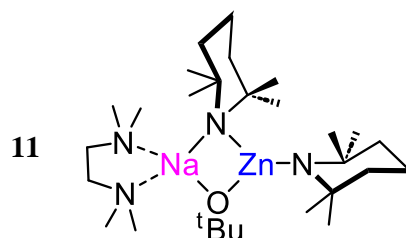
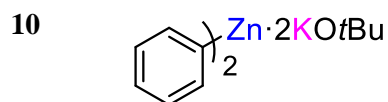
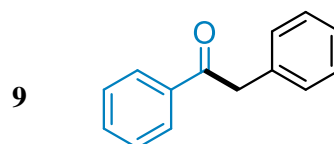
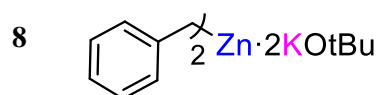
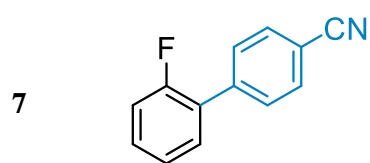
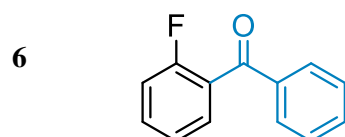
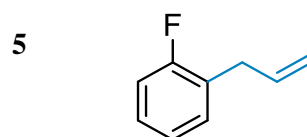
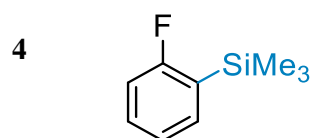
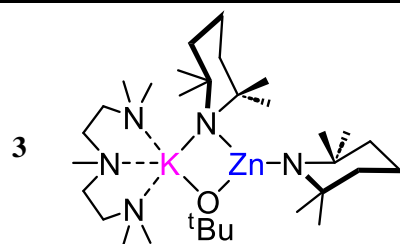
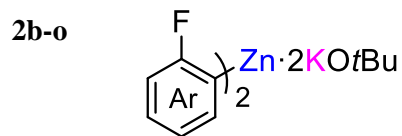
Compound

1a

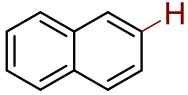
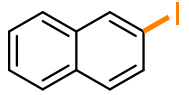
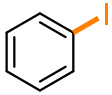
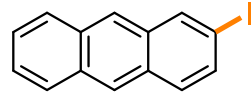
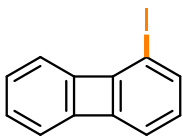
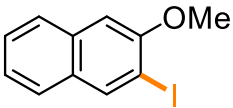
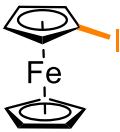
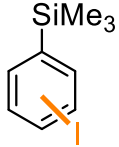
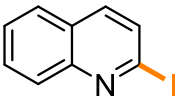
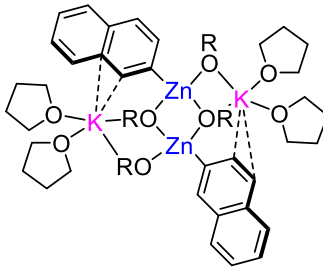
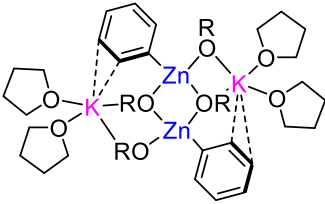
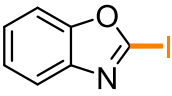
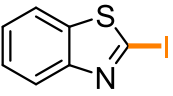
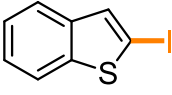
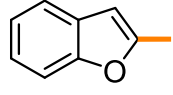


2a

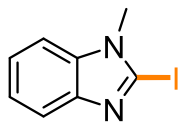




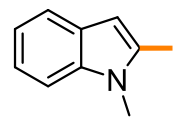
## Chapter 5

Number	Compound	Number	Compound
1		2a	
2b		2c	
2d		2e	
2f		2g	
2h		3a	
3b		4	$(\text{THF})_3\text{KZn}(\text{Fc})_3$
5a		5b	
5c		5d	

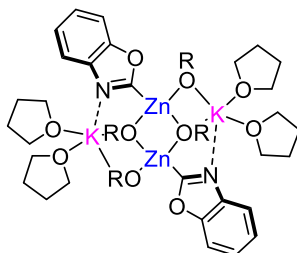
5e



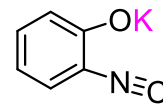
5f



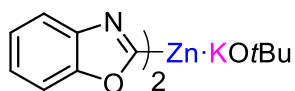
6



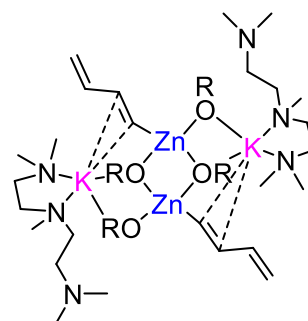
7



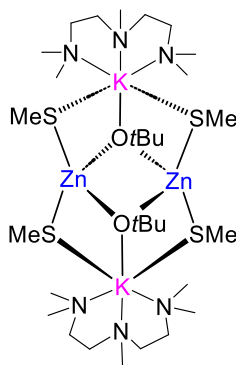
8



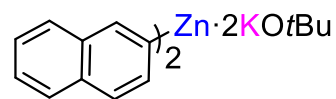
9



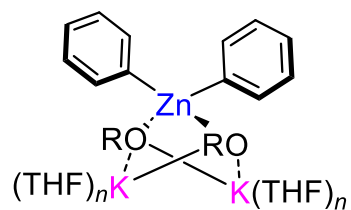
10



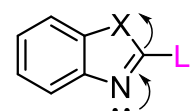
I



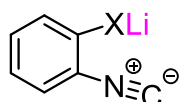
II



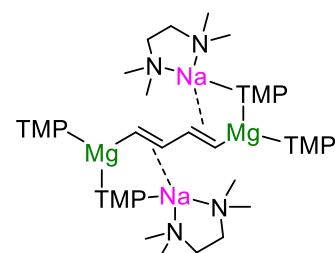
III



IV

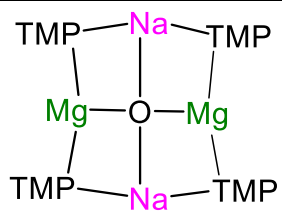


V



---

VI



VII

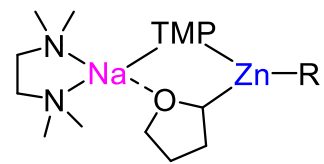


# Table of Contents

<b>Acknowledgements</b>	<b><i>i</i></b>
<b>Abstract</b>	<b><i>iv</i></b>
<b>Publications</b>	<b><i>vi</i></b>
<b>Conference Presentations</b>	<b><i>vii</i></b>
<b>List of Common Abbreviations</b>	<b><i>viii</i></b>
<b>Tables of Numbered Compounds</b>	<b><i>xi</i></b>
<b>Chapter 1: Alkali-Metal Alkoxides as Additives in Polar Organometallic Chemistry</b>	<b><i>1</i></b>
<b>1.1 Alkali-Metal Alkoxides and Group 1 Organometallics</b>	<b><i>1</i></b>
1.1.1 The Inception of the Lochmann-Schlosser Superbase	<i>2</i>
1.1.2 The LINK reagent: an Amide variant of the LIC-KOR Superbase	<i>4</i>
<b>1.2 Constitutional Complexity in Mixed AM-OR/RLi Aggregates</b>	<b><i>5</i></b>
<b>1.3 Applications of Alkali-Metal Alkoxides as Additives to Promote Mg and Zn/halogen Exchange Reactions</b>	<b><i>9</i></b>
1.3.1 Organolithiums Reagents in Metal/Halogen Exchange	<i>9</i>
1.3.2 Turbo Grignard Reagents in Metal/Halogen Exchange	<i>10</i>
1.3.3 Alkali-Metal Mediated Cooperative Bimetallic Chemistry	<i>13</i>
1.3.4 Alkali-Metal Alkoxide Additives in Mg/halogen Exchange	<i>14</i>
1.3.5 Lithium Alkoxide Additives in Zn/halogen Exchange	<i>17</i>
<b>1.4 Aims of the Thesis</b>	<b><i>19</i></b>
<b>1.5 References</b>	<b><i>20</i></b>
<b>Chapter 2: Untangling the Complexity of Lithium/Magnesium Alkyl/Alkoxy Combinations Utilised in Mg/Br Exchange</b>	<b><i>24</i></b>
<b>2.1 Introduction</b>	<b><i>25</i></b>
<b>2.2 Aims</b>	<b><i>26</i></b>
<b>2.3 Results and Discussion</b>	<b><i>27</i></b>
2.3.1 Assessing the Reactivity of Different Li and Mg Alkyl/Alkoxide Mixtures Towards 2-Bromoanisole	<i>27</i>
2.3.2 Structural and Spectroscopic Analysis of Mg/Br Exchange of 2-Bromoarenes	<i>28</i>
2.3.3 Structural and Spectroscopic Analysis of Mg/Br Exchange of 4-Bromoarenes	<i>31</i>
2.3.4 Electrophilic Interceptions of Mixed Aryl/Alkoxy Lithium Magnesiates 1a-b and Tetra(aryl) Lithium Magnesiates 2a-b	<i>34</i>
2.3.5 Spectroscopic Investigations into the Exchange Reagent (sBu <sub>2</sub> Mg·LiOR')	<i>35</i>
2.3.6 Alkoxide Effects in sBu <sub>2</sub> Mg·LiOR' combinations	<i>37</i>
2.3.7 Investigations to Determine the Active Exchange Reagent in sBu <sub>2</sub> Mg·LiOR' (R' = 2-ethylhexyl)	<i>39</i>
<b>2.4 Conclusions</b>	<b><i>43</i></b>
<b>2.5 Experimental</b>	<b><i>44</i></b>
2.5.1 Synthesis of Starting Materials	<i>44</i>
2.5.2 Synthesis of Mixed Aryl/Alkoxy Lithium Magnesiates [LiMgAr <sub>2</sub> (OR')] <sub>2</sub> 1a-b	<i>46</i>

2.5.3 Synthesis of Tetra(aryl) Lithium Magnesiates $[\text{Li}_2\text{Mg}(\text{Ar})_4]$ 2a-b, 6	48
2.5.4 Synthesis of $[\text{LiMg}_5\text{Bu}_2(\text{OR})]_2$ (OR = dmem) (6)	50
2.5.5 Electrophilic functionalisation studies	50
<b>2.5.6 GC reaction monitoring</b>	<b>52</b>
<b>2.6 References</b>	<b>54</b>
<b>Chapter 3: Assessing Alkali-Metal Effects in Mixed-Ligand Alkyl/Alkoxide Alkali-Metal Magnesiates Complexes</b>	
<b>3.1 Introduction</b>	<b>58</b>
<b>3.2 Aims</b>	<b>59</b>
<b>3.3 Results and Discussion</b>	<b>60</b>
3.3.1 Synthesis and Characterisation of Mixed Alkyl/Alkoxy Alkali-Metal Magnesiates	60
3.3.2 Assessing the Alkali-Metal Effect and Mg/Br Exchange Capabilities of Alkyl/Alkoxy Magnesiates 4-6	67
3.3.3 Structural and Spectroscopic Investigations of Mg/Br Exchange Products	69
3.3.4 Assessing Alkoxide Effects in Mixed Alkyl/Alkoxy Magnesiates and their Reactivity	70
<b>3.4 Conclusions</b>	<b>75</b>
<b>3.5 Experimental</b>	<b>76</b>
3.5.1 Synthesis of alkali metal alkoxides $\text{M}(\text{dmem})$ (AM = Li, 1; Na, 2; K, 3) and $\text{MOR}'$ (R = 2-ethylhexyl)	76
3.5.2 Synthesis of Alkyl/alkoxy magnesiates $[\text{MMg}(\text{CH}_2\text{SiMe}_3)_2(\text{dmem})]_2$ (M= Li, 4; Na, 5; (THF)K, 6)	78
3.5.3 Synthesis of $[\text{Mg}(\text{CH}_2\text{SiMe}_3)(\text{dmem})]_2$ 7	81
3.5.4 Synthesis of $[\text{Mg}(\text{Ar})(\text{dmem})]_2$ (Ar = <i>o</i> -OMe-C <sub>6</sub> H <sub>4</sub> ) 8	81
3.5.5 Synthesis of $[\text{MMg}(\text{CH}_2\text{SiMe}_3)_2\text{OR}']_2$ (R' = 2-Ethylhexyl) (M = Na, 9; K, 10)	82
3.5.6 Synthesis of $[\text{MMg}(\text{Ar})_2\text{OR}']_2$ (R' = 2-Ethylhexyl) (Ar = <i>o</i> -OMe-C <sub>6</sub> H <sub>4</sub> ) (M = Na, 11; K, 12)	83
3.5.7 Aqueous Quench of Insoluble Putative $\text{KAr}$ (Ar = <i>o</i> -OMe-C <sub>6</sub> H <sub>4</sub> )	84
3.5.8 Mg/Br exchange of 2-bromoanisole with $[(\text{TMEDA})_2\text{K}_2\text{MgR}_4]$ (R = $\text{CH}_2\text{SiMe}_3$ )	85
<b>3.6 References</b>	<b>86</b>
<b>Chapter 4: Alkali-Metal-Alkoxide Powered Zincation of Fluoroarenes Employing Zinc Bis-Amide <math>\text{Zn}(\text{TMP})_2</math></b>	
<b>4.1 Introduction</b>	<b>91</b>
<b>4.2 Aims</b>	<b>97</b>
<b>4.3 Results and Discussion</b>	<b>98</b>
4.3.1 Zincate screening towards metalation of 1,3,5-trifluorobenzene	98
4.3.2 Investigating the role of $\text{KOtBu}$ towards the activation of $\text{Zn}(\text{TMP})_2$	99
4.3.3 Expanding the substrate scope of fluoroarene metalation	104
4.3.4 Further functionalisation of potassium zincate intermediates	107
4.3.5 Extension to the zincation of non-activated arenes	108
4.3.6 Formation of sodium zincates using a $\text{Zn}(\text{TMP})_2/\text{NaOtBu}$ combination	110
<b>4.4 Conclusions</b>	<b>112</b>
<b>4.5 Experimental</b>	<b>114</b>
4.5.1 Synthesis of $[(\text{PMDETA})\text{KZn}(\text{TMP})_2\text{OtBu}]$ (3)	114

4.5.2 Synthesis of $(\text{THF})_3\text{K}_2\text{Zn}(\text{C}_6\text{F}_3\text{H}_2)_2(\text{OtBu})_2$ 2a	114
4.5.3 Synthesis of higher order potassium zincates $(\text{THF})_3\text{K}_2\text{Zn}(\text{Ar})_2(\text{OtBu})_2$ 2b-2o	115
4.5.4 Electrophilic quenches of potassium zincate 2d	122
4.5.5 Synthesis of 8 $(\text{THF})_2\text{K}_2\text{Zn}(\text{Bz})_2(\text{OtBu})_2$ (Bz = $\text{CH}_2\text{Ph}$ ) (toluene zincation)	123
<b>4.5.6 Synthesis of 1,2-diphenylethanone 9 via arylation of 8</b>	<b>125</b>
4.5.7 Synthesis of $[\text{K}_2\text{Zn}(\text{Ph})_2(\text{OtBu})_2]$ 10 (benzene zincation)	125
4.5.8 Synthesis of sodium zincates 11, 12 and 13	125
<b>4.6 References</b>	<b>128</b>
<b>Chapter 5: Zincation of Non-Activated Arenes with an Alkoxide Powered <math>\text{Zn}(\text{TMP})_2</math> Base</b>	<b>132</b>
<b>5.1 Introduction</b>	<b>132</b>
<b>5.2 Aims</b>	<b>135</b>
<b>5.3 Results and Discussion</b>	<b>136</b>
5.3.1 Reaction Optimisation for Regioselective Zincation of Naphthalene	136
5.3.2 Solid and Solution State Complexity in the Zincation of Non-Activated Arenes	138
5.3.3 Regioselective Iodinations of Non-Activated Arenes via Alkoxide Mediated Zincations	141
5.3.4 Investigations into the Zincation of 5-Membered Fused Heterocycles	144
5.3.5 Cleave and Capture Chemistry using $\text{Zn}(\text{TMP})_2/2\text{KOtBu}$	149
<b>5.4 Conclusions and Future Work</b>	<b>153</b>
<b>5.4 Experimental</b>	<b>154</b>
5.5.1 Synthesis of Organometallic Compounds 3a-b, 4, 6, 7, 9 and 10	154
5.5.2 Synthesis of Iodoarenes Compounds 2a-g and 5a-f	157
5.5.3 Selected crystallographic parameters for compounds 3a-b, 4, 6, 9 and 10	162
<b>5.6 References</b>	<b>169</b>
<b>Chapter 6 - Conclusions and Outlook</b>	<b>173</b>
<b>Chapter 7 – General Experimental Techniques and Procedures</b>	<b>177</b>
<b>7.1 Schlenk Techniques</b>	<b>177</b>
<b>7.2 Glovebox</b>	<b>178</b>
<b>7.3 Solvent Purification</b>	<b>179</b>
<b>7.4 Reagent Purification</b>	<b>179</b>
<b>7.5 Standardisation of Organometallic Reagents</b>	<b>179</b>
<b>7.6 Synthesis of <math>\text{Zn}(\text{TMP})_2</math></b>	<b>180</b>
<b>7.7 Analytical Procedures</b>	<b>181</b>
<b>7.8 References</b>	<b>182</b>



# Chapter 1: Alkali-Metal Alkoxides as Additives in Polar Organometallic Chemistry

Alkali-metal alkoxides (AM-OR) are commercially available and indispensable reagents in synthetic chemistry, offering a versatile range of applications.<sup>1,2</sup> They are renowned for their relatively strong basicity and nucleophilic properties which can be tuned by altering the substituents on the parent alcohol of which they are derived from. They find essential use in organic synthesis, by facilitating deprotonative metalations, nucleophilic substitutions and condensation reactions effecting a range of C-C, C-N, C-O and C-S bond forming processes where in some cases the alkoxide is used as a catalyst.<sup>3-5</sup> Boasting their versatility, alkali-metal alkoxides have also been found to act as powerful single electron transfer (SET) donors to aromatic molecules and alkyl iodides so are used in many radical processes in organic chemistry.<sup>6,7</sup> However, the predominant focus of this *Chapter* will be the use of these Group 1 alkoxides as additives in polar organometallic chemistry which is the underpinning theme in this thesis. This *Chapter* provides a concise overview on the current *state-of-the-art* on this area of research including current understanding of their activating effect as well their most representative applications in synthesis when used in combination with s-block metal and zinc organometallic reagents.

## 1.1 Alkali-Metal Alkoxides and Group 1 Organometallics

The use of Group 1 metal alkoxides as additives to activate s-block organometallics is a phenomenon that was first noticed over 70 years ago, where the addition of varying amounts of AM-OR (AM = Li, Na) to organolithium (RLi) or organosodium (RNa) reagents was found to rapidly accelerate styrene and diene polymerisation.<sup>8,9</sup> This discovery led to the emergence of a wide range of powerful monometallic and bimetallic s-block reagents, which have been subsequently coined in the literature as “superbases” due to their ability to carry out challenging deprotonative metalation reactions (C-H to C-Metal).<sup>10</sup> Typical combinations comprise of an alkyllithium (RLi, R = alkyl) and a heavier AM-OR component (Figure 1). The working hypothesis behind the activation of alkyllithiums by alkali-metal alkoxides is the formation of mixed-metal/mixed-ligand aggregates, switching on cooperative effects between the different metals giving rise to a synergic mixture which offers an enhanced reactivity to the monometallic reagents used to form the superbase.<sup>11</sup>

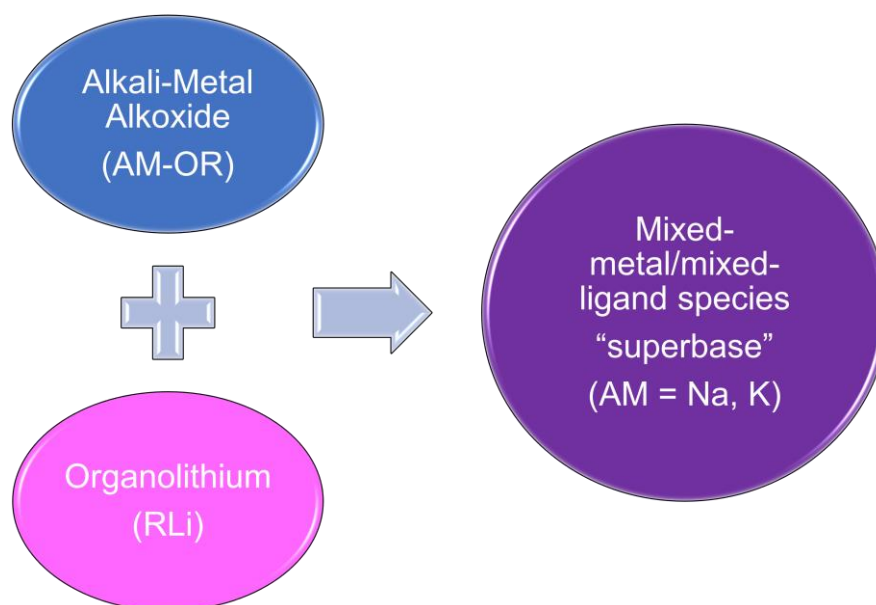
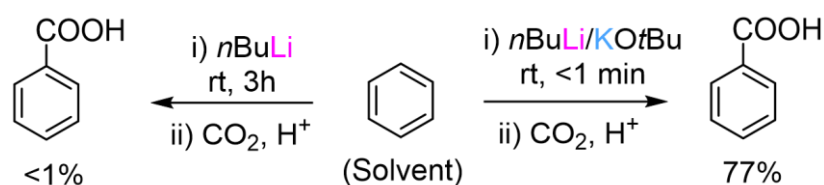


**Figure 1.** Combination of heavier AM-OR (AM = Na, K) with RLi to form superbasic mixed-metal/mixed-ligand species

### 1.1.1 The Inception of the Lochmann-Schlosser Superbase

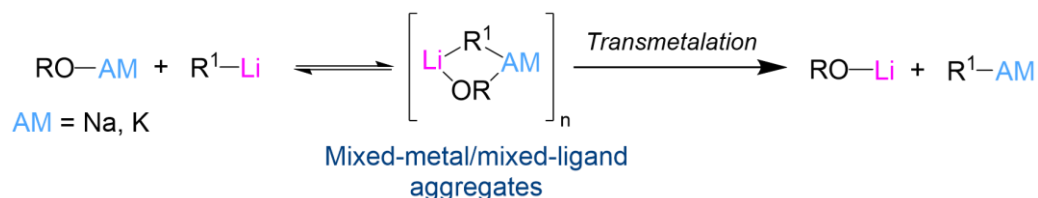
The quintessential example of these superbase reagents is the famous Lochmann-Schlosser superbase, or "LIC-KOR" base due to its  $n\text{BuLi}/\text{KO}t\text{Bu}$  composition. Reported independently by Lochmann (1966)<sup>12</sup> and Schlosser (1967)<sup>13</sup> the LIC-KOR base remains a commonly used metalating reagent 50 years after its discovery due to its unique reactivity in deprotonative metalation reactions.<sup>10</sup> This is exemplified by the deprotonation of benzene, as in the absence of a Lewis donor  $n\text{BuLi}$  is completely inert towards benzene whereas in less than one minute at room temperature the LIC-KOR superbase can metalate the arene in an efficient manner (Scheme 1) when benzene is used as a solvent.<sup>13</sup>



**Scheme 1.** Contrasting basicity of  $n\text{BuLi}$  and LIC-KOR towards the metalation of benzene

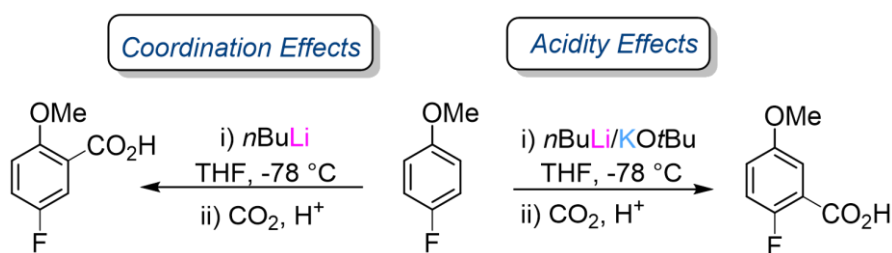
Schlosser states that although the combination of  $n\text{BuLi}$  and  $\text{KO}t\text{Bu}$  will eventually lead to the eventual transmetalation of the two species, driven by the formation of a highly insoluble alkylpotassium ( $n\text{BuK}$ ) and the oxophilicity of Li to form  $\text{LiO}t\text{Bu}$ , it is unlikely that the highly reactive alkylpotassium species formed is the active base.<sup>14,15</sup> This is due to the fact that organopotassium reagents are known to cleave ethereal solvents such as tetrahydrofuran (THF) (even at  $-78\text{ }^\circ\text{C}$ ) and are prone to self-degradation due to their lack of thermal stability, whereas superbasic mixtures are known to be stable in ethereal solvents up to  $-50\text{ }^\circ\text{C}$ .<sup>14</sup>

Moreover, comparative reactivity studies between organopotassium and LICKOR bases have shown that the latter provides higher yields with a greater control of the regioselectivity.<sup>14</sup> This supports the hypothesis that the unique reactivity observed for these reagents is due to the formation of a mixed-metal/mixed-ligand “ate” species, before eventual transmetalation is observed (Scheme 2).



**Scheme 2.** Proposed formation of mixed alkyl/alkoxy bimetallic aggregates in superbases mixtures

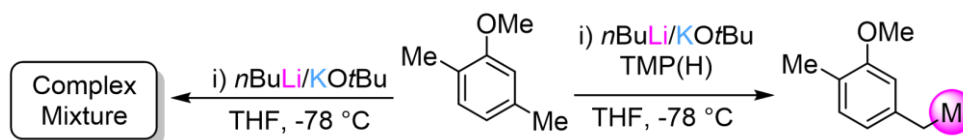
Highlighting its use in organic synthesis, the LIC-KOR superbase can provide (in some cases) complementary selectivities to those observed using conventional organolithium reagents. Schlosser noticed this investigating the metalation of fluoroanisoles where *n*-butyllithium is known to metalate 4-fluoro or 2-fluoroanisole ortho to the OMe directing group.<sup>16</sup> This is known as “Directed *ortho* Metalation” (DoM)<sup>17</sup> where a Lewis donor group provides a coordinating docking site for the incoming organolithium reagent, subsequently inducing its deaggregation and facilitating the metalation step via a complex induced proximity effect (CIPE).<sup>18</sup> Contrastingly, the superbase mixture of *n*BuLi/KOtBu selectively metalates *ortho* to the fluorine atom which is the most acidic site in terms of pKa in the fluoroarene (Scheme 3).<sup>16</sup> It is thought that KOtBu provides a twofold activation of *n*BuLi by forming the aforementioned mixed-metal/mixed-ligand ate species whilst also facilitating the deaggregation of the organolithium reagent to form smaller, kinetically more reactive species.<sup>11</sup> Thus, in absence of this need for additional deaggregation, the LIC-KOR base favours the deprotonation of the most acidic site ortho to the fluorine.



**Scheme 3.** Controlling the regioselectivity of metalation of 4-fluoroanisole with LIC-KOR by overriding CIPE with acidifying effects

### 1.1.2 The LiNK reagent: an Amide variant of the LIC-KOR Superbase

An important adaptation of the Lochmann-Schlosser superbase was developed more recently by O'Shea and co-workers by introducing the amine TMP(H) (2,2',6,6'-tetramethylpiperidine) to the LIC-KOR base making a three component mixture of  $n\text{BuLi}/\text{KO}t\text{Bu}/\text{TMP(H)}$  with the catchy name, LiNK reagent.<sup>19</sup> Another way to view this base is a combination of the utility amide  $\text{LiTMP}$  with  $\text{KO}t\text{Bu}$ . O'Shea noted profound differences in the regioselectivities observed in metalations of substituted toluenes carried out by the LIC-KOR base and the LiNK base. For example, a complex mixture of products is observed when 2,5-dimethylanisole is treated with the standard LIC-KOR base at  $-78\text{ }^\circ\text{C}$  in THF. However, when employing the LiNK base, a selective benzylic metalation is achieved in the *meta* position (Scheme 4). The observed regioselectivity has been rationalised by the ability of this base to induce an anion migration of the kinetic *ortho*-aryl position to the benzylic site as evidenced by NMR spectroscopic studies using catalytic amounts of TMP(H). More recently the LiNK base was shown to be compatible with more user-friendly conditions operating at  $0\text{ }^\circ\text{C}$  and room temperature in hydrocarbon solvents for the selective lateral metalations of toluenes, xylenes and benzyloxy silanes.<sup>20</sup> Kobayashi recently employed the LiNK reagent under catalytic conditions for the deprotonation of nonactivated alkylarenes and subsequent addition to imines and alkenes forming new C-C bonds.<sup>21</sup>



**Scheme 4.** Contrasting metalation regioselectivities of 2,5-dimethylanisole with LIC-KOR superbase and LiNK reagent

Despite their popularity and synthetic utility, superbase reagents have some considerable drawbacks with respect to relative functional group tolerance, the need for ethereal solvents used under cryogenic conditions and the control of regioselectivity due to the extreme reactivity of these species. For example, when treating naphthalene with the LIC-KOR superbase, Schlosser reported an extremely complex mixture of products containing two monometalated and ten dimetalated isomers (see *Chapter 5, section 5.1*).

## 1.2 Constitutional Complexity in Mixed AM-OR/RLi Aggregates

Although there is a general consensus the highly reactive nature of the superbase is of a synergic kind due to the formation of mixed-metal/mixed-ligand aggregates there is still a relatively poor understanding of the solution and solid-state behaviour of the LIC-KOR superbase. This is due to its poor solubility and incompatibility with common organic solvents making the characterisation of such species particularly challenging. Schlosser proposed that the special reactivities observed for these bimetallic combinations could be due to the formation of multiple mixed aggregates of varying alkyl/alkoxide content in solution.

Lochmann and Boche reported the first crystallographically characterised co-complex formed from a superbase type mixture in which the combination of  $n\text{BuLi}$  and  $\text{LiOtBu}$  forms a tetrameric mixed aggregate  $[\text{nBuLi}\cdot\text{LiOtBu}]_4$  in the solid state (Figure 2).<sup>22</sup> The molecular structure revealed two distinct Li environments (Li and Li' in Figure 2) in which four Li centres are coordinated to two  $n\text{Bu}$  groups and one alkoxide then the remaining four Li centres exhibit the reverse by coordinating two alkoxide groups and one  $n\text{Bu}$  fragment. Albeit this structure is monometallic, it can offer some clues into the possible aggregates present in the mixed metal LIC-KOR system. The authors comment that the difference in size between Li and K could of course affect the resultant aggregation of the LIC-KOR base in solution and in the solid state. Nevertheless, this report laid the foundations for the subsequent spectroscopic and crystallographic investigations into superbase type mixtures.

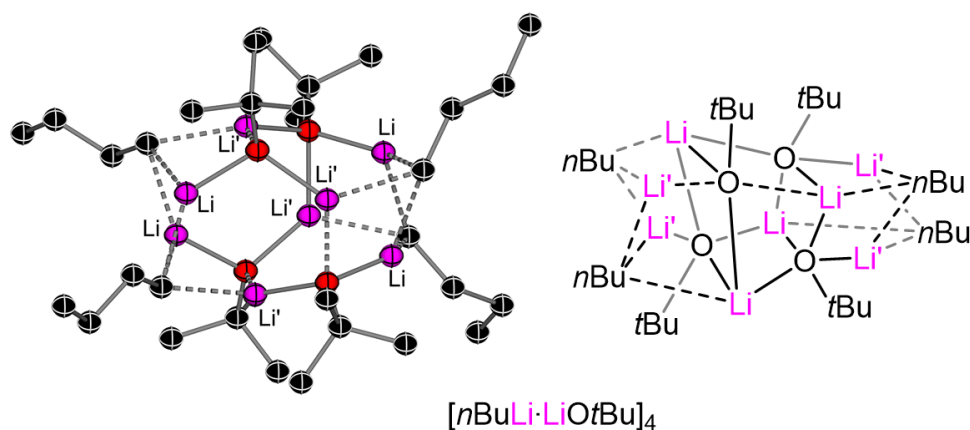


**Figure 2.** Molecular structure (LHS) and chemdraw representation (RHS) of  $[\text{nBuLi}\cdot\text{LiOtBu}]_4$ . Displacement ellipsoids at 50% probability and all hydrogen atoms omitted for clarity.<sup>22</sup>

Somewhat contradictory to these findings, Lochmann and Bauer assessed the solution behaviour of an equimolar mixture of trityllithium and caesium 3-ethyl-3-heptoxide by rigorous NMR spectroscopic studies concluding a complete transmetalation of the metals occurs.<sup>23</sup> The authors found no evidence of the formation of mixed aggregates in solution citing the complete formation of caesium trityl and the corresponding lithium alkoxide.

Although in this report it was also cautiously stated that it is challenging to extrapolate these findings to the LIC-KOR superbase as clear differences are observed in the reactivities and stability of alkylpotassium reagents and superbase mixtures (*vide supra*). This highlights a common theme throughout this thesis in that the nature of the two chosen metals and the organo/alkoxide fragments govern the aggregates formed and how subtle alterations to the mixture can result in dramatic changes on the constitution of the organometallic complexes formed.

Another important landmark in this area of research was the structural authentication of a mixed organosodium/lithium alkoxide co-complex achieved from combining *n*BuLi with sodium 2,4,6-trimethylphenoxide by Streitwieser by using hexane as a solvent and TMEDA (N,N,N',N'-tetramethylethylenediamine) as a Lewis donor.<sup>24</sup> Furnishing an octanuclear cluster [TMEDA·Na-CH<sub>2</sub>(o-Li-3,5-Me<sub>2</sub>-C<sub>6</sub>H<sub>2</sub>)]<sub>4</sub>, its structure is rationalised in terms of the lateral metalation of the alkoxide fragment giving rise to lithium-4,6-dimethyl-2-sodiummethylphenoxide which is tetrameric in the solid state (Figure 3). The structure comprises a central distorted Li<sub>4</sub>O<sub>4</sub> cubane with perpendicular interactions between each lithium vertex and a benzylic fragment. The sodium atoms lie on the periphery of the Li<sub>4</sub>O<sub>4</sub> cage, solvated by the bidentate donor TMEDA and form perpendicular interactions with a metalated benzylic C atom forming a Li···C···Na···O ring completed with Na-O electrostatic interactions. The structure is said to be dictated by the Li-O bonding preference, thus the Li<sub>4</sub>O<sub>4</sub> motif maximises the number of Li-O bonds and the authors state the Na-O coordination is of minor importance in the coordination sphere of the five coordinate O atom. The authors proposed that the lithium alkoxides may have a key role in governing the formation of mixed aggregates in solution due to this preferential Li-O bonding which could exist in more standard superbase mixtures (i.e. *n*BuLi/KO*t*Bu). Indeed, the bonding in this structure fits well with hard soft acid base (HSAB) theory in which the smaller alkali metal (Li) prefers direct contacts with oxygen and the heavier alkali metal (Na) adopts interactions with the softer carbanionic centre.

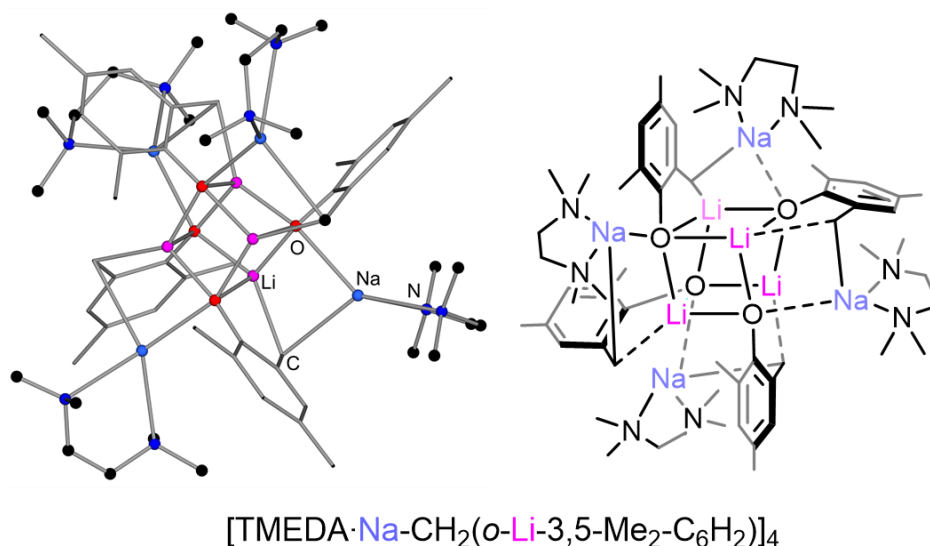


**Figure 3.** Molecular structure (LHS) and chemdraw representation of [TMEDA·Na-CH<sub>2</sub>(o-Li-3,5-Me<sub>2</sub>-C<sub>6</sub>H<sub>2</sub>)<sub>4</sub>]. Structure modelled as balls and sticks with all hydrogen atoms omitted and benzylic fragments drawn as wire frames for clarity.<sup>24</sup>

Despite the discovery of the LIC-KOR superbase over five decades ago, it was only in 2014 that the first ever mixed-metal/mixed-ligand aggregate containing all components of a superbase was reported. Strohmann was able to capture a snapshot into the metalation of benzene by the classical *n*BuLi/KOtBu superbase in THF at -78 °C revealing a five component [(PhK)<sub>4</sub>(PhLi)(LiOtBu)(THF)<sub>6</sub>(C<sub>6</sub>H<sub>6</sub>)<sub>2</sub>] (Figure 4).<sup>25</sup> Reminiscent of the bonding interactions present in the structure reported by Streitwieser, the interior of the complex is built on both hard Li atoms interactions with the alkoxide fragment and three of the phenyl groups. The central unit comprises a PhLi and LiOtBu moiety forming a {Li-C-Li-O} four membered ring where the Ph ligands reside in the same plane as the Li atoms suggesting significant  $\sigma$  character. The softer K atoms surround this central ring forming  $\pi$  interactions in a perpendicular fashion to the *ipso*-carbons of the metalated ring. Two of the K atoms form two of these electrostatic interactions with metalated Ph moieties and their coordination sphere satisfied by two THF molecules and a  $\eta^1$ -coordinating benzene ligand. The remaining two K atoms above and below the central {Li-C-Li-O} ring form  $\pi$  interactions with two Ph moieties and form additional contacts to the O atom in the alkoxide fragment and a THF donor molecule. Reaffirming the preference of the softer alkali metal (K) to form contacts with the softer carbanionic centres. The superbasic nature of this compound was confirmed in neat toluene by the formation of benzyl potassium at -40 °C. DFT calculations suggest that an initial coordination of the  $\pi$  system in toluene to the K atoms (replacing a labile THF donor molecule) could facilitate this deprotonation by bringing the substrate in close proximity to the anionic Ph moiety.

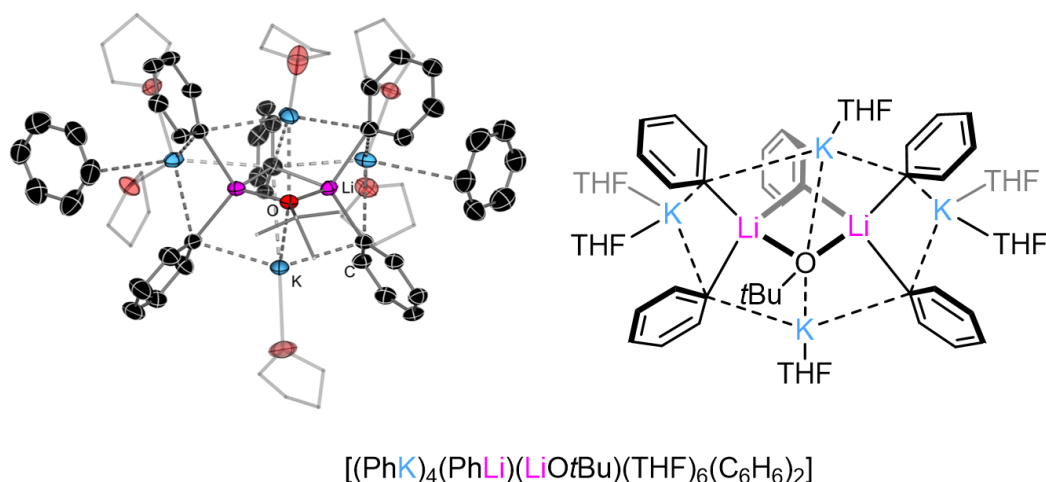


**Figure 4.** Molecular structure (LHS) and chemdraw representation (RHS) of  $[(\text{PhK})_4(\text{PhLi})(\text{LiOtBu})(\text{THF})_6(\text{C}_6\text{H}_6)_2]$ . Displacement ellipsoids at 50% probability and all hydrogen atoms omitted with C atoms in THF drawn as wire frames for clarity.<sup>25</sup>

A fundamental aspect in the characterisation of superbases in solution is the relative stability and solubility of these combinations in organic solvents often attributed to the formation of  $n\text{BuK}$  which is thermally unstable often undergoing  $\beta$ -hydride elimination and removing it from the equilibrium shown in Scheme 2. Recently, Klett and co-workers sought to employ the more lipophilic neopentyl lithium (NpLi) reagent, in absence of any  $\beta$  hydrogens, in combination with  $\text{KO}t\text{Bu}$  to hopefully reveal a more soluble and thermally stable superbase mixture. The combination of NpLi and  $\text{KO}t\text{Bu}$  in hexane afforded a white precipitate which was confirmed as NpK in a very moderate yield of 30%. Subsequent crystallisation experiments of the resulting mother liquor led to the characterisation of multiple mixed aggregates of the form  $[\text{Li}_4\text{K}_4(\text{Np})_n(\text{OtBu})_{8-n}]$  (where  $n = 1, 2$  or  $3$ ) and the authors note a significant decrease in the stability of the complex with increasing Np content.<sup>26</sup> The first of the compounds to be characterised was the bimetallic  $[\text{Li}_4\text{K}_4(\text{Np})_3(\text{OtBu})_5]$  fragment (Figure 5). The structural make-up of this mixed aggregate has a remarkable resemblance to that of Mulvey's previously reported all alkoxide octameric  $[\text{Li}_4\text{K}_4(\text{OtBu})_8]$  structure which adopts a breastplate arrangement.<sup>27</sup> The eight metal centres occupy the vertices of a truncated tetrahedron, leading to four  $\text{Li}_2\text{K}_2$  triangles capped by bridging Np groups and four  $\text{Li}_2\text{K}_2$  trapeziums capped by  $\text{OtBu}$  groups. Detailed spectroscopic studies by Klett suggest the presence of multiple mixed-metal/mixed-ligand aggregates in solution with varying Np/ $\text{OtBu}$  ratios. This seminal report by Klett further endorses Schlosser's initial considerations that multiple reactive bimetallic mixed aggregates can co-exist in solution within RLi/AM-OR superbase mixtures.<sup>14</sup>



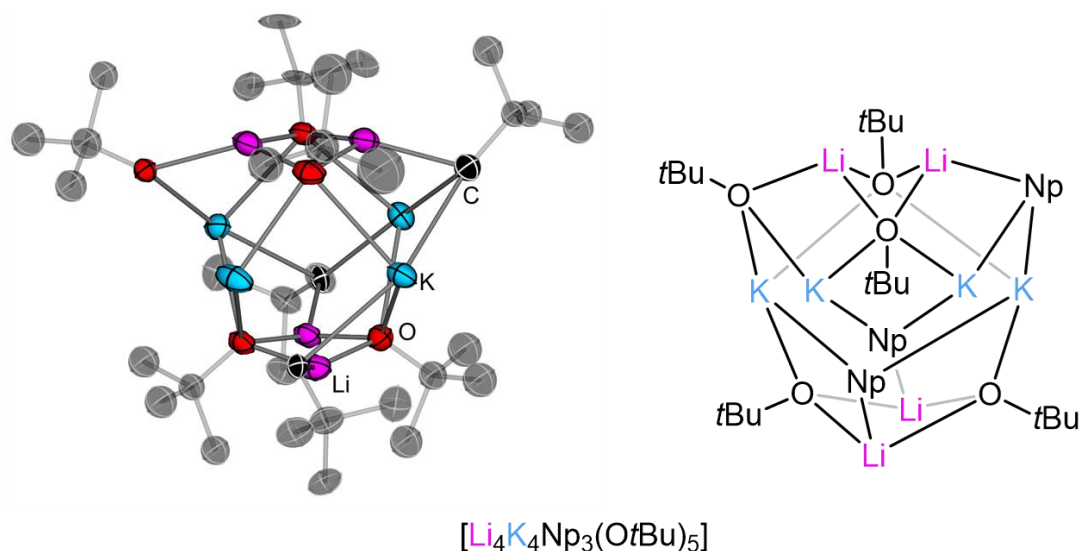


**Figure 5.** Molecular structure (LHS) and chemdraw representation (RHS) of  $[(\text{Li}_4\text{K}_4\text{Np}_3)(\text{OtBu})_5]$ . Displacement ellipsoids at 30% probability and all hydrogen atoms omitted for clarity.<sup>26</sup>

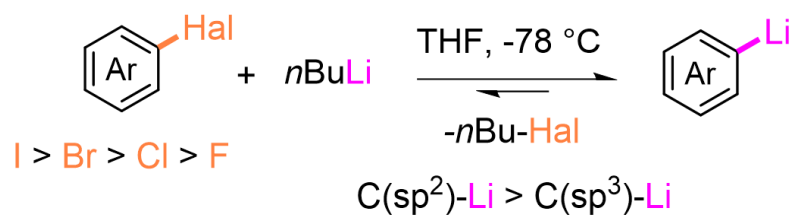
The aforementioned contributions have been integral to the current understanding of the modulus operandi of the LIC-KOR superbases, yet its true constitution remains difficult to ascertain and is a topic of debate amongst the polar organometallic chemistry community.<sup>11,28</sup> What we can be certain of is the diverse and structural complexity observed for mixed-metal/mixed-ligand superbase aggregates which can co-exist in equilibrium giving rise to the unique synergic reactivity observed for commonly used superbases.

### 1.3 Applications of Alkali-Metal Alkoxides as Additives to Promote Mg and Zn/halogen Exchange Reactions

#### 1.3.1 Organolithium Reagents in Metal/Halogen Exchange

The unique reactivity of AM-OR/RLi combinations has sparked a stream of related studies into the activation of di-organomagnesium and diorganozinc reagents. Primarily this work has focused on the addition of stoichiometric amounts of alkali metal alkoxides to dialkylmagnesium or zinc reagents for metal/halogen exchange (*vide infra*). Discovered independently by Gilman<sup>29</sup> and Wittig<sup>30</sup> at the end of the 1930s, using highly reactive alkyllithium reagents, metal/halogen exchange constitutes a cornerstone reaction in organic synthesis and is one of the most powerful methodologies to functionalise aromatic halides.<sup>31</sup> Li/halogen exchange is a kinetically driven process in which a more stabilised carbanion ( $\text{C}(\text{sp}^2)\text{-Li}$  Vs  $\text{C}(\text{sp}^3)\text{-Li}$ ) is produced upon reaction of an alkyllithium reagent typically with an aryl halide (Scheme 5).<sup>32</sup> The stronger the C-Hal (Hal = halogen) bond the slower the

lithium/halogen exchange process,<sup>33</sup> so these reactions occur much more frequently with aryl iodides or bromides.



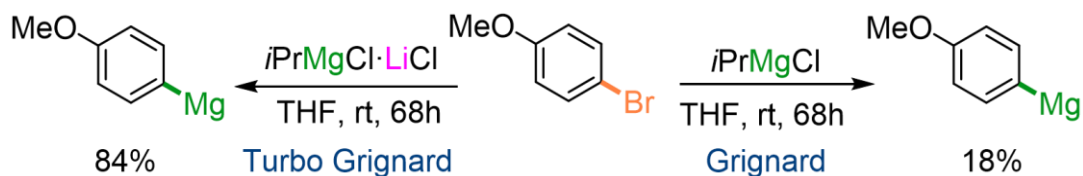
**Scheme 5.** General scheme for Lithium/halogen exchange of aromatic halides

Ethereal solvents such as THF are known to accelerate the rate of lithium/halogen exchange, likely through deaggregation of the organolithium reagent affording smaller and more kinetically activated species. However, organolithium reagents are known to decompose in THF by an initial  $\alpha$ -metalation of the heterocycle which undergoes a reverse [3+2] cycloaddition forming a lithium enolate and ethylene.<sup>34</sup> Hence, these reactions are almost exclusively carried out under cryogenic conditions. Unfortunately, due to the high reactivity of the organolithium reagents used many unwanted side reactions are possible such as Li-H exchange, Wurtz coupling, benzyne formation and nucleophilic additions.<sup>35-37</sup> Despite the increased stability of the aryllithium product, such species still contain a highly polarised  $\text{Li}^{\delta+}\text{-C}^{\delta-}$  bond which can itself participate in the aforementioned side reactions. This poses major challenges using highly decorated aromatic halides containing functional groups like  $\text{NO}_2$ , CN or carbonyl moieties.

### 1.3.2 Turbo Grignard Reagents in Metal/Halogen Exchange

An alternative class of reagents for metal/halogen exchange reactions are Grignard reagents ( $\text{RMgX}$ ). Compared to organolithium reagents, Grignard species contain a considerably less polarised M-C bond due to the increased electronegativity of magnesium compared with lithium ( $\text{Mg } \chi = 1.31$  vs  $\text{Li } \chi = 0.98$ ).<sup>32</sup> Thus, many of the unwanted side reactions prominent in Li/halogen exchange reactions can be avoided using these tamer organomagnesium reagents which can operate at room temperature.<sup>38</sup> This allows for the magnesiumation of highly functionalized aromatic halides, via Mg/halogen exchange, containing sensitive functional groups like nitro, cyano and ester moieties.<sup>38,39</sup> However, a decrease in the M-C bond polarity is accompanied with a sluggish kinetic profile for Mg/halogen exchange requiring extremely electron deficient substrates for success in these processes.<sup>40</sup> Overcoming this issue, pioneering work from Knochel in 2004 led to the inception of “Turbo Grignard reagents” describing a profound enhancement in the reactivity of conventional Grignard reagents towards aromatic halides when a stoichiometric equivalent of  $\text{LiCl}$  was added to the reaction e.g.,  $i\text{PrMgCl} \cdot \text{LiCl}$ .<sup>40</sup> For example, Knochel reports that treating 4-bromoanisole with

*i*PrMgCl in THF after 68h affords an 18% yield of Mg/Br yet under the same reactions conditions an 84% yield could be achieved by simply adding LiCl to the reaction medium (Scheme 6).<sup>40</sup> Owing to their popularity and synthetic utility Turbo Grignard reagents are now commercially available commodities and have been subject of several reviews<sup>15,31,41</sup> detailing their applications in organic synthesis. *i*PrMgCl·LiCl even won the EROS (Encyclopaedia of Reagents for Organic Synthesis) best reagent award in 2011.<sup>15</sup>



**Scheme 6.** Mg/Br exchange of 4-bromoanisole with Grignard and Turbo Grignard reagents

Despite the widespread use of Turbo Grignard reagents, the activating role of LiCl remained poorly understood despite much investigation within the organometallic community. Grignard reagents themselves exhibit extremely complex solution chemistry forming a diversity of species bearing various ligands co-existing in fast equilibria, epitomised by the Schlenk equilibria (Figure 6), of which the composition depends on the experimental conditions. The addition of LiCl only compounds this complexity further. Straub and Knochel putatively proposed, via theoretical calculations, that LiCl could act as a means to deaggregate the Grignard (e.g., *i*PrMgCl) reagent forming a highly soluble and more reactive monomeric mixed metal species (e.g. [*i*PrMg( $\mu$ -Cl)<sub>2</sub>Li]) (Figure 6).<sup>42</sup>

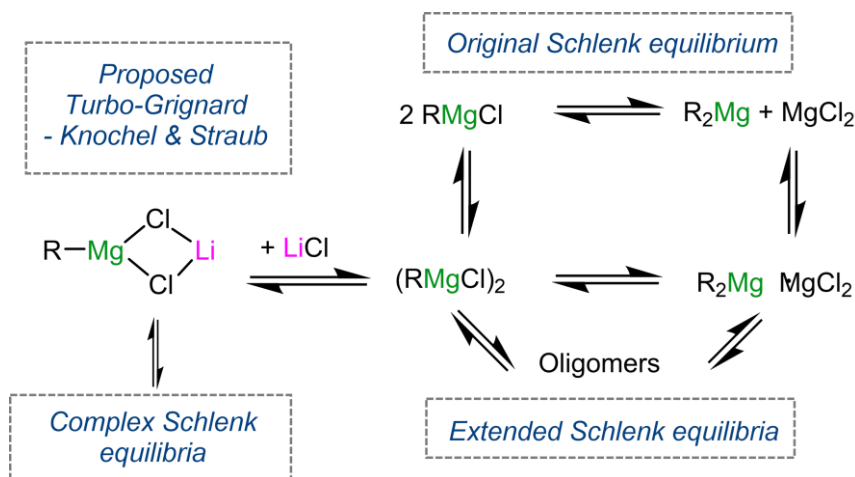


**Figure 6.** Original and extended Schlenk equilibria and proposed Turbo Grignard motif by Knochel and Straub

Solution studies by Stalke offered further support to the presence of such bimetallic aggregates in solution however it was also revealed that a multitude of species comprising of different aggregation states and ligand distribution can be present in equilibria (which is also dependant on concentration and temperature).<sup>43,44</sup> A breakthrough in the solid-state characterisation of the related Turbo-Hauser [TMP(THF)Mg( $\mu$ -Cl)<sub>2</sub>Li(THF)<sub>2</sub>] (TMP =

2,2,6,6-tetramethylpiperidide) base by Mulvey demonstrated that the bimetallic motif proposed by Knochel was indeed adopted in the solid state confirmed by X-Ray crystallography (Figure 7a).<sup>45</sup> Strohmann has very recently added another piece to the ever evolving Turbo Grignard puzzle with the characterisation of a di-organomagnesium species  $[t\text{Bu}_2\text{Mg}(\text{THF})(\mu\text{-Cl})\text{Li}(\text{THF})_2]$  (Figure 7b) from a mixture of  $t\text{BuMgCl}$  and  $t\text{BuLi}$ .<sup>46</sup> Due to the highly dynamic Schlenk equilibrium it's possible that such di-organomagnesium reagents could be present in solution and therefore should be considered when discussing the reactivity of commonly used Turbo Grignard reagents.

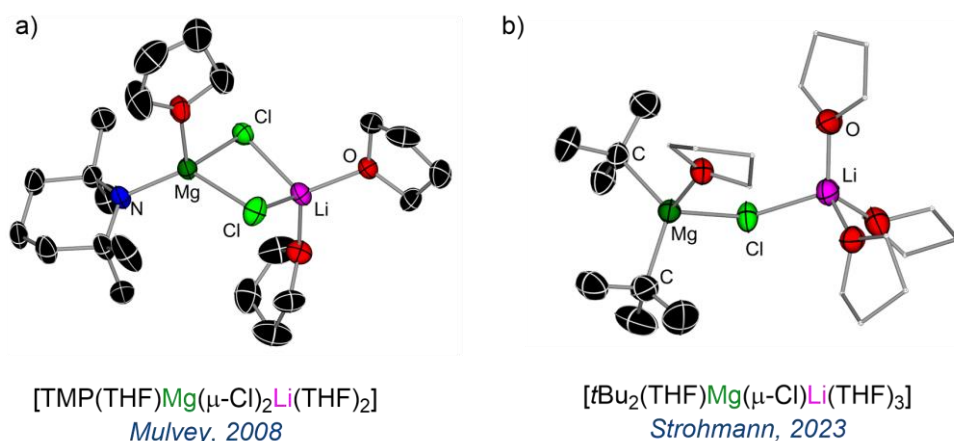


**Figure 7.** a) Molecular structure of  $[\text{TMP}(\text{THF})\text{Mg}(\mu\text{-Cl})_2\text{Li}(\text{THF})_2]$  with displacement ellipsoids at 50% probability and all hydrogen atoms omitted for clarity b) Molecular structure of  $[\text{tBu}_2(\text{THF})\text{Mg}(\mu\text{-Cl})\text{Li}(\text{THF})_3]$  with displacement ellipsoids at 50% probability, all hydrogen atoms omitted and C atoms in THF drawn as wire frames for clarity

As recently as 2023, Eisenstein and co-workers used *ab-initio* molecular dynamics (AIMD) simulations, a well-suited method for studying highly dynamic systems in solution,<sup>47,48</sup> to model Turbo Grignard reagents based on  $\text{CH}_3\text{MgCl}$  and the related Schlenk associated compounds  $\text{MgCl}_2$  and  $(\text{CH}_3)_2\text{Mg}$ .<sup>49</sup> This extremely detailed and elegant study confirmed a synergistic role of  $\text{LiCl}$  for the determination of the compounds present in Turbo Grignard reagents.  $\text{LiCl}$  shifts the Schlenk equilibrium to favour a higher concentration of dialkylmagnesium whilst forming smaller, more soluble bimetallic  $\text{Li}:\text{Mg}:\text{Cl}$  clusters. Eisenstein concluded that the initial proposals by Knochel and Straub, along with the recent discovery of  $t\text{Bu}_2\text{Mg}\cdot\text{LiCl}(\text{THF})_4$  by Strohmann align well their AIMD simulations. Despite the plethora of studies on the behaviour of Turbo Grignard there is still a call by the authors to further investigate the fragmentation of  $\text{Li}:\text{Mg}:\text{X}$  clusters as a function of the alkyl substituent, the halide used and/or the choice of solvent.

These different studies support that the presence of both metals, Mg and Li, is required for the unique reactivity observed for Turbo Grignard reagents. In essence, the high reactivity typically associated with organolithium reagents is paired with the high selectivity of

organomagnesium reagents offering a synergic type of bimetallic species capable of facile magnesium/halogen exchange under more user-friendly conditions.

### 1.3.3 Alkali-Metal Mediated Cooperative Bimetallic Chemistry

The first example of an alkali-metal zincate dates back to 1859 when Wanklyn reported the formation of the mixed sodium/zinc trisalkyl compound  $\text{NaZnEt}_3$ , from the reaction between diethylzinc ( $\text{ZnEt}_2$ ) with sodium metal. In 1951, Wittig later coined the term “ates” for the first time to define such mixed metal species when evaluating the reactivity of  $\text{PhLi}$  vs  $\text{LiMgPh}_3$  for the arylation of alpha-beta unsaturated ketones.<sup>50</sup> Pioneering work from Weiss followed, with structural studies elucidating the structures of many alkali metal magnesiates and zincates such as  $[(\text{PMDETA})\text{Li}_2\text{MgPh}_4]$ <sup>51</sup> and  $[\text{Li}_2\text{ZnMe}_4]$ .<sup>52</sup> Thus, molecular structures of the form  $\text{AMM}'_2\text{R}_4$  ( $\text{AM} = \text{Li, Na, K; M} = \text{Mg, Zn...}$ ) are commonly referred to as “Weiss motifs”.<sup>53</sup> Since these important landmarks, alkali-metal magnesiates and zincates have found widespread applications in organic synthesis, particularly in cornerstone transformations such as metal-halogen exchange or deprotonative metalation.<sup>15,31,54</sup> Mechanistic investigations which combine the isolation of key reaction intermediates with DFT calculations have attributed the special reactivity profiles of these heterobimetallic reagents to their bimetallic communication between their two different metals. Typically, the high reactivity of a group 1 alkali metal (e.g., Li, Na, K) organometallic is paired with the high selectivity of a less electropositive metal (e.g., Mg, Zn, Al) often in the presence of Lewis donor ligands to afford soluble, monomeric and highly reactive bimetallic ate compounds (Figure 8). The ligand set is often comprised of alkyl, amide, alkoxide or aryl groups leading to homoleptic or heteroleptic mixed metal species. A 1:1 ratio of alkali metal ( $\text{AM}$ ) to the lower polarity metal ( $\text{M}'$ ) affords a ‘lower order’ species of the form  $\text{AMMR}_3$ , formally a monoanionic ate. This ratio can be increased to a 2:1 mixture giving rise to ‘higher order’ ates of the form  $\text{AMM}'_2\text{R}_4$  formally dianionic ates and typically the more reactive of the two. The subject of many in-depth reviews,<sup>15,55–58</sup> alkali-metal mediated processes involving cooperative heterobimetallics has found its use in a variety of synthetic transformations such as deprotonative metalation, metal/halogen exchange and is now increasingly used in catalytic protocols.<sup>59,60</sup> Not exclusive to main group metals, our group has recently developed a host of bimetallic ate complexes pairing alkali metals with earth abundant transition metals such as Fe, Co and Ni.<sup>61–63</sup>

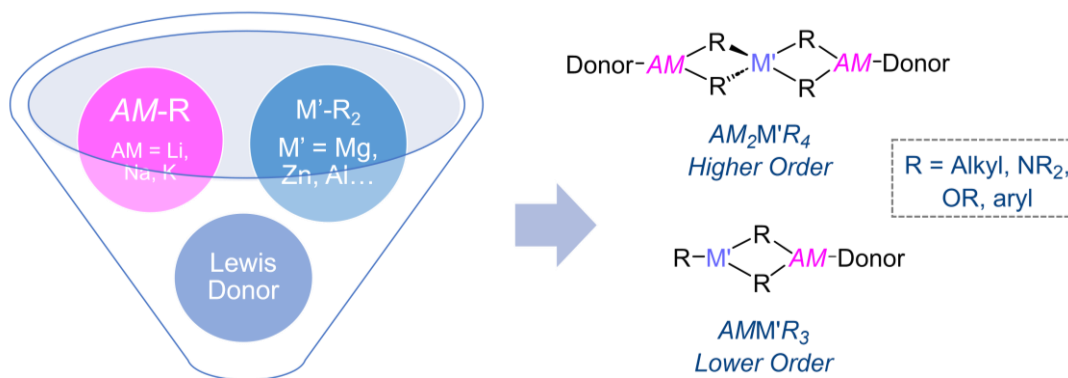
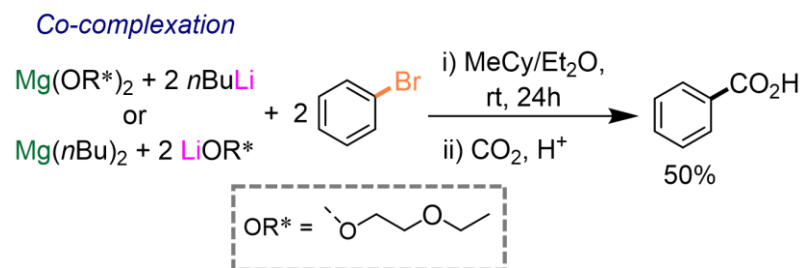


**Figure 8.** General formation of lower order and higher order heterobimetallic ates

### 1.3.4 Alkali-Metal Alkoxide Additives in Mg/halogen Exchange

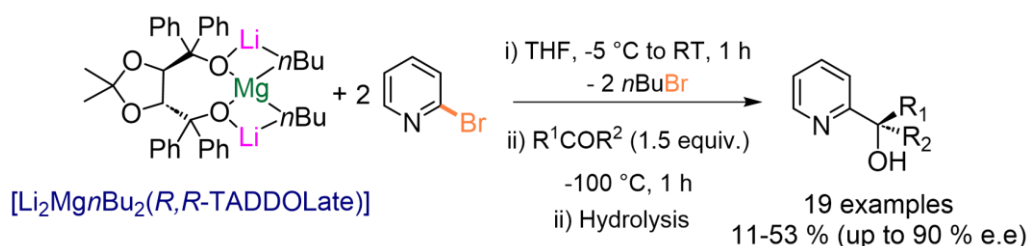
Shifting our focus to alkali-metal alkoxide additives in these heterobimetallic systems, they have been used primarily in metal/halogen exchange processes. Within Group 1/Group 2 bimetallic combinations, early work by Screttas showed that the addition of magnesium alkoxides to alkyl/aryl sodium (or potassium) compounds induces the solubilisation of the heavier alkali organyl in non-polar solvents, a benefit attributed to the formation of mixed-metal aggregates.<sup>64-68</sup> For example, the dissolution of PhNa is achieved by the addition of a soluble magnesium alkoxide (magnesium 2-ethoxyethoxide,  $\text{Mg}(\text{O}(\text{CH}_2)_2\text{OEt})_2$  or  $\text{Mg}(\text{OR}^*)_2$ ; ( $\text{R}^* = (\text{CH}_2)_2\text{OEt}$ ) which was shown to act like a magnesium containing superbase by the deprotonation of toluene. Screttas demonstrated that these mixtures could also be reached by the co-complexation of  $\text{MgPh}_2$  and the corresponding  $\text{NaOR}^*$ . Spectroscopic studies suggested the formation of higher order sodium magnesiate  $[\text{Na}_2\text{MgPh}_2(\text{OR}^*)_2]$  leading to this synergistic reactivity.<sup>64,66</sup> A similar study employing  $\text{Mg}(\text{OR}^*)_2$  in combination with two equivalents of  $n\text{BuLi}$  led to the remarkable metal/halogen exchange of bromobenzene at room temperature in a mixture of methylcyclohexane (MeCy)/diethyl ether ( $\text{Et}_2\text{O}$ ) (Scheme 7).<sup>69,70</sup> The authors point to the formation of a mixed alkyl/alkoxy lithium magnesiate, however they were unable to accurately deduce the active exchange reagent or indeed confirm which metal had actually carried out the metal/halogen exchange. The subsequent studies herein suggest this was indeed a Mg/Br exchange, not a Li/Br exchange, although this was unclear at the time.



**Scheme 7.** Room temperature metal/halogen exchange of bromobenzene using  $n\text{BuLi}$  in combination with a soluble magnesium alkoxide  $\text{Mg(OR}^*)$  ( $\text{OR}^* = (\text{O}(\text{CH}_2)_2\text{OEt})$ )

Richey reported a similar enhancement of the reactivity of  $\text{Et}_2\text{Mg}$  towards bromobenzene using various AM-OR additives more commonly used in organic synthesis such as  $\text{LiOtBu}$ ,  $\text{NaOMe}$ ,  $\text{KOMe}$  or  $\text{KOPh}$ .<sup>71</sup> Dialkylmagnesium reagents such as  $\text{Et}_2\text{Mg}$  are typically inert towards such substrates, yet Richey realised an almost quantitative Mg/Br exchange of bromo and iodobenzene using a mixture of  $\text{Et}_2\text{Mg}$  with the aforementioned AM-OR additives. The special reactivity of these mixtures described by Screttas and Richey is attributed to the formation of mixed alkyl/alkoxy alkali-metal magnesiate however information on the exact constitution of these mixtures remained scarce.

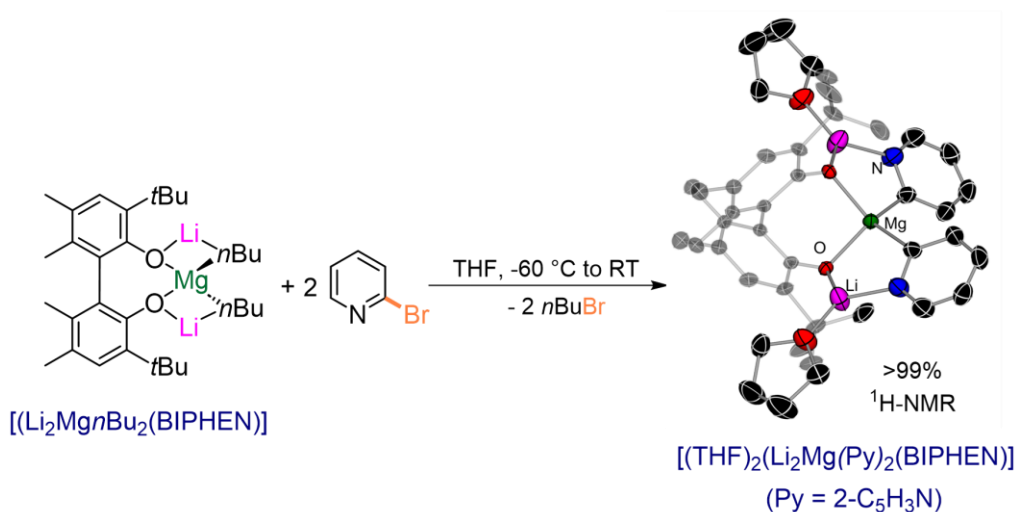
Later, Gros and Mongin developed more sophisticated systems using AM-OR additives for asymmetric synthesis via Mg/halogen exchange. Treatment of higher order tetra(alkyl)  $\text{Li}_2\text{MgnBu}_4$  with one equivalent of the chiral diol R,R-TADDOL (TADDOL= $\alpha,\alpha,\alpha,\alpha$ -tetraaryl-1,3-dioxolane-4,5-dimethanol, aryl =  $\text{C}_6\text{H}_5$ ), led to the proposed formation of chiral lithium magnesiate  $[\text{Li}_2\text{MgnBu}_2(\text{R,R-TADDOLate})]$ . Bromo and iodopyridines were found to undergo Mg/halogen exchange with this alkyl/alkoxy lithium magnesiate in THF under mild conditions and were subsequently added to aldehydes at  $-100^\circ\text{C}$  to give enantioenriched pyridylcarbinols in moderate yields (11-53%, up to 90% e.e) (Scheme 8).<sup>72</sup>



**Scheme 8.** Mg/Br exchange of bromopyridines by  $[\text{Li}_2\text{MgnBu}_2(\text{R,R-TADDOLate})]$

O'Hara was able to shed some light on the constitution of the lithium magnesiate species responsible for these Mg/halogen exchange of such bromopyridines and the metalated intermediates formed post magnesiation.<sup>73</sup> Using a racemic version of  $\text{Li}_2$ -(rac)-BIPHEN (di)alkoxide in combination with  $n\text{Bu}_2\text{Mg}$  the mixed alkyl/alkoxy magnesiate  $[\text{Li}_2\text{MgnBu}_2((\text{rac})\text{-BIPHEN})\cdot(\text{THF})_3]$  (BIPHEN- $\text{H}_2=5,5',6,6'$ -tetramethyl-3,3'-di-tert-butyl-

1,1'-biphenyl-2,2'-diol) could be crystallographically characterised (Scheme 9). Exhibiting a distorted tetrahedral geometry, the Mg centre is bound to both (*rac*)-BIPHEN oxygen atoms and two butyl groups. Both lithium atoms form contacts between an oxygen centre and a butyl group whilst their coordination sphere is satisfied by THF. NMR spectroscopic studies seemed to suggest this bimetallic motif is retained in solution. Treatment of this lithium magnesiate with two equivalents of 2-bromopyridine and structurally mapping the reaction afforded the replacement of the two butyl groups attached to Mg with two pyridyl moieties post Mg/Br exchange forming  $[(\text{THF})_2\text{Li}_2\text{Mg}(\text{Py})_2(\text{BIPHEN})]$  (Scheme 9). Notably, the pyridyl-nitrogens coordinate the lithium cations providing some information towards the stability of these metalated intermediates in solution. Despite an isolated crystalline yield of 47% for this metalated intermediate,  $^1\text{H-NMR}$  spectroscopy confirms a quantitative Mg/Br exchange.

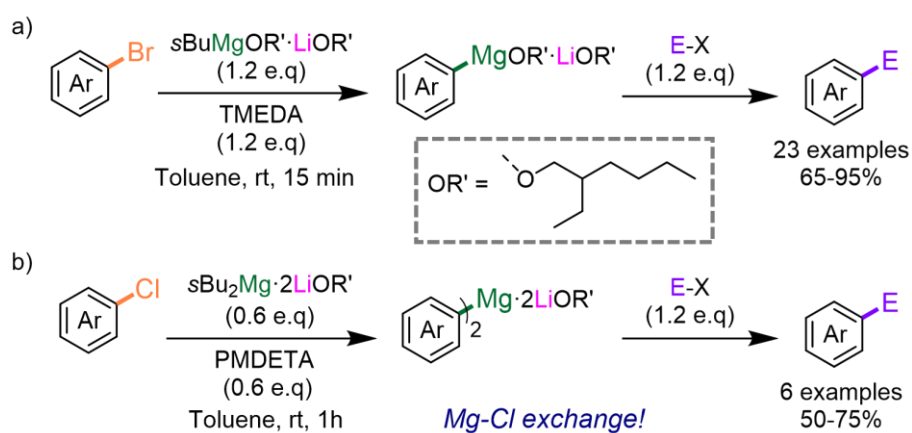


**Scheme 9.** Quantitative Mg/Br exchange of 2-bromopyridine with  $[(\text{Li}_2\text{Mg}n\text{Bu}_2(\text{BIPHEN}))]$  forming  $[(\text{THF})_2\text{Li}_2\text{Mg}(\text{Py})_2(\text{BIPHEN})]$ . Molecular structure of  $[(\text{THF})_2\text{Li}_2\text{Mg}(\text{Py})_2(\text{BIPHEN})]$  with displacement ellipsoids at 50% probability and all hydrogen atoms omitted for clarity

Harnessing the synthetic utility of lithium alkoxide additives in Mg/halogen exchange, Knochel demonstrated the formation of a powerful exchange reagent of the form  $s\text{BuMg}(\text{OR}')\cdot\text{LiOR}'$  ( $\text{OR}' = 2\text{-ethylhexyl}$ ) for the *in-situ* generation of a wide range of aryl and hetero-aryl magnesiates in toluene. The lipophilic nature of the long chain alkoxide additive, derived from 2-ethylhexanol, allows for solubility of the magnesiated intermediates in toluene in comparison to Turbo Grignard reagents which require an ethereal solvent for solubility and efficient reactivity. Such magnesium intermediates were initially described by Knochel as  $\text{ArMg}(\text{OR}')\cdot\text{LiOR}'$  and were found to react efficiently with different electrophiles such as aldehydes, ketones and allyl bromides whilst also participating in Kumada and Negishi (via transmetalation with  $\text{ZnCl}_2$ ) Pd-catalysed cross-couplings with aryl bromides/chlorides forming more value added products (Scheme 10a).<sup>74</sup> Interestingly, this alkoxide mediated Mg/halogen exchange approach was found to be significantly faster than when using Turbo



Grignard reagents (up to 110 times faster) delivering quantitative Mg/Br exchange of bromoarenes in just 15 minutes at ambient temperature. Indeed, solvent effects proved to be prominent in these systems as a switch to THF from toluene drastically diminishes the extent of Mg/halogen exchange of the alkoxide containing reagents. An even more powerful exchange reagent containing two reactive alkyl ligands could be accessed in the form of  $s\text{Bu}_2\text{Mg}\cdot 2\text{LiOR}'$ , upgrading these systems to perform the notoriously challenging Mg/Cl exchange in the presence of Lewis donor PMDETA (Scheme 10b).<sup>74</sup> Knochel proposed the formation of higher order *bis*-aryl magnesiate intermediates via an atom economical Mg/Cl exchange which were then quenched with various electrophiles. Although the appeal of these mixed-metal/mixed-ligand exchange reagents to a synthetic chemist is clear, there is much ambiguity attached to the nature and the constitution of the exchange reagent and metalated intermediates formed post Mg/Br exchange which will be examined in depth in *Chapter 2*.

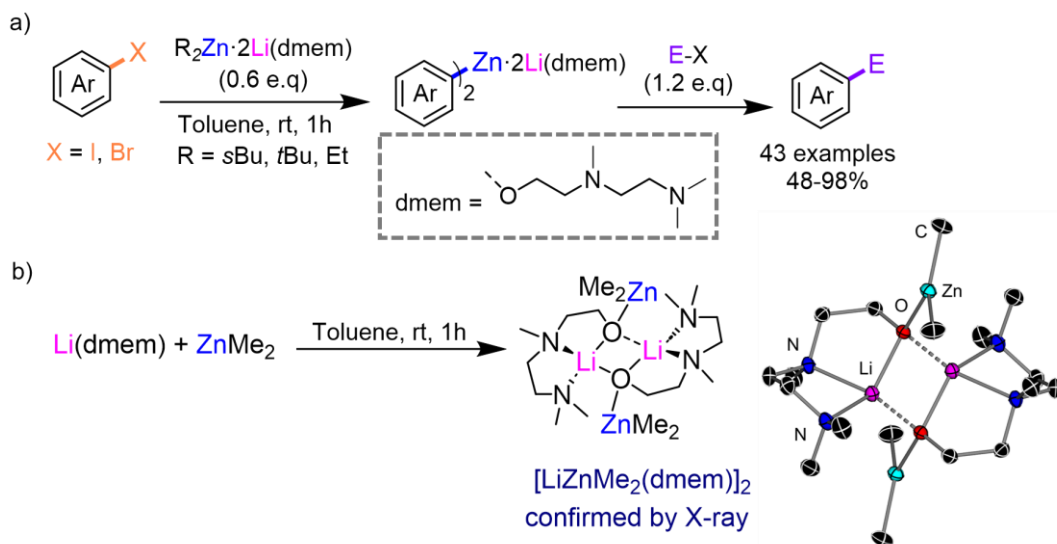


**Scheme 10.** a) Mg/Br exchange in toluene under ambient conditions promoted by soluble  $s\text{BuMg}(\text{OR}')\cdot\text{LiOR}'$  and  $s\text{Bu}_2\text{Mg}\cdot 2\text{LiOR}'$  (OR' = 2-ethylhexyl)

### 1.3.5 Lithium Alkoxide Additives in Zn/halogen Exchange

Knochel has successfully evolved this chemistry to encompass Zn/I and Zn/Br exchange processes through the activation of dialkylzinc reagents with lithium alkoxide additives.<sup>75</sup> Interestingly, when N-donor atoms were included in the alcohol chain, with 2-[[2-(dimethylamino)ethyl]methylamino]ethanol ((H)dmem) containing two N-coordination sites, the reactivity of  $\text{R}_2\text{Zn}\cdot 2\text{LiOR}$  towards iodoarenes is greatly enhanced. Demonstrating the synthetic utility of these systems, the proposed *bis*-aryl zincated intermediates were shown to participate directly in Negishi cross-coupling reactions or react with other electrophiles providing an extensive substrate scope (Scheme 11a). Substrates containing highly sensitive functional groups (e.g.,  $\text{NO}_2$ , CN), often problematic using polar organometallic reagents, are tolerated in this system providing a complementary substrate scope to the aforementioned

$s\text{Bu}_2\text{Mg}\cdot 2\text{LiOR}'$  ( $\text{OR}' = 2\text{-ethylhexyl}$ ) exchange reagent. In collaboration with the Knochel group, studies within our group demonstrated that two equivalents of  $\text{Li}(\text{dmem})$  alkoxide were needed to activate the dialkylzinc species towards Zn/halogen exchange. For example, whilst  $\text{ZnEt}_2$  was completely inert towards two equivalents of 2-iodoanisole and the addition of one equivalent of  $\text{Li}(\text{dmem})$  gave a conversion of just 23% after ten minutes at room temperature, the addition of two equivalents of  $\text{Li}(\text{dmem})$  gave an almost quantitative conversion (95%) under the same conditions. Detailed spectroscopic studies, including  $^1\text{H}$ -DOSY studies, suggested the formation of a higher order mixed alkyl/alkoxy lithium zincate,  $[\text{Li}_2\text{Zn}s\text{Bu}_2(\text{dmem})_2]$  upon co-complexation of  $s\text{Bu}_2\text{Zn}$  and two equivalents of  $\text{Li}(\text{dmem})$ .<sup>75</sup> Although such a species could not be structurally authenticated, the formation of mixed alkyl/alkoxy zincates was confirmed by the isolation of dimeric  $[\text{LiZnMe}_2(\text{dmem})]_2$ ; a related lower order lithium zincate (Scheme 11b). Notably, this structure encapsulates the intramolecular stabilisation of Li by the *N*-donor atoms present in the alkoxide chain. This special coordination to Li can perhaps help to explain the overall stability of the system and the marked alkoxide effect observed when longer chain alkoxides are used in absence of Lewis donors as one could expect a higher aggregation of the lithium zincates forming less reactive oligomers. As expected, addition of a second equivalent of alkoxide to  $[\text{LiZnMe}_2(\text{dmem})]_2$  greatly enhances the reactivity of this system towards Zn/I exchange consistent with the formation of higher order lithium zincates in solution.



**Scheme 11.** a) Zn/halogen exchange of bromo and iodoarenes with  $\text{R}_2\text{Zn}\cdot 2\text{Li}(\text{dmem})$  exchange reagent and subsequent reaction with electrophiles b) Co-complexation of  $\text{Li}(\text{dmem})$  and  $\text{ZnMe}_2$  forming of  $[\text{LiZnMe}_2(\text{dmem})]_2$  and molecular structure of  $[\text{LiZnMe}_2(\text{dmem})]_2$  with displacement ellipsoids at 50% probability and all hydrogen atoms omitted for clarity

## **1.4 Aims of the Thesis**

Broadly, this thesis aims to gain a deeper understanding into the role played by alkali-metal alkoxides additives in the activation of dialkylmagnesium (*Chapters 2 and 3*) and bis-amidozinc reagents (*Chapters 4 and 5*). Combining NMR spectroscopic and X-Ray crystallographic techniques, each chapter looks to meticulously analyse the constitution of such heterobimetallic mixtures and the reaction pathways in operation with respect to two cornerstone reactions in organic synthesis: metal/halogen exchange (*Chapters 2 and 3*) and deprotonative metalation (*Chapters 4 and 5*). The results presented hereafter highlight the synthetic utility of such mixed-metal/mixed ligand systems whilst calling attention to the complexity induced by alkali-metal alkoxides.

## 1.5 References

- 1 D. Caine, in *Encyclopedia of Reagents for Organic Synthesis*, John Wiley & Sons, Ltd, Chichester, UK, 2006.
- 2 D. E. Pearson, C. A. Buehler, C. Michael and D. Stobbe, *Chem. Rev.*, 1973, **74**, 45–86.
- 3 J. Madasu, S. Shinde, R. Das, S. Patel and A. Shard, *Org. Biomol. Chem.*, 2020, **18**, 8346–8365.
- 4 V. Hardouin Duparc, R. M. Shakaroun, M. Slawinski, J.-F. Carpentier and S. M. Guillaume, *Eur. Polym. J.*, 2020, **134**, 109858.
- 5 R. M. Kissling and M. R. Gagné, *J. Org. Chem.*, 2001, **66**, 9005–9010.
- 6 S. Zhou, G. M. Anderson, B. Mondal, E. Doni, V. Ironmonger, M. Kranz, T. Tuttle and J. A. Murphy, *Chem. Sci.*, 2014, **5**, 476–482.
- 7 C. Sun and Z. Shi, *Chem. Rev.*, 2014, **114**, 9219–9280.
- 8 A. A. Morton, F. D. Marsh, R. D. Coombs, A. L. Lyons, S. E. Penner, H. E. Ramsden, V. B. Baker, E. L. Little and R. L. Letsinger, *J. Am. Chem. Soc.*, 1950, **72**, 3785–3792.
- 9 H. L. Hsieh and C. F. Wofford, *J. Polym. Sci. Part A-1 Polym. Chem.*, 1969, **7**, 449–460.
- 10 L. Lochmann and M. Janata, *Cent. Eur. J. Chem.*, 2014, **12**, 537–548.
- 11 L. J. Bole and E. Hevia, *Nat. Synth.*, 2022, **1**, 195–202.
- 12 L. Lochmann, J. Pospíšil and D. Lím, *Tetrahedron Lett.*, 1966, **7**, 257–262.
- 13 M. Schlosser, *J. Organomet. Chem.*, 1967, **8**, 9–16.
- 14 M. Schlosser and S. Strunk, *Tetrahedron Lett.*, 1984, **25**, 741–744.
- 15 S. D. Robertson, M. Uzelac and R. E. Mulvey, *Chem. Rev.*, 2019, **119**, 8332–8405.
- 16 G. Katsoulos, S. Takagishi and M. Schlosser, *Synlett*, 1991, **1991**, 731–732.
- 17 V. Snieckus, *Chem. Rev.*, 1990, **90**, 879–933.
- 18 M. C. Whisler, S. MacNeil, V. Snieckus and P. Beak, *Angew. Chem. Int. Ed.*, 2004, **43**, 2206–2225.

- 19 P. Fleming and D. F. O'Shea, *J. Am. Chem. Soc.*, 2011, **133**, 1698–1701.
- 20 A. Manvar, P. Fleming and D. F. O'Shea, *J. Org. Chem.*, 2015, **80**, 8727–8738.
- 21 Y. Yamashita, H. Suzuki, I. Sato, T. Hirata and S. Kobayashi, *Angew. Chem. Int. Ed.*, 2018, **57**, 6896–6900.
- 22 M. Marsch, K. Harms, L. Lochmann and G. Boche, *Angew. Chemie Int. Ed. English*, 1990, **29**, 308–309.
- 23 W. Bauer and L. Lochmann, *J. Am. Chem. Soc.*, 1992, **114**, 7482–7489.
- 24 S. Harder and A. Streitwieser, *Angew. Chemie Int. Ed. English*, 1993, **32**, 1066–1068.
- 25 C. Unkelbach, D. F. O'Shea and C. Strohmman, *Angew. Chem. Int. Ed.*, 2014, **53**, 553–556.
- 26 P. Benrath, M. Kaiser, T. Limbach, M. Mondeshki and J. Klett, *Angew. Chem. Int. Ed.*, 2016, **55**, 10886–10889.
- 27 W. Clegg, A. M. Drummond, S. T. Liddle, E. Mulvey and A. Robertson, *Chem. Commun.*, 1999, 1569–1570.
- 28 J. Klett, *Chem. – A Eur. J.*, 2021, **27**, 888–904.
- 29 R. L. Bebb and H. Gilman, *J. Am. Chem. Soc.*, 1939, **61**, 106–109.
- 30 G. Wittig, U. Pockels and H. Dröge, *Berichte der Dtsch. Chem. Gesellschaft (A B Ser.)*, 1938, **71**, 1903–1912.
- 31 D. Tilly, F. Chevallier, F. Mongin and P. C. Gros, *Chem. Rev.*, 2014, **114**, 1207–1257.
- 32 A. Music and D. Didier, *Synlett*, 2019, **30**, 1843–1849.
- 33 W. Langham, R. Q. Brewster and H. Gilman, *J. Am. Chem. Soc.*, 1941, **63**, 545–549.
- 34 R. E. Mulvey, V. L. Blair, W. Clegg, A. R. Kennedy, J. Klett and L. Russo, *Nat. Chem.*, 2010, **2**, 588–591.
- 35 M. Schlosser, L. Guio and F. Leroux, *J. Am. Chem. Soc.*, 2001, **123**, 3822–3823.
- 36 B. D. E. Applequist, D. F. O. Brien and D. F. O. Brien, *J. Am. Chem. Soc.*, 1963, **85**, 743–748.
- 37 E. Martin, D. L. Hughes and S. J. Lancaster, *Inorg. Chim. Acta.*, 2010, **363**, 275–278.
- 38 P. Knochel, W. Dohle, N. Gommermann, F. F. Kneisel, F. Kopp, T. Korn, I.

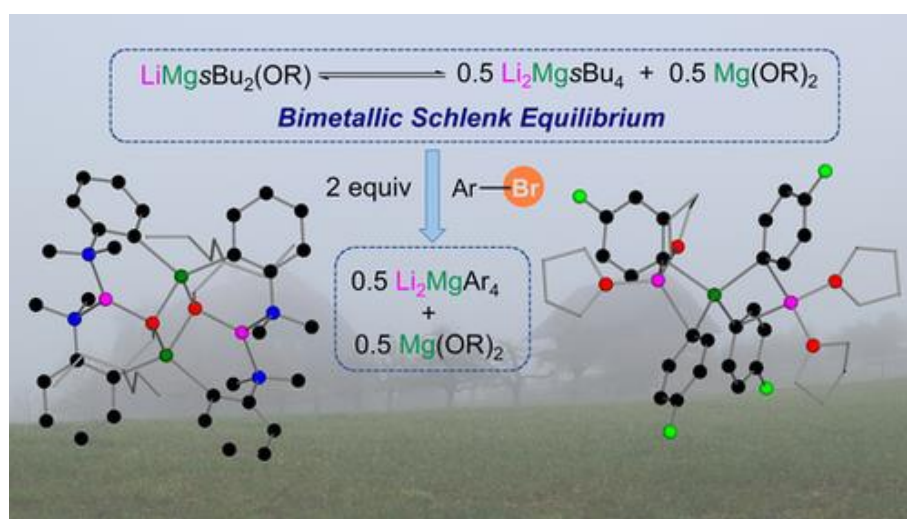
- Sapountzis and V. A. Vu, *Angew. Chem. Int. Ed.*, 2003, **42**, 4302–4320.
- 39 I. Sapountzis and P. Knochel, *Angew. Chem. Int. Ed.*, 2002, **41**, 1610–1611.
- 40 A. Krasovskiy and P. Knochel, *Angew. Chem. Int. Ed.*, 2004, **43**, 3333–3336.
- 41 D. S. Ziegler, B. Wei and P. Knochel, *Chem. Eur. J.*, 2019, **25**, 2695–2703.
- 42 A. Krasovskiy, B. F. Straub and P. Knochel, *Angew. Chem. Int. Ed.*, 2006, **45**, 159–162.
- 43 R. Neufeld, T. L. Teuteberg, R. Herbst-Irmer, R. A. Mata and D. Stalke, *J. Am. Chem. Soc.*, 2016, **138**, 4796–4806.
- 44 R. Neufeld and D. Stalke, *Chem. Eur. J.*, 2016, **22**, 12624–12628.
- 45 P. García-Álvarez, D. V. Graham, E. Hevia, A. R. Kennedy, J. Klett, R. E. Mulvey, C. T. O’Hara and S. Weatherstone, *Angew. Chemie*, 2008, **120**, 8199–8201.
- 46 A. Hermann, R. Seymen, L. Brieger, J. Kleinheider, B. Grabe, W. Hiller and C. Strohmann, *Angew. Chem. Int. Ed.*, 2023, **62**, 4–8.
- 47 R. M. Peltzer, O. Eisenstein, A. Nova and M. Cascella, *J. Phys. Chem. B*, 2017, **121**, 4226–4237.
- 48 R. M. Peltzer, J. Gauss, O. Eisenstein and M. Cascella, *J. Am. Chem. Soc.*, 2020, **142**, 2984–2994.
- 49 M. de Giovanetti, S. H. Hopen Eliasson, A. C. Castro, O. Eisenstein and M. Cascella, *J. Am. Chem. Soc.*, 2023, **145**, 16305–16309.
- 50 G. Wittig, F. J. Meyer and G. Lange, *Justus Liebigs Ann. Chem.*, 1951, **571**, 167–201.
- 51 T. Greiser, J. Kopf, D. Thoennes and E. Weiss, *Chem. Ber.*, 1981, **114**, 209–213.
- 52 E. Weiss and R. Wolfrum, *Chem. Ber.*, 1968, **101**, 35–40.
- 53 E. Weiss, *Angew. Chemie Int. Ed. English*, 1993, **32**, 1501–1523.
- 54 R. E. Mulvey, F. Mongin, M. Uchiyama and Y. Kondo, *Angew. Chem. Int. Ed.*, 2007, **46**, 3802–3824.
- 55 A. Harrison-Marchand and F. Mongin, *Chem. Rev.*, 2013, **113**, 7470–7562.
- 56 F. Mongin and A. Harrison-Marchand, *Chem. Rev.*, 2013, **113**, 7563–7727.
- 57 T. X. Gentner and R. E. Mulvey, *Angew. Chem. Int. Ed.*, 2021, **60**, 9247–9262.
- 58 R. E. Mulvey, *Acc. Chem. Res.*, 2009, **42**, 743–755.

- 59 J. M. Gil-Negrete and E. Hevia, *Chem. Sci.*, 2021, 1982–1992.
- 60 A. M. Borys and E. Hevia, *Trends Chem.*, 2021, **3**, 803–806.
- 61 L. C. H. Maddock, T. Nixon, A. R. Kennedy, M. R. Probert, W. Clegg and E. Hevia, *Angew. Chem. Int. Ed.*, 2018, **57**, 187–191.
- 62 A. Logallo, M. Mu, M. García-Melchor and E. Hevia, *Angew. Chem. Int. Ed.*, , DOI:10.1002/anie.202213246.
- 63 A. M. Borys and E. Hevia, *Angew. Chem. Int. Ed.*, 2021, **60**, 24659–24667.
- 64 C. G. Screttas and M. Micha-Screttas, *Organometallics*, 1984, **3**, 904–907.
- 65 C. G. Screttas and M. Micha-Screttas, *J. Organomet. Chem.*, 1986, **316**, 1–12.
- 66 C. G. Screttas and M. Micha-Screttas, *J. Organomet. Chem.*, 1985, **290**, 1–13.
- 67 C. G. Screttas and B. R. Steele, *J. Org. Chem.*, 1988, **53**, 5151–5153.
- 68 C. G. Screttas and B. R. Steele, *J. Org. Chem.*, 1989, **54**, 1013–1017.
- 69 M. Micha-Screttas, C. G. Screttas, B. R. Steele and G. A. Heropoulos, *Tetrahedron Lett.*, 2002, **43**, 4871–4873.
- 70 C. S. Salteris, I. D. Kostas, M. Micha-Screttas, B. R. Steele, G. A. Heropoulos, C. G. Screttas and A. Terzis, *J. Organomet. Chem.*, 1999, **590**, 63–70.
- 71 E. M. Hanawalt, J. Farkas and H. G. Richey, *Organometallics*, 2004, **23**, 416–422.
- 72 D. Catel, O. Payen, F. Chevallier, F. Mongin and P. C. Gros, *Tetrahedron*, 2012, **68**, 4018–4028.
- 73 J. Francos, P. C. Gros, A. R. Kennedy and C. T. O’Hara, *Organometallics*, 2015, **34**, 2550–2557.
- 74 D. S. Ziegler, K. Karaghiosoff and P. Knochel, *Angew. Chem. Int. Ed.*, 2018, **57**, 6701–6704.
- 75 M. Balkenhohl, D. S. Ziegler, A. Desaintjean, L. J. Bole, A. R. Kennedy, E. Hevia and P. Knochel, *Angew. Chem. Int. Ed.*, 2019, **58**, 12898–12902.

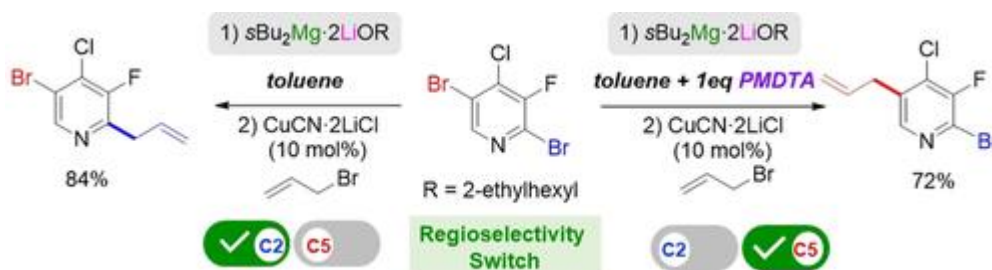
## Chapter 2: Untangling the Complexity of Lithium/Magnesium Alkyl/Alkoxy Combinations Utilised in Mg/Br Exchange

This Chapter is adapted from the following two publications in peer reviewed journals:

- 1) *Untangling the Complexity of Lithium/Magnesium Alkyl/Alkoxy Combinations utilized in Mg/Br Exchange*, L. J. Bole, **N. R. Judge**, and E. Hevia, *Angew. Chem. Int. Ed.*, **2021**, 60, 7626.



- 2) *Regioselective Bromine/Magnesium Exchange for the Selective Functionalization of Polyhalogenated Arenes and Heterocycles*, A. Desaintjean, T. Haupt, L. J. Bole, **N. R. Judge**, E. Hevia and P. Knochel, *Angew. Chem. Int. Ed.*, **2021**, 60, 1513.



This work was carried out in collaboration with the group of Prof. Paul Knochel. Initial reaction optimisation, substrate scope and electrophilic functionalisation were carried out by two PhD students from the Knochel group: Alexandre Desaintjean and Tobias Haupt (Ludwig-Maximilians-Universität, München, Department Chemie) and are not included in this Thesis but are referenced.



Contributing authors to the manuscript and their role:

Leonie J. Bole: Led the project and provided supervision to Neil Judge and conducted synthesis and characterisation of compounds **1a** and **5** included in this *Chapter*. Performed majority of NMR spectroscopic experiments into constitution of exchange reagent. Wrote the first draft of the manuscript and parts of the Supporting Information.

Neil Judge: Synthesis and characterisation of compounds **1b**, **2a-b** and **6** and related NMR spectroscopic investigations. Performed all GC reaction monitoring studies. Performed studies relating to interconversions between **6** and **1a**. Aided in the writing of the manuscript and Supporting Information.

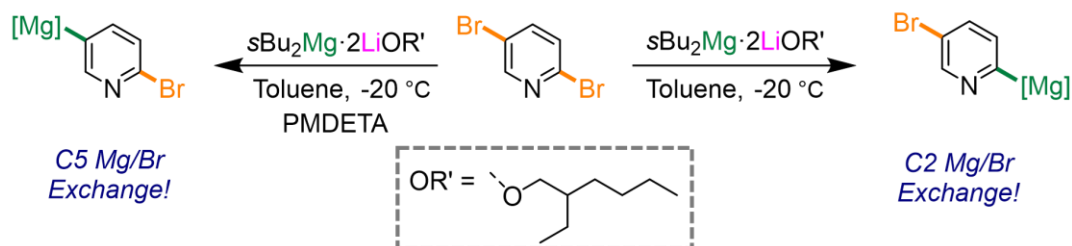
Eva Hevia: Principal Investigator, conceived the project, secured the funding, directed the work, and revised the final version of the manuscript with contributions from all authors.

## 2.1 Introduction

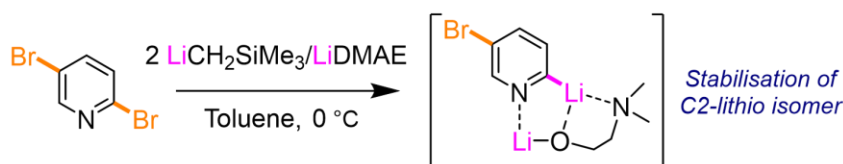
As outlined in *Chapter 1* the addition of AM-OR additives to dialkylmagnesium reagents can greatly enhance their ability to undergo Mg/halogen exchange under ambient conditions (see *Chapter 1*, **section 1.3.4**).<sup>1-4</sup> Epitomised by Knochel's incredibly powerful exchange reagent  $s\text{Bu}_2\text{Mg}\cdot 2\text{LiOR}'$  (OR' = 2-ethylhexyl), such mixed alkyl/alkoxy lithium magnesiates were able to perform not only Mg/Br exchange but also the challenging Mg/Cl exchange forming a wide range of polyfunctionalised aryl and hetero-aryl magnesiates.<sup>5</sup> In his initial report Knochel proposed the formation of higher order lithium magnesiates of the form  $[\text{Li}_2\text{Mg}(s\text{Bu})_2(\text{OR}')_2]$  as the active exchange reagent in  $s\text{Bu}_2\text{Mg}\cdot 2\text{LiOR}'$ , however this possibility was not structurally or spectroscopically investigated.<sup>2</sup> Recent developments by the Knochel group have successfully employed this reagent in toluene for the regioselective Mg/halogen exchange of polyhalogenated aromatics and heterocycles.<sup>6</sup> Assessing the role of Lewis donor additives revealed that the addition of *N,N,N',N'',N''*-pentamethyldiethylenetriamine (PMDETA) can finely tune the regioselectivity of Mg/Br exchange. For example, treatment of 2,5-dibromopyridine with  $s\text{Bu}_2\text{Mg}\cdot 2\text{LiOR}'$  in toluene afforded the quantitative Mg/Br exchange in the C2 position of the aromatic heterocycle (Scheme 1a). However, the addition of PMDETA results in a regioselectivity switch to exclusively perform the Mg/Br exchange in the C5 position. Previous reports using organolithium reagents have demonstrated the kinetically favoured C2-lithiated isomer rapidly isomerises to the more thermodynamically stable C5-lithiated product.<sup>7,8</sup> Gros has elegantly shown that this isomerisation can be thwarted and the kinetically favoured C2 regioselectivity retained by the addition of lithium aminoalkoxide (LiDMAE) (DMAE =  $\text{O}(\text{CH}_2)_2\text{NMe}_2$ ).<sup>9</sup> The authors propose a stabilisation of the 2-lithio-bromopyridine intermediates by chelation and stabilisation of the Li atom by the lithium alkoxide additive (Scheme 1b), although this

pyridyl/alkoxy lithium adduct could not be isolated and structurally characterised. Initial thoughts from Knochel suggested the perceived regioselectivity switch using  $s\text{Bu}_2\text{Mg}\cdot 2\text{LiOR}'$  in the presence of PMDETA results from the Lewis donor providing coordinative saturation of the Li centres preventing an initial coordination of the pyridyl nitrogen to the metal centres (vital for C2 Mg/Br exchange) thus favouring the Mg/Br exchange in the C5 position.

a) *Knochel, 2021*



b) *Gros, 2008*



**Scheme 1. a)** Regioselective Mg/Br exchange of 2,5-dibromopyridine using  $s\text{Bu}_2\text{Mg}\cdot 2\text{LiOR}'$  (OR' = 2-ethylhexyl) in the presence and absence of PMDETA b) Proposed stabilisation of 2-lithio-bromopyridines by LiDMAE (DMAE =  $\text{O}(\text{CH}_2)_2\text{NMe}_2$ )

## 2.2 Aims

This *Chapter* looks to provide an in-depth analysis on the constitution and reactivity pathways involved in the mixed alkyl/alkoxy lithium magnesiate exchange reagent  $s\text{Bu}_2\text{Mg}\cdot 2\text{LiOR}'$  used by Knochel. By using detailed NMR spectroscopic and X-ray crystallographic techniques we aim to examine the formation of the proposed bimetallic exchange reagent and reveal the nature of the metalated intermediates post Mg/halogen exchange. As highlighted in *Chapter 1*, the addition of alkali metal alkoxides to various other Group 1/Group 2 organometallic compounds can result in a high level of complexity of the mixed metal aggregates formed in solution and in the solid state. Thus, we find it both intriguing and important to shed some light on this powerful exchange reagent and its unique reactivity.

## 2.3 Results and Discussion

### 2.3.1 Assessing the Reactivity of Different Li and Mg Alkyl/Alkoxide Mixtures Towards 2-Bromoanisole

We started our studies examining the reactivity of various Li and Mg mixed alkyl/alkoxide mixtures towards our model substrate 2-bromoanisole (Table 1). Using the originally reported combination of two equivalents of *s*BuLi and one equivalent of the long chain magnesium alkoxide Mg(OR')<sub>2</sub> (OR' = 2-ethylhexyl) in a 2:1 ratio led to the full magnesiumation of two equivalents of 2-bromoanisole after 40 minutes at room temperature (entry 1). The same conversion was observed when mixing *s*Bu<sub>2</sub>Mg with two equivalents of LiOR' (entry 2), hinting at the formation of the same type of active mixed-metal bimetallic species, which contrasts with the almost total lack of reactivity of *s*Bu<sub>2</sub>Mg towards 2-bromoanisole (5% yield, entry 5). Interestingly, 2-bromoanisole can also undergo quantitative Mg/Br exchange when using a 1:1 mixture of *s*Bu<sub>2</sub>Mg and LiOR' (entry 3). Exposing the key role of the alkoxide employed to mediate this transformation, using the relevant chelating lithium alkoxide Li(dmem) derived from 2-[[2-(dimethylamino)ethyl]methylamino]ethanol (dmem(H))<sup>10</sup> only a modest 20% yield of the magnesiumation product was observed. Studies using different combinations of Li and Mg alkoxides also revealed that when 1.5 equivalents of Mg(OR')<sub>2</sub> were added to the initial LiOR'/*s*Bu<sub>2</sub>Mg combination the Mg/Br was totally shutdown (*vide infra*).

**Table 1.** Screening of Mg/Br exchange capabilities of mixed Li and Mg alkyl/alkoxy mixtures

i) Exchange Reagent (1 equiv)  
Toluene, rt, 40 min  
ii) NH<sub>4</sub>Cl

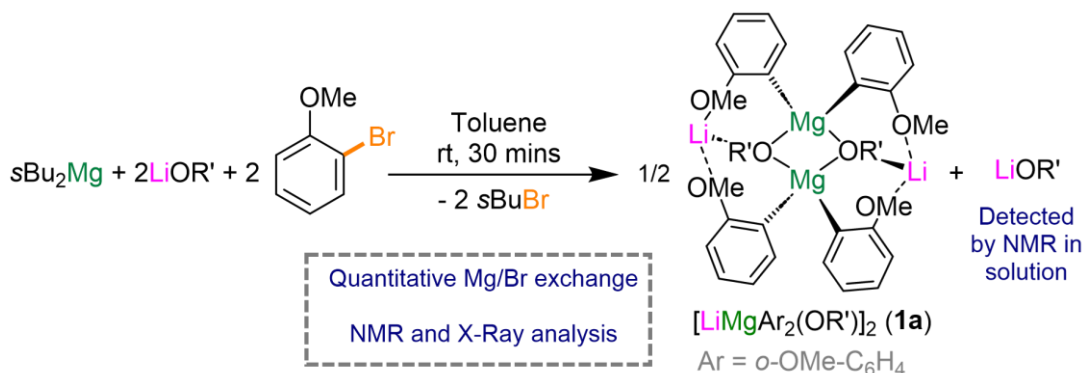
Entry	Exchange reagent <sup>[a]</sup>	Yield [%] <sup>[b]</sup>
1	2 <i>s</i> BuLi + Mg(OR') <sub>2</sub>	99
2	2 LiOR' + <i>s</i> Bu <sub>2</sub> Mg	99
3	LiOR' + <i>s</i> Bu <sub>2</sub> Mg	99
4	Li(dmem) + <i>s</i> Bu <sub>2</sub> Mg	20
5	<i>s</i> Bu <sub>2</sub> Mg	5
6	LiOR' + <i>s</i> Bu <sub>2</sub> Mg + 1.5 Mg(OR') <sub>2</sub>	0

[a] OR' = 2-ethylhexyl and dmem = CH<sub>2</sub>CH<sub>2</sub>N(CH<sub>3</sub>)CH<sub>2</sub>CH<sub>2</sub>N(CH<sub>3</sub>)<sub>2</sub> [b] Yields were determined by GC analysis of reaction aliquots after an aqueous quench using hexamethylbenzene as internal standard. Formation only of anisole and unreacted 2-bromoanisole were the only products observed.

### 2.3.2 Structural and Spectroscopic Analysis of Mg/Br Exchange of 2-Bromoarenes

Taking a deeper look at this reaction, we attempted to examine the constitution of the organometallic intermediates of Mg/Br exchange before electrophilic interception. Two equivalents of 2-bromoanisole were added to a solution of toluene containing *s*Bu<sub>2</sub>Mg and two equivalents of LiOR' and stirred for 30 minutes. A crop of crystals suitable for X-Ray crystallography revealed the formation of a dimeric mixed aryl/alkoxy lithium magnesiate [LiMgAr<sub>2</sub>(OR')]<sub>2</sub> (Ar = *o*-OMe-C<sub>6</sub>H<sub>4</sub>) (**1a**) (Scheme 2) as a product of Mg/Br exchange confirmed by the fact that Mg is now coordinated to the *ortho*-C of two anisyl groups, occupying the position previously filled by a Br atom. Alkoxide bridges complete the Mg coordination sphere. Contrastingly, the Li atom only binds to one OR' ligand, achieving further coordinative stabilisation via two OMe groups from the metalated anisole molecules. This compound was also crystallised by fellow student in the group Leonie J. Bole and is included in her PhD dissertation, and so crystallographic parameters will not be discussed here.<sup>11</sup> NMR spectroscopic analysis confirmed the quantitative formation of lithium magnesiate **1** in-situ with concomitant formation of two equivalents of *s*BuBr as a by-product of the Mg/Br exchange confirming both alkyl ligands are active towards 2-bromoanisole.

Despite employing two equivalents of lithium alkoxide in this reaction just one equivalent of LiOR' is incorporated into the structure of  $[\text{LiMgAr}_2(\text{OR}')_2]_2$  (Ar = *o*-OMe-C<sub>6</sub>H<sub>4</sub>) (**1a**). Indeed, NMR spectroscopic analysis of the mother liquor of **1a** confirmed the presence of a free equivalent of LiOR' in solution, which is also observed monitoring this reaction by *in-situ* <sup>1</sup>H-NMR monitoring.



**Scheme 2.** Mg/Br exchange of 2-bromoanisole confirmed by both X-ray crystallography and NMR spectroscopy forming  $[\text{LiMgAr}_2(\text{OR}')_2]_2$  (**1a**) (Ar = *o*-OMe-C<sub>6</sub>H<sub>4</sub>)

An identical motif is observed carrying out the reaction with 2-bromo-*N,N*-dimethylaniline resulting in the formation of  $[\text{LiMgAr}_2(\text{OR}')_2]_2$  (Ar = 2-NMe<sub>2</sub>-C<sub>6</sub>H<sub>4</sub>) (**1b**) (Figure 1) obtained in a 46% yield as a crystalline solid. <sup>1</sup>H NMR monitoring studies showed that the reaction of two equivalents of 2-bromo-*N,N*-dimethylaniline with a combination of  $s\text{Bu}_2\text{Mg}/2\text{LiOR}'$  led to the quantitative formation of **1b**. Featuring a centrosymmetric four-membered {MgOMgO} ring, each Mg binds to the *ipso* C of two aryl groups, occupying the position previously filled by a Br atom, and two alkoxy bridges. The two C<sub>*ipso*</sub>-Mg bonds have lengths of 2.1519(4) Å (C(9)′-Mg(1)) and 2.2176(4) Å (C(18)-Mg(1)), typical for this type of environment.<sup>12–14</sup> In contrast, each Li coordinates to one alkoxy bridge in addition to two NMe<sub>2</sub> groups. These distinct coordination preferences between Li and Mg generate an unusual ring-fused structure comprising four 6-membered {LiNCCMgO} rings which share their Mg and O vertices forming the central {MgOMgO} ring (Figure 1). The dimeric structures of **1a** and **1b** are retained in solution, even upon addition of bulk THF, demonstrating the robustness of this mixed alkyl/alkoxy aggregate. Lithium magnesiates **1a** and **1b** represent two rare examples of direct insights into the products of alkoxy mediated metal/halogen exchange reactions, with the only other notable exception being O'Hara's aforementioned  $[(\text{THF})_2\text{Li}_2\text{Mg}(\text{Py})_2(\text{BIPHEN})]$  (see Chapter 1, Scheme 9).<sup>7,15</sup>

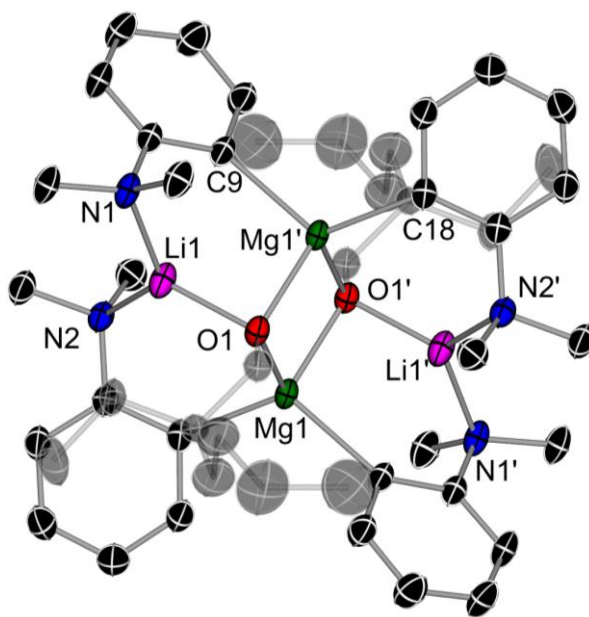
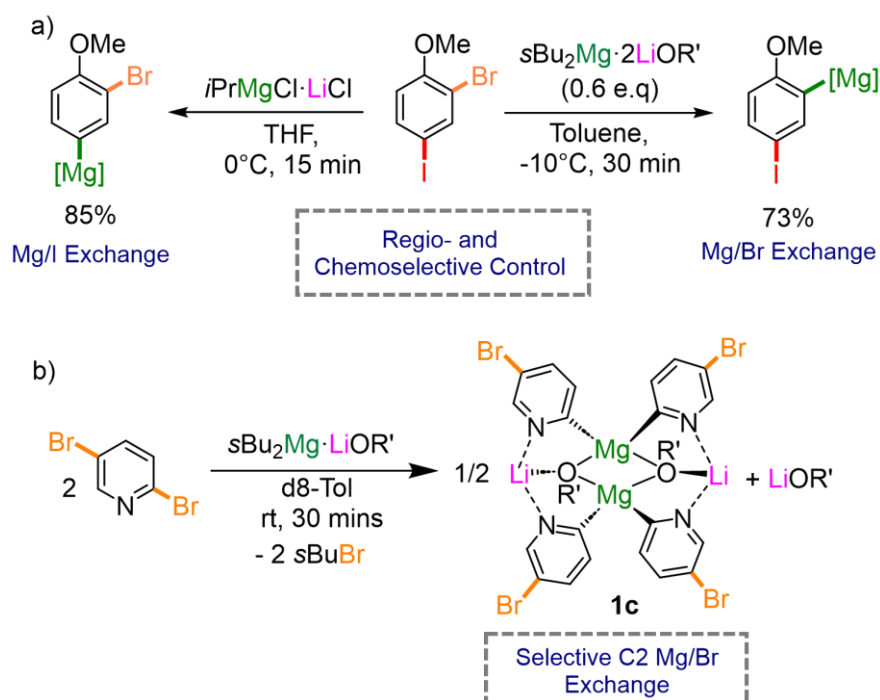


**Figure 1.** Molecular structure of  $[\text{LiMgAr}_2(\text{OR}')_2]$  ( $\text{Ar} = 2\text{-NMe}_2\text{-C}_6\text{H}_4$ ) (**1b**) with displacement ellipsoids at 50% probability and all H atoms omitted for clarity.

The quantitative Mg/Br exchange of 2-bromoanisole and 2-bromo-*N,N*-dimethylaniline, forming lower order mixed aryl/alkoxy magnesiate **1a** and **1b** respectively, was also achieved by using a 1:1 ratio of *s*Bu<sub>2</sub>Mg and LiOR' (confirmed by NMR spectroscopy and X-Ray crystallography). This is consistent with our findings that a free equivalent of LiOR' is found in the filtrate of these crystalline compounds and that only one equivalent of LiOR' is present in the dimeric crystalline structures of  $[\text{LiMgAr}_2(\text{OR}')_2]$ . These results initially led us to believe that intermediates **1a** and **1b** were the rational products of Mg/Br exchange carried out by a lower order lithium magnesiate exchange reagent,  $[\text{LiMg}s\text{Bu}_2(\text{OR}')]$ , and the second equivalent of LiOR' is merely a spectator in these reactions. While these findings support Knochel's initial proposal attributing the enhanced reactivity of *s*BuMg<sub>2</sub>·LiOR combinations to the formation of a lithium magnesiate, they also demonstrate that the presence of just one equivalent of LiOR is sufficient to quantitatively promote the Mg-Br exchange which makes unlikely the involvement of higher order lithium magnesiate,  $[\text{Li}_2\text{Mg}(s\text{Bu})_2(\text{OR}')_2]$  as initially proposed.<sup>2</sup>

The special coordination environment of the Li centres interacting with an O or N donor atom in the structures of **1a** and **1b** respectively can help aid the rationale behind the regioselectivities reported from the Knochel group. For example, treating 2-bromo-4-iodoanisole with *s*Bu<sub>2</sub>Mg·2LiOR', in toluene, led to an unexpected regioselective Mg/Br exchange (Scheme 3a). A quite surprising outcome given that C-I bonds are significantly more reactive towards metal/halogen exchange than stronger C-Br bonds.<sup>16</sup> Indeed, using the conventional Turbo Grignard reagent *i*PrMgCl·LiCl in THF leads to a regioselective Mg/I exchange as expected (Scheme 3a). This remarkable regioselectivity observed deploying

$s\text{Bu}_2\text{Mg}\cdot 2\text{LiOR}'$  is likely due to the absence of a donor solvent which allows the exchange reagent to interact with the methoxy substituent in the substrate, likely through dative  $\text{Li}\cdots\text{O}$  interactions, favouring Complex induced proximity effect (CIPE) type reactivity.<sup>17,18</sup> A similar type of CIPE reactivity could be envisaged for the regioselectivity observed with 2,5-dibromopyridine forming similar intermediates to **1a-b** upon reaction with  $s\text{Bu}_2\text{Mg}\cdot 2\text{LiOR}'$ , in the absence of a donor, in which the pyridyl N atom interacts with the Li atoms stabilising the C2 metalated product **1c** (Scheme 3b) which was characterised by NMR spectroscopy, including  $^1\text{H}$ -DOSY NMR. However, as previously mentioned in Scheme 1a, addition of PMDETA shuts down this lithium directing effect providing coordinative saturation of the alkali-metal which switches the regioselectivity of the Mg/Br exchange to the C5 position.

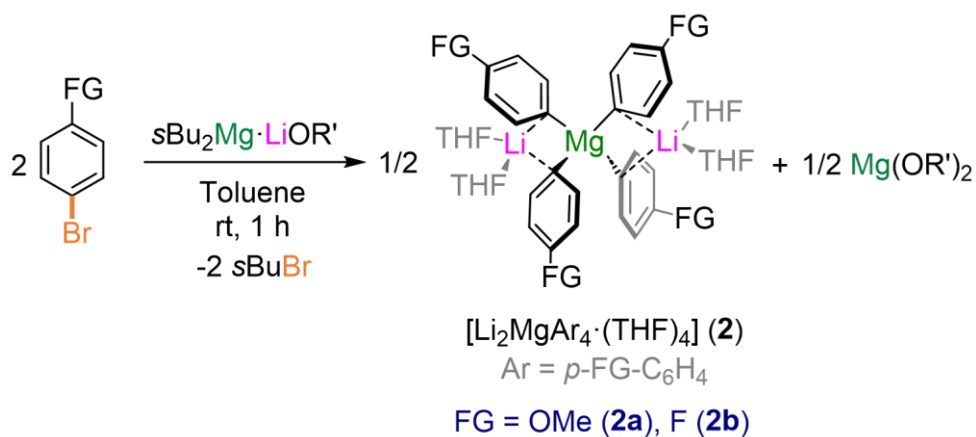


**Scheme 3.** a) Regio- and chemoselective Mg/Br exchange of 2-bromo-4-iodoanisole using  $s\text{Bu}_2\text{Mg}\cdot 2\text{LiOR}'$  ( $\text{OR}' = 2\text{-ethylhexyl}$ ) b) Regioselective C2 Mg/Br exchange of 2,5-dibromopyridine forming **1c**

### 2.3.3 Structural and Spectroscopic Analysis of Mg/Br Exchange of 4-Bromoarenes

Adding further interest, given the molecular structures of **1a-b** and the importance of the *ortho* directing groups to the stability of these metalated intermediates, we wondered what the consequences of using substrates where the functional group is more remote would be i.e., *para*-substituted bromoarenes. Thus, when a combination of  $s\text{Bu}_2\text{Mg}$  and  $\text{LiOR}'$  was reacted with two equivalents of 4-bromoanisole and 4-bromo-fluorobenzene over the course of one hour a large amount of white precipitate formed which could be solubilised upon the addition of THF and gentle heating. Cooling to room temperature afforded a crop of colourless crystals. Surprisingly, X-ray crystallographic analysis on these crystals revealed the formation of an

entirely different type of lithium magnesiate, namely the homoleptic tetra(aryl)lithium magnesiates  $[(\text{THF})_4\text{Li}_2\text{MgAr}_4]$  ( $\text{Ar} = 4\text{-OMe-C}_6\text{H}_4$ , **2a**;  $\text{Ar} = 4\text{-F-C}_6\text{H}_4$ , **2b**) which do not possess any alkoxide ligand. These compounds could be isolated in 74 and 60% isolated crystalline yields respectively (Scheme 4). Despite the moderate crystalline yields,  $^1\text{H-NMR}$  studies indicate these Mg/Br exchange reactions are almost quantitative in  $d_8$ -toluene. Thus, simply changing the substitution pattern of the bromoarene has led to a completely different type of metalated intermediate of Mg/Br exchange despite using the same exchange reagent,  $s\text{Bu}_2\text{Mg}\cdot\text{LiOR}'$ .



**Scheme 4.** Mg/Br exchange of 4-bromoanisole and 4-bromo-fluorobenzene with  $s\text{Bu}_2\text{Mg}\cdot\text{LiOR}'$  leading to tetra(aryl)lithium magnesiate intermediates  $[\text{Li}_2\text{MgAr}_4\cdot(\text{THF})_4]$  (**2**) with release of  $\text{Mg}(\text{OR}')_2$

Puzzled by the lack of alkoxide content in higher order lithium magnesiates **2a** and **2b**, analysis of the mother liquor in this case confirmed the Mg/Br exchange reaction occurs with concomitant elimination of  $\text{Mg}(\text{OR}')_2$  (Figure 2) (determined by  $^1\text{H}$  and  $^{13}\text{C}$  NMR ( $\text{Mg}(\text{OR}')_2$  independently synthesised by reaction of  $n\text{Bu}_2\text{Mg}$  and 2 equivalents of 2-ethylhexanol). Crucially, carrying out this reaction with an additional equivalent of  $\text{LiOR}'$  present,  $s\text{Bu}_2\text{Mg}\cdot 2\text{LiOR}'$ , the same tetra(aryl) lithium magnesiate products are obtained with a free equivalent of  $\text{LiOR}'$  found in solution.



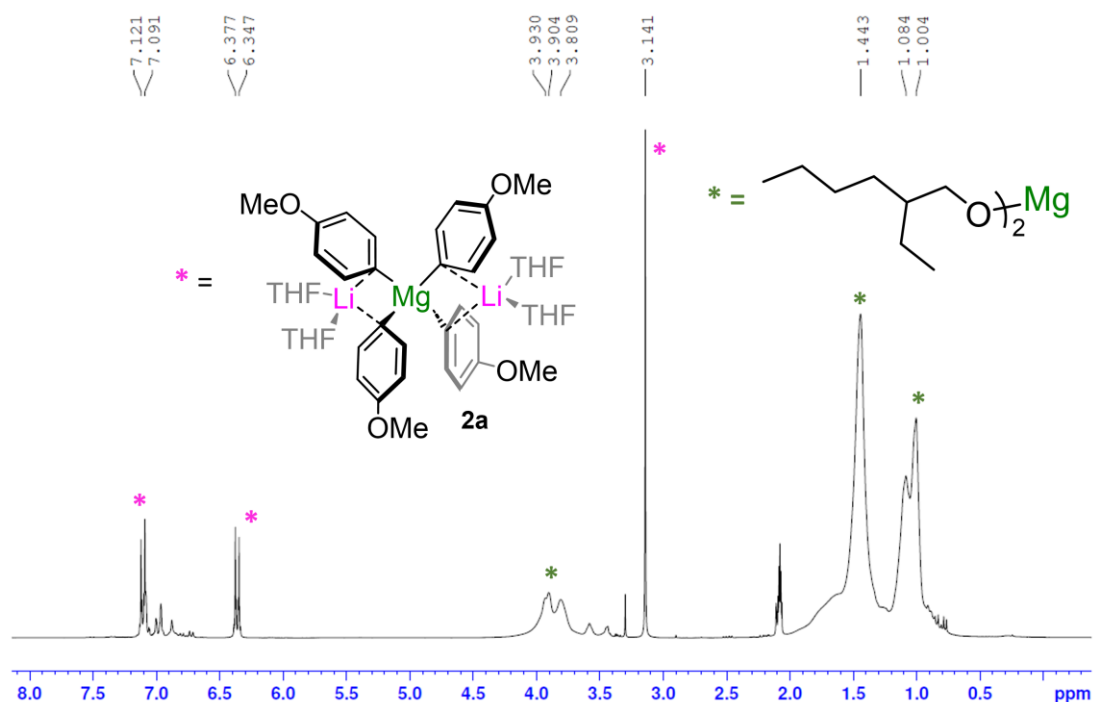


**Figure 2.**  $^1\text{H-NMR}$  spectra in  $d_8\text{-THF}$  of the filtrate from crystalline homoleptic tetra(aryl)lithium magnesiate  $[(\text{THF})_4\text{Li}_2\text{MgAr}_4]$  ( $\text{Ar} = 4\text{-OMe-C}_6\text{H}_4$ , **2a**) showing formation of  $\text{Mg}(\text{OR}')_2$  post  $\text{Mg}/\text{Br}$  exchange

The molecular structures of **2a** and **2b** were established by X-ray crystallography (Figure 3). Diverging markedly from lower order mixed aryl/alkoxy lithium magnesiates **1a** and **1b**, **2a** and **2b** exhibit a monomagnesium constitution, with a 2:1 Li:Mg ratio where all anionic groups are the relevant C4-substituted aryls resulting from  $\text{Mg}/\text{Br}$  exchange of 4-bromoanisole and 4-bromo-fluorobenzene respectively. Both structures contain a C4-coordinated Mg atom flanked by two THF-solvated Li cations, displaying a bent  $\text{Li}\cdots\text{Mg}\cdots\text{Li}$  arrangement [ $159.05(8)^\circ$  and  $152.96(11)^\circ$  for **2a** and **2b** respectively]. The central Mg centres in both structures display distorted tetrahedral geometries with average bond angles of  $108.2^\circ$  (range =  $105.7^\circ$ -  $114.0^\circ$  and  $109.1^\circ$  (range =  $102.6^\circ$ -  $114.2^\circ$  for **2a** and **2b** respectively). Unlike in **1a-b**, here the lithium centres do not interact with the donor substituents on the aromatic rings, which are now located too remote, and instead they adopt a perpendicular disposition to the aromatic rings, binding to their *ipso* C via  $\pi$  type interactions in a similar manner as previously reported by Weiss for the higher order sodium magnesiate  $[(\text{PMDETA})_2\text{Na}_2\text{MgPh}_4]$  which was prepared by co-complexation of two equivalents of  $\text{PhNa}\cdot\text{PMDETA}$  with  $\text{MgPh}_2$ .<sup>19,20</sup> The average Mg-C  $\sigma$ -bond distance for this structure, 2.29 Å, is similar to that found in lithium magnesiates **2a** (2.23 Å) and **2b** (2.24 Å).

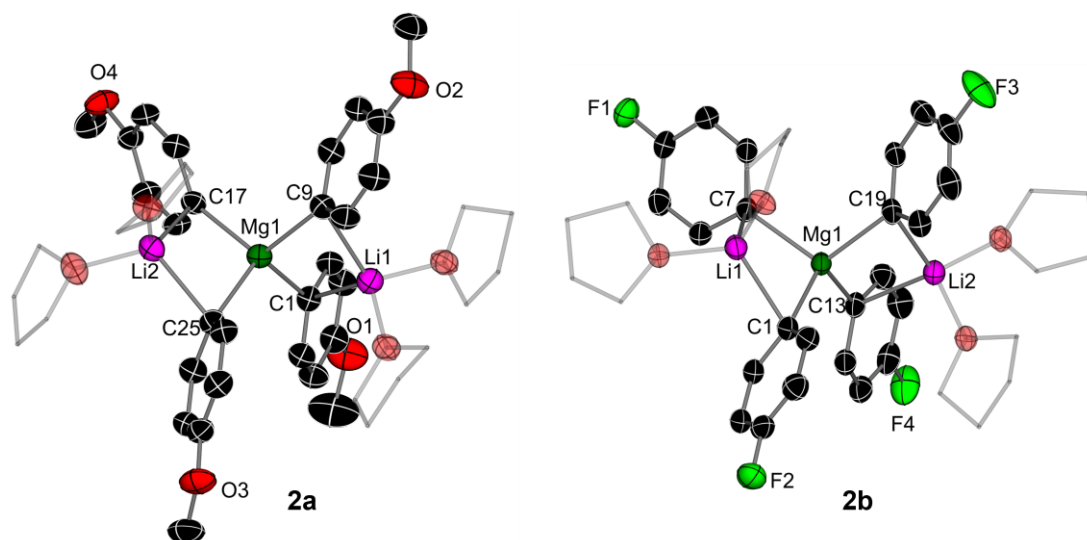
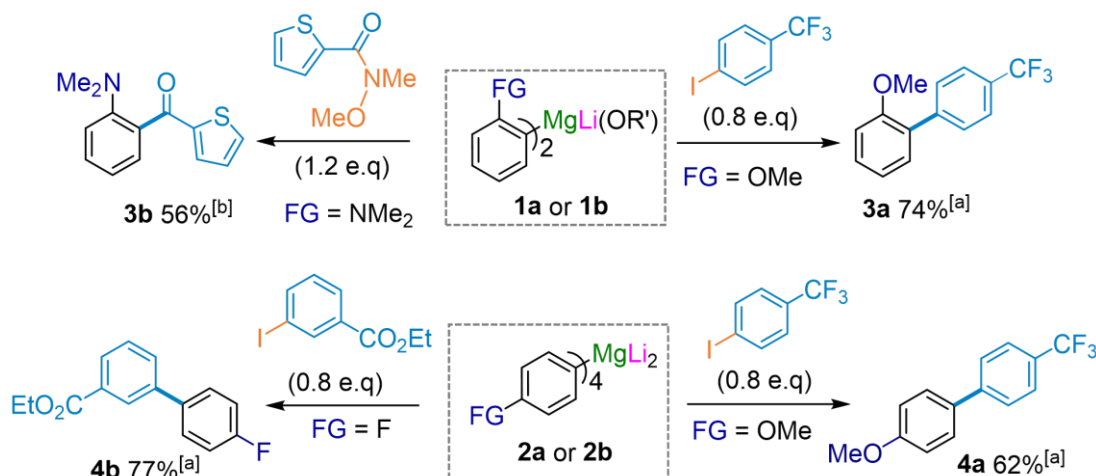


**Figure 3.** Molecular structures of **2a** and **2b** with displacement ellipsoids at 50% probability, all H atoms omitted, and with C atoms in THF molecules drawn as wire frames for clarity.

### 2.3.4 Electrophilic Interceptions of Mixed Aryl/Alkoxy Lithium Magnesiates **1a-b** and Tetra(aryl) Lithium Magnesiates **2a-b**

$^1\text{H}$  NMR monitoring of the reactions of the  $\text{LiOR}/s\text{Bu}_2\text{Mg}$  bimetallic combination with these different bromoarenes showed that **1a-b** and **2a-b** are in each case the only organometallic product of the reaction and that their formation did not result from a disproportionation during the crystallisation process. It should also be noted that these species are the sole organometallic species present in solution when using the original  $2s\text{BuLi}/\text{Mg}(\text{OR})_2$  combination reported by Knochel,<sup>5</sup> offering further support to the *in situ* formation of the same exchange reagent.

To ascertain whether the different composition of **1a-b** and **2a-b** could have an influence on their further functionalisation, electrophilic interception studies were carried out (Scheme 5). Thus, transmetalation of mixed aryl/alkoxy magnesiate **1a** and homoleptic tetra(aryl) magnesiates **2a-b** with  $\text{ZnCl}_2$  followed by Pd catalysed cross-coupling with 4-iodo-trifluoromethylbenzene or ethyl-3-iodobenzoate led to the formation of asymmetric bis(arenes) **3a**, **4a** and **4b** in good yields ranging from 62 to 77%. In addition, **1b** reacts with a Weinreb amide to form acylation product **3b** in a 56% yield. While these quenching studies demonstrate the synthetic utility of these mixed-metal complexes and their ability to undergo C-C bond forming processes, they also illustrate how on many occasions the constitution of the active organometallic species can remain concealed, limiting the understanding on how such bimetallic reagents operate. This is particularly relevant for these reactions, where using the same exchange reagent and same reaction conditions, produces different types of magnesium aryl species.



**Scheme 5.** Comparative electrophilic interception studies of **1a-2b** and **2a-b** prepared in situ via Mg/Br exchange with 0.6 equiv of the 2 *s*BuLi·Mg(OR)<sub>2</sub> combination. [a] ZnCl<sub>2</sub> (1.3 equiv.), E<sup>+</sup> (0.8 equiv.), Pd(OAc)<sub>2</sub> (4 mol%), SPhos (8 mol%) [b] E<sup>+</sup> (1.2 equiv.), 25°C, 12 h.

### 2.3.5 Spectroscopic Investigations into the Exchange Reagent (*s*Bu<sub>2</sub>Mg·LiOR')

Puzzled by the contrasting compositions of **1a-b** versus **2a-b**, we next probed the constitution of the exchange reagent *s*Bu<sub>2</sub>Mg/LiOR' in toluene solutions using a combination of NMR experiments including <sup>1</sup>H-DOSY NMR. These studies revealed the presence of two distinct organometallic species in solution containing *s*Bu groups in two different environments (Figure 4b). One species whose M-CH fragment of the *s*Bu groups resonates at  $\delta = 0.40$  ppm in the <sup>1</sup>H NMR spectrum (Figure 4b) belongs to a compound which also contains alkoxide ligands (both sets of resonances exhibit almost identical diffusion coefficients (*D*) by <sup>1</sup>H-DOSY NMR,  $D = 4.30 \times 10^{-10} \text{ m}^2 \text{ s}^{-1}$ ). These data support the formation of co-complexation product [LiMg<sub>5</sub>Bu<sub>2</sub>(OR')] (**I**) (Figure 4b). The second species displays an upfield shifted multiplet at  $\delta = -0.26$  ppm which is intermediate between those chemical shifts found for the single metal reagents *s*BuLi ( $\delta = -1.09$  ppm) and *s*Bu<sub>2</sub>Mg ( $\delta = 0.05$  ppm). Moreover, <sup>1</sup>H-DOSY NMR experiments indicate that this signal belongs to a species that contains only *s*Bu groups ( $D = 6.02 \times 10^{-10} \text{ m}^2 \text{ s}^{-1}$ ), which coupled with the homoleptic constitution of the exchange products **2a-2b**, suggest that this second species may be homoleptic tetra(alkyl) [Li<sub>2</sub>Mg<sub>5</sub>Bu<sub>4</sub>] (**II**) (Figure 4a-b). Further support for this interpretation was found when [Li<sub>2</sub>Mg<sub>5</sub>Bu<sub>4</sub>] (**II**) was prepared independently via co-complexation of two equivalents of *s*BuLi with *s*Bu<sub>2</sub>Mg which gave a colourless oil with its <sup>1</sup>H NMR spectrum showing a multiplet at  $\delta = -0.26$  ppm, the same chemical shift as that found in the *s*Bu<sub>2</sub>Mg/LiOR' mixture (Figure 4c).

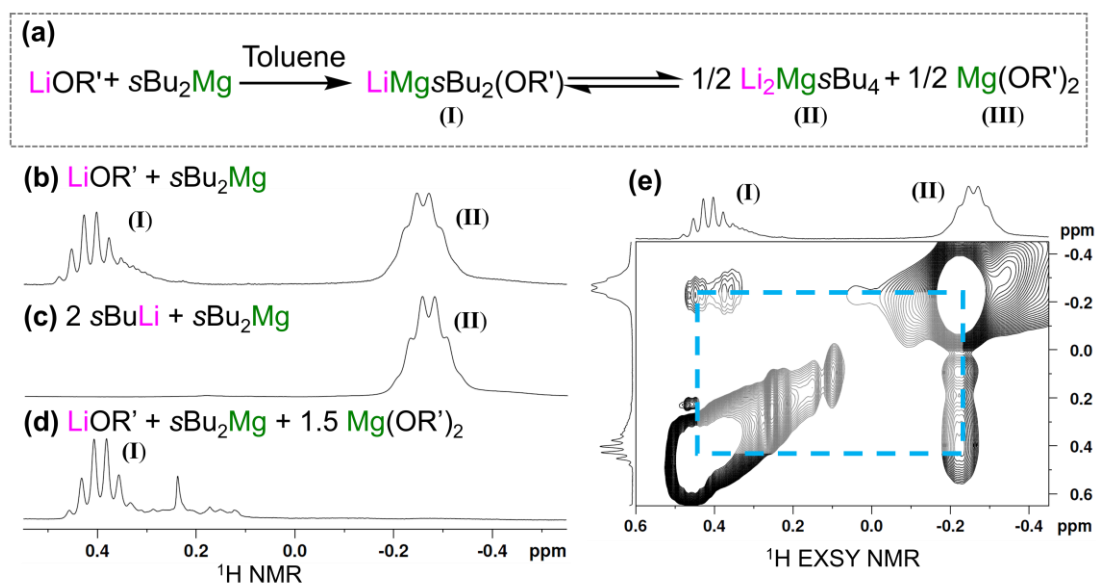
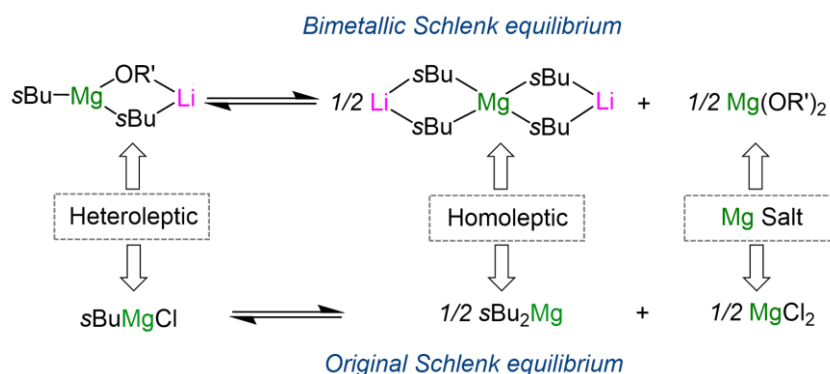


**Figure 4.** a) Proposed equilibrium of  $[\text{LiMgsBu}_2(\text{OR}')]$  (**I**) with  $[\text{Li}_2\text{MgsBu}_4]$  (**II**) and  $\text{Mg}(\text{OR}')_2$  (**III**). Section of  $^1\text{H}$  NMR spectra (from 0.5 to -0.5 ppm) in  $d_8$ -toluene of: (b)  $\text{LiOR}' + s\text{Bu}_2\text{Mg}$ ; (c)  $2 s\text{BuLi} + s\text{Bu}_2\text{Mg}$  and (d)  $\text{LiOR}' + s\text{Bu}_2\text{Mg} + 1.5 \text{Mg}(\text{OR}')_2$ . (e) Section of  $^1\text{H}$ -EXSY NMR spectrum of  $\text{LiOR}' + s\text{Bu}_2\text{Mg}$  in  $d_8$ -toluene.

Furthermore,  $^1\text{H}$ -EXSY NMR experiments indicate that lithium magnesiate **I** and **II** are in equilibrium with each other (Figure 4e). An explanatory possible equilibrium is depicted in Figure 4a, with the combination of equimolar amounts of  $s\text{Bu}_2\text{Mg}$  and  $\text{LiOR}'$  forming mixed alkyl/alkoxy co-complex  $[\text{LiMgsBu}_2(\text{OR}')]$  (**I**) which in turn is in equilibrium with tetra(alkyl)  $[\text{Li}_2\text{MgsBu}_4]$  (**II**) and  $\text{Mg}(\text{OR}')_2$  (**III**). Adding credence to this interpretation it was found that adding increasing amounts of  $\text{Mg}(\text{OR}')_2$  (**III**) to a  $s\text{Bu}_2\text{Mg}/\text{LiOR}'$  combination caused the gradual decrease of (**II**) in solution, until it disappears completely after 1.5 e.q of  $\text{Mg}(\text{OR}')_2$  in total. This suggests that under these conditions the equilibrium lies towards the formation of (**I**). While studies on homo(alkyl) alkali-metal magnesiate have described that higher and lower order species can be in equilibrium with each other,<sup>21–23</sup> the type of equilibrium depicted in Figure 4 for mixed alkyl/alkoxy species is, as far as we can ascertain, unknown in lithium magnesiate chemistry. It bears a strong resemblance with the well-established classical Schlenk equilibrium in Grignard reagent chemistry where heteroleptic  $\text{RMgX}$  reagents are in equilibrium with the homoleptic species,  $\text{MgR}_2$  and  $\text{MgX}_2$  (Scheme 6) (See *Chapter 1, section 1.3.2*). Related to these findings, O'Hara has recently found that a sodium dialkyl magnesiate supported by a biphenolate ligand  $[\text{Na}_2\text{Mg}(\text{BIPHEN})n\text{Bu}_2]$  is in equilibrium with all alkoxy sodium magnesiate  $[\text{Na}_2\text{Mg}(\text{BIPHEN})_2]$  along with  $\text{Na}_2\text{MgnBu}_4$  although, in this case, all species involved within the equilibrium have the same 2:1 alkali metal:magnesium ratio (See *Chapter 1, section 1.3.4*).<sup>7,15</sup>



**Scheme 6.** Comparison of the conventional Schlenk equilibrium with proposed bimetallic Schlenk type equilibrium of  $[\text{LiMg}(\text{sBu})_2(\text{OR}')]$  (**I**) with  $[\text{Li}_2\text{Mg}(\text{sBu})_4]$  (**II**) and  $\text{Mg}(\text{OR}')_2$  (**III**)

### 2.3.6 Alkoxide Effects in $\text{sBu}_2\text{Mg} \cdot \text{LiOR}$ combinations

The high solubility of  $[\text{LiMg}(\text{sBu})_2(\text{OR}')]$  (**I**) and  $[\text{Li}_2\text{Mg}(\text{sBu})_4]$  (**II**) in hydrocarbon solvents precluded their crystallization and structure elucidation. For  $[\text{Li}_2\text{Mg}(\text{sBu})_4]$  (**II**) a related structure to that reported for  $[(\text{TMEDA})_2\text{Li}_2\text{Mg}(\text{CH}_2\text{SiMe}_3)_4]$  can be expected,<sup>23</sup> which in a similar manner to higher order lithium magnesiate **2a** and **2b**, exhibits a trinuclear  $\text{Li} \cdots \text{Mg} \cdots \text{Li}$  motif where each alkyl bridges between Mg and Li. Although Mulvey has shown that higher order alkali metal magnesiate can also exist as solvent separated ion pairs in the solid state however this required an excess of DABCO (1,4-diazabicyclo[2.2.2]octane) which can sequester the alkali metal cations leaving interstitial  $\{\text{Mg}n\text{Bu}_4\}^2$  anions in the solid state.<sup>24</sup>

In the case of (**I**), using the alkoxide  $\text{Li}(\text{dmem})$  [ $\text{dmem} = \text{CH}_2\text{CH}_2\text{N}(\text{CH}_3)\text{CH}_2\text{CH}_2\text{N}(\text{CH}_3)_2$ ] previously used in Zn/I exchange reactions with lithium zincates<sup>10</sup> (see Chapter 1, Section 1.3.4) which contains two amide groups, in a co-complexation reaction with one equivalent of  $\text{sBu}_2\text{Mg}$  led to the isolation of dimeric mixed alkyl/alkoxy magnesiate  $[\text{LiMg}(\text{sBu})_2(\text{dmem})]_2$  (**5**) in a 35% crystalline yield (Figure 5a). X-ray crystallographic studies revealed a step ladder motif for **5** (Figure 5b), comprising outer Li-C rungs and inner Mg-O rungs, a common motif observed for s-block organometallic solid state structures.<sup>25–27</sup> Along the ladder edge, internal  $\text{NMe}_2$  substituents from the alkoxide ligands and another  $\text{sBu}$  group coordinate to Li and Mg respectively to complete the dimer. Alternatively, **5** can be viewed as two dinuclear  $\{\text{LiOMgC}\}$  rings which combine laterally through the Mg-O edges to form a tetranuclear ladder.

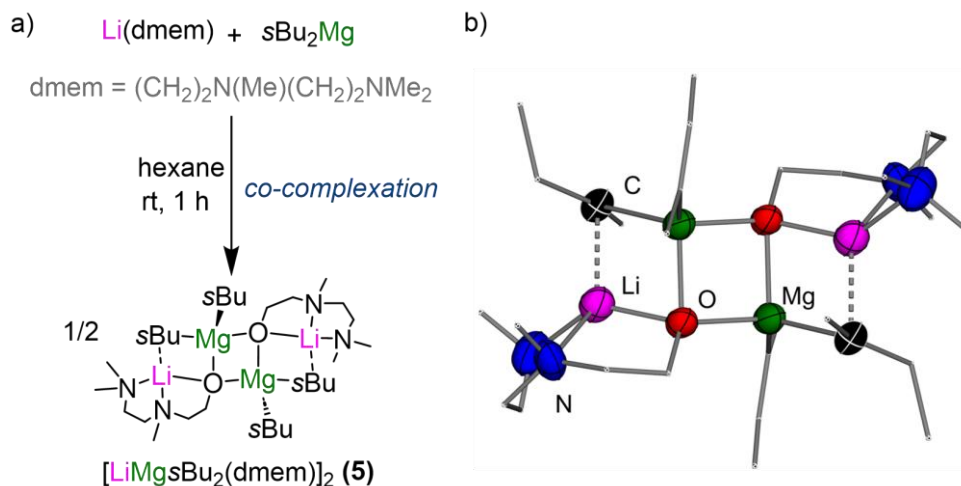
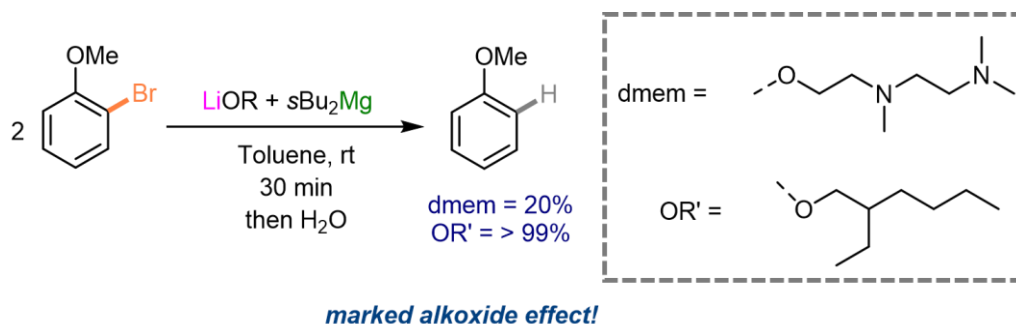


**Figure 5.** a) Co-complexation of  $\text{Li}(\text{dmem})$  with  $\text{sBu}_2\text{Mg}$  forming mixed alkyl/alkoxy magnesiate  $[\text{LiMgsBu}_2(\text{dmem})]_2$  (**5**) b) Molecular structure of **5** with displacement ellipsoids at 50% probability, all H atoms omitted, and with C atoms in the alkoxy and  $\text{sBu}$  fragments drawn as wire frames for clarity

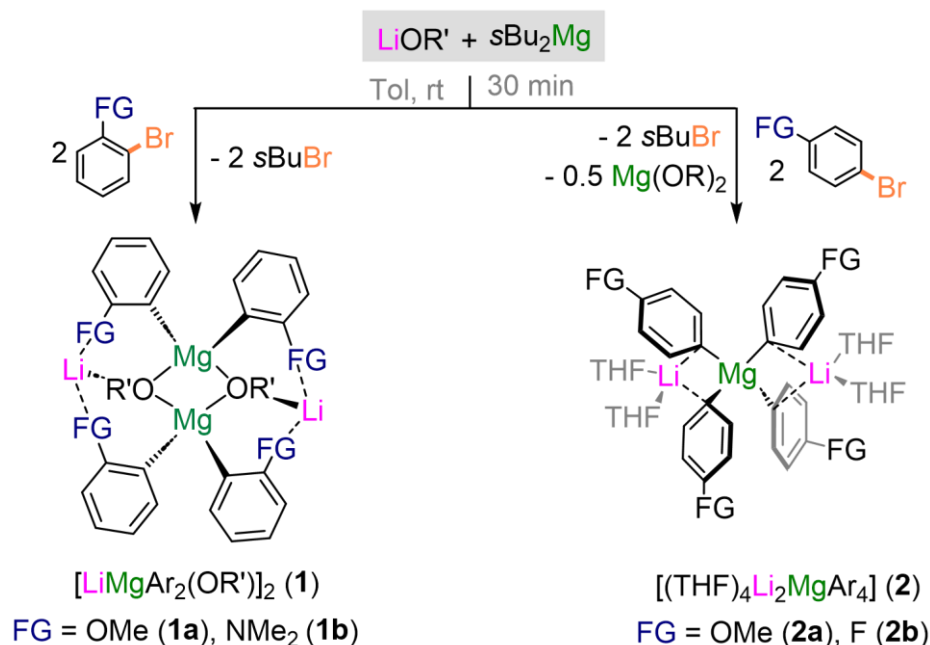
It is important to note that  $^1\text{H-NMR}$  studies confirmed that  $[\text{LiMgsBu}_2(\text{dmem})]_2$  (**5**) is the sole organometallic product formed on co-complexation of  $\text{Li}(\text{dmem})$  and  $\text{sBu}_2\text{Mg}$  and no redistribution to a higher order tetra(alkyl) magnesiate  $\text{Li}_2\text{MgsBu}_4$  (**II**) and  $\text{Mg}(\text{dmem})_2$  as observed using the long chain alkoxy  $\text{LiOR}'$  ( $\text{R} = 2\text{-ethylhexyl}$ ). Remarkably, simply changing the substituents on the alkoxy ligand and incorporating the  $\text{dmem}$  ligand seems to preclude the induction of a bimetallic Schlenk type equilibrium (Scheme 6), forming a more rigid and robust magnesiate **5** which is less prone to redistribution in solution. Moreover,  $[\text{LiMgsBu}_2(\text{dmem})]_2$  **5** reacts sluggishly with 2-bromoanisole in toluene at room temperature after one hour, with a markedly reduced yield of 20% compared to the quantitative reactivity observed when the Mg/Br exchange is carried out with  $\text{LiOR}'$  ( $\text{R} = 2\text{-ethylhexyl}$ ) (Scheme 7). The lower likelihood of highly reactive  $\text{Li}_2\text{MgsBu}_4$  (**II**) forming under the conditions exercised allows explanation to the poor yield observed for Mg/Br exchange when using pure isolated crystals of **5**. Another explanation can be drawn from the structural features, showing coordinative saturation of both lithium atoms within the dimer. Given our proposal of a CIPE-pathway of action, complete satisfaction of lithium's coordination sphere would not allow for substrate interaction, thus impacting overall reactivity.



**Scheme 7.** Alkoxide effects in Mg/Br exchange of 2-bromoanisole with  $s\text{Bu}_2\text{Mg} + \text{LiOR}'$  or  $\text{Li}(\text{dmem})$

### 2.3.7 Investigations to Determine the Active Exchange Reagent in $s\text{Bu}_2\text{Mg} \cdot \text{LiOR}'$ ( $\text{R}' = 2\text{-ethylhexyl}$ )

While these findings shed light on the constitutions of these mixed alkyl/alkoxide mixtures in solution, it was still not clear why two completely different types of aryl lithium magnesiate products form during the Mg/Br exchange process with substituted bromoarenes (Scheme 8). The isolation of mixed aryl/alkoxy lower order lithium magnesiates **1a-b** when *ortho* substituted bromoarenes are treated with  $s\text{Bu}_2\text{Mg} \cdot \text{LiOR}'$  compared to the higher order tetra(aryl) magnesiates **2a-b** obtained when *para* substituted bromoarenes are employed posed the question of which species was responsible for the Mg/Br exchange reaction.



**Scheme 8.** Reactions of  $s\text{Bu}_2\text{Mg} \cdot \text{LiOR}'$  with 2-bromo and 4-bromo-substituted arenes (25°C, toluene, 30 min, using 2 equivalents of the relevant bromoarene)

At first glance, it appeared that **1a-b** resulting from the reaction with 2-bromo substituted substrates could be the products if the exchange process was effected by

[LiMg $s$ Bu $_2$ (OR')] (**I**). In contrast, homoleptic **2a-b** seemed more likely to be formed via reaction of 4-bromo substituted arenes with [Li $_2$ Mg $s$ Bu $_4$ ] (**II**) due to their lack of alkoxide content. In order to establish if both systems, **I** and **II**, could be active towards Mg-Br exchange, we first carried out the reaction of [Li $_2$ Mg $s$ Bu $_4$ ] (**II**) with four equivalents of 2-bromoanisole in toluene to produce tetra(aryl) lithium magnesiate [(THF) $_2$ Li $_2$ Mg(2-OMe-C $_6$ H $_4$ ) $_4$ ] (**6**) in a 90% isolated yield (Figure 6).  $^1$ H NMR monitoring studies showed the quantitative conversion of 2-bromoanisole into **6** accompanied by  $s$ BuBr. The molecular structure of **6** was established by X-Ray crystallography. Exhibiting a contacted ion pair magnesiate structure reminiscent to that of **2a**, **6** displays a distorted tetrahedral structure with Mg bonded to four *ortho*-metalated molecules of anisole, while Li interacts with OMe groups of two anisyl groups as well as a THF ligand. To maximise these Li-OMe contacts the Li $\cdots$ Mg $\cdots$ Li vector in **6** is significantly more bent than in **2a** [88.15(11) $^\circ$  vs 159.05(18) $^\circ$ ], while the lengths of the Mg-C bonds in both complexes are almost identical (average values, 2.223 and 2.2313 Å for **6** and **2a** respectively). Considering the alkyl-rich constitution of higher order magnesiate **II**, coupled with its ability to quantitatively promote Mg/Br exchange of 2-bromoanisole, the selective formation of **2a** when 2-bromoanisole was reacted with the LiOR'/ $s$ Bu $_2$ Mg combination became even more puzzling. In an attempt to mimic the reaction conditions when using this mixed alkyl/alkoxide reagent, one molar equivalent of Mg(OR') $_2$  (which is the other product observed from disproportionation of [LiMg $s$ Bu $_2$ (OR')] (**I**) into [Li $_2$ Mg $s$ Bu $_4$ ] (**II**)) was introduced to a suspension of [(THF) $_2$ Li $_2$ Mg(2-OMe-C $_6$ H $_4$ ) $_4$ ] (**6**) in toluene which led to the quantitative formation of lower order exchange product [LiMg(2-OMe-C $_6$ H $_4$ ) $_2$ (OR')] $_2$  (**2a**) (Figure 6) (confirmed by NMR spectroscopy).



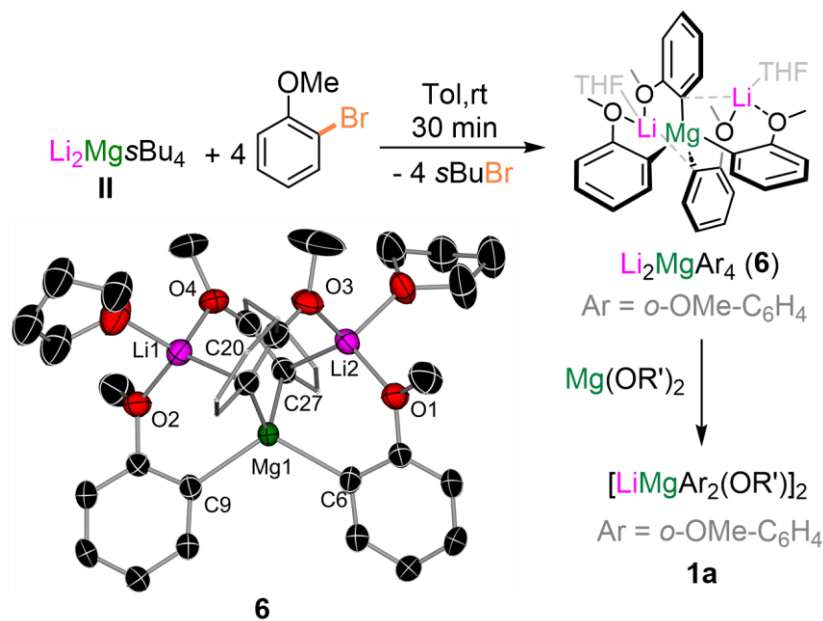


**Figure 6.** Synthesis of  $[(\text{THF})_2\text{Li}_2\text{Mg}(2\text{-OMe-C}_6\text{H}_4)_4]$  (**6**) via Mg/Br exchange of four equivalents of 2-bromoanisole with  $[\text{Li}_2\text{Mg}s\text{Bu}_4]$  (**II**) and subsequent conversion into **1a** via co-complexation with  $\text{Mg}(\text{OR}')_2$ . Molecular structure of **6** with displacement ellipsoids at 50% probability, all H atoms omitted, and with C atoms in THF molecules drawn as wire frames for clarity

Adding a new layer of complexity, these results set at least two different scenarios to explain the formation of mixed alkyl/alkoxides **1a-b** during the exchange reactions. On one hand, *in situ* generated tetra(alkyl) magnesiate (**II**) could be responsible for the Mg/Br exchange in all cases, furnishing  $[\text{LiMgAr}_4]$  (**2**) intermediates that in the case of *ortho*-substituted Ar groups can undergo co-complexation with the concomitantly generated  $\text{Mg}(\text{OR}')_2$  (**III**) furnishing **1a-b** (as depicted in Scheme 9). Alternatively the more kinetically activated *ortho*-substituted bromoarenes<sup>28</sup> could react preferentially with mixed(alkyl) alkoxide magnesiate **6** whereas, for less reactive 4-substituted substrates, the exchange may occur via tetra(alkyl) magnesiate (**II**). However, this second option seems less likely as using isolated crystals of related mixed(alkyl) alkoxide magnesiate **5** towards 2-bromoanisole led to significantly lower conversions (Scheme 7), a behaviour also noticed in Zn/I exchange reactions using  $[\text{LiZnEt}_2(\text{dmem})]$ .<sup>10</sup> Additionally, dianionic higher order alkali metal *ates*, like (**II**), are known to be more reactive than their lower order congeners, like (**I**).<sup>29-36</sup> Especially revealing was the fact that when an excess of 1.5 equiv of  $\text{Mg}(\text{OR}')_2$  (**III**) was added to the equimolar mixture of  $\text{LiOR}'$  and  $s\text{Bu}_2\text{Mg}$  (pushing the bimetallic Schlenk equilibrium depicted in Scheme 3 towards the exclusive formation of  $[\text{LiMg}s\text{Bu}_2(\text{OR}')]$  (**I**) in solution (Figure 4d), the exchange process is completely suppressed with no conversion seen after 40 minutes (Table 1, entry 6).



interception as shown in Scheme 3 affording in all cases the relevant functionalized substituted arene **3a-b**, **4a-b**.

## 2.4 Conclusions

Through detailed NMR spectroscopic and X-Ray crystallographic studies we have been able to shed light on the constitution and *modus operandi* of the mixed alkyl/alkoxy bimetallic exchange reagent,  $s\text{Bu}_2\text{Mg}\cdot\text{LiOR}'$ , originally reported by the Knochel group. Isolation and characterisation of the metalated intermediates post Mg/Br exchange helped unveil the complex nature of this system which could produce two entirely different bimetallic products  $[\text{LiMgAr}_2(\text{OR}')]$  (**1a-b**) and  $[\text{Li}_2\text{MgAr}_4]$  (**2a-b**), based on the substitution pattern of the bromoarene used. By carefully investigating the constitution of equimolar mixtures of  $s\text{Bu}_2\text{Mg}$  and  $\text{LiOR}'$  we have uncovered a novel bimetallic Schlenk type equilibrium between the mixed alkyl/alkoxy lithium magnesiate  $[\text{LiMgsBu}_2(\text{OR}')]$  (**I**) and higher order  $[\text{Li}_2\text{MgsBu}_4]$  (**II**) and magnesium alkoxide  $[\text{Mg}(\text{OR}')_2]$  (**III**).

Manipulation of the Schlenk equilibrium by adding variable amounts of  $[\text{Mg}(\text{OR}')_2]$  and subsequent control experiments suggest that while the inclusion of the chosen alkoxide is essential for solubility and allowing this complex equilibrium to be present, the true active species within these reactions is a dianionic, homoalkyl lithium magnesiate,  $[\text{Li}_2\text{MgsBu}_4]$  (**II**) leading to homoaryl reaction intermediates,  $[\text{Li}_2\text{MgAr}_4]$ . However, we were able to reveal that in the case of *ortho* substituted bromoarenes such intermediates can undergo co-complexation with  $\text{Mg}(\text{OR}')_2$  to form mixed aryl/alkoxy  $[\text{LiMgAr}_2(\text{OR}')]$  intermediates favoured by interactions with the Li atoms and the *ortho*-donor atoms present in the substrate.

Additionally, a switch to a chelating alkoxide (dmem) resulted in a reduced propensity of these mixtures to undergo Mg/Br exchange likely due to the formation of more a robust and rigid mixed alkyl/alkoxy magnesiate (**5**) which does not participate in a Schlenk type redistribution process. Moreover, the chelating nature of the alkoxide ligand, providing coordinative saturation of the alkali-metal, may also have a detrimental effect on the reactivity preventing a CIPE type mechanism.

The studies presented within this Chapter are complementary to those reported by the Knochel group whilst exploring the synthetic potential of these reagents further. With the knowledge acquired in these studies we were set to assess the role of the alkali-metal and the nature of the alkoxide ligand in these exchange reagents, which became the main focus in Chapter 3.

## 2.5 Experimental

A link is provided below for the Electronic Supporting Information (ESI) from the peer reviewed article on which this experimental section is based:

[downloadSupplement \(wiley.com\)](#)

### 2.5.1 Synthesis of Starting Materials

#### Synthesis of $s\text{Bu}_2\text{Mg}$

To an argon-flushed 750 mL Schlenk flask, 100 mL of dry  $\text{Et}_2\text{O}$  was added followed by 40 mmol of  $s\text{BuMgCl}$  (20 mL, 20 M in  $\text{Et}_2\text{O}$ ) and cooled to 0 °C in an ice bath. Taking advantage of the Schlenk equilibrium, 20 mmol of 1,4-dioxane (1.7 mL) was then added dropwise, resulting in a thick, white suspension which was stirred at 0 °C overnight. Filtration of this suspension through a plug of cellite and glasswool resulted in a colourless solution of  $s\text{Bu}_2\text{Mg}$  in  $\text{Et}_2\text{O}$ . All  $\text{Et}_2\text{O}$  was then removed under reduced pressure to give a pale-yellow oil which was then re-dissolved in 20 mL of dry hexane. The dialkylmagnesium reagent was standardised in THF via iodometric titration<sup>38</sup> – typical concentration 0.41 M.  **$^1\text{H-NMR}$  (300.1 MHz,  $\text{D}_8\text{-Tol}$ ):**  $\delta$  / ppm = 3.50 (s, residual 1,4-dioxane), 3.30 (q, residual  $\text{Et}_2\text{O}$ ), 1.87 (quint., 4H,  $\text{CH}_2$ ,  $s\text{Bu}$ ), 1.51 (d, 6H,  $\text{CH}_3$ ,  $s\text{Bu}$ ), 1.20 (t, 6H,  $\text{CH}_3$ ,  $s\text{Bu}$ ), 0.82 (t, residual  $\text{Et}_2\text{O}$ ), 0.05 (sext., 2H,  $\text{CH}$ ,  $s\text{Bu}$ ).  **$^{13}\text{C}\{^1\text{H}\}\text{-NMR}$  (75.5 MHz,  $\text{D}_8\text{-Tol}$ ):**  $\delta$  / ppm = 65.1 (residual  $\text{Et}_2\text{O}$ ), 31.1 ( $\text{CH}$ ,  $s\text{Bu}$ ), 20.2 ( $\text{CH}_3$ ,  $s\text{Bu}$ ), 19.8 ( $\text{CH}_2$ ,  $s\text{Bu}$ ), 17.1 ( $\text{CH}_3$ ,  $s\text{Bu}$ ), 13.7 (residual  $\text{Et}_2\text{O}$ ).

**Note:** This reagent is highly temperature sensitive and requires continuous storage at -30 °C or below. It must be used within 3 or 4 days of synthesis to ensure purity. Full spectroscopic characterisation can be found within this document –  $\text{Et}_2\text{O}$  present within spectra as it cannot be completely removed under vacuum.

#### Synthesis of $\text{Mg}(\text{OR}')_2$ (III)

In an argon-filled Schlenk tube, 1 mmol of  $n\text{Bu}_2\text{Mg}$  (2 mL, 0.5 M in heptane) was cooled to 0 °C. To this, 2 mmol, 0.32 mL of 2-ethylhexanol was added and the mixture was then allowed to warm to room temperature overnight. Removal of all volatiles under reduced pressure resulted in a colourless oil, determined to be spectroscopically pure  $\text{Mg}(\text{OR}')_2$  (III).  **$^1\text{H-NMR}$  (300.1 MHz,  $\text{D}_8\text{-Tol}$ , 298 K):**  $\delta$  / ppm = 4.0-3.66 (br. m, 4H,  $\text{OCH}_2$ ), 1.89-1.31 (br. m, 18 H,  $\text{CH}_2 \times 2$  (Et) +  $\text{CH}$  +  $(\text{CH}_2)_3$ ,  $\text{OR}'$ ), 1.18-0.93 (br. m, 12H,  $\text{CH}_3 \times 2$ ,  $\text{OR}'$ ).  **$^{13}\text{C}\{^1\text{H}\}\text{-NMR}$  (75.5 MHz,  $\text{D}_8\text{-Tol}$ ):**  $\delta$  / ppm = 67.4 ( $\text{OCH}_2$ ,  $\text{OR}$ ), 45.4 ( $\text{OCH}_2\text{C}(\text{H})$ ,  $\text{OR}'$ ), 30.7 ( $\text{CH}_2$ ,  $\text{OR}'$ ), 29.9 ( $\text{CH}_2$ ,  $\text{OR}'$ ), 24.2 ( $\text{CH}_2$ , Et,  $\text{OR}'$ ), 23.7 ( $\text{CH}_2$ ,  $\text{OR}'$ ), 14.6 ( $\text{CH}_3$ , Et,  $\text{OR}'$ ), 11.0 ( $\text{CH}_3$ ,  $\text{OR}'$ ).

### Synthesis of LiOR' (R = 2-ethylhexyl)

In an argon-filled Schlenk flask, 1.00 mmol of *n*BuLi (0.63 mL, 1.60 M) was added to 5 mL of dry hexane and cooled to 0 °C. To this, 0.16 mL of ROH was added and the mixture was then allowed to stir at room temperature for 1 h. Removal of all volatiles under reduced pressure resulted in a colourless oil – LiOR'. **<sup>1</sup>H-NMR (300.1 MHz, D<sub>8</sub>-Tol, 298 K):** δ / ppm = 3.96-3.68 (br. m, 2H, OCH<sub>2</sub>), 1.70 (br. m, 1H, CH<sub>2</sub> x1, Et), 1.46 (br. s, 8 H, CH<sub>2</sub> x1 (Et) + CH + (CH<sub>2</sub>)<sub>3</sub>, OR'), 1.09 (br. t, 3H, CH<sub>3</sub>, OR'), 1.01 (br. t, 3H, CH<sub>3</sub>, OR'). **<sup>7</sup>Li-NMR (156 MHz, D<sub>8</sub>-Tol, 298 K):** δ / ppm = 0.86 (LiOR). **<sup>13</sup>C{<sup>1</sup>H}-NMR (75.5 MHz, D<sub>8</sub>-Tol, 298 K):** δ / ppm = 68.2 (OCH<sub>2</sub>, OR'), 46.6 (OCH<sub>2</sub>C(H), OR'), 31.1 (CH<sub>2</sub>, OR'), 30.2 (CH<sub>2</sub>, OR'), 24.2 (CH<sub>2</sub>, Et, OR'), 24.0 (CH<sub>2</sub>, OR'), 14.5 (CH<sub>3</sub>, Et, OR'), 11.4 (CH<sub>3</sub>, OR').

### Synthesis of exchange reagent *s*Bu<sub>2</sub>Mg·LiOR' (R = 2-ethylhexyl)

To an argon-flushed Schlenk, 1 mmol of *n*BuLi (0.63 mL, 1.6 M in hexane) when *n* = 1 was added to 5 mL of hexane, cooled to 0 °C and 1 mmol, 0.16 mL of R'OH added when *n* = 1 (2 mmol, 0.32 mL when *n* = 2). The reaction mixture was then stirred at room temperature for 1 hour before addition of 1 mmol of *s*Bu<sub>2</sub>Mg (2.44 mL, 0.41 M in hexane) to give a colourless, slightly oily mixture which was stirred at room temperature for 1 hour. After co-complexation occurred, all solvent was removed *in vacuo* to give a colourless oil which was then reconstituted in 5 mL of dry toluene, giving a 0.2 M solution (or 1.0 mL of D<sub>8</sub>-Tol added to give a 1.0 M solution for NMR studies).

Species present:

LiMg<sub>5</sub>Bu<sub>2</sub>(OR') (I)

Li<sub>2</sub>Mg<sub>5</sub>Bu<sub>4</sub> (II)

Mg(OR')<sub>2</sub> (III)

**<sup>1</sup>H-NMR (300.1 MHz, D<sub>8</sub>-Tol, 298 K):** δ / ppm = 3.91-3.59 (br. m, 2H, OCH<sub>2</sub> of (30) and (26)), 3.36 (s, 1,4-dioxane), 3.13 (q, Et<sub>2</sub>O), 1.8 (m, 5H, CH<sub>2</sub> of *s*Bu + CH<sub>2</sub> x1, \* Et of OR'), 1.69 (d, 2H, CH<sub>3</sub>, *s*Bu, (30)), 1.52 (d, 4H, CH<sub>3</sub>, *s*Bu (33)), 1.43 (br. m, 14H, CH<sub>2</sub> x1, \* Et of OR' + CH, CH<sub>2</sub> and CH<sub>3</sub>, OR' of (30) and (26)), 0.89 (br. m, 6h, CH<sub>3</sub>, *s*Bu, (30) and (33)), 0.42 (m, CH, *s*Bu, 30), -0.26 (sext., CH, 33). \* = diastereotopic protons. **<sup>7</sup>Li-NMR (156 MHz, D<sub>8</sub>-Tol, 298 K):** δ / ppm = 0.35 (br. s, (30) and (33)). **<sup>13</sup>C{<sup>1</sup>H}-NMR (75.5 MHz, D<sub>8</sub>-Tol, 298 K):** δ / ppm = 67.7 (OCH<sub>2</sub>, (26)), 66.7 (OCH<sub>2</sub>, (30)), 65.8 (Et<sub>2</sub>O), 44.5 (CH, OR', (30)), 43.8 (CH, OR', (26)), 33.2 (CH<sub>2</sub>, *s*Bu, (30)), 31.7 (CH<sub>2</sub>, *s*Bu, (33)), 31.3 (CH<sub>2</sub>, OR'), 29.5 (CH<sub>2</sub>, OR', (30) + (26)), 24.6 (CH<sub>2</sub>, OR', (26)), 23.9 (CH<sub>2</sub>, OR', (30) and (26)), 22.3 (CH<sub>3</sub>, *s*Bu, (30)), 20.4 (CH<sub>3</sub>, *s*Bu, (33)), 20.2 (CH, *s*Bu, (33)), 19.4 (CH, *s*Bu, (30)), 18.4 (CH<sub>3</sub>, OR', (30) and

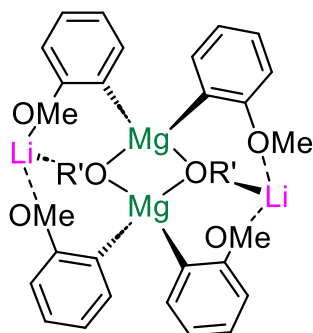
(26)), 17.2 (CH<sub>3</sub>, OR', (30) and (26)), 14.3 (CH<sub>3</sub>, sBu, (33)), 11.2 (CH<sub>3</sub>, sBu, (30)). ‡ = Confirmed by [<sup>1</sup>H, <sup>1</sup>H]-COSY and [<sup>1</sup>H, <sup>13</sup>C]-HSQC NMR spectra

#### Synthesis of Li<sub>2</sub>Mg<sub>2</sub>OBu<sub>4</sub> (II)

Under inert atmosphere, 2 mmol of sBuLi (1.42 mL, 1.4 M in cyclohexane) was added to 5 mL of dry hexane, followed by 1 mmol of sBu<sub>2</sub>Mg (2.44 mL, 0.41 M in hexane) resulting in a colourless, oily mixture. After stirring the reaction at room temperature for 1 hour, all volatiles were removed *in vacuo* to give a colourless oil – Li<sub>2</sub>Mg<sub>2</sub>OBu<sub>4</sub> (33). <sup>1</sup>H-NMR (300.1 MHz, D<sub>8</sub>-Tol, 298 K): δ / ppm = 3.05 (q, residual Et<sub>2</sub>O), 1.82 (br. m, 8H, CH<sub>2</sub>, sBu), 1.48 (d, 12H, CH<sub>3</sub>, sBu), 1.20 (t, 12H, CH<sub>3</sub>, sBu), -0.28 (br. m, 4H, CH, sBu). <sup>7</sup>Li-NMR (156 MHz, D<sub>8</sub>-Tol, 298 K): δ / ppm = 0.13 (Li<sub>2</sub>Mg<sub>2</sub>OBu<sub>4</sub>, II). <sup>13</sup>C{<sup>1</sup>H}-NMR (75.5 MHz, D<sub>8</sub>-Tol, 298 K): δ / ppm = 65.9 (Et<sub>2</sub>O), 31.5 (CH<sub>2</sub>, sBu), 19.9 (CH, sBu), ‡ 19.7 (CH<sub>3</sub>, sBu), ‡ 16.9 (CH<sub>3</sub>, sBu), 14.3 (Et<sub>2</sub>O). ‡Confirmed by [<sup>1</sup>H, <sup>13</sup>C]-HSQC NMR spectrum.

### 2.5.2 Synthesis of Mixed Aryl/Alkoxy Lithium Magnesiates [LiMgAr<sub>2</sub>(OR')]<sub>2</sub> 1a-b

#### Synthesis of [LiMgAr<sub>2</sub>(OR')]<sub>2</sub> (Ar = *o*-OMe-C<sub>6</sub>H<sub>4</sub>) (1a)

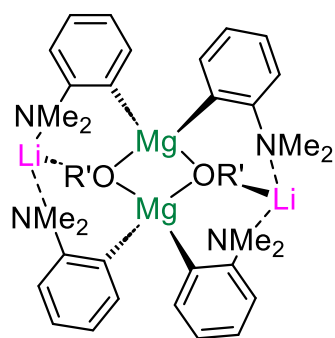


In an argon-flushed Schlenk flask, 1 mmol of the exchange reagent was prepared from Mg(OR')<sub>2</sub> and two equivalents of sBuLi (or from sBu<sub>2</sub>Mg + *n*LiOR' (*n* = 1 or 2)). Once reconstituted in 5 mL toluene to achieve a pale-yellow solution (0.2 M), 2 mmol of 2-bromoanisole (0.25 mL) was added. The resulting colourless solution was stirred at room temperature for 30 minutes and became slightly turbid. All volatiles were then removed under vacuum to give a white, waxy solid. This was then suspended in 2 mL hexane and solubilised with 2 mL of dry toluene with gentle heating applied. Slow cooling to room temperature resulted in a crop of colourless crystals – dimeric compound 1a. Yield: 165 mg, 22%. <sup>1</sup>H-NMR (300.1 MHz, D<sub>8</sub>-Tol, 298 K): δ / ppm = 8.06 (d, 4H, C-*H*<sub>ortho</sub>), 7.20 (t, 4H, C-*H*<sub>meta</sub>), 7.12 (t, 4H, C-*H*<sub>para</sub> + D<sub>8</sub>-Tol), 6.67 (d, 4H, C-*H*<sub>meta</sub>), 3.80 (m, 4H, OCH<sub>2</sub>, OR'), 3.31 (s, 12H, OMe, Ar), 1.52 (m, 2H, C-*H*, OR'), 1.34-0.91 (m, 16H, CH<sub>2</sub> (Et), (CH<sub>2</sub>)<sub>3</sub>, OR'), 0.73 (t, 6H, CH<sub>3</sub>, Et, OR'), 0.65 (t, 6H, CH<sub>3</sub>, OR'). <sup>7</sup>Li-NMR (156 MHz, D<sub>8</sub>-Tol, 298 K): δ / ppm = 1.41 [LiMgAr<sub>2</sub>(OR')]<sub>2</sub>. <sup>13</sup>C{<sup>1</sup>H}-NMR (75.5 MHz, D<sub>8</sub>-Tol, 298 K): δ / ppm = 166.3 (C<sub>q</sub>-OMe), 150.9 (C<sub>q</sub>-Mg), 143.2 (C<sub>Ar</sub>-H), 127.4 (C<sub>Ar</sub>-H), 123.3 (C<sub>Ar</sub>-H), 123.3 (C<sub>Ar</sub>-H), 109.4 (C<sub>Ar</sub>-H), 66.6 (OCH<sub>2</sub>, OR'), 55.9 (OMe, Ar), 44.3 (C-*H*, OR), 31.1 (CH<sub>2</sub>, Et, OR'), 29.4 (CH<sub>2</sub>, OR'), 24.0 (CH<sub>2</sub>, OR'), 23.4 (CH<sub>2</sub>, OR'), 14.2 (CH<sub>3</sub>, Et, OR'), 11.0 (CH<sub>3</sub>, OR'). This compound crystallises with a molecule of toluene, however, this is not present in the final spectra or

elemental analysis results. Anal. calcd. for  $C_{44}H_{62}Li_2Mg_2O_6$ : C, 70.51; H, 8.34. Found: C, 70.56; H, 8.42.

**Note:** NMR spectroscopic analysis of the filtrate of compound **1a** revealed the presence of residual compound **1a** and free LiOR' visible by both  $^1H$  and  $^{13}C\{^1H\}$  NMR spectra

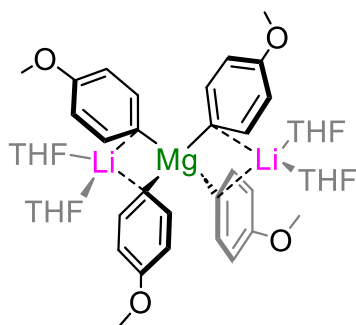
Synthesis of  $[LiMgAr_2(OR')]_2$  (Ar = *o*-NMe<sub>2</sub>-C<sub>6</sub>H<sub>4</sub>) (**1b**)



In an argon-flushed Schlenk flask, 1 mmol of the exchange reagent was prepared from  $Mg(OR')_2$  and two equivalents of *s*BuLi (or from *s*Bu<sub>2</sub>Mg + *n*LiOR' (*n* = 1 or 2)). Once reconstituted in 5 mL toluene to achieve a pale yellow solution, 2 mmol of 2-bromo-*N,N*-dimethylaniline (0.29 mL) was added. The resulting colourless solution was stirred at room temperature for 30 minutes and became slightly turbid. All volatiles were then removed under vacuum to give a white, waxy solid. This was then suspended in 3 mL hexane and solubilised with dropwise addition of THF with gentle heating applied. Slow cooling to room temperature resulted in a crop of colourless crystals – compound **1b**. Yield: 185 mg, 23%. Anal. calcd. for  $C_{48}H_{76}Li_2Mg_2N_4O_2$ : C, 71.74; H, 9.53; N, 6.97. Found: C, 71.02; H, 9.63; N, 6.65.  $^1H$ -NMR (300.1 MHz, D<sub>8</sub>-Tol, 298 K):  $\delta$  / ppm = 8.08 (m, 4H, C-*H*<sub>ortho</sub>), 7.22 (m, 4H, C-*H*<sub>meta</sub>), 7.13-7.09 (m, 4H, C-*H*<sub>para</sub> + D<sub>8</sub>-Tol), 6.89 (d, 4H, C-*H*<sub>meta</sub>), 4.06 (d, 4H, OCH<sub>2</sub>, OR), 2.35 (t, 24H, NMe<sub>2</sub>, Ar), 1.54 (m, 2H, C-*H*, OR), 1.37-0.91 (m, 16H, CH<sub>2</sub> (Et), (CH<sub>2</sub>)<sub>3</sub>, OR), 0.83 (t, 6H, CH<sub>3</sub>, Et, OR), 0.63 (t, 6H, CH<sub>3</sub>, OR).  $^7Li$ -NMR (156 MHz, D<sub>8</sub>-Tol, 298 K):  $\delta$  / ppm = 1.22  $[LiMg(OR)Ar_2]_2$ .  $^{13}C\{^1H\}$ -NMR (75.5 MHz, D<sub>8</sub>-Tol, 298 K):  $\delta$  / ppm = 161.2 (C<sub>Ar</sub>-Mg), 142.8 (C<sub>Ar</sub>-H), 126.9 (C<sub>Ar</sub>-H), 123.8 (C<sub>Ar</sub>-H), 114.7 (C<sub>Ar</sub>-H), 68.9 (OCH<sub>2</sub>, OR), 47.3 (NMe<sub>2</sub>, Ar), 43.8 (C-*H*, OR), 30.9 (CH<sub>2</sub>, Et, OR), 29.8 (CH<sub>2</sub>, OR), 24.0 (CH<sub>2</sub>, OR), 23.5 (CH<sub>2</sub>, OR), 14.5 (CH<sub>3</sub>, Et, OR), 11.3 (CH<sub>3</sub>, OR).

### 2.5.3 Synthesis of Tetra(aryl) Lithium Magnesiates [Li<sub>2</sub>Mg(Ar)<sub>4</sub>] 2a-b, 6

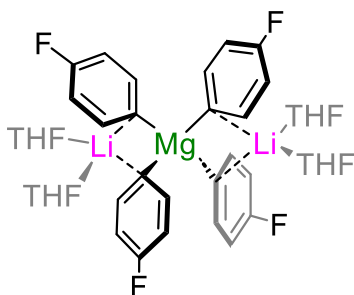
#### Synthesis of [Li<sub>2</sub>MgAr<sub>4</sub>·(THF)<sub>4</sub>] (Ar = *p*-OMe-C<sub>6</sub>H<sub>4</sub>) (2a)



In an argon-flushed Schlenk flask, 1 mmol of the exchange reagent was prepared from Mg(OR')<sub>2</sub> and two equivalents of *s*BuLi (or from *s*Bu<sub>2</sub>Mg + *n*LiOR' (*n* = 1 or 2)). Once reconstituted in 5 mL toluene to achieve a pale-yellow solution, 2 mmol of 4-bromoanisole (0.25 mL) was added at -10 °C, resulting in a white suspension after approximately 10 minutes, which was then warmed to room temperature and stirred for one hour. After filtration of the supernatant, the remaining white solid was suspended in 3 mL hexane and solubilised with dropwise addition of dry THF and gentle heating applied. Slow cooling to room temperature resulted in a crop of colourless crystals – compound **2a**. Yield: 100 mg, 21%. <sup>1</sup>H-NMR (300.1 MHz, D<sub>8</sub>-THF, 298 K): δ / ppm = 7.77 (d, 8H, C-*H*<sub>ortho</sub>), 6.55 (d, 8H, C-*H*<sub>meta</sub>), 3.61 (THF), 3.66 (s, 12H, OMe, Ar), 1.78 (THF). <sup>7</sup>Li-NMR (156 MHz, D<sub>8</sub>-THF, 298 K): δ / ppm = -0.21 (s, Li<sub>2</sub>MgAr<sub>4</sub>, **32**). <sup>13</sup>C{<sup>1</sup>H}-NMR (75.5 MHz, D<sub>8</sub>-THF, 298 K): δ / ppm = 158.1 (C<sub>q</sub>-OMe), 144.0 (C<sub>q</sub>-Mg), 111.6 (C<sub>ortho</sub>-H + C<sub>meta</sub>-H), 68.0 (THF), 54.3 (OMe, Ar), 26.2 (THF).

**Note:** Despite the moderate crystalline yield, repeating the reaction on a bulk scale and performing a hydrolysis step reveals an 83% yield of Mg/Br exchange as determined by GC against 20 mol% C<sub>6</sub>Me<sub>6</sub>.

#### Synthesis of [Li<sub>2</sub>MgAr<sub>4</sub>·(THF)<sub>4</sub>] (Ar = *p*-F-C<sub>6</sub>H<sub>4</sub>) (2b)

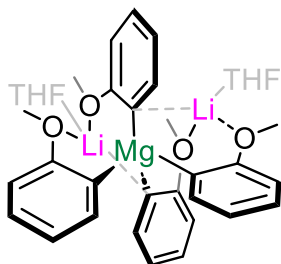


In an argon-flushed Schlenk flask, 1 mmol of the exchange reagent was prepared from Mg(OR')<sub>2</sub> and two equivalents of *s*BuLi (or from *s*Bu<sub>2</sub>Mg + *n*LiOR' (*n* = 1 or 2)). Once reconstituted in 5 mL toluene to achieve a pale-yellow solution, 2 mmol of 1-fluoro-4-bromobenzene (0.22 mL) was added at -10 °C. The resulting pale-yellow solution was stirred at this temperature for one hour. The reaction was allowed to warm to room temperature and stirred for a further one hour. All volatiles were then removed under vacuum to give a yellow oil. Addition of 3 mL of hexane to this oil immediately afforded a white solid to crash from solution and this mixture was allowed to stir for a further one hour. The white solid was then isolated via cannula filtration and dried under vacuum (250 mg, 60%). This solid was then recrystallised from 3 mL of hexane and solubilised with dropwise addition of THF with gentle heating applied. Slow cooling to room temperature resulted in a crop of colourless



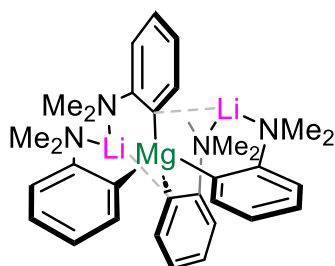
crystals – compound **3b**. Yield: 100 mg, 15%. Anal. calcd. for  $C_{40}H_{48}F_4Li_2MgO_4$ , 67.95; H, 6.84. Found: C, 67.23; H, 7.83.  $^1H$ -NMR (300.1 MHz,  $D_8$ -THF, 298 K):  $\delta$  / ppm = 7.79 (d, 8H,  $C_{Ar-H}$ ), 6.60 (d, 8H,  $C_{Ar-H}$ ), 3.58 (THF), 1.74 (THF).  $^7Li$ -NMR (156 MHz,  $D_8$ -THF, 298 K):  $\delta$  / ppm = -0.02 [(THF) $_4$ Li $_2$ MgAr $_4$ ].  $^{19}F$ -NMR (282.4 MHz,  $D_8$ -THF, 298 K):  $\delta$  / ppm = -123.69 (br. tt,  $C_q-F$ ).  $^{13}C\{^1H\}$ -NMR (75.5 MHz,  $D_8$ -THF, 298 K):  $\delta$  / ppm = 172.7 ( $C_q$ -Mg), 163.8-160.2 (d,  $C_q-F$ ,  $^2J$  = 235.30 Hz), 142.6 ( $C_{Ar-H}$ ), 111.6 ( $C_{Ar-H}$ ), 68.4 (THF), 26.4 (THF).

#### Synthesis of $[Li_2MgAr_4 \cdot (THF)_2]$ (Ar = *o*-OMe- $C_6H_4$ ) (**6**)



In an argon-flushed Schlenk flask, 1 mmol of  $Li_2Mg_5Bu_4$  (**II**) was prepared and stirred at room temperature for one hour before removing all volatiles under reduced pressure. To this, four equivalents of 2-bromoanisole (4 mmol, 0.5 mL) resulting in a thick white suspension. After one hour at room temperature, all volatiles were removed under reduced pressure and the resulting white solid suspended in 5 mL of hexane. Solubility was gained upon the addition of 5 mL of THF and application of gentle heating. Controlled cooling to room temperature resulted in a crop of colourless crystals – compound **6**. Yield, 195 mg, 32%.  $^1H$ -NMR (300.1 MHz,  $D_8$ -THF, 298 K):  $\delta$  / ppm = 7.74 (d, 4H,  $C_{Ar-H}$ ), 6.88 (td, 4H,  $C_{Ar-H}$ ), 6.69 (t, 4H,  $C_{Ar-H}$ ), 6.61 (d, 4H,  $C_{Ar-H}$ ), 3.61 (THF), 3.58 (s, 12H, OMe), 1.77 (THF).  $^7Li$ -NMR (156 MHz,  $D_8$ -THF, 298 K):  $\delta$  / ppm = -1.14 ( $Li_2MgAr_4$ , **34**).  $^{13}C\{^1H\}$ -NMR (75.5 MHz,  $D_8$ -THF, 298 K):  $\delta$  / ppm = 168.5 ( $C_q$ -OMe), 161.9 ( $C_q$ -Mg), 143.9 ( $C_{Ar-H}$ ), 125.4 ( $C_q$ -H), 121.8 ( $C_{Ar-H}$ ), 110.2 ( $C_{Ar-H}$ ), 68.0 (THF), 56.9 (OMe), 26.2 (THF).

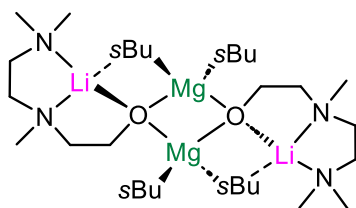
#### Synthesis of $[Li_2MgAr_4 \cdot (THF)_2]$ (Ar = *o*-NMe $_2$ - $C_6H_4$ )



In an argon-flushed Schlenk flask, 1 mmol of  $Li_2Mg_5Bu_4$  (**II**) was prepared and stirred at room temperature for one hour before removing all volatiles under reduced pressure. To this, four equivalents of 2-bromodimethylaniline (4 mmol, 0.58 mL) resulting in a thick white suspension. After one hour at room temperature, all volatiles were removed under reduced pressure and the resulting white solid suspended washed with hexane (2 x 10 mL). White precipitate confirmed as  $[Li_2MgAr_4 \cdot (THF)_2]$  (Ar = *o*-NMe $_2$ - $C_6H_4$ ) by NMR spectroscopy. Yield, 300 mg, 58%.  $^1H$ -NMR (300.1 MHz,  $D_8$ -THF, 298 K):  $\delta$  / ppm = 7.80 (m, 4H,  $C_{Ar-H}$ ), 6.83 (m, 8H,  $C_{Ar-H}$ ), 6.62 (m, 4H,  $C_{Ar-H} \times 2$ ), 2.65 (s, 24H, NMe $_2$ ).  $^7Li$ -NMR (156 MHz,  $D_8$ -THF, 298 K):  $\delta$  / ppm = 0.96 [ $Li_2MgAr_4$ ].  $^{13}C\{^1H\}$ -NMR (75.5 MHz,  $D_8$ -THF, 298 K):  $\delta$  / ppm = 162.7 ( $C_q$ -NMe $_2$ ), 129.43 ( $C_q$ -Mg), 128.6 ( $C_{Ar-H}$ ), 125.1 ( $C_{Ar-H}$ ), 122.3 ( $C_{Ar-H}$ ), 114.4 ( $C_{Ar-H}$ ), 46.9 (NMe $_2$ ).

### 2.5.4 Synthesis of [LiMg<sub>2</sub>Bu<sub>2</sub>(OR)]<sub>2</sub> (OR = dmem) (**6**)

#### Synthesis of [LiMg<sub>2</sub>Bu<sub>2</sub>(OR)]<sub>2</sub> (OR = dmem) (**6**)

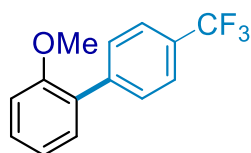


In an argon-filled Schlenk-flask, 1mmol of Li(dmem) (synthesis and characterisation described in **Chapter 3**) was dissolved in 5 mL of dry hexane. To this, 1 mmol of sBu<sub>2</sub>Mg (2.44 mL, 0.41 M in hexane) was added affording a thick, white suspension which was then allowed to stir at ambient

temperature for 1 hour to ensure complete co-complexation. Gentle heating of this mixture then afforded a colourless solution which deposited a crop of colourless block crystals upon slow cooling to room temperature. Analysis of these by X-ray crystallography proved them to be the dimeric co-complex **5**. Yield: 201 mg, 35%. Anal. calcd. for C<sub>30</sub>H<sub>66</sub>Li<sub>2</sub>Mg<sub>2</sub>N<sub>4</sub>O<sub>2</sub>: C, 61.98; H, 12.14; N, 9.64. Found: C, 61.59; H, 12.02; N, 10.03. <sup>1</sup>H-NMR (300.1 MHz, D<sub>8</sub>-Tol, **298 K**):<sup>‡</sup> δ / ppm = 4.09-3.61 (m, 2H, OCH<sub>2</sub>, OR), 2.52-1.7 (br. m, 19H, CH<sub>2</sub>, sBu + CH<sub>2</sub> and CH<sub>3</sub>, OR), 1.73 (br. d, CH<sub>3</sub>, sBu<sub>2</sub>Mg), 1.66 (br. m, CH<sub>2</sub>, sBu bridging), 1.56 (br. m, CH<sub>2</sub>, sBu terminal), 1.37 (t x 2, 6H, CH<sub>3</sub>, sBu of sBu<sub>2</sub>Mg and compound **37** bridging and terminal), -0.11 (CH, sBu, sBu<sub>2</sub>Mg), -0.33 (CH, sBu, terminal), -0.66 (CH, sBu, bridging). <sup>7</sup>Li-NMR (156 MHz, D<sub>8</sub>-Tol, **298 K**): δ / ppm = 0.49 [LiMg<sub>2</sub>Bu<sub>2</sub>(OR)]<sub>2</sub>. <sup>13</sup>C{<sup>1</sup>H}-NMR (75.5 MHz, D<sub>8</sub>-Tol, **298 K**):<sup>‡</sup> δ / ppm = 60.5 (OCH<sub>2</sub>CH<sub>2</sub>, OR), 59.3 (OCH<sub>2</sub>), 56.8 (CH<sub>2</sub>, OR), 53.5 (CH<sub>2</sub>, OR), 45.6 (CH<sub>3</sub>, OR), 43.1 (CH<sub>3</sub>, OR), 34.0 (CH<sub>2</sub>, sBu, bridging), 32.7 (CH<sub>2</sub>, sBu, terminal), 31.9 (CH<sub>2</sub>, sBu, sBu<sub>2</sub>Mg), 23.2 (CH<sub>3</sub>, sBu<sub>2</sub>Mg + sBu bridging), 21.2 (CH<sub>3</sub>, sBu terminal), 20.0 (CH, sBu, sBu<sub>2</sub>Mg), 19.3 (CH, sBu terminal), 18.8 (CH, sBu bridging), 17.8 (CH<sub>3</sub>, sBu, sBu<sub>2</sub>Mg), 17.1 (CH<sub>3</sub>, sBu, bridging), 16.9 (CH<sub>3</sub>, sBu, terminal). ‡ = Confirmed by [<sup>1</sup>H,<sup>1</sup>H]-COSY and [<sup>1</sup>H,<sup>13</sup>C]-HSQC NMR spectra

### 2.5.5 Electrophilic functionalisation studies

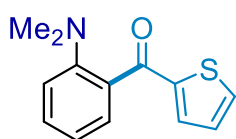
#### Synthesis of 2-methoxy-4'-(trifluoromethyl)-1,1'-biphenyl (**3a**)



In an argon-flushed Schlenk flask, 0.6 mmol of the exchange reagent was prepared from Mg(OR')<sub>2</sub> and two equivalents of sBuLi. To this, 0.5 mmol of 2-bromoanisole (65 μL) was added at room temperature in toluene. After stirring at 25 °C for 30 min, ZnCl<sub>2</sub> (1.00 M in THF, 0.65 mL, 0.65 mmol), Pd(OAc)<sub>2</sub> (5 mg, 4 mol%), SPhos (17 mg, 8 mol%) and 1-iodo-4-(trifluoromethyl)benzene (109 mg, 0.40 mmol) were added and the reaction mixture was stirred at room temperature overnight. After work-up, the crude product was purified *via* column chromatography (*isohexane*, R<sub>f</sub> = 0.27) to give the product **3a** (84 mg, 333 μmol, 83%

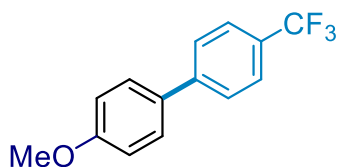
yield) as a colourless oil. **<sup>1</sup>H-NMR (400 MHz, CDCl<sub>3</sub>, 298K)** δ / ppm = 7.67 (m, 4H), 7.44 – 7.29 (m, 2H), 7.12 – 6.96 (m, 2H), 3.84 (s, 3H). **<sup>13</sup>C-NMR (101 MHz, CDCl<sub>3</sub>, 298K)** δ / ppm = 156.6, 142.4 (d, *J* = 1.5 Hz), 130.9, 130.0, 129.6, 129.4, 129.0 (q, *J* = 32.3 Hz), 125.0 (q, *J* = 3.8 Hz), 124.5 (q, *J* = 271.8 Hz), 121.1, 111.5, 55.7. **<sup>19</sup>F-NMR (375 MHz, CDCl<sub>3</sub>, 298K)** δ / ppm = -62.4. IR (ATR, cm<sup>-1</sup>)  $\tilde{\nu}$  = 1616, 1600, 1586, 1488, 1464, 1437, 1404, 1321, 1298, 1263, 1239, 1161, 1118, 1106, 1067, 1056, 1027, 1007, 855, 840, 803, 752, 731, 716. MS (EI, 70 eV, %) *m/z* = 253 (15), 252 (100), 251 (12), 237 (17), 233 (11), 217 (71), 188 (12), 183 (15), 168 (61), 139 (19), 118 (12). HRMS (EI, 70 eV) *m/z*: calc. for C<sub>14</sub>H<sub>11</sub>OF<sub>3</sub>: 252.0762; found 252.0757.

#### Synthesis of (2-(azaneyl)phenyl)(thiophen-2-yl)methanone (**3b**)



In an argon-flushed Schlenk flask, 0.6 mmol of the exchange reagent was prepared from Mg(OR')<sub>2</sub> and two equivalents of *s*BuLi. To this, 0.5 mmol of 2-bromodimethylaniline (72 μL) was added at room temperature in toluene. After stirring at 25 °C for 30 min, *N*-methoxy-*N*-methylthiophene-2-carboxamide (103 mg, 0.60 mmol) was added and the reaction mixture was stirred at room temperature overnight. After work-up, the crude product was purified *via* column chromatography (isohexane:ethyl acetate = 96:4, R<sub>f</sub> = 0.17) to give the product **4b** (65 mg, 281 μmol, 56% yield) as a yellow oil. **<sup>1</sup>H-NMR (400 MHz, CDCl<sub>3</sub>, 298K)** δ / ppm = 7.67 (dd, *J* = 4.9, 1.2 Hz, 1H), 7.54 (dd, *J* = 3.8, 1.2 Hz, 1H), 7.38 (td, *J* = 7.5, 1.6 Hz, 2H), 7.10 (dd, *J* = 4.9, 3.8 Hz, 1H), 6.99 (d, *J* = 8.1 Hz, 1H), 6.89 (t, *J* = 7.6 Hz, 1H), 2.80 (s, 6H). **<sup>13</sup>C-NMR (101 MHz, CDCl<sub>3</sub>, 298K)** δ / ppm = 190.3, 151.1, 144.9, 134.7, 134.2, 131.6, 130.4, 129.0, 128.0, 118.6, 116.6, 43.6. IR (ATR, cm<sup>-1</sup>)  $\tilde{\nu}$  = 2934, 2866, 2799, 1634, 1594, 1562, 1497, 1450, 1431, 1410, 1354, 1300, 1284, 1265, 1230, 1217, 1163, 1144, 1096, 1043, 954, 881, 842, 753, 725. MS (EI, 70 eV, %) *m/z* = 231 (29), 215 (13), 214 (100), 199 (64), 198 (87), 184 (20), 181 (21), 132 (10), 97 (14). HRMS (EI, 70 eV) *m/z*: calc. for C<sub>13</sub>H<sub>13</sub>NOS: 231.0718; found: 231.0712.

#### Synthesis of 4-methoxy-4'-(trifluoromethyl)-1,1'-biphenyl (**4a**)

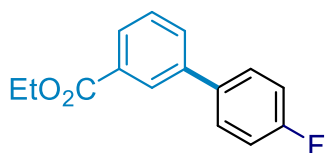


In an argon-flushed Schlenk flask, 0.6 mmol of the exchange reagent was prepared from Mg(OR')<sub>2</sub> and two equivalents of *s*BuLi. To this, 0.5 mmol of 2-bromoanisole (65 μL) was added at room temperature in toluene. To this, 0.5 mmol of 4-bromoanisole (63 μL) was added at room temperature. After stirring at 25 °C for 30 min, ZnCl<sub>2</sub> (1.00 M in THF, 0.65 mL, 0.65 mmol), Pd(OAc)<sub>2</sub> (5 mg, 4 mol%), SPhos (17 mg, 8 mol%) and 1-iodo-4-(trifluoromethyl)benzene (109 mg, 0.40 mmol) were added and the reaction mixture was stirred at room temperature overnight. After work-up, the crude product was

purified *via* column chromatography (isohexane:ethyl acetate = 99:1,  $R_f = 0.24$ ) to give the product **4a** (63 mg, 250  $\mu\text{mol}$ , 62% yield) as a white solid.

**$^1\text{H-NMR}$  (400 MHz,  $\text{CDCl}_3$ , 298K)**  $\delta$  / ppm = 7.66 (d,  $J = 1.8$  Hz, 4H), 7.55 (d,  $J = 8.8$  Hz, 2H), 7.01 (d,  $J = 8.9$  Hz, 2H), 3.87 (s, 3H).  **$^{13}\text{C-NMR}$  (101 MHz,  $\text{CDCl}_3$ , 298K)**  $\delta$  / ppm = 160.0, 144.4 (d,  $J = 1.3$  Hz), 132.3, 128.8 (q,  $J = 32.5$  Hz), 128.5, 127.0, 125.8 (q,  $J = 3.8$  Hz), 124.5 (q,  $J = 271.8$  Hz), 114.6, 55.5.  **$^{19}\text{F-NMR}$  (375 MHz,  $\text{CDCl}_3$ , 298K)**  $\delta$  / ppm = -62.3. **IR (ATR,  $\text{cm}^{-1}$ )**  $\tilde{\nu} = 2970, 2930, 2868, 1652, 1606, 1584, 1494, 1464, 1412, 1384, 1374, 1306, 1280, 1242, 1232, 1152, 1132, 1104, 1042, 1024, 978, 942, 912, 836, 814, 764, 742, 694$ . **MS (EI, 70 eV, %)**  $m/z = 253$  (15), 252 (100), 237 (44), 209 (67), 188 (10), 183 (14). **HRMS (EI, 70 eV)**  $m/z$ : calc. for  $\text{C}_{14}\text{H}_{11}\text{OF}_3$ : 252.0762; found 252.0757.

#### Synthesis of ethyl 4'-fluoro-[1,1'-biphenyl]-3-carboxylate (**4b**)



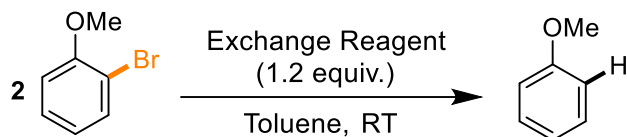
To this, 0.5 mmol of 1-bromo-4-fluorobenzene (55  $\mu\text{L}$ ) was added at room temperature. After stirring at 25  $^\circ\text{C}$  for 30 min,  $\text{ZnCl}_2$  (1.00 M in THF, 0.65 mL, 0.65 mmol),  $\text{Pd}(\text{OAc})_2$  (5 mg, 4 mol%), SPhos (17 mg, 8 mol%) and ethyl 3-iodobenzoate (110 mg, 0.40 mmol) were added and the reaction solution was stirred at room temperature overnight. After work-up, the crude product was purified *via* column chromatography (isohexane:ethyl acetate = 19:1,  $R_f = 0.45$ ) to give the product **4b** (75 mg, 307  $\mu\text{mol}$ , 77% yield) as a pale yellow oil.  **$^1\text{H-NMR}$  (400 MHz,  $\text{CDCl}_3$ , 298K)**  $\delta$  / ppm = 8.35 – 8.13 (m, 1H), 8.02 (ddd,  $J = 7.8, 1.7, 1.2$  Hz, 1H), 7.80 – 7.72 (m, 1H), 7.63 – 7.55 (m, 2H), 7.51 (td,  $J = 7.7, 0.5$  Hz, 1H), 7.19 – 7.10 (m, 2H), 4.41 (q,  $J = 7.1$  Hz, 2H), 1.42 (t,  $J = 7.1$  Hz, 3H).  **$^{13}\text{C-NMR}$  (101 MHz,  $\text{CDCl}_3$ , 298K)**  $\delta$  / ppm = 166.6, 162.9 (d,  $J = 247.1$  Hz), 140.6, 136.5 (d,  $J = 3.2$  Hz), 131.4, 131.3, 129.0 (d,  $J = 3.9$  Hz), 128.9, 128.5, 128.2, 115.9 (d,  $J = 21.5$  Hz), 61.3, 14.5.  **$^{19}\text{F-NMR}$  (375 MHz,  $\text{CDCl}_3$ , 298K)**  $\delta$  / ppm = -115.0. **IR (ATR,  $\text{cm}^{-1}$ )**  $\tilde{\nu} = 2982, 1714, 1608, 1598, 1584, 1514, 1478, 1440, 1392, 1368, 1304, 1268, 1236, 1172, 1158, 1108, 1084, 1042, 1012, 1000, 958, 928, 914, 892, 860, 836, 816, 754, 734, 716, 692, 664$ . **MS (EI, 70 eV, %)**  $m/z = 244$  (47), 216 (35), 200 (12), 199 (100), 171 (49), 170 (100), 169 (10), 85 (11). **HRMS (EI, 70 eV)**  $m/z$ : calc. for  $\text{C}_{15}\text{H}_{13}\text{O}_2\text{F}$ : 244.0900; found 244.0895.

## 2.5.6 GC reaction monitoring

### Mg/Br exchange of 2-bromoanisole with different exchange reagents

Exchange reagents prepared as described in **Section 2.5**. 2-Bromoanisole (1.67 e.q, 1.67 mL, 1.0 M in toluene containing 20 mol%  $\text{C}_6\text{Me}_6$ ) was then added at room temperature and stirred

for 40 minutes. The reaction was then quenched with 10 mL of sat. aq.  $\text{NH}_4\text{Cl}$  solution and extracted with ethyl acetate (1x 25mL, 2x 20 mL). The combined organic extracts were washed with brine (1 x 10 mL), dried over  $\text{MgSO}_4$  and filtered. A 50  $\mu\text{L}$  aliquot was diluted in 1 mL of ethyl acetate, filtered and then analysed by GC using an internal calibration curve.



Exchange Reagent	Time [min]	Yield [%]
$\text{Mg}(\text{OR})_2 + 2 \text{ sBuLi}$	40	>99
$\text{sBu}_2\text{Mg} + 2 \text{ LiOR}$	40	>99
$\text{sBu}_2\text{Mg} + \text{LiOR}$	40	>99
$\text{LiMg sBu}_2(\text{dmem})$ ( <b>5</b> ) (isolated crystals)	40	20
$\text{sBu}_2\text{Mg}$	40	5
$\text{sBu}_2\text{Mg} + \text{LiOR} + 1.5 \text{ Mg}(\text{OR})_2$	40	0
$\text{Li}_2\text{Mg sBu}_4$ ( <b>II</b> )	40	>99

## 2.6 References

- 1 L. J. Bole and E. Hevia, *Nat. Synth.*, 2022, **1**, 195–202.
- 2 D. S. Ziegler, B. Wei and P. Knochel, *Chem. Eur. J.*, 2019, **25**, 2695–2703.
- 3 J. Farkas, S. J. Stoudt, E. M. Hanawalt, A. D. Pajerski and H. G. Richey, *Organometallics*, 2004, **23**, 423–427.
- 4 C. G. Screttas and B. R. Steele, *J. Org. Chem.*, 1989, **54**, 1013–1017.
- 5 D. S. Ziegler, K. Karaghiosoff and P. Knochel, *Angew. Chem. Int. Ed.*, 2018, **57**, 6701–6704.
- 6 A. Desaintjean, T. Haupt, L. J. Bole, N. R. Judge, E. Hevia and P. Knochel, *Angew. Chem. Int. Ed.*, 2021, **60**, 1513–1518.
- 7 C. Yeardley, A. R. Kennedy, P. C. Gros, S. Touchet, M. Fairley, R. McLellan, A. J. Martínez-Martínez and C. T. O'Hara, *Dalton Trans.*, 2020, **49**, 5257–5263.
- 8 P. C. Gros and Y. Fort, *European J. Org. Chem.*, 2009, 4199–4209.
- 9 A. Doudouh, C. Woltermann and P. C. Gros, *J. Org. Chem.*, 2007, **72**, 4978–4980.
- 10 M. Balkenhohl, D. S. Ziegler, A. Desaintjean, L. J. Bole, A. R. Kennedy, E. Hevia and P. Knochel, *Angew. Chem. Int. Ed.*, 2019, **58**, 12898–12902.
- 11 L. J. Bole, Exploiting Chemical Cooperativity in Main-Group Organometallics for C-C, C-N, C-H Bond Formation and C-Halogen Functionalisation, University of Bern, 2020.
- 12 C. Bakewell, A. J. P. White and M. R. Crimmin, *J. Am. Chem. Soc.*, 2016, **138**, 12763–12766.
- 13 W. Clegg, B. Conway, P. García-Álvarez, A. R. Kennedy, R. E. Mulvey, L. Russo, J. Sassmannshausen and T. Tuttle, *Chem. Eur. J.*, 2009, **15**, 10702–10706.
- 14 D. R. Armstrong, A. R. Kennedy, R. E. Mulvey and R. B. Rowlings, *Angew. Chem. Int. Ed.*, 1999, **38**, 131–133.
- 15 J. Francos, P. C. Gros, A. R. Kennedy and C. T. O'Hara, *Organometallics*, 2015, **34**, 2550–2557.
- 16 W. Langham, R. Q. Brewster and H. Gilman, *J. Am. Chem. Soc.*, 1941, **63**, 545–549.
- 17 P. Beak and V. Snieckus, *Acc. Chem. Res.*, 1982, **15**, 306–312.

- 18 M. C. Whisler, S. MacNeil, V. Snieckus and P. Beak, *Angew. Chem. Int. Ed.*, 2004, **43**, 2206–2225.
- 19 M. Geissler, J. Kopf and E. Weiss, *Chem. Ber.*, 1989, **122**, 1395–1402.
- 20 E. Weiss, *Angew. Chemie Int. Ed. English*, 1993, **32**, 1501–1523.
- 21 L. M. Seitz and T. L. Brown, *J. Am. Chem. Soc.*, 1966, **88**, 4140–4147.
- 22 S. E. Baillie, W. Clegg, P. García-Álvarez, E. Hevia, A. R. Kennedy, J. Klett and L. Russo, *Chem. Commun.*, 2011, **47**, 388–390.
- 23 S. E. Baillie, W. Clegg, P. García-Álvarez, E. Hevia, A. R. Kennedy, J. Klett and L. Russo, *Organometallics*, 2012, **31**, 5131–5142.
- 24 P. C. Andrikopoulos, D. R. Armstrong, E. Hevia, A. R. Kennedy, R. E. Mulvey and C. T. O. Hara, 2005, 1131–1133.
- 25 R. E. Mulvey, *Chem. Soc. Rev.*, 1991, **20**, 167.
- 26 A. Downard and T. Chivers, *Eur. J. Inorg. Chem.*, 2001, 2193–2201.
- 27 W. Clegg, S. H. Dale, D. V. Graham, R. W. Harrington, E. Hevia, L. M. Hogg, A. R. Kennedy and R. E. Mulvey, *Chem. Commun.*, 2007, 1641–1643.
- 28 L. Shi, Y. Chu, P. Knochel and H. Mayr, *J. Org. Chem.*, 2009, **74**, 2760–2764.
- 29 O. Bayh, H. Awad, F. Mongin, C. Hoarau, F. Trécourt, G. Quéguiner, F. Marsais, F. Blanco, B. Abarca and R. Ballesteros, *Tetrahedron*, 2005, **61**, 4779–4784.
- 30 R. E. Mulvey, F. Mongin, M. Uchiyama and Y. Kondo, *Angew. Chem. Int. Ed.*, 2007, **46**, 3802–3824.
- 31 D. Catel, O. Payen, F. Chevallier, F. Mongin and P. C. Gros, *Tetrahedron*, 2012, **68**, 4018–4028.
- 32 L. Davin, A. Hernán-Gómez, C. McLaughlin, A. R. Kennedy, R. McLellan and E. Hevia, *Dalton Trans.*, 2019, **48**, 8122–8130.
- 33 H. Awad, F. Mongin, F. Trécourt, G. Quéguiner, F. Marsais, F. Blanco, B. Abarca and R. Ballesteros, *Tetrahedron Lett.*, 2004, **45**, 6697–6701.
- 34 M. De Tullio, A. M. Borys, A. Hernán-Gómez, A. R. Kennedy and E. Hevia, *Chem Catal.*, 2021, **1**, 1308–1321.
- 35 M. Fairley, L. Davin, A. Hernán-Gómez, J. García-Álvarez, C. T. O'Hara and E. Hevia, *Chem. Sci.*, 2019, **10**, 5821–5831.

- 36 J. M. Gil-Negrete and E. Hevia, *Chem. Sci.*, 2021, 1982–1992.
- 37 T. X. Gentner and R. E. Mulvey, *Angew. Chem. Int. Ed.*, 2021, **60**, 9247–9262.
- 38 A. Krasovskiy and P. Knochel, *Synthesis*, 2006, 890–891.



## Chapter 3: Assessing Alkali-Metal Effects in Mixed-Ligand Alkyl/Alkoxide Alkali-Metal Magnesiates Complexes

This Chapter is adapted from a publication in a peer reviewed journal:

*Assessing Alkali-Metal Effects in the Structures and Reactivity of Mixed-Ligand Alkyl/Alkoxide Alkali-Metal Magnesiates*, N. R. Judge, L. J. Bole and E. Hevia, *Chem. Eur. J.*, 2022, **28**, e2021041.



Contributing authors to the manuscript and their role:

Neil Judge: Designed and performed all experimental work, analysed and processed all data, wrote the first draft of the manuscript and the supporting information.

Leonie J. Bole: Synthesis and characterisation of compound **8** from a related project.

Eva Hevia: Principal Investigator, conceived the project, secured the funding, directed the work, and revised the final version of the manuscript with contributions from all authors.

### 3.1 Introduction

The unique activating effects of alkali-metal alkoxides when added to other s-block organometallics is a well-established phenomenon in polar organometallic chemistry (*Chapter 1*).<sup>1-4</sup> Typified by the LIC-KOR (Lochmann-Schlosser) superbases, combining potassium *tert*-butoxide with *n*-butyllithium greatly enhances the metalation capabilities of this mixture when compared to those of their monometallic counterparts.<sup>5-8</sup> This synergistic behavior has been attributed to the formation of mixed alkyl/alkoxy bimetallic  $[\text{LiK}(\text{OR}')\text{R}]_n$  aggregates though the true constitution of these species has remained a matter of debate for many years.<sup>9,10</sup> Using the more hydrocarbon soluble bimetallic combination, namely  $\text{NpLi/KO}^t\text{Bu}$  ( $\text{Np} = \text{Neopentyl}$ ), Klett has impressively structurally characterized the  $[\text{Li}_4\text{K}_4\text{Np}_3(\text{O}^t\text{Bu})_5]$  aggregate where the alkyl groups bind to both potassium and lithium leading to an intermediary bond polarity and distinct reactivity to those observed for alkyl potassium or alkyl lithium reagents (Figure 5 in *Chapter 1*).<sup>11</sup> The constitution of these bimetallic aggregates seems fluid with several species of distinct composition co-existing in solution.

These alkoxide-mediated activating effects are known beyond organolithium chemistry. Thus, early studies by Richey Jr have shown that various dialkylmagnesium reagents can effectively undergo Mg/halogen exchange reactions with several aryl bromides and iodides when Group 1 metal alkoxides are used as additives.<sup>12</sup> This boost in reactivity was attributed to the formation of more reactive triorganomagnesiates anions, although the role that the alkali-metal could play in these transformations was not really considered at the time. More recently, Knochel has exploited the synthetic utility of these alkyl/alkoxide systems combining  $s\text{Bu}_2\text{Mg}$  with two equivalents of  $\text{LiOR}'$  ( $\text{R}' = 2\text{-ethylhexyl}$ ) to promote fast and regioselective Mg/Br exchange of a wide range of aryl and heteroaryl bromides. The power of this approach has also been demonstrated by accomplishing more challenging Mg/Cl exchange of significantly less reactive aryl chlorides.<sup>13</sup> Further studies assessing Mg/Br exchanges on dibromo-substituted heterocyclic substrates have revealed that their regioselectivity is intimately connected to the presence of Lewis donors as additives.<sup>14</sup> Thus, when 2,5-dibromopyridine is reacted with  $s\text{Bu}_2\text{Mg} \cdot 2\text{LiOR}'$  selective activation of the C2 position is observed whereas the presence of one equivalent of PMDETA (*N,N,N',N'',N''*-pentamethyldiethylenetriamine) triggers a regioselectivity switch inducing selective Mg/Br exchange at the C5-position (Figure 1a).

Through isolation of key organometallic intermediates and NMR spectroscopic investigations, our collaborative work with Knochel has established that lithium and its coordinative saturation play a key role in controlling the regioselectivity of these reactions. Intrigued by these findings we took a closer look into the constitution of the exchange reagent,

uncovering the presence of a bimetallic Schlenk-type equilibrium between the mixed alkyl/alkoxy magnesiate  $[\text{LiMg}\text{sBu}_2(\text{OR}')]$  (**I**), alkyl rich  $[\text{Li}_2\text{Mg}\text{sBu}_4]$  (**II**) and magnesium alkoxide  $\text{Mg}(\text{OR}')_2$  (Figure 1b). Surprisingly, these studies suggest that  $[\text{Li}_2\text{Mg}\text{sBu}_4]$  (**II**) is the active species performing the Mg/Br exchange, the mixed alkyl/alkoxy magnesiate  $[\text{LiMg}\text{sBu}_2(\text{OR}')]$  (**I**) species is actually unreactive in this process.<sup>15</sup> Building on this work and inspired by recent studies in s-block bimetallic chemistry which have established the key mediating role played by the alkali-metal in main group heterobimetallic systems with applications in homogeneous catalysis,<sup>16–18</sup> organic synthesis<sup>19,20</sup> and small molecule activation processes,<sup>21</sup> here we extend our studies on mixed-alkyl/alkoxide alkali-metal magnesiate chemistry to sodium and potassium. By systematically changing the alkali-metal, we evaluate the constitution of these heterobimetallic systems in both solution and in the solid state and investigate their reactivity towards Mg/Br exchange reactions using 2-bromoanisole which has been chosen as a model substrate.

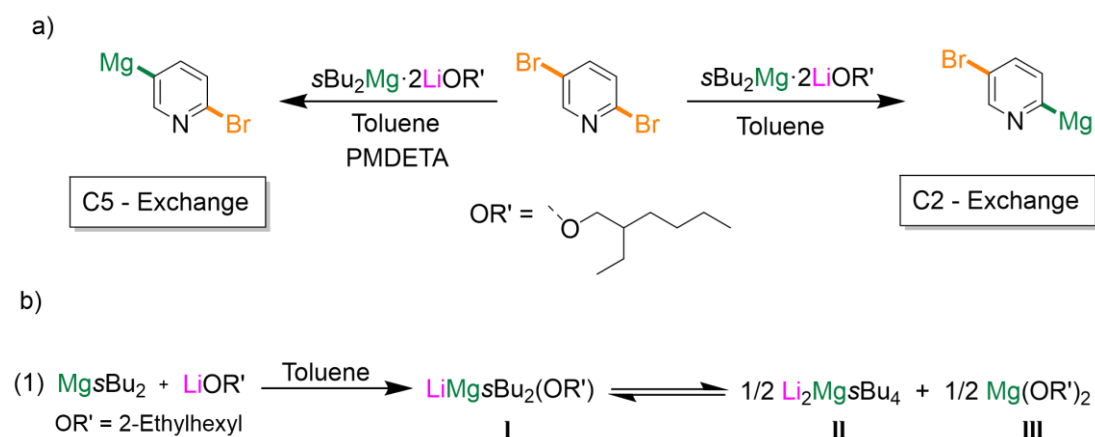


**Figure 1.** (a) Regioselectivity switch of Mg/Br exchange reactions of 2,5-dibromopyridine mediated by  $\text{sBu}_2\text{Mg} \cdot 2\text{LiOR}'$  combination. (b) Bimetallic Schlenk equilibrium for  $[\text{LiMg}\text{sBu}_2(\text{OR}')]$  (**I**).

### 3.2 Aims

Expanding on the knowledge acquired in *Chapter 2* when assessing the structural and reactivity implications of adding lithium alkoxides to dialkylmagnesium reagents, here we look to deepen our understanding of alkyl/alkoxide alkali metal magnesiates. In this *Chapter* we systematically investigate the use of sodium and potassium alkoxides. Our group, along with many others, has established in many cases clear alkali-metal effects in certain types of transformations such as deprotonative metalations and catalytic regimes when studying main group bimetallic compounds.<sup>16,18,22–24</sup> Thus, in this *Chapter* our focus was to probe how the alkali metal can influence not only the structure and composition of alkyl/alkoxide alkali-metal magnesiates but also their reactivity towards bromoarenes in Mg/Br exchange processes with particular focus on the metalated intermediates formed in these reactions.

### 3.3 Results and Discussion

#### 3.3.1 Synthesis and Characterisation of Mixed Alkyl/Alkoxy Alkali-Metal Magnesiates

An effective strategy to access heterobimetallic complexes is the combination (or more accurately co-complexation) of the required monometallic counterparts.<sup>25,26</sup> This approach has been successfully used by Mulvey for the synthesis of mixed alkyl/alkoxide [(TMEDA)MMg(O*t*Bu)*n*Bu<sub>2</sub>]<sub>2</sub> complexes by combining MO*t*Bu (M= Na, K) with *n*Bu<sub>2</sub>Mg in the presence of bidentate Lewis donor TMEDA (TMEDA= *N,N,N',N'*-tetramethylethylenediamine).<sup>27</sup> For our studies we chose the alkoxide derived from 2-{[2-(dimethylamino)ethyl] methylamino}ethanol (dmemH) which has already shown promise in lithium zincate chemistry<sup>28</sup> where the addition of 2 molar equivalents of Li(dmem) to Zn*n*Bu<sub>2</sub> allows the activation of both alkyl groups on zinc to promote challenging Zn/I and Zn/Br exchanges. Moreover, the two additional N-coordinating sites located in the backbone of the alkoxide ligand should allow for intramolecular stabilization of the alkali metals via chelation and subsequently preclude aggregation, which can also contribute towards the formation of kinetically more reactive species.

Homometallic M(dmem) (M= Li, **1**; Na, **2**; K, **3**) were prepared *in situ* by straightforward deprotonation of dmehH with MCH<sub>2</sub>SiMe<sub>3</sub> in hexane quantitatively forming the desired alkali metal alkoxides. In the case of [Li(dmem)]<sub>6</sub> **1** and [Na(dmem)]<sub>4</sub> **2** these alkoxides could be isolated as crystalline solids (85 and 87% yield respectively) and structurally authenticated in the solid state by X-ray crystallography (Figure 2). Lithium alkoxide **1** adopts a hexameric Li<sub>6</sub>O<sub>6</sub> aggregate boasting a hexagonal prism type structure via the central Li-O interactions (Figure 2, left). The tridentate alkoxide ligand uses just one of its N atoms to satisfy the coordination sphere of the alkali metal. The pendent nitrogen atom bearing two methyl groups does not partake in bonding and sits on the periphery of the central Li<sub>6</sub>O<sub>6</sub> core. In contrast, the heavier alkali metal sodium demands additional stabilisation from the alkoxide ligand owing to its larger size. The sodium atom in **2** is therefore chelated by all three donor atoms within the alkoxide ligand where both nitrogen atoms now form dative interactions to the alkali metal resulting in a tetrameric cubane structure with a Na<sub>4</sub>O<sub>4</sub> core (Figure 2, right). It should be noticed that hexameric and tetrameric arrangements as those shown by **1** and **2** are common motifs displayed by other alkali metal alkoxides, although external donor ligands like THF or TMEDA are typically present.<sup>29, 30</sup> The structure of these two alkoxides helps us to understand their excellent solubility in non-polar solvents such as hexane and toluene as the more ionic M<sub>x</sub>O<sub>x</sub> core is surrounded and sheltered by the rest of the chelating ligand with a more lipophilic character. This is in stark contrast to commonly

employed alkali metal alkoxides such as potassium *tert*-butoxide (KO*t*Bu) which require the addition of macrocyclic crown ethers to enhance their solubility in non-polar solvents.<sup>31</sup>

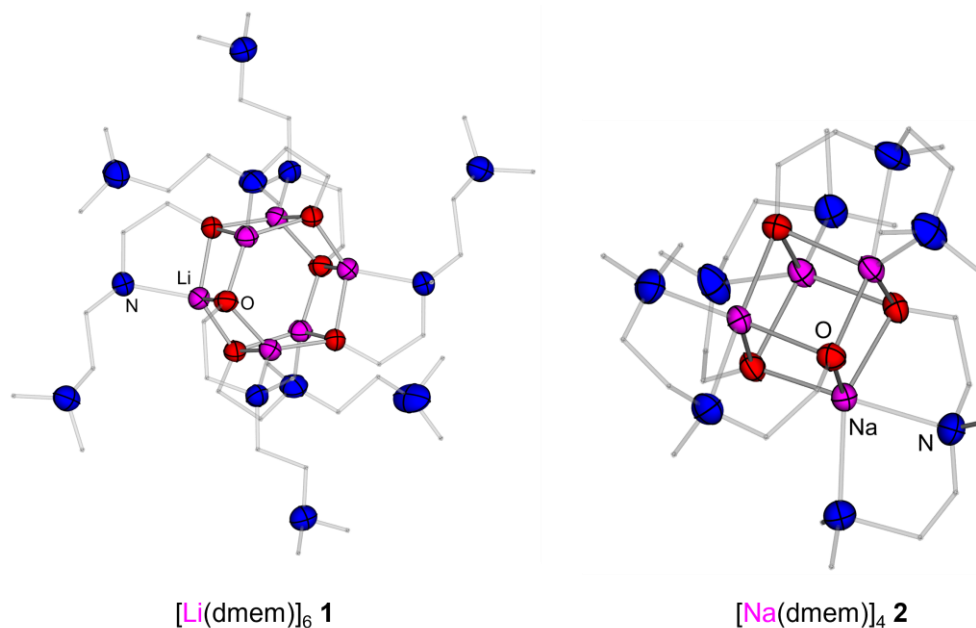


**Figure 2.** Molecular structures of **1** and **2** with displacement ellipsoids at 50% probability, all H atoms omitted, and with C atoms in alkoxide substituents drawn as wire frames for clarity.

Co-complexation reactions of equimolar amounts of M(dmef) and Mg(CH<sub>2</sub>SiMe<sub>3</sub>)<sub>2</sub> were then investigated (Figure 3). Lacking of β-hydrogens, this dialkyl(magnesium) offers more thermal stability than, for example, sBu<sub>2</sub>Mg<sup>32</sup> making the isolation of the organometallic intermediates more accessible. These reactions lead to the isolation of mixed alkyl/alkoxy alkali-metal magnesiates [MMg(CH<sub>2</sub>SiMe<sub>3</sub>)<sub>2</sub>(dmef)]<sub>2</sub> (M= Li, **4**; Na, **5**; (THF)K, **6**) (Figure 3) as crystalline solids in a 54, 35 and 29% yields respectively. While these isolated yields are moderate, NMR analysis of the reaction filtrates showed that they formed quantitatively. These mixed-metal species could also be prepared using a second co-complexation approach, by reacting heteroleptic [Mg(CH<sub>2</sub>SiMe<sub>3</sub>)(dmef)] (**7**) (obtained by deprotonation of dmef(H) with Mg(CH<sub>2</sub>SiMe<sub>3</sub>)<sub>2</sub> with the relevant alkali-metal alkyl MCH<sub>2</sub>SiMe<sub>3</sub> (Figure 3).

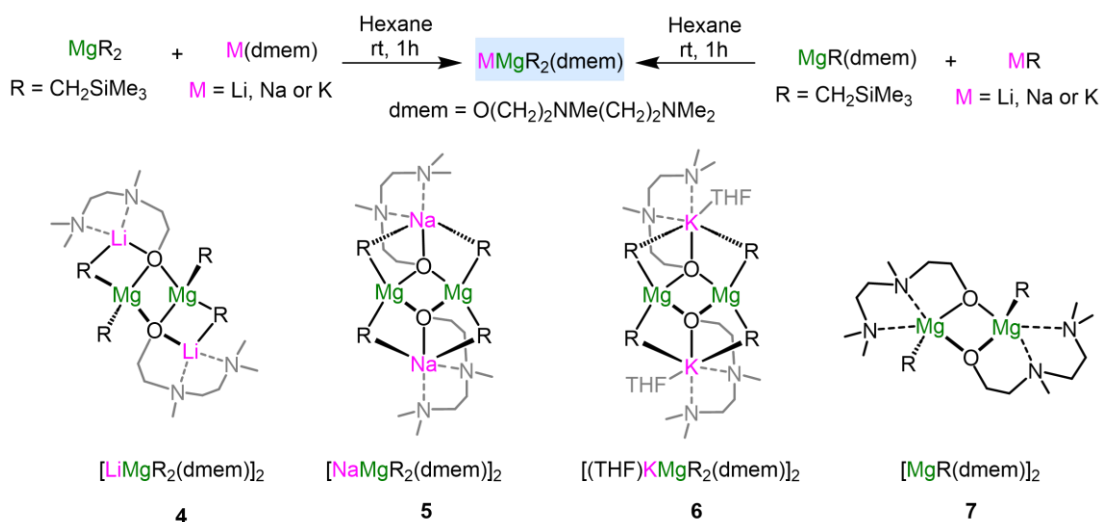


**Figure 3.** Co-complexation routes to access mixed alkyl/alkoxy alkali-metal magnesiates **4-6** with Chemdraw representations of compounds **4-7**.

Compounds **4-7** were characterized by multinuclear NMR and their molecular structures were established by X-ray crystallography (Figure 4). All are dimers featuring a central four-membered {MgOMgO} unit. For heterobimetallic compounds **4-6**, while each Mg center binds to two alkoxide and two alkyl groups, the presence of a different alkali-metal and its coordination preferences dictates the overall structure of the complex. In each case the alkoxide ligand binds in a tridentate fashion to the alkali-metal, via its O and two N sites. Featuring a centrosymmetric structure, lithium magnesiate **4** exhibits a ladder motif reminiscent to those previously reported for lithium amides<sup>33-38</sup> comprising outer Li-C rungs and inner alkoxy O-Mg rungs. Completing the structure along the ladder edge internal NMe<sub>2</sub> and NMe coordinate to Li whereas a terminal alkyl group binds to Mg. This structure can also be envisaged as two dinuclear {LiOMgC} rings which combine laterally via their Mg-O edges to generate this tetranuclear ladder. Within this motif one alkyl group is terminal on Mg (Mg-C5, 2.146(14) Å) whereas the other bridges Mg and Li (Mg-C1 2.205(14) Å, Li-C1, 2.273(3) Å) (Table 1). This structure is analogous to that previously reported by our group for [LiMg<sub>2</sub>Bu<sub>2</sub>(dmем)]<sub>2</sub> using the same chelating alkoxide ligand (see Chapter 2, Figure 5).<sup>15</sup>

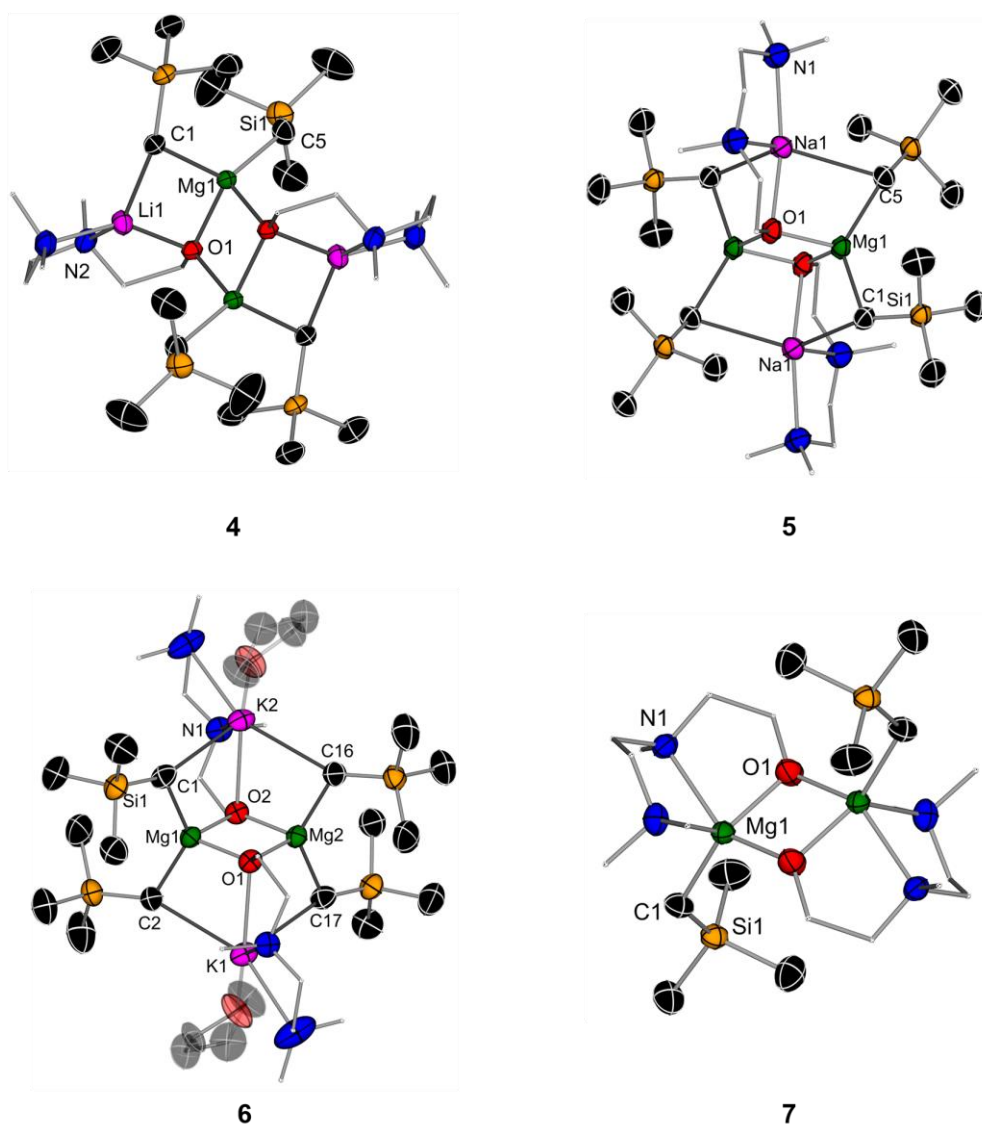


**Figure 4.** Molecular structures of compounds **4-7** with displacement ellipsoids at 50% probability, all H atoms omitted and with C atoms in the alkoxide substituent drawn as wire frames only for clarity. Equivalent atoms in **4, 5,** and **6** generated by  $(3/2 - x, 1/2 - y, 2/3 - z)$ ,  $(1 - x, 1 - y, 1 - z)$  and  $(1 - x, -y, 1 - z)$  respectively.

Contrastingly, heavier congeneric sodium and potassium magnesiate **5** and **6** exhibit a different dimeric motif where now all alkyl groups bridge the alkali-metal and Mg. Instead of forming a ladder-type structure, **5** and **6** display an incomplete double cubane motif with a missing vertex in each cube. This arrangement is known for other monometallic and heterobimetallic complexes<sup>39-43</sup> including mixed alkyl alkoxide alkali-metal magnesiate<sup>44,45</sup> and manganate complexes.<sup>46</sup> The structures of **5** and **6** can also be described as inverse crowns,<sup>47-50</sup> comprising a cationic octagonal  $\{(MCMgC)\}^{2+}$  ring which hosts two alkoxide anions in its core. Each alkoxide coordinates to two Mg atoms and one alkali-metal (M) using its O atom and two N atoms to chelate the latter. Thus in **5** Na displays pentacoordination, whereas in **6** K attains hexacoordination by solvation of a molecule of THF (Figure 4). Inspecting the Mg-C and Mg-O bond distances in these compounds did not reveal any

significant differences (Table 1). These bonds anchor the structure to which the alkali-metals are affixed by a combination of M-C and M-O ancillary bonds which as expected become more elongated as the size of the alkali metal cation increases (Table 1).

**Table 1.** Selected bond distances (Å) and angles (°) in the crystal structures of compounds **4-7**.

<b>[LiMg(CH<sub>2</sub>SiMe<sub>3</sub>)<sub>2</sub>(dmem)]<sub>2</sub> (4)</b>			
Mg1 – C1	2.205(14)	Li1 – C1	2.273(3)
Mg1 – C5	2.146(14)	Li1 – O1	1.978(2)
Mg1 – O1	2.033(9)	Li1 ... Mg1	2.779(2)
Mg ... Mg	3.030(8)	Mg1-O1-Mg1	96.350(4)
O1-Mg1-O1	83.650(4)		
<b>[NaMg(CH<sub>2</sub>SiMe<sub>3</sub>)<sub>2</sub>(dmem)]<sub>2</sub> (5)</b>			
Mg1 – C1	2.191(2)	Na1 – C1	2.686(3)
Mg1 – C5	2.204(3)	Na1 – C5	2.882(3)
Mg1 – O1	2.018(16)	Na1 – O1	2.421(18)
Mg ... Mg	3.057(14)	Mg1 ... Na1	3.132(12)
O1-Mg1-O1	81.613(8)	Mg1-O1-Mg1	98.387(7)
<b>[(THF)KMg(CH<sub>2</sub>SiMe<sub>3</sub>)<sub>2</sub>(dmem)]<sub>2</sub> (6)</b>			
Mg1 – C1	2.188(3)	K1 – C2	3.131(3)
Mg1 – C2	2.193(3)	K2 – C1	3.173(3)
Mg1 – O1	2.027(18)	K1 – O1	2.740(17)
Mg ... Mg	2.996(11)	Mg1 ... K1	3.589(10)
O1-Mg1-O2	84.610(7)	Mg1-O1-Mg2	95.320(7)
O1-Mg2-O2	84.80(7)	Mg1-O2-Mg2	95.253(7)
<b>[Mg(CH<sub>2</sub>SiMe<sub>3</sub>)(dmem)]<sub>2</sub> (7)</b>			
Mg1 – C1	2.177(2)	Mg ... Mg	3.090(13)
Mg1 – O1	1.995(17)	Mg1-O1-Mg1	101.476(7)
O1-Mg1-O1	78.524(7)		

The structures of **4-6** can be compared to that of the monometallic alkylmagnesium alkoxide **7** which also exhibits a dimeric motif with a similar {MgOMgO} ring, although in this case the Mg atoms are also chelated by the N atoms on the alkoxide chain. Consistent with its neutral constitution, the Mg-O distance in **4** (1.995(17) Å) is slightly shorter than those



found in magnesiate species **4-6**. This trend is also observed for the Mg-C bond distances [2.177(2) Å] although it should also be noted that in **7** the alkyl groups bind terminal to the Mg centers (Table 1). Using cryoscopic molecular weight determinations Coates reported in 1968 that alkylmagnesium alkoxides tend to form tetramers and higher oligomers via intermolecular Mg-O donor acceptor bonds in non-coordinating solvents such as benzene; whereas coordinating solvents such as THF can favour the formation of dimeric structures.<sup>51</sup> Many examples of structurally characterised alkylmagnesium alkoxides adopt tetrameric structures<sup>52,53</sup> or higher oligomer biscubanes.<sup>54</sup> The intramolecular coordinating abilities of the tridentate chelating alkoxide used here prevents the oligomerisation of **4** where the dimer is soluble even in non-polar solvents such as hexane.

The constitution of mixed alkyl/alkoxy magnesiates **4-6** in solution (C<sub>6</sub>D<sub>6</sub>) was also studied using multinuclear NMR spectroscopy including <sup>1</sup>H-DOSY NMR studies. This was imperative to assess if these complexes exist as the sole compounds in solution or if alternatively they are in equilibrium with other organometallic species as previously shown for related lithium magnesiates [LiMg<sub>3</sub>Bu<sub>2</sub>(OR')] (R' = 2-ethylhexyl) (Figure 1).<sup>15</sup> Related to these findings, O'Hara has also reported that heteroleptic alkali metal magnesiates [(rac)BIPHEN]M<sub>2</sub>MgnBu<sub>2</sub>(THF)<sub>4</sub> (M = Li or Na), containing the bis(aryloxy) group BIPHEN (BIPHEN = 5,5',6,6'-tetramethyl-3,3'-di-tert-butyl-1,1'-biphenyl-2,2'-diol) undergo a redistribution process in THF solution to form the homoleptic alkoxy [(rac)BIPHEN]<sub>2</sub>M<sub>2</sub>Mg(THF)<sub>4</sub> and alkyl rich magnesiates [M<sub>2</sub>MgnBu<sub>4</sub>(THF)<sub>4</sub>].<sup>55,56</sup> Interestingly, for **4-6**, the presence of the tridentate alkoxide ligand seems to impose a greater stability of these bimetallic species in solution as no evidence of ligand redistribution and formation of other organometallic compounds in solution were observed. This was supported by <sup>1</sup>H-DOSY NMR spectroscopic studies which indicated that in all cases a single molecular entity is formed containing both alkyl and alkoxide groups (see Figure 5 for <sup>1</sup>H-DOSY NMR spectra of lithium magnesiate **4**). For example, in lithium magnesiate **4** the independent diffusion co-efficient for the alkoxide fragment is  $D = 4.55 \times 10^{-10} \text{ m}^2/\text{s}$  and a similar value is obtained for the alkyl fragment at  $D = 4.46 \times 10^{-10} \text{ m}^2/\text{s}$  suggesting they belong to the same organometallic entity (Figure 5).

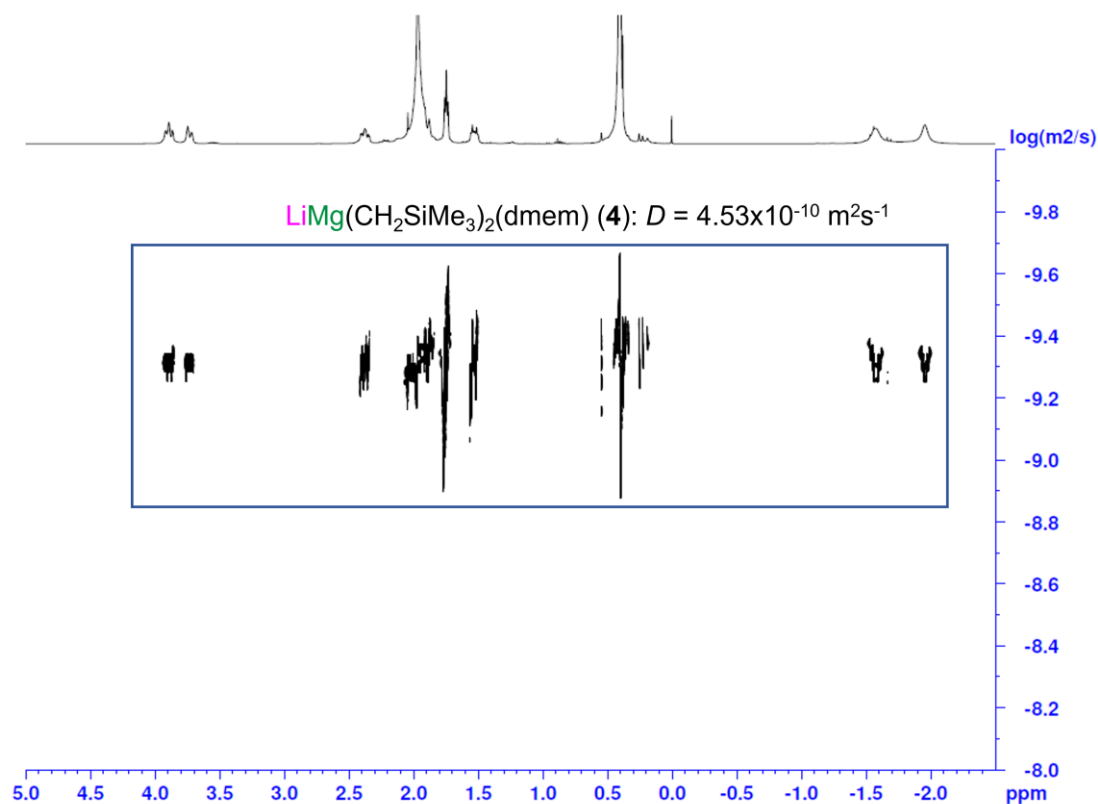


**Figure 5.**  $^1\text{H}$ -DOSY NMR spectrum of  $[\text{LiMg}(\text{CH}_2\text{SiMe}_3)_2(\text{dmep})]_2$  **4** in  $\text{C}_6\text{D}_6$

In the case of lithium magnesiate **4**, two different signals are observed for the M-CH<sub>2</sub> groups in the  $^1\text{H}$  and  $^{13}\text{C}$  NMR spectra (-1.56 and -1.96 ppm and -4.8 and -6.7 ppm, respectively) which is consistent with the retention, in solution, of its structure in the solid state where one alkyl group is terminal while the other one bridges Li and Mg. In contrast, sodium magnesiate **5** and potassium magnesiate **6** displays only one signal in the  $^1\text{H}$  and  $^{13}\text{C}$  NMR (-1.8 and -6.3 ppm (**5**) and -1.78 and -6.3 ppm (**6**), respectively) for the equivalent M-CH<sub>2</sub> groups which bridge between the Mg and alkali metal centres in the solid-state structures. While the M-CH<sub>2</sub> signal at 298 K in the  $^1\text{H}$  NMR spectra for sodium magnesiate **5** is broad; at 333 K this peak converges to a sharper singlet suggesting there is a degree of fluxionality in solution.

Furthermore,  $^1\text{H}$ -DOSY NMR was used to estimate the molecular weight of sodium magnesiate **5** in  $\text{C}_6\text{D}_6$  solution via Stalke's external calibration curve (ECC)<sup>57</sup> method using tetraphenylanthracene as an internal standard (Figure 6). The determined molecular weight  $MW_{det}$  of **5**, based on the independent diffusion coefficients of multiple non-overlapping signals in the  $^1\text{H}$  NMR spectra, was found to be 555 g/mol. However, the calculated and expected molecular weight  $MW_{calc}$  of monomeric sodium magnesiate **5** is 366.95 g/mol whilst the dimeric form has an  $MW_{calc}$  733.9 g/mol. The  $MW_{det}$  of **5** is intermediate between the expected molecular weights for **5** existing as a monomer or a dimer. This supports the claim that in  $\text{C}_6\text{D}_6$  solution at 298K there is a degree of fluxionality in the structure of **5** (possibly a

monomer/dimer equilibrium) resulting in the broad signals observed in the  $^1\text{H}$  NMR spectra at room temperature. It is important to note that no redistribution to higher order sodium magnesiate  $\text{Na}_2\text{MgR}_4$  and magnesium alkoxide  $\text{Mg}(\text{dmem})_2$  is detected as previously reported for  $[\text{LiMg}_s\text{Bu}_2(\text{OR}')]_2$  ( $\text{R}' = 2$ -ethylhexyl) using a long chain alkoxide (see Figure 4, Chapter 2). Additionally, in  $\text{D}_8$ -THF only one sharp singlet for the M- $\text{CH}_2$  signal is observed at  $-2.06$  ppm suggesting the formation of a singular molecular entity.

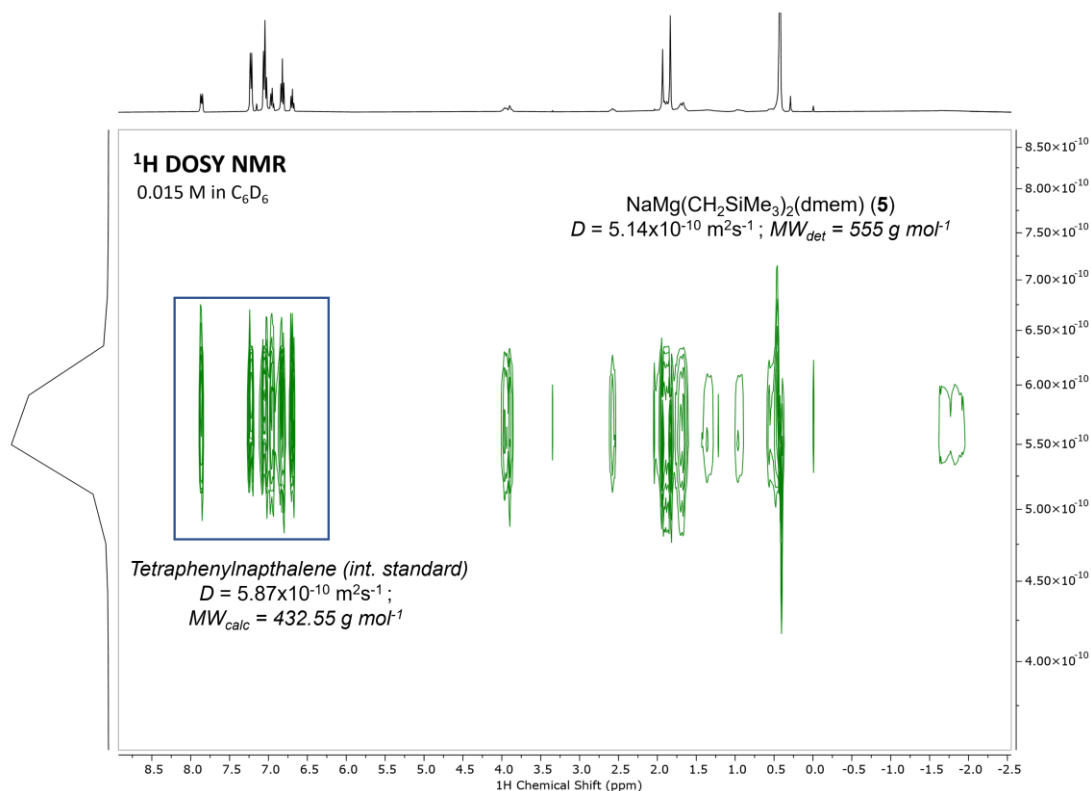


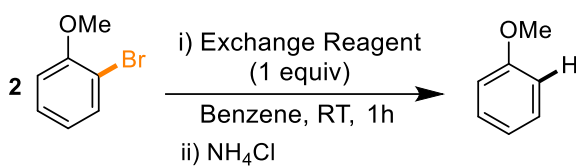
**Figure 6.**  $^1\text{H}$ -DOSY NMR and molecular weight estimations of  $[\text{NaMg}(\text{CH}_2\text{SiMe}_3)_2(\text{dmem})_2]$  **5** in  $\text{C}_6\text{D}_6$  at 298 K.

### 3.3.2 Assessing the Alkali-Metal Effect and Mg/Br Exchange Capabilities of Alkyl/Alkoxy Magnesiates 4-6

Next, we investigated the ability of magnesiates **4-6** to undergo Mg/Br exchange using 2-bromoanisole as a model substrate. Since these bimetallic complexes contain two alkyl groups which potentially can undergo exchange, reactions were carried out with two equivalents of 2-bromoanisole in benzene at room temperature for one hour, followed by an aqueous quench and subsequent analysis by GC to determine the extent of Mg/Br exchange (Table 2). Significantly, monometallic Mg species,  $\text{Mg}(\text{CH}_2\text{SiMe}_3)_2$  and  $[\text{Mg}(\text{CH}_2\text{SiMe}_3)(\text{dmem})]_2$  **7**, are completely inactive towards 2-bromoanisole (entries 1 and 2). In contrast, lithium magnesiate **4** gave a 41% conversion to anisole (entry 3). While this yield is moderate, it should be noted that our previous studies using  $[\text{LiMg}_s\text{Bu}_2(\text{OR}')]_2$  ( $\text{R}' = 2$ -

ethylhexyl) have shown that this mixed alkyl(alkoxide) magnesiate reacts sluggishly towards 2-bromoanisole (see Chapter 2, section 2.3.1).<sup>15</sup> Replacing Li by Na, using magnesiate **5** slightly increase in the yield of the exchange product (45%, entry 4) which can be further improved to 59% (entry 5) using potassium magnesiate **6**. Crucially, this result demonstrated that both alkyl groups in **6** are active towards Mg/Br exchange by delivering a conversion above 50%.

**Table 2.** Screening of Mg/Br exchange capabilities of mixed alkyl/alkoxy alkali metal magnesiates towards 2-bromoanisole.



Entry	Exchange reagent <sup>[a]</sup>	Yield [%] <sup>[b]</sup>
1	MgR <sub>2</sub>	0
2	RMg(dmcm) ( <b>7</b> )	0
3	LiMgR <sub>2</sub> (dmcm) ( <b>4</b> )	41
4	NaMgR <sub>2</sub> (dmcm) ( <b>5</b> )	45
5	KMgR <sub>2</sub> (dmcm) ( <b>6</b> )	59
6	K(dmcm) + Mg <i>n</i> Bu <sub>2</sub>	75
7	K(dmcm) + Mg <i>s</i> Bu <sub>2</sub>	52

[a] R = CH<sub>2</sub>SiMe<sub>3</sub> and dmcm = CH<sub>2</sub>CH<sub>2</sub>N(CH<sub>3</sub>)CH<sub>2</sub>CH<sub>2</sub>N(CH<sub>3</sub>)<sub>2</sub>. [b] Yields were determined by GC analysis of reaction aliquots after an aqueous quench using hexamethylbenzene as internal standard. Formation only of anisole and unreacted 2-bromoanisole were observed.

Intrigued by these findings that show a clear alkali-metal and alkoxide effect, we next assessed the influence of the alkyl groups, combining equimolar amounts of K(dmcm) with equimolar amounts of Mg*n*Bu<sub>2</sub> and Mg*s*Bu<sub>2</sub> which *a priori* can be expected to be more reactive than Mg(CH<sub>2</sub>SiMe<sub>3</sub>)<sub>2</sub>. Interestingly, while this was the case for Mg*n*Bu<sub>2</sub> (75%, entry 6), using Mg*s*Bu<sub>2</sub> gave similar conversions to those observed for **6** (52%, entry 7) which was somewhat surprising given that the *s*Bu group has been the alkyl substituent of choice in related Li/Mg and Li/Zn systems investigating Mg/X and Zn/X exchange using alkoxide ligands.<sup>13,28</sup> It should be noted that when LiOR' (R' = 2-ethylhexyl) is paired with Mg*s*Bu<sub>2</sub>, the active exchange reagent is Li<sub>2</sub>Mg*s*Bu<sub>4</sub> due to the presence of the bimetallic Schlenk equilibrium

depicted in Figure 1 and that when this equilibrium is manipulated towards the exclusive formation of mixed alkyl/alkoxide [LiMg<sub>2</sub>Bu<sub>2</sub>(OR')] the exchange process is suppressed (see Chapter 2, section 2.3.4).<sup>15</sup> This scenario is not possible for magnesiates **4-6** which in solution retain their mixed alkyl/alkoxide constitution (*vide supra*). Our studies show a clear enhancement of reactivity when potassium is used as a metal partner with Mg contrasting with early work by Richey Jr. where adding different Group 1 metal alkoxides to MgEt<sub>2</sub> enabled Mg/Br exchange in bromobenzene, though no definite trend in reactivity could be seen dependent on the alkali-metal.<sup>12</sup>

### 3.3.3 Structural and Spectroscopic Investigations of Mg/Br Exchange Products

To gain further insights into the reactivity of **6** with 2-bromoanisole we next turned our focus to the isolation of the metalated intermediate prior to hydrolysis. Carrying the reaction out in benzene we noticed the almost immediate formation of a white precipitate which could not be redissolved in other organic solvents including polar THF. Removal of this solid by filtration furnished a light-yellow solution which on cooling deposited crystals of [MgAr(dmef)]<sub>2</sub> (**8**) (Ar = *o*-OMe-C<sub>6</sub>H<sub>4</sub>) in a 30% crystalline yield (Figure 7). X-ray crystallographic studies established the molecular structure of **7** which shares the same dimeric motif as that described for **7** but now each Mg binds to an *ortho*-metalated anisyl group via its C atom. Despite their structural similarity, it should be noted that **8** is not accessible by reacting **7** with 2-bromoanisole (Table 2, entry 2), demonstrating that its formation is synergic in origin as it is mediated by potassium magnesiate **6** (Figure 7).

<sup>1</sup>H NMR analysis of the reaction filtrates also confirm that **5** is the only organometallic species present in solution. While the lack of solubility in organic solvents of the solid formed during this reaction precluded its NMR characterisation, its aqueous quench with subsequent GC analysis showed the formation of anisole. Thus, we can tentatively propose that the formation of **8** occurs with the concomitant precipitation of [KAr]<sub>n</sub> (Ar = *o*-OMe-C<sub>6</sub>H<sub>4</sub>) (Figure 7). Adding a new layer of complexity to the behaviour of these mixed alkyl/alkoxide species, these results indicate that while potassium magnesiate **6** can efficiently promote Mg/Br exchange of 2-bromoanisole, the putative intermediate of this reaction [KMgAr<sub>2</sub>(dmef)] (**int-1**) undergoes redistribution into single metal components **8** and [KAr]<sub>n</sub> (Ar = *o*-OMe-C<sub>6</sub>H<sub>4</sub>) which may be driven by the poor solubility of the potassium species. This type of equilibrium is reminiscent to that present in Lochman-Schlosser *n*BuLi/KOtBu combinations, where an initial mixed metal alkyl/alkoxide intermediate is formed which eventually evolves into the exchange products LiOtBu and *n*BuK.<sup>6</sup> Ultimately, caution should be taken when using these bimetallic reagents in organic synthesis, since while 2-bromoanisole can be efficiently

converted into anisole via Mg/Br exchange and aqueous quench, two entirely different organometallic species are formed which could be expected to have very different properties in terms of stability, reactivity and functional group tolerance, and could therefore effect further functionalisation of their aromatic moieties.

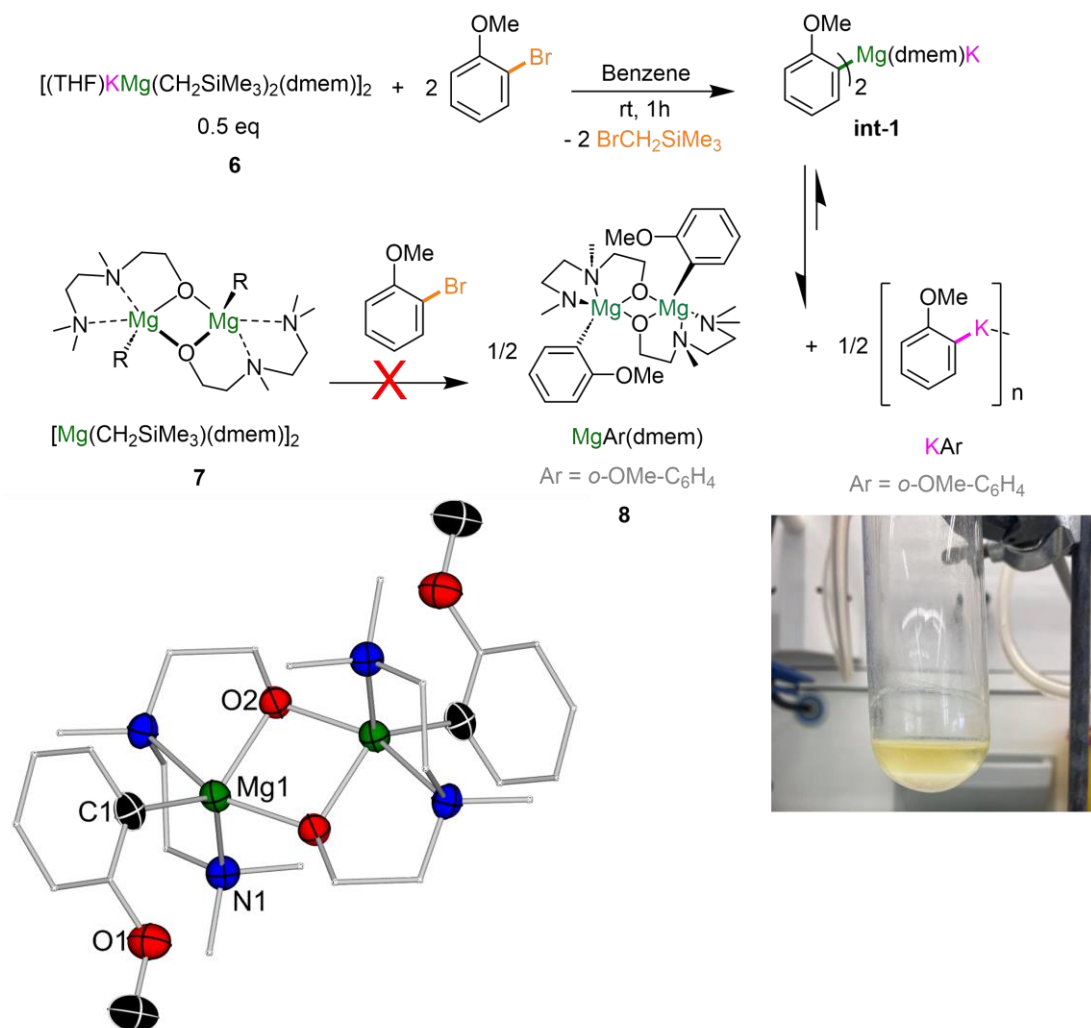


**Figure 7.** Isolation of  $[\text{MgAr}_2(\text{dmem})]$  (**8**) via reaction of potassium magnesiate **6** with two equivalents of 2-bromoanisole and proposed concomitant formation of an insoluble potassium aryl  $[\text{KAr}]_n$ . Molecular structure of compound **8** (bottom left) with displacement ellipsoids at 50% probability, all H atoms omitted and with C atoms in the alkoxide substituent drawn as wire frames only for clarity. Equivalent atoms in **8** generated by  $(1-x, 1-y, 1-z)$ . Bottom left picture depicts the reaction mixture in a Schlenk flask to highlight the white solid crashing from the reaction mixture.

### 3.3.4 Assessing Alkoxide Effects in Mixed Alkyl/Alkoxy Magnesiates and their Reactivity

Puzzled by these findings, we next decided to probe whether the redistribution process shown in Figure 7 would also affect related sodium and potassium magnesiates containing the long chain aliphatic alkoxide  $\text{OR}'$  ( $\text{R}' = 2\text{-ethylhexyl}$ ). Co-complexation of  $\text{MOR}'$  with equimolar amounts of  $\text{Mg}(\text{CH}_2\text{SiMe}_3)_2$  led to the formation of  $[\text{MMg}(\text{CH}_2\text{SiMe}_3)_2(\text{OR}')_2]$  ( $\text{M} =$

Na, **9**; K, **10**). Whilst sodium magnesiate **9** could only be isolated as a colourless oil, potassium magnesiate **10** was isolated as a crystalline solid in a 55% yield.  $^1\text{H}$  and  $^{13}\text{C}$  NMR characterisation of these compounds show similar behaviour as sodium and potassium magnesiates **4** and **5** respectively, existing as single molecular entities in  $\text{C}_6\text{D}_6$  solutions without undergoing the bimetallic Schlenk equilibrium depicted in Figure 1b, previously reported for  $[\text{LiMg}_s\text{Bu}_2(\text{OR}')_2]$  ( $\text{R}' = 2\text{-ethylhexyl}$ ).<sup>15</sup> Indeed, analysis of the  $^1\text{H}$ -NMR spectra obtained upon co-complexing  $\text{LiOR}'$  with  $\text{Mg}(\text{CH}_2\text{SiMe}_3)_2$  revealed a more complex situation than observed with the sodium and potassium congeners in which multiple species are present. Independent synthesis of higher order lithium magnesiate  $\text{Li}_2\text{Mg}(\text{CH}_2\text{SiMe}_3)_4$  and analysis of the  $^1\text{H}$ -NMR spectra in  $\text{C}_6\text{D}_6$  confirmed its presence in the aforementioned mixture demonstrating that the nature of the alkali metal can have a profound effect on the constitution of the bimetallic entities produced from these co-complexation reactions. The use of heavier alkali metal alkoxides (Na and K) in co-complexation reactions with dialkyl magnesium reagents has completely precluded the redistribution of these mixed alkyl/alkoxy magnesiates into higher order tetraalkyl magnesiates, as seen with Li, via the bimetallic Schlenk type equilibrium depicted in Figure 1b. Due to this marked alkali metal effect, mixed alkyl/alkoxy potassium magnesiate **10** could be isolated as a crystalline solid and its molecular structure was established by X-ray crystallographic studies (Figure 8a).

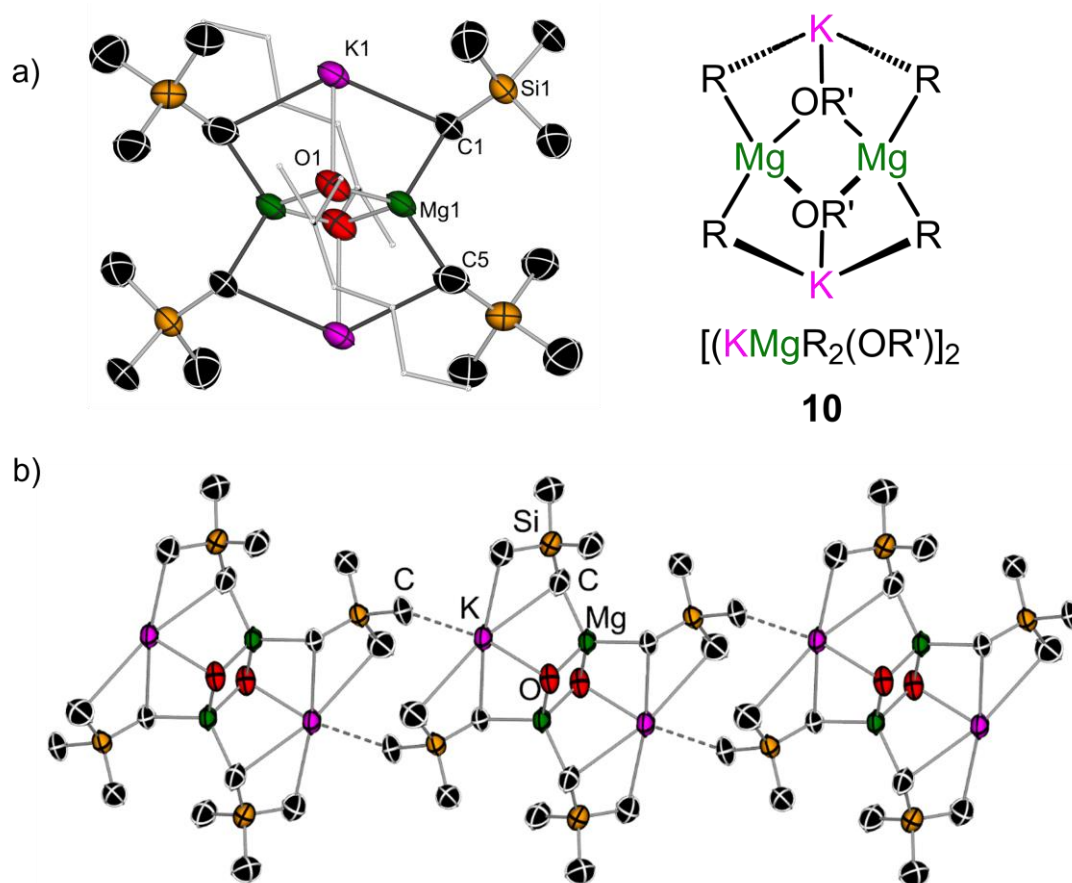


**Figure 8.** a) Dimeric fragment and chemdraw representation of  $[\text{KMg}(\text{CH}_2\text{SiMe}_3)_2\text{OR}']_2$  ( $\text{OR}' = 2\text{-ethylhexyl}$ ) **10**  
 b) 1D linear Polymeric X-ray crystal structure of **10**. Displacement ellipsoids at 50% probability, all H atoms omitted and with C atoms in the alkoxide substituent drawn as wire frames only for clarity.

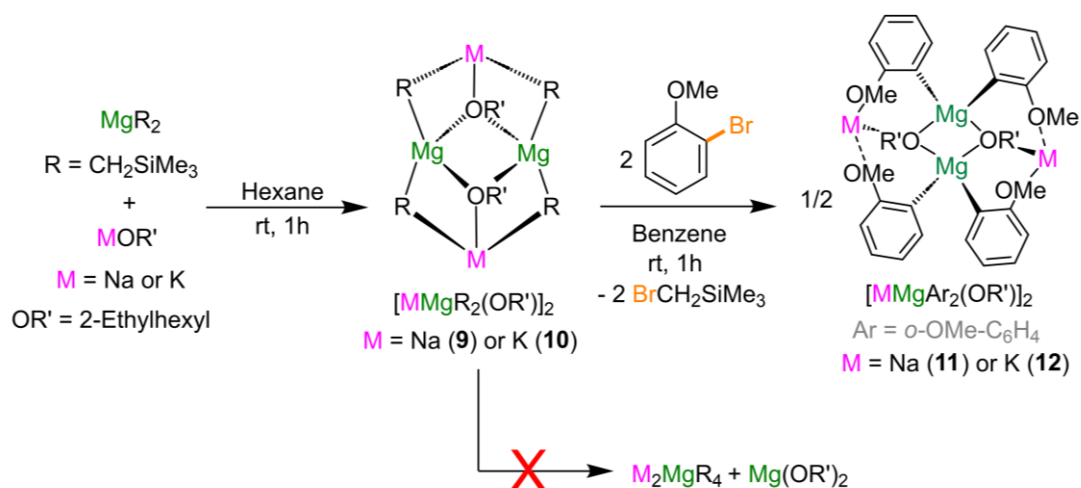
Despite the aliphatic constitution of the alkoxide groups lacking additional coordination sites the core structure of **10** is almost identical to that described for potassium magnesiate **6** containing the chelating alkoxide, displaying comparable geometrical parameters (Table 3). Coordinatively unsaturated K centres in **10** attain further stabilisation by forming anagostic  $\text{K}\cdots\text{Me}$  interactions with one Me group from the  $\text{CH}_2\text{SiMe}_3$  ligands on a neighbouring  $[\text{KMg}(\text{CH}_2\text{SiMe}_3)_2(\text{OR}')_2]$  dimeric unit giving rise to a linear 1D polymeric arrangement (Figure 8b).



**Table 3.** Selected bond distances (Å) in the crystal structures of compounds **6** & **10**

[(THF)KMg(CH <sub>2</sub> SiMe <sub>3</sub> ) <sub>2</sub> (dmem)] <sub>2</sub> ( <b>6</b> )			
Mg1 – C1	2.188(3)	K1 – C2	3.131(3)
Mg1 – C2	2.193(3)	K2 – C1	3.173(3)
Mg1 – O1	2.027(18)	K1 – O1	2.740(17)
Mg ... Mg	2.996(11)	Mg1 ... K1	3.589(10)
[KMg(CH <sub>2</sub> SiMe <sub>3</sub> ) <sub>2</sub> (OR')] <sub>2</sub> ( <b>10</b> ) (R = 2-ethylhexyl)			
Mg1 – C1	2.146(4)	K1 – C1	3.146(5)
Mg1 – C5	2.179(5)	K1 – C5	3.196(9)
Mg1 – O1	2.005(3)	K1 – O1	2.628(9)
Mg ... Mg	3.007(2)	Mg1 ... K1	3.435(3)

Both sodium magnesiate **9** and potassium magnesiate **10** react with two equivalents of our model substrate 2-bromoanisole in benzene at room temperature affording conversions to anisole, after a hydrolysis step, of 75 and 76% respectively after just one hour. Contrasting with **6**, using potassium magnesiate **10**, no solid precipitation is observed before the hydrolysis step. <sup>1</sup>H NMR monitoring of this reaction showed that after 3 hours, all of **10** has reacted with 2-bromoanisole producing two equivalents of BrCH<sub>2</sub>SiMe<sub>3</sub> and mixed aryl/alkoxide [KMgAr<sub>2</sub>(OR')]<sub>2</sub> (**12**) (Ar = *o*-OMe-C<sub>6</sub>H<sub>4</sub>) which is stable in solution and does not undergo any redistribution process. The same reactivity was observed for sodium derivative **9** in forming [NaMgAr<sub>2</sub>(OR')]<sub>2</sub> (**11**) (Scheme 1) although in this case after 3h at room temperature unreacted 2-bromoanisole is detected in solution (75% conversion), illustrating the importance of the choice of alkali-metal for the efficiency of the Mg/Br exchange process.



**Scheme 1.** Synthesis of alkyl/alkoxy magnesiate **9** and **10** and their reactivity with 2-bromoanisole to form metalated intermediates **11** and **12** respectively.

Magnesiate **11** and **12** were characterised in solution by  $^1\text{H}$  and  $^{13}\text{C}$  NMR spectroscopy.  $^1\text{H}$  DOSY NMR studies on these species confirm their mixed aryl/alkoxide constitution. The molecular structure of sodium magnesiate **11** was also confirmed by X-ray crystallographic studies (Figure 9), in which each Mg binds to two *ortho*-metalated anisole groups, occupying the position previously filled by the Br atoms, completing their coordination by bonding to two alkoxide ligands. Each Na binds to one alkoxide group and two OMe substituents from the anisyl fragments. The Na atoms in **11** find additional stabilisation by  $\pi$ -engaging in a preferred  $\eta^3$ -fashion with the aryl groups of neighbouring dimeric units creating an intricate 3D polymeric arrangement overall (Figure 9).

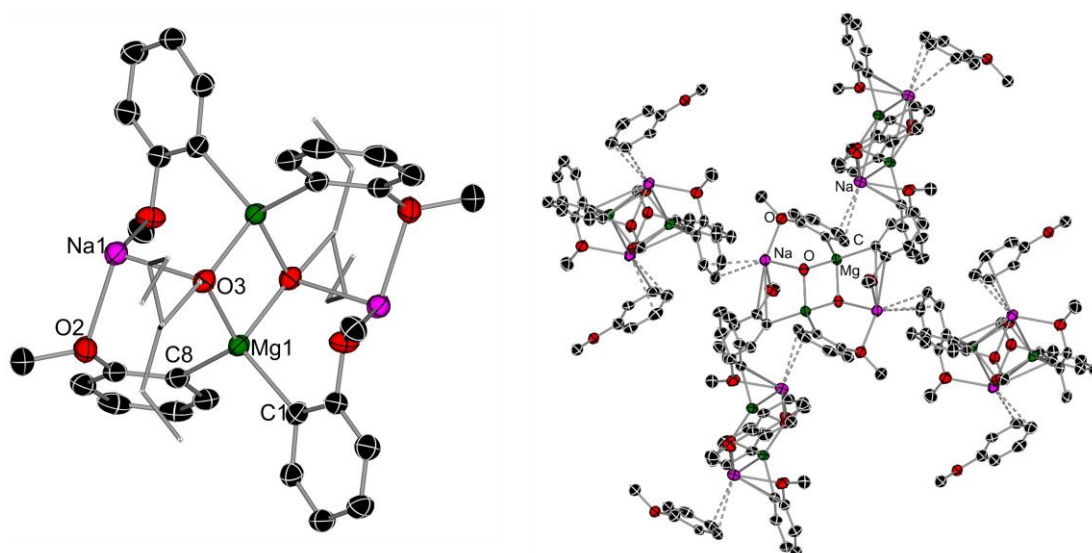


**Figure 9.** Dimeric fragment of  $[\text{NaMg}(\text{Ar})_2(\text{OR}')_2]$  ( $\text{Ar} = o\text{-OMe-C}_6\text{H}_4$ ;  $\text{OR}' = 2\text{-ethylhexyl}$ ) **11** (left) and Polymeric X-ray crystal structure of  $[\text{NaMg}(\text{Ar})_2(\text{OR}')_2]$  ( $\text{Ar} = o\text{-OMe-C}_6\text{H}_4$ ;  $\text{OR}' = 2\text{-ethylhexyl}$ ) **11** (right). Displacement ellipsoids at 50% probability, all H atoms omitted and with C atoms in the alkoxide substituent drawn as wire frames only for clarity.

This motif is closely related to the one we have previously reported for the product of Mg/Br exchange obtained from treating 2-bromoanisole with an equimolar mixture of  $Mg_sBu_2$  and  $LiOR'$  (see Chapter 2, section 2.3.2).<sup>14</sup> However on this occasion this compound is obtained by direct exchange with  $Li_2Mg_sBu_4$  to give a  $Li_2MgAr_4$  intermediate which in turn undergoes co-complexation with  $Mg(OR')_2$  also present in the reaction media via the bimetallic Schlenk equilibrium depicted in Figure 1b.<sup>15</sup> As aforementioned, while we do not observe the presence of this equilibrium for potassium magnesiates **6** and **10**, we decided to benchmark its reactivity towards 2-bromoanisole against that of higher order potassium magnesiate  $K_2Mg(CH_2SiMe_3)_4$  which can be isolated as its TMEDA solvate by combining TMEDA,  $KCH_2SiMe_3$  and  $Mg(CH_2SiMe_3)_2$  in a 2:2:1 ratio.<sup>58</sup> Interestingly, when reacting this alkyl rich reagent with four equivalents of 2-bromoanisole we only observed a 57% conversion, revealing that the mixed alkyl/alkoxide species is in this specific case a more powerful exchange reagent.

### 3.4 Conclusions

By assessing the reactivity towards 2-bromoanisole of several mixed alkyl/alkoxide alkali-metal magnesiates, systematically changing the alkali-metal and alkoxide group, new light has been shed on the activating effect of alkali-metal alkoxides when used as additives with organomagnesium reagents to mediate Mg/Br exchanges. A notable alkali-metal effect has been uncovered, with the formation of the stable mixed alkyl/alkoxide  $[MMg(alkyl)_2(OR')]$  ( $OR' = 2$ -ethylhexyl) species when  $M = Na, K$ , which, in solution are not affected by the bimetallic Schlenk equilibrium previously reported for related lithium/magnesiates. Furthermore, an increase in reactivity has been noticed when using  $K$  instead of  $Li$  as a bimetallic partner with  $Mg$ , consistent with the alkali-metal playing a prominent role in mediating the Mg/Br exchange process. These findings also show the close interplay between the nature of the alkoxide group employed and the constitution of the exchange products prior to electrophilic interception. Thus, uncovering a new element of complexity, while the long aliphatic alkoxide  $OR'$  bimetallic intermediate  $[KMgAr_2(OR')]_2$  (**12**) is stable in arene solutions, employing the chelating alkoxide, *dmem*, led to the formation of the single metal species  $[MgAr(dmem)]_2$  (**8**) with concomitant precipitation of  $[KAr]_n$ . The different composition of these exchange products can profoundly affect the further functionalization of the aryl fragment when using these systems in organic synthetic transformations.

### 3.5 Experimental

A link is provided below for the Electronic Supporting Information (ESI) from the peer reviewed article on which this experimental section is based:

[downloadSupplement \(wiley.com\)](#)

#### 3.5.1 Synthesis of alkali metal alkoxides M(dm<sub>em</sub>) (AM = Li, 1; Na, 2; K, 3) and MOR' (R = 2-ethylhexyl)

##### Synthesis of Li(dm<sub>em</sub>) 1

Li(dm<sub>em</sub>) was synthesised according to synthetic procedures and spectral data were in accord with previous reports.<sup>28</sup>

To an argon-flushed Schlenk flask, 10 mmol (6.3 mL, 1.6 M in hexane) of *n*BuLi was added to 10 mL of hexane and cooled to -40 °C. To this, an equimolar amount of 2-(2-(dimethylamino)ethyl(methyl)amino)ethane-1-ol (1.6 mL, 10 mmol) was added giving a fine, white suspension. The reaction mixture was warmed to room temperature and stirred for four hours in total giving a pale-yellow solution. The solution was then concentrated under vacuum until precipitation occurred – it was then stored at -30 °C overnight to induce further precipitation. Isolation by filtration was carried out the following day and the white solid dried under reduced pressure before being stored in the glovebox. Yield: 1.3 g, 8.5 mmol, 85%. A small portion of this white solid Li(dm<sub>em</sub>) was redissolved in hexane and placed in the freezer at -30 °C to yield a crop of colourless crystals suitable for X-Ray crystallography. **<sup>1</sup>H-NMR (400 MHz, C<sub>6</sub>D<sub>6</sub>, 298 K):** δ / ppm = 4.18-4.15 (br. t, 2H, OCH<sub>2</sub>, dm<sub>em</sub>), 2.72-2.63 (br. m, 6H, CH<sub>2</sub>N(Me), N(Me)CH<sub>2</sub> and CH<sub>2</sub>NMe<sub>2</sub>, dm<sub>em</sub>), 2.40 (br. s, 3H, NMe, dm<sub>em</sub>), 2.23 (br. s, 6H, NMe<sub>2</sub>, dm<sub>em</sub>). **<sup>13</sup>C{<sup>1</sup>H}-NMR (101 MHz, C<sub>6</sub>D<sub>6</sub>, 298 K):** δ / ppm = 65.8 (CH<sub>2</sub>N(Me), dm<sub>em</sub>), 61.6 (OCH<sub>2</sub>, dm<sub>em</sub>), 57.6 (CH<sub>2</sub>NMe<sub>2</sub>, dm<sub>em</sub>), 57.3 (N(Me)CH<sub>2</sub>, dm<sub>em</sub>), 45.9 (NMe<sub>2</sub>, dm<sub>em</sub>), 39.9 (NMe, dm<sub>em</sub>). **<sup>7</sup>Li-NMR (156 MHz, C<sub>6</sub>D<sub>6</sub>, 298 K):** δ / ppm 0.81 (Li- dm<sub>em</sub>).

##### Synthesis of Na(dm<sub>em</sub>) 2

To an argon-flushed Schlenk flask (15 mmol, 1.66 g) of NaCH<sub>2</sub>SiMe<sub>3</sub> was added to 30 mL of hexane and cooled to -40°C. To this, an equimolar amount of 2-(2-(dimethylamino)ethyl(methyl)amino)ethane-1-ol (15 mmol, 2.4 mL) was added giving a clear, colourless solution. The reaction mixture was warmed to room temperature and stirred for one hour in total giving a pale-yellow solution. The solution was then concentrated under vacuum until precipitation occurred – it was then stored at -30°C overnight to induce further precipitation. Isolation by filtration was carried out the following day and the off-white solid dried under reduced pressure before being stored in the glovebox. Yield: 2.2 g, 87%. A small portion of this white solid Na(dm<sub>em</sub>) was redissolved in hexane and placed in the freezer at -

30 °C to yield a crop of colourless crystals suitable for X-ray crystallography. **<sup>1</sup>H-NMR (400 MHz, C<sub>6</sub>D<sub>6</sub>, 298 K):** δ / ppm = 4.03 (br. t, 2H, OCH<sub>2</sub>, dmem), 2.53 (br. t, 2H, CH<sub>2</sub>NMe<sub>2</sub>, dmem), 2.39 (br.t, 2H, CH<sub>2</sub>N(Me), dmem), 2.30-2.25 (s, 3H, NMe, dmem & br.t, 2H, CH<sub>2</sub>N(Me), dmem), 2.12 (s, 6H, NMe<sub>2</sub>, dmem). **<sup>13</sup>C{<sup>1</sup>H}-NMR (101 MHz, C<sub>6</sub>D<sub>6</sub>, 298 K):** δ / ppm = 63.5 (CH<sub>2</sub>N(Me), dmem), 61.5 (OCH<sub>2</sub>, dmem), 57.5 (CH<sub>2</sub>NMe<sub>2</sub>, dmem), 55.6 (N(Me)CH<sub>2</sub>, dmem), 45.3 (NMe<sub>2</sub>, dmem), 42.1 (NMe, dmem).

### Synthesis of K(dmem) 3

Note: K(dmem) synthesised and used *in-situ*.

To an argon-flushed Schlenk flask (1 mmol, 126 mg) of KCH<sub>2</sub>SiMe<sub>3</sub> was added to 5 mL of hexane and cooled to -40 °C. To this, an equimolar amount of 2-(2-(dimethylamino)ethyl(methyl)amino)ethane-1-ol (1 mmol, 0.16 mL) was added giving a clear, colourless solution. The reaction mixture was warmed to room temperature and stirred for one hour in total giving a pale-yellow solution. The solution was then concentrated under vacuum to afford K(dmem) as a yellow oil. **<sup>1</sup>H-NMR (400 MHz, C<sub>6</sub>D<sub>6</sub>, 298 K):** δ / ppm = 4.1 (t, 2H, OCH<sub>2</sub>, dmem), 2.63 (t, 2H, CH<sub>2</sub>NMe<sub>2</sub>, dmem), 2.48 (br.t, 2H, CH<sub>2</sub>N(Me), dmem), 2.37-2.32 (s, 3H, NMe, dmem & br.t, 2H, CH<sub>2</sub>N(Me), dmem), 2.2 (s, 6H, NMe<sub>2</sub>, dmem). **<sup>13</sup>C{<sup>1</sup>H}-NMR (101 MHz, C<sub>6</sub>D<sub>6</sub>, 298 K):** δ / ppm = 64.1 (CH<sub>2</sub>N(Me), dmem), 61.3 (OCH<sub>2</sub>, dmem), 57.9 (CH<sub>2</sub>NMe<sub>2</sub>, dmem), 56.9 (N(Me)CH<sub>2</sub>, dmem), 45.9 (NMe<sub>2</sub>, dmem), 42.3 (NMe, dmem).

### Synthesis of Li(OR') R = 2-ethylhexyl

LiOR' was synthesised according to synthetic procedures and spectral data were in accord with previous reports.<sup>14</sup>

In an argon-filled Schlenk flask, 1.00 mmol of *n*BuLi (0.63 mL, 1.60 M) was added to 5 mL of dry hexane and cooled to 0 °C. To this, 0.16 mL of ROH was added and the mixture was then allowed to stir at room temperature for 1 h. Removal of all volatiles under reduced pressure resulted in a colourless oil – LiOR'. **<sup>1</sup>H-NMR (300.1 MHz, D<sub>8</sub>-Tol, 298 K):** δ / ppm = 3.96-3.68 (br. m, 2H, OCH<sub>2</sub>), 1.70 (br. m, 1H, CH<sub>2</sub> x1, Et),<sup>‡</sup> 1.46 (br. s, 8 H, CH<sub>2</sub> x1 (Et) + CH + (CH<sub>2</sub>)<sub>3</sub>, OR'), 1.09 (br. t, 3H, CH<sub>3</sub>, OR'), 1.01 (br. t, 3H, CH<sub>3</sub>, OR'). **<sup>7</sup>Li-NMR (156 MHz, D<sub>8</sub>-Tol, 298 K):** δ / ppm = 0.86 (LiOR). **<sup>13</sup>C{<sup>1</sup>H}-NMR (75.5 MHz, D<sub>8</sub>-Tol, 298 K):** δ / ppm = 68.2 (OCH<sub>2</sub>, OR'), 46.6 (OCH<sub>2</sub>C(H), OR'), 31.1 (CH<sub>2</sub>, OR'), 30.2 (CH<sub>2</sub>, OR'), 24.2 (CH<sub>2</sub>, Et, OR'), 24.0 (CH<sub>2</sub>, OR'), 14.5 (CH<sub>3</sub>, Et, OR'), 11.4 (CH<sub>3</sub>, OR').

### Synthesis of Na(OR') R = 2-ethylhexyl

To an argon-flushed Schlenk flask (1 mmol, 110 mg) of NaCH<sub>2</sub>SiMe<sub>3</sub> was added to 5 mL of hexane and cooled to -40°C. To this, an equimolar amount of 2-ethylhexanol (1 mmol, 0.16 mL) was added giving a clear, colourless solution. The reaction mixture was warmed to room

temperature and stirred for one hour in total giving a pale-yellow solution. The solution was then concentrated under vacuum to afford NaOR' as a yellow oil.  $^1\text{H-NMR}$  (400 MHz,  $\text{C}_6\text{D}_6$ , 298 K):  $\delta$  / ppm = 3.95-3.83 (br. m, 2H,  $\text{OCH}_2$ ), 1.73 (br. m, 1H,  $\text{CH}_2 \times 1$ , Et), 1.50 (br. s, 8 H,  $\text{CH}_2 \times 1$  (Et) +  $\text{CH}$  +  $(\text{CH}_2)_3$ , OR'), 1.14 (br. t, 3H,  $\text{CH}_3$ , OR'), 1.05 (br. t, 3H,  $\text{CH}_3$ , OR').  $^{13}\text{C}\{^1\text{H}\}$ -NMR (75.5 MHz,  $\text{C}_6\text{D}_6$ , 298 K):  $\delta$  / ppm = 68.1 ( $\text{OCH}_2$ , OR'), 45.9 ( $\text{OCH}_2\text{C}(\text{H})$ , OR'), 31.0 ( $\text{CH}_2$ , OR'), 30.1 ( $\text{CH}_2$ , OR'), 24.1 ( $\text{CH}_2$ , Et, OR'), 24.0 ( $\text{CH}_2$ , OR'), 14.5 ( $\text{CH}_3$ , Et, OR'), 11.5 ( $\text{CH}_3$ , OR').

#### Synthesis of $\text{K}(\text{OR}') \text{R} = 2\text{-ethylhexyl}$

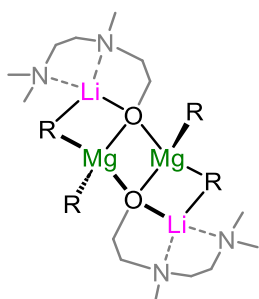
Note: KOR synthesised and used *in-situ*

To an argon-flushed Schlenk flask (1 mmol, 126 mg) of  $\text{KCH}_2\text{SiMe}_3$  was added to 5 mL of hexane and cooled to  $-40^\circ\text{C}$ . To this, an equimolar amount of 2-ethylhexanol (1 mmol, 0.16 mL) was added giving a clear, colourless solution. The reaction mixture was warmed to room temperature and stirred for one hour in total giving a pale-yellow solution. The solution was then concentrated under vacuum to afford KOR' as a yellow oil.  $^1\text{H-NMR}$  (400 MHz,  $\text{C}_6\text{D}_6$ , 298 K):  $\delta$  / ppm = 3.93-3.78 (br. m, 2H,  $\text{OCH}_2$ ), 1.74 (br. m, 1H,  $\text{CH}_2 \times 1$ , Et), 1.46 (br. s, 8 H,  $\text{CH}_2 \times 1$  (Et) +  $\text{CH}$  +  $(\text{CH}_2)_3$ , OR'), 1.12 (br. t, 3H,  $\text{CH}_3$ , OR'), 1.02 (br. t, 3H,  $\text{CH}_3$ , OR').  $^{13}\text{C}\{^1\text{H}\}$ -NMR (75.5 MHz,  $\text{C}_6\text{D}_6$ , 298 K):  $\delta$  / ppm = 69.5 ( $\text{OCH}_2$ , OR'), 46.8 ( $\text{OCH}_2\text{C}(\text{H})$ , OR'), 31.1 ( $\text{CH}_2$ , OR'), 30.1 ( $\text{CH}_2$ , OR'), 23.7 ( $\text{CH}_2$ , Et, OR'), 24.0 ( $\text{CH}_2$ , OR'), 14.2 ( $\text{CH}_3$ , Et, OR'), 11.5 ( $\text{CH}_3$ , OR').

### 3.5.2 Synthesis of Alkyl/alkoxy magnesiates

#### $[\text{MMg}(\text{CH}_2\text{SiMe}_3)_2(\text{dmem})]_2$ (M= Li, 4; Na, 5; (THF)K, 6)

##### Synthesis of $[\text{LiMg}(\text{CH}_2\text{SiMe}_3)_2(\text{dmem})]_2$ 4



In an argon flushed Schlenk flask, 1 mmol of  $\text{Li}(\text{dmem})$  was prepared as described in section 3.5.1.  $\text{Mg}(\text{CH}_2\text{SiMe}_3)_2$  (1mmol, 0.2g) was then added to a solution of  $\text{Li}(\text{dmem})$  in hexane (5 mL) and stirred for one hour at room temperature to give a fine white suspension. Gentle heating with a heat gun afforded a pale-yellow solution that was allowed to slowly cool to room temperature affording a colourless crop of crystals – compound 4. Yield: 190mg, 54%. Anal. Calcd. for  $\text{C}_{30}\text{H}_{78}\text{Li}_2\text{Mg}_2\text{N}_4\text{O}_2\text{Si}_4$  C, 51.34; H, 11.20; N, 7.98. Found: C, 50.47; H, 11.12; N, 8.41.

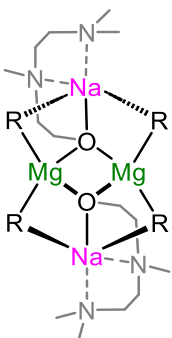
**Alternative synthesis:** In an argon-flushed Schlenk flask, 1 mmol of  $\text{Mg}(\text{CH}_2\text{SiMe}_3)(\text{dmem})$  7 (257 mg) was solubilised in hexane (5 mL) and to this solution was added 1 mmol  $\text{LiCH}_2\text{SiMe}_3$  (94 mg). The reaction was allowed to stir for one hour at room temperature to give a fine white suspension. Gentle heating with a heat gun afforded a pale-yellow solution

that was allowed to slowly cool to room temperature affording a colourless crop of crystals – compound **4**.

**<sup>1</sup>H-NMR (400 MHz, C<sub>6</sub>D<sub>6</sub>, 298 K):**  $\delta$  / ppm = 3.92-3.72 (m, 2H, OCH<sub>2</sub>, dmem), 2.41-2.35 (m, 1H, CH, dmem), 1.97 (br.s, 11H, CH<sub>2</sub>, NMe & NMe<sub>2</sub>, dmem), 1.75 (t, 2H, CH<sub>2</sub>N(Me), dmem), 1.55-1.51 (m, 1H, CH, dmem), 0.40 (s, 18H, 6 x CH<sub>3</sub>, CH<sub>2</sub>SiMe<sub>3</sub>), -1.56 (s, 2H, 1 x CH<sub>2</sub>, CH<sub>2</sub>SiMe<sub>3</sub>), -1.96 (s, 2H, 1 x CH<sub>2</sub>, CH<sub>2</sub>SiMe<sub>3</sub>). **<sup>13</sup>C{<sup>1</sup>H}-NMR (101 MHz, C<sub>6</sub>D<sub>6</sub>, 298 K):**  $\delta$  / ppm = 60.6 (CH<sub>2</sub>N(Me), dmem), 58.8 (OCH<sub>2</sub>, dmem), 56.7 (CH<sub>2</sub>NMe<sub>2</sub>, dmem), 54.3 (N(Me)CH<sub>2</sub>, dmem), 45.9 (NMe<sub>2</sub>, dmem), 42.1 (NMe, dmem), 5.3 (3 x CH<sub>3</sub>, CH<sub>2</sub>SiMe<sub>3</sub>), 4.9 (3 x CH<sub>3</sub>, CH<sub>2</sub>SiMe<sub>3</sub>), -4.8 (CH<sub>2</sub>, CH<sub>2</sub>SiMe<sub>3</sub>), -6.7 (CH<sub>2</sub>, CH<sub>2</sub>SiMe<sub>3</sub>). **<sup>7</sup>Li-NMR (156 MHz, C<sub>6</sub>D<sub>6</sub>, 298 K):**  $\delta$  / ppm = 0.67.

<sup>1</sup>H-DOSY NMR spectroscopic studies indicate the formation of a single molecular entity [LiMg(CH<sub>2</sub>SiMe<sub>3</sub>)<sub>2</sub>(dmem)]<sub>2</sub> (**4**) based on the independent diffusion coefficients of the chemical shifts in the <sup>1</sup>H NMR spectra. [LiMg(CH<sub>2</sub>SiMe<sub>3</sub>)<sub>2</sub>(dmem)]<sub>2</sub> (**4**):  $D = 4.53 \times 10^{-10} \text{ m}^2 \text{ s}^{-1}$

#### Synthesis of [NaMg(CH<sub>2</sub>SiMe<sub>3</sub>)<sub>2</sub>(dmem)]<sub>2</sub> **5**



In an argon flushed Schlenk flask, 1 mmol of Na(dmem) was prepared as described in section 3.5.1. Mg(CH<sub>2</sub>SiMe<sub>3</sub>)<sub>2</sub> (1mmol, 0.2g) was then added to a solution of Na(dmem) in hexane (5 mL) and stirred for one hour at room temperature to give a pale yellow solution. The solution was then stored at -30 °C overnight affording a colourless crop of crystals – compound **5**. Yield: 110mg, 35%. Anal. Calcd. for C<sub>30</sub>H<sub>78</sub>Na<sub>2</sub>Mg<sub>2</sub>N<sub>4</sub>O<sub>2</sub>Si<sub>4</sub> C, 49.10; H, 10.71; N, 7.63. Found: C, 48.88; H, 10.67; N, 7.77.

**Alternative synthesis:** In an argon-flushed Schlenk flask, 1 mmol of Mg(CH<sub>2</sub>SiMe<sub>3</sub>)(dmem) **7** (257 mg) was solubilised in hexane (5 mL) and to this solution was added 1 mmol NaCH<sub>2</sub>SiMe<sub>3</sub> (110 mg). The reaction was allowed to stir for one hour at room temperature to give a pale yellow solution. The solution was then stored at -30 °C overnight affording a colourless crop of crystals – compound **5**.

**<sup>1</sup>H-NMR (400 MHz, C<sub>6</sub>D<sub>6</sub>, 298 K):**  $\delta$  / ppm = 3.95-3.86 (m, 2H, OCH<sub>2</sub>, dmem), 2.57 (m, 1H, CH, dmem), 1.93-1.84 (m overlapping, 11H, 2 x CH, NMe & NMe<sub>2</sub>, dmem), 1.75 (m, 3H, 1 x CH, CH<sub>2</sub>N(Me), dmem), 0.40 (s, 18H, 6 x CH<sub>3</sub>, CH<sub>2</sub>SiMe<sub>3</sub>), -1.51-(-1.84) (v.br.m, 4H, 2 x CH<sub>2</sub>, CH<sub>2</sub>SiMe<sub>3</sub>). **<sup>1</sup>H-NMR (400 MHz, C<sub>6</sub>D<sub>6</sub>, 333 K):**  $\delta$  / ppm = 3.91 (m, 2H, OCH<sub>2</sub>, dmem), 2.58 (m, 1H, CH, dmem), 1.98-1.90 (m overlapping, 11H, 2 x CH, NMe & NMe<sub>2</sub>, dmem), 1.80 (m, 3H, 1 x CH, CH<sub>2</sub>N(Me), dmem), 0.36 (s, 18H, 6 x CH<sub>3</sub>, CH<sub>2</sub>SiMe<sub>3</sub>), -1.80 (s, 4H, 2 x CH<sub>2</sub>, CH<sub>2</sub>SiMe<sub>3</sub>). **<sup>13</sup>C{<sup>1</sup>H}-NMR (101 MHz, C<sub>6</sub>D<sub>6</sub>, 333 K):**  $\delta$  / ppm = 63.6 (CH<sub>2</sub>N(Me),

dmem), 58.7 (OCH<sub>2</sub>, dmem), 57.5 (CH<sub>2</sub>NMe<sub>2</sub>, dmem), 56.3 (N(Me)CH<sub>2</sub>, dmem), 46.0 (NMe<sub>2</sub>, dmem), 40.5 (NMe, dmem), 4.8 (3 x CH<sub>3</sub>, CH<sub>2</sub>SiMe<sub>3</sub>), -6.3 (CH<sub>2</sub>, CH<sub>2</sub>SiMe<sub>3</sub>),

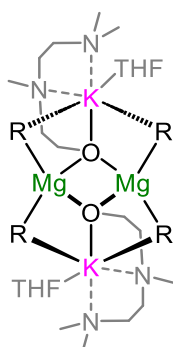
**<sup>1</sup>H-NMR (300.1 MHz, D<sub>8</sub>-THF, 298 K):** δ / ppm = 3.75-3.72 (m, 2H, OCH<sub>2</sub>, dmem), 2.57 (m, 2H, CH<sub>2</sub>, dmem), 2.40-2.30 (m overlapping, 7H, 2 x CH<sub>2</sub>, 1 x CH<sub>3</sub>, dmem), 2.25 (m, 6H, 2 x CH<sub>3</sub>, dmem), -0.07 (s, 18H, 6 x CH<sub>3</sub>, CH<sub>2</sub>SiMe<sub>3</sub>), -2.06 (s, 4H, 2 x CH<sub>2</sub>, CH<sub>2</sub>SiMe<sub>3</sub>).

**<sup>13</sup>C{<sup>1</sup>H}-NMR (101 MHz, D<sub>8</sub>-THF, 298 K):** δ / ppm = 64.4 (CH<sub>2</sub>N(Me), dmem), 59.0 (OCH<sub>2</sub>, dmem), 57.5 (CH<sub>2</sub>NMe<sub>2</sub>, dmem), 53.5 (N(Me)CH<sub>2</sub>, dmem), 45.7 (NMe<sub>2</sub>, dmem), 43.4 (NMe, dmem), 4.2 (6 x CH<sub>3</sub>, CH<sub>2</sub>SiMe<sub>3</sub>), -7.2 (2 x CH<sub>2</sub>, CH<sub>2</sub>SiMe<sub>3</sub>).

<sup>1</sup>H-DOSY NMR spectroscopic studies indicate the formation of a single molecular entity NaMg(CH<sub>2</sub>SiMe<sub>3</sub>)<sub>2</sub>(dmem) (**5**) based on the independent diffusion coefficients of the chemical shifts in the <sup>1</sup>H NMR spectra.

NaMg(CH<sub>2</sub>SiMe<sub>3</sub>)<sub>2</sub>(dmem) (**5**):  $D = 5.14 \times 10^{-10} \text{ m}^2 \text{ s}^{-1}$

#### Synthesis of [(THF)KMg(CH<sub>2</sub>SiMe<sub>3</sub>)<sub>2</sub>(dmem)]<sub>2</sub> **6**



In an argon flushed Schlenk flask, 1 mmol of K(dmem) was prepared as described in section 3.5.1. Mg(CH<sub>2</sub>SiMe<sub>3</sub>)<sub>2</sub> (1mmol, 0.2g) was then added to a solution of K(dmem) in hexane (5 mL) and stirred for one hour at room temperature to give a fine off-white suspension. Gentle heating of the suspension with a heat gun and addition of THF (0.25 mL) afforded a pale-yellow solution. The solution was then stored at -30 °C overnight affording a colourless crop of crystals – compound **3**. Yield: 110mg, 29%. Anal. Calcd. for C<sub>30</sub>H<sub>78</sub>K<sub>2</sub>Mg<sub>2</sub>N<sub>4</sub>O<sub>2</sub>Si<sub>4</sub> C, 47.03; H, 10.26; N, 7.31. Found: C, 46.51; H, 10.11; N, 7.02.

**Alternative synthesis:** In an argon-flushed Schlenk flask, 1 mmol of Mg(CH<sub>2</sub>SiMe<sub>3</sub>)(dmem) **7** (257 mg) was solubilised in hexane (5 mL) and to this solution was added 1 mmol KCH<sub>2</sub>SiMe<sub>3</sub> (110 mg). The reaction was allowed to stir for one hour at room temperature to give a fine white suspension. Gentle heating of the suspension with a heat gun and addition of THF (0.25 mL) afforded a pale-yellow solution. The solution was then stored at -30 °C overnight affording a colourless crop of crystals– compound **6**.

**<sup>1</sup>H-NMR (300.1 MHz, C<sub>6</sub>D<sub>6</sub>, 298 K):** δ / ppm = 3.96 (t, 2H, OCH<sub>2</sub>, dmem), 2.35 (br. m, 2H, CH<sub>2</sub>, dmem), 1.88 (m overlapping, 5H, 1 x CH<sub>2</sub>, 1 x CH<sub>3</sub>, dmem), 1.72 (m, 8H, 1 x CH<sub>2</sub>, 2 x CH<sub>3</sub>, dmem), 0.44 (s, 18H, 6 x CH<sub>3</sub>, CH<sub>2</sub>SiMe<sub>3</sub>), -1.78 (s, 4H, 2 x CH<sub>2</sub>, CH<sub>2</sub>SiMe<sub>3</sub>). **<sup>13</sup>C{<sup>1</sup>H}-NMR (101 MHz, C<sub>6</sub>D<sub>6</sub>, 298 K):** δ / ppm = 62.3 (CH<sub>2</sub>N(Me), dmem), 57.2 (OCH<sub>2</sub>, dmem), 54.6 (CH<sub>2</sub>NMe<sub>2</sub>, dmem), 53.4 (N(Me)CH<sub>2</sub>, dmem), 43.0 (NMe<sub>2</sub>, dmem), 38.7 (NMe, dmem), 2.9 (6 x CH<sub>3</sub>, CH<sub>2</sub>SiMe<sub>3</sub>), -6.3 (2 x CH<sub>2</sub>, CH<sub>2</sub>SiMe<sub>3</sub>).

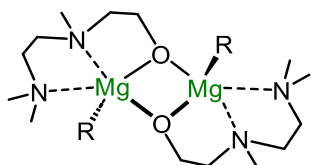


$^1\text{H}$ -DOSY NMR spectroscopic studies indicate the formation of a single molecular entity  $[(\text{THF})\text{KMg}(\text{CH}_2\text{SiMe}_3)_2(\text{dmem})]_2$  (**6**) based on the independent diffusion coefficients of the chemical shifts in the  $^1\text{H}$  NMR spectra.

$[(\text{THF})\text{KMg}(\text{CH}_2\text{SiMe}_3)_2(\text{dmem})]_2$  (**6**):  $D = 4.60 \times 10^{-10} \text{ m}^2\text{s}^{-1}$

### 3.5.3 Synthesis of $[\text{Mg}(\text{CH}_2\text{SiMe}_3)(\text{dmem})]_2$ **7**

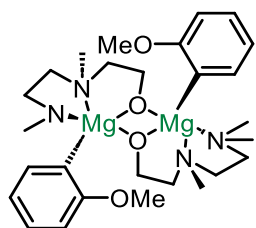
#### Synthesis of $[\text{Mg}(\text{CH}_2\text{SiMe}_3)(\text{dmem})]_2$ **7**



In an argon-flushed Schlenk flask, 1 mmol of  $\text{Mg}(\text{CH}_2\text{SiMe}_3)_2$  (1 mmol, 0.2 g) was suspended in hexane (5 mL) and cooled to  $0^\circ\text{C}$ . Hdmem (1 mmol, 0.16 mL) was then added dropwise forming a fine white suspension which was allowed to stir at room temperature for 1 h. Gentle heating of the suspension with a heat gun afforded a pale yellow solution. The solution was then stored at  $-30^\circ\text{C}$  overnight affording a colourless crop of crystals – compound **7**. Yield: 150 mg, 60%. Anal. Calcd. for  $\text{C}_{11}\text{H}_{28}\text{MgN}_2\text{OSi}$  C, 51.46; H, 10.99; N, 10.91. Found: C, 50.89; H, 10.76; N, 10.87.  $^1\text{H}$ -NMR (300.1 MHz,  $\text{C}_6\text{D}_6$ , 298 K):  $\delta$  / ppm = 3.82–3.53 (2 x m, 2H,  $\text{OCH}_2$ , dmem), 1.88 (m overlapping, 13H, 2 x  $\text{CH}_2$ , 3 x  $\text{CH}_3$ , dmem), 1.75–1.54 (2 x m, 2H, 1 x  $\text{CH}_2$ , dmem), 0.44 (s, 9H, 3 x  $\text{CH}_3$ ,  $\text{CH}_2\text{SiMe}_3$ ), -1.49 (–1.66) (2 x d, 4H, 2 x  $\text{CH}_2$ ,  $\text{CH}_2\text{SiMe}_3$ ).  $^{13}\text{C}\{^1\text{H}\}$ -NMR (101 MHz,  $\text{C}_6\text{D}_6$ , 298 K):  $\delta$  / ppm = 62.2 ( $\text{CH}_2\text{N}(\text{Me})$ , dmem), 58.6 ( $\text{OCH}_2$ , dmem), 56.7 ( $\text{CH}_2\text{NMe}_2$ , dmem), 52.0 ( $\text{N}(\text{Me})\text{CH}_2$ , dmem), 47.2 ( $\text{NMe}$ , dmem), 45.7 ( $\text{NMe}$ , dmem), 38.7 ( $\text{NMe}$ , dmem), 5.5 (6 x  $\text{CH}_3$ ,  $\text{CH}_2\text{SiMe}_3$ ), -8.4 (2 x  $\text{CH}_2$ ,  $\text{CH}_2\text{SiMe}_3$ ).

### 3.5.4 Synthesis of $[\text{Mg}(\text{Ar})(\text{dmem})]_2$ (Ar = *o*-OMe- $\text{C}_6\text{H}_4$ ) **8**

#### Synthesis of $[\text{Mg}(\text{Ar})(\text{dmem})]_2$ (Ar = *o*-OMe- $\text{C}_6\text{H}_4$ ) **8**

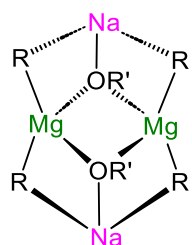


In an argon flushed Schlenk flask 1 mmol of  $\text{K}(\text{dmem})$  **3** was prepared as described in section 3.5.1.  $\text{Mg}(\text{CH}_2\text{SiMe}_3)_2$  (1 mmol, 0.2 g) was then added to a solution of  $\text{K}(\text{dmem})$  in hexane (5 mL) and stirred for one hour at room temperature to give a fine off-white suspension. All solvent was removed under vacuum to give a white solid which was dissolved in benzene (5 mL). To this solution was added 2-bromoanisole (2 mmol, 0.25 mL) at room temperature and allowed to stir for 1 h affording a pale-yellow suspension. All solvent removed under vacuum to afford an off-white solid that was then suspended in hexane (5 mL). Toluene (approx. 2 mL) was added whilst vigorously heating the suspension. The pale-yellow filtrate was then isolated via cannula filtration and the solution was then stored at  $-30^\circ\text{C}$  overnight affording a colourless crop of crystals – compound **8**. Yield: 80 mg, 30%. Anal.

Calcd. for  $C_{35}H_{56}Mg_2N_4O_4$  C, 65.13; H, 8.75; N, 8.68. Found: C, 64.28; H, 8.79; N, 8.87. Note: **8** crystallises with a single molecule of toluene.  **$^1H$ -NMR (300.1 MHz,  $D_8$ -Tol, 298 K):**  $\delta$  / ppm = 7.84 (m, 1H,  $C_{Ar-H}$ ), 7.30 (m, 1H,  $C_{Ar-H}$ ), 7.17 (m, 1H,  $C_{Ar-H}$ ), 6.71 (d, 1H,  $C_{Ar-H}$ ), 3.68 (m, 2H,  $OCH_2$ , dmem), 3.55 (s, 3H,  $CH_3$ ,  $OMe$ ), 2.56 (m, 1H, 1 x CH, dmem), 2.40-2.13 (br. m, 8H, 1 x  $CH_2$ , 2 x  $CH_3$ , dmem), 2.03 (m, 1H, 1 x CH, dmem), 1.97 (s, 3H, 1 x  $CH_3$ , dmem), 1.55 (m, 1H, 1 x CH, dmem), 1.32 (m, 1H, 1 x CH, dmem).  **$^{13}C\{^1H\}$ -NMR (75.5 MHz,  $D_8$ -Tol, 298 K):**  $\delta$  / ppm = 168.1 ( $C_{Ar-Mg}$ ), 158.4 ( $C_{Ar-q}$ ), 141.8 ( $C_{Ar-H}$ ), 125.3 ( $C_{Ar-H}$ ), 120.5 ( $C_{Ar-H}$ ), 106.3 ( $C_{Ar-H}$ ), 62.2 ( $CH_2N(Me)$ , dmem), 59.0 ( $OCH_2$ , dmem), 56.8 ( $CH_2NMe_2$ , dmem), 53.4 ( $N(Me)CH_2$ , dmem), 50.5 ( $NMe_2$ , dmem), 34.0 ( $NMe$ , dmem).

### 3.5.5 Synthesis of $[MMg(CH_2SiMe_3)_2OR']_2$ ( $R' = 2$ -Ethylhexyl) ( $M = Na$ , **9**; $K$ , **10**)

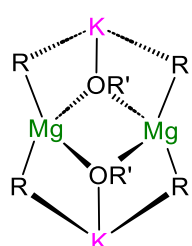
#### Synthesis of $[NaMg(CH_2SiMe_3)_2OR']_2$ **9** ( $R' = 2$ -Ethylhexyl)



In an argon-flushed Schlenk flask, 1 mmol of  $NaOR'$  was prepared as described in section 3.5.1.  $Mg(CH_2SiMe_3)_2$  (1mmol, 0.2 g) was then added to a fine suspension of  $NaOR'$  in hexane (5 mL) and stirred for one hour at room temperature to give a pale yellow solution. All solvent was removed under vacuum to afford a clear colourless oil – compound **9**.  **$^1H$ -NMR (300.1 MHz,  $C_6D_6$ , 298 K):**  $\delta$  / ppm = 3.50 (m, 2H,  $OCH_2$ ,  $OR'$ ), 1.36 (br. m, 9H, 1 x  $CH$ , 4 x  $CH_2$ ,  $OR'$ ), 0.98 (br. t, 3H,  $CH_3$ ,  $OR'$ ), 0.92 (br. t, 3H,  $CH_3$ ,  $OR'$ ), 0.28 (s, 18H, 6 x  $CH_3$ ,  $CH_2SiMe_3$ ), -2.1 (s, 4H, 2 x  $CH_2$ ,  $CH_2SiMe_3$ ).  **$^{13}C\{^1H\}$ -NMR (101 MHz,  $C_6D_6$ , 298 K):**  $\delta$  / ppm = 66.5 ( $OCH_2$ ,  $OR'$ ), 45.4 ( $OCH_2C(H)$ ,  $OR'$ ), 30.9 ( $CH_2$ ,  $OR'$ ), 29.6 ( $CH_2$ ,  $OR'$ ), 24.3 ( $CH_2$ , Et,  $OR'$ ), 23.7 ( $CH_2$ ,  $OR'$ ), 14.3 ( $CH_3$ , Et,  $OR'$ ), 11.1 ( $CH_3$ ,  $OR'$ ), 4.6 (6 x  $CH_3$ ,  $CH_2SiMe_3$ ), -6.2 (2 x  $CH_2$ ,  $CH_2SiMe_3$ ).

**$^1H$ -NMR (300.1 MHz,  $C_6D_6$ , 298 K):**  $\delta$  / ppm = 3.50 (m, 2H,  $OCH_2$ ,  $OR'$ ), 1.36 (br. m, 9H, 1 x  $CH$ , 4 x  $CH_2$ ,  $OR'$ ), 0.98 (br. t, 3H,  $CH_3$ ,  $OR'$ ), 0.92 (br. t, 3H,  $CH_3$ ,  $OR'$ ), 0.28 (s, 18H, 6 x  $CH_3$ ,  $CH_2SiMe_3$ ), -2.1 (s, 4H, 2 x  $CH_2$ ,  $CH_2SiMe_3$ ).  **$^{13}C\{^1H\}$ -NMR (101 MHz,  $C_6D_6$ , 298 K):**  $\delta$  / ppm = 66.5 ( $OCH_2$ ,  $OR'$ ), 45.4 ( $OCH_2C(H)$ ,  $OR'$ ), 30.9 ( $CH_2$ ,  $OR'$ ), 29.6 ( $CH_2$ ,  $OR'$ ), 24.3 ( $CH_2$ , Et,  $OR'$ ), 23.7 ( $CH_2$ ,  $OR'$ ), 14.3 ( $CH_3$ , Et,  $OR'$ ), 11.1 ( $CH_3$ ,  $OR'$ ), 4.6 (6 x  $CH_3$ ,  $CH_2SiMe_3$ ), -6.2 (2 x  $CH_2$ ,  $CH_2SiMe_3$ ).

#### Synthesis of $[KMg(CH_2SiMe_3)_2OR']_2$ **10** ( $R' = 2$ -Ethylhexyl)



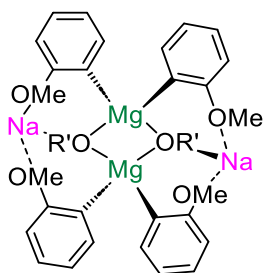
In an argon-flushed Schlenk flask, 1 mmol of  $KOR'$  was prepared as described in section 3.5.1.  $Mg(CH_2SiMe_3)_2$  (1mmol, 0.2 g) was then added to a solution of  $KOR'$  in hexane (5 mL) and stirred for one hour at room temperature to give a colourless solution. The solution was then stored at -30 °C overnight affording a colourless crop of crystals – compound **10**.

Yield: 200 mg, 55%. Anal. Calcd. for  $C_{24}H_{61}K_2Mg_2O_2Si_4$  C, 52.36; H, 10.71. Found: C, 52.1; H, 10.7.  **$^1H$ -NMR (300.1 MHz,  $C_6D_6$ , 298 K):**  $\delta$  / ppm = 3.49 (m, 2H,  $OCH_2$ ,  $OR'$ ), 1.60-1.23 (br. m, 9H, 1 x  $CH$ , 4 x  $CH_2$ ,  $OR'$ ), 1.00 (br. m, 6H, 2 x  $CH_3$ ,  $OR'$ ), 0.30 (s, 18H, 6 x  $CH_3$ ,  $CH_2SiMe_3$ ), -1.92 (s, 4H, 2 x  $CH_2$ ,  $CH_2SiMe_3$ ).  **$^{13}C\{^1H\}$ -NMR (101 MHz,  $C_6D_6$ , 298 K):**  $\delta$  / ppm = 67.2 ( $OCH_2$ ,  $OR'$ ), 45.3 ( $OCH_2C(H)$ ,  $OR'$ ), 30.9 ( $CH_2$ ,  $OR'$ ), 29.8 ( $CH_2$ ,  $OR'$ ), 24.3

(CH<sub>2</sub>, Et, OR'), 23.8 (CH<sub>2</sub>, OR'), 14.5 (CH<sub>3</sub>, Et, OR'), 11.2 (CH<sub>3</sub>, OR'), 5.1 (6 x CH<sub>3</sub>, CH<sub>2</sub>SiMe<sub>3</sub>), -3.1 (2 x CH<sub>2</sub>, CH<sub>2</sub>SiMe<sub>3</sub>).

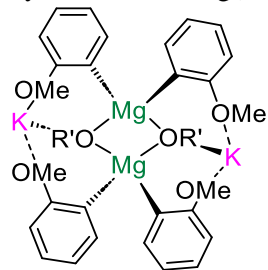
### 3.5.6 Synthesis of [MMg(Ar)<sub>2</sub>OR']<sub>2</sub> (R' = 2-Ethylhexyl) (Ar = *o*-OMe-C<sub>6</sub>H<sub>4</sub>) (M = Na, **11**; K, **12**)

#### Synthesis of [NaMg(Ar)<sub>2</sub>OR']<sub>2</sub> (R' = 2-Ethylhexyl) (Ar = *o*-OMe-C<sub>6</sub>H<sub>4</sub>) **11**



In an argon-flushed Schlenk flask, 1 mmol of NaOR' was prepared as described in section 3.5.1. Mg(CH<sub>2</sub>SiMe<sub>3</sub>)<sub>2</sub> (1mmol, 0.2 g) was then added to a fine suspension of NaOR' in hexane (5 mL) and stirred for one hour at room temperature to give a pale yellow solution. All solvent was removed under vacuum to give a white solid which was dissolved in benzene (5 mL). To this solution was added 2-bromoanisole (2 mmol, 0.25 mL) at room temperature and allowed to stir for 1h affording a pale-yellow suspension. All solvent removed under vacuum to afford an off-white solid that was then suspended in hexane (5 mL). Toluene (approx. 3 mL) was added with gentle heating to give a pale-yellow solution. Allowing the solution to slowly cool to room temperature overnight afforded a colourless crop of crystals – compound **11**. Yield: 210 mg, 54%. Anal. Calcd. for C<sub>44</sub>H<sub>62</sub>Mg<sub>2</sub>Na<sub>2</sub>O<sub>6</sub> C, 67.62; H, 8.00. Found: C, 66.47; H, 7.93. **<sup>1</sup>H-NMR (300.1 MHz, C<sub>6</sub>D<sub>6</sub>, 298 K):** δ / ppm = 8.21 (m, 2H, C<sub>Ar</sub>-H), 7.31-7.17 (m, 4H, 2 x C<sub>Ar</sub>-H), 6.67 (d, 2H, C<sub>Ar</sub>-H), 3.88 (m, 2H, OCH<sub>2</sub>, OR'), 3.23 (s, 6H, 2 x CH<sub>3</sub>, OMe), 1.42-1.04 (br. m, 9H, 1 x CH, 4 x CH<sub>2</sub>, OR'), 0.84 (br. t, 3H, CH<sub>3</sub>, OR'), 0.76 (br. t, 3H, CH<sub>3</sub>, OR'). **<sup>13</sup>C{<sup>1</sup>H}-NMR (101 MHz, C<sub>6</sub>D<sub>6</sub>, 298 K):** δ / ppm = 167.2 (C<sub>Ar</sub>-Mg), 154.5 (C<sub>Ar</sub>-q), 143.9 (C<sub>Ar</sub>-H), 127.0 (C<sub>Ar</sub>-H), 122.5 (C<sub>Ar</sub>-H), 109.7 (C<sub>Ar</sub>-H), 67.2 (OCH<sub>2</sub>, OR'), 55.8 (OCH<sub>2</sub>C(H), OR'), 44.5 (CH<sub>2</sub>, OR'), 30.8 (CH<sub>2</sub>, OR'), 29.3 (CH<sub>2</sub>, Et, OR'), 23.7 (CH<sub>2</sub>, OR'), 14.5 (CH<sub>3</sub>, Et, OR'), 10.8 (CH<sub>3</sub>, OR').

<sup>1</sup>H-DOSY NMR spectroscopic studies indicate the formation of a single molecular entity [NaMg(*o*-OMe-C<sub>6</sub>H<sub>4</sub>)<sub>2</sub>(OR')]<sub>2</sub> (**11**) based on the independent diffusion coefficients of the chemical shifts in the <sup>1</sup>H NMR spectra. [NaMg(*o*-OMe-C<sub>6</sub>H<sub>4</sub>)<sub>2</sub>(OR')]<sub>2</sub> (**11**): *D* = 4.04x10<sup>-10</sup> m<sup>2</sup>s<sup>-1</sup>.

**Synthesis of [KMg(Ar)<sub>2</sub>OR']<sub>2</sub> (R' = 2-Ethylhexyl) (Ar = *o*-OMe-C<sub>6</sub>H<sub>4</sub>) **12****

In an argon flushed J. Young's NMR tube isolated crystals of potassium magnesiate **7** (0.1 mmol, 36 mg) were dissolved in C<sub>6</sub>D<sub>6</sub> (0.5 mL). To this solution 0.2 mmol of 2-bromoanisole (25 μL) was then added at room temperature and the reaction monitored by NMR spectroscopy to give quantitative conversion to compound **7** after 3h

at room temperature with concomitant formation of BrCH<sub>2</sub>SiMe<sub>3</sub>. **<sup>1</sup>H-NMR (300.1 MHz, C<sub>6</sub>D<sub>6</sub>, 298 K):** δ / ppm = 8.02 (m, 2H, 2 x C<sub>Ar-H</sub>), 7.19 (m, 2H, 2 x C<sub>Ar-H</sub>), 6.67 (d, 2H, C<sub>Ar-H</sub>), 3.93 (m, 2H, OCH<sub>2</sub>, OR'), 3.41 (s, 6H, 2 x CH<sub>3</sub>, OMe), 2.11 (s, 4H, 2 x CH<sub>2</sub>, BrCH<sub>2</sub>SiMe<sub>3</sub>), 1.38 (V. br m, 9H, 1 x CH, 4 x CH<sub>2</sub>, OR'), 0.94 (m, 6H, 2 x CH<sub>3</sub>, OR'), -0.03 11 (s, 12H, 2 x CH<sub>2</sub>, BrCH<sub>2</sub>SiMe<sub>3</sub>). **<sup>13</sup>C{<sup>1</sup>H}-NMR (101 MHz, C<sub>6</sub>D<sub>6</sub>, 298 K):** δ / ppm = 167.1 (C<sub>Ar-Mg</sub>), 158.2 (C<sub>Ar-q</sub>), 143.5 (C<sub>Ar-H</sub>), 121.7 (C<sub>Ar-H</sub>), 114.3 (C<sub>Ar-H</sub>), 108.7 (C<sub>Ar-H</sub>), 67.5 (OCH<sub>2</sub>, OR'), 55.0 (OCH<sub>2</sub>C(H), OR'), 44.6 (CH<sub>2</sub>, OR'), 30.9 (CH<sub>2</sub>, OR'), 29.7 (CH<sub>2</sub>, Et, OR'), 23.8 (CH<sub>2</sub>, OR'), 17.7 (CH<sub>2</sub>, BrCH<sub>2</sub>SiMe<sub>3</sub>), 14.5 (CH<sub>3</sub>, Et, OR'), 10.9 (CH<sub>3</sub>, OR'), -2.6 (CH<sub>3</sub>, BrCH<sub>2</sub>SiMe<sub>3</sub>).

<sup>1</sup>H-DOSY NMR spectroscopic studies indicate the formation of a single molecular entity [KMg(*o*-OMe-C<sub>6</sub>H<sub>4</sub>)<sub>2</sub>(OR')] (**12**) based on the independent diffusion coefficients of the chemical shifts in the <sup>1</sup>H NMR spectra. [KMg(*o*-OMe-C<sub>6</sub>H<sub>4</sub>)<sub>2</sub>(OR')] (**12**): *D* = 3.4x10<sup>-10</sup> m<sup>2</sup>s<sup>-1</sup>

**3.5.7 Aqueous Quench of Insoluble Putative KAr (Ar = *o*-OMe-C<sub>6</sub>H<sub>4</sub>)**

In an argon flushed Schlenk flask 1 mmol of K(dmcm) was prepared as described in section **3.5.1**. Mg(CH<sub>2</sub>SiMe<sub>3</sub>)<sub>2</sub> (1mmol, 0.2 g) was then added to a solution of K(dmcm) in hexane (5 mL) and stirred for one hour at room temperature to give a fine off-white suspension. All solvent was removed under vacuum to give a white solid which was dissolved in benzene (5 mL). To this solution was added 2-bromoanisole (2 mmol, 0.25 mL) at room temperature and allowed to stir for 1h affording a pale-yellow suspension. All solvent removed under vacuum to afford an off-white solid that was then suspended in hexane (5 mL). The solid was isolated via cannula filtration and washed with hexane (10 mL) giving the putative KAr (Ar = *o*-OMe-C<sub>6</sub>H<sub>4</sub>) species (0.20 g). An aqueous quench was then performed with NH<sub>4</sub>Cl. The aqueous layer was then extracted with 1 x 25 mL and 2 x 20 mL of EtOAc (70 mL total), before combining all organic layers and drying over MgSO<sub>4</sub>. A 50 μL aliquot was diluted in 1 mL of ethyl acetate then subjected to GC analysis which shows the formation of anisole (30 mg, 28%). (20 mol% of hexamethylbenzene as internal standard).

### **3.5.8 Mg/Br exchange of 2-bromoanisole with [(TMEDA)<sub>2</sub>K<sub>2</sub>MgR<sub>4</sub>] (R = CH<sub>2</sub>SiMe<sub>3</sub>)**

In an argon flushed Schlenk flask 1 mmol of [(TMEDA)<sub>2</sub>K<sub>2</sub>MgR<sub>4</sub>] was prepared as described in literature procedures<sup>58</sup> by co-complexation of K(CH<sub>2</sub>SiMe<sub>3</sub>) (2 mmol, 0.253 g) and Mg(CH<sub>2</sub>SiMe<sub>3</sub>)<sub>2</sub> (1 mmol, 0.2 g) in hexane (10 mL) forming a white suspension. After allowing the suspension to stir at room temperature for one hour two equivalents TMEDA (2 mmol, 0.3 mL) was then added affording a pale-yellow solution. All solvent was removed under vacuum to afford an off-white solid which was dissolved in benzene (5 mL). To this solution was added 2-bromoanisole (4 mmol, 0.5 mL) at room temperature and allowed to stir for one hour. An aqueous quench was then performed with NH<sub>4</sub>Cl. The aqueous layer was then extracted with 1 x 25 mL and 2 x 20 mL of EtOAc (70 mL total), before combining all organic layers and drying over MgSO<sub>4</sub>. A 50 μL aliquot was diluted in 1 mL of ethyl acetate then subjected to GC analysis which shows the formation of anisole in a 57% yield. (20 mol% of hexamethylbenzene as internal standard).

### 3.6 References

- 1 M. Schlosser, *J. Organomet. Chem.*, 1967, **8**, 9–16.
- 2 P. Caubère, *Chem. Rev.*, 1993, **93**, 2317–2334.
- 3 L. Lochmann, J. Pospíšil and D. Lím, *Tetrahedron Lett.*, 1966, **7**, 257–262.
- 4 L. Lochmann and M. Janata, *Cent. Eur. J. Chem.*, 2014, **12**, 537–548.
- 5 M. Schlosser, *Angew. Chem. Int. Ed.*, 2005, **44**, 376–393.
- 6 M. Schlosser and S. Strunk, *Tetrahedron Lett.*, 1984, **25**, 741–744.
- 7 L. Lochmann, *Eur. J. Inorg. Chem.*, 2000, 1115–1126.
- 8 F. Mongin and A. Harrison-Marchand, *Chem. Rev.*, 2013, **113**, 7563–7727.
- 9 S. D. Robertson, M. Uzelac and R. E. Mulvey, *Chem. Rev.*, 2019, **119**, 8332–8405.
- 10 J. Klett, *Chem. – A Eur. J.*, 2021, **27**, 888–904.
- 11 P. Benrath, M. Kaiser, T. Limbach, M. Mondeshki and J. Klett, *Angew. Chem. Int. Ed.*, 2016, **55**, 10886–10889.
- 12 J. Farkas, S. J. Stoudt, E. M. Hanawalt, A. D. Pajerski and H. G. Richey, *Organometallics*, 2004, **23**, 423–427.
- 13 D. S. Ziegler, K. Karaghiosoff and P. Knochel, *Angew. Chem. Int. Ed.*, 2018, **57**, 6701–6704.
- 14 A. Desaintjean, T. Haupt, L. J. Bole, N. R. Judge, E. Hevia and P. Knochel, *Angew. Chem. Int. Ed.*, 2021, **60**, 1513–1518.
- 15 L. J. Bole, N. R. Judge and E. Hevia, *Angew. Chem. Int. Ed.*, 2021, **60**, 7626–7631.
- 16 J. M. Gil-Negrete and E. Hevia, *Chem. Sci.*, 2021, 1982–1992.
- 17 A. M. Borys and E. Hevia, *Trends Chem.*, 2021, **xx**, 8–11.
- 18 M. De Tullio, A. M. Borys, A. Hernán-Gómez, A. R. Kennedy and E. Hevia, *Chem Catal.*, 2021, **1**, 1308–1321.
- 19 T. X. Gentner and R. E. Mulvey, *Angew. Chem. Int. Ed.*, 2021, **60**, 9247–9262.
- 20 A. Harrison-Marchand and F. Mongin, *Chem. Rev.*, 2013, **113**, 7470–7562.
- 21 M. J. Evans, M. D. Anker, C. L. McMullin, S. E. Neale and M. P. Coles, *Angew. Chem. Int. Ed.*, 2021, **60**, 22289–22292.

- 22 T. X. Gentner, A. R. Kennedy, E. Hevia and R. E. Mulvey, *ChemCatChem*, 2021, **13**, 2371–2378.
- 23 D. B. Pardue, S. J. Gustafson, R. A. Periana, D. H. Ess and T. R. Cundari, *Comput. Theor. Chem.*, 2013, **1019**, 85–93.
- 24 A. M. Borys and E. Hevia, *Trends Chem.*, 2021, **3**, 803–806.
- 25 P. Mastropierro, Z. Livingstone, S. D. Robertson, A. R. Kennedy and E. Hevia, *Organometallics*, 2020, **39**, 4273–4281.
- 26 P. Mastropierro, A. R. Kennedy and E. Hevia, *Eur. J. Inorg. Chem.*, 2020, **2**, 1016–1022.
- 27 N. D. R. Barnett, W. Clegg, A. R. Kennedy, R. E. Mulvey and S. Weatherstone, *Chem. Commun.*, 2005, **190**, 375–377.
- 28 M. Balkenhohl, D. S. Ziegler, A. Desaintjean, L. J. Bole, A. R. Kennedy, E. Hevia and P. Knochel, *Angew. Chem. Int. Ed.*, 2019, **58**, 12898–12902.
- 29 B. T. Ko and C. C. Lin, *J. Am. Chem. Soc.*, 2001, **123**, 7973–7977.
- 30 X. Song, Z. Wang, J. Zhao and T. S. A. Hor, *Chem. Commun.*, 2013, **49**, 4992–4994.
- 31 R. Curci and F. di Furia, *Int. J. Chem. Kinet.*, 1975, **7**, 341–349.
- 32 A. R. Kennedy, J. Klett, R. E. Mulvey and S. D. Robertson, *Eur. J. Inorg. Chem.*, 2011, 4675–4679.
- 33 D. R. Armstrong, D. Barr, W. Clegg, S. M. Hodgson, R. E. Mulvey, D. Reed, R. Snaith and D. S. Wright, *Angew. Chem. Int. Ed.*, 1989, **20**, 4719–4727.
- 34 R. E. Mulvey, *Chem. Soc. Rev.*, 1991, **20**, 167.
- 35 D. R. Baker, R. E. Mulvey, W. Clegg and P. A. O’Neil, *J. Am. Chem. Soc.*, 1993, **115**, 6472–6473.
- 36 A. R. Kennedy, R. E. Mulvey and A. Robertson, *Chem. Commun.*, 1998, **0**, 89–90.
- 37 R. E. Mulvey, *Chem. Soc. Rev.*, 1998, **27**, 339–346.
- 38 A. Downard and T. Chivers, *Eur. J. Inorg. Chem.*, 2001, 2193–2201.
- 39 W. Clegg, S. H. Dale, D. V. Graham, R. W. Harrington, E. Hevia, L. M. Hogg, A. R. Kennedy and R. E. Mulvey, *Chem. Commun.*, 2007, 1641–1643.
- 40 M. M. Olmstead, W. J. Grigsby, D. R. Chacon, T. Hascall and P. P. Power, *Inorg.*

- Chim. Acta.*, 1996, **251**, 273–284.
- 41 S. Sakamoto, T. Imamoto and K. Yamaguchi, *Org. Lett.*, 2001, **3**, 1793–1795.
- 42 K. Merz, S. Block, R. Schoenen and M. Driess, *J. Chem. Soc. Dalton Trans.*, 2003, **3**, 3365–3369.
- 43 S. E. Baillie, E. Hevia, A. R. Kennedy and R. E. Mulvey, *Organometallics*, 2007, **26**, 204–209.
- 44 E. Hevia, A. R. Kennedy, R. E. Mulvey and S. Weatherstone, *Angew. Chem. Int. Ed.*, 2004, **43**, 1709–1712.
- 45 K. J. Drewette, K. W. Henderson, A. R. Kennedy, R. E. Mulvey, C. T. O’Hara and R. B. Rowlings, *Chem. Commun.*, 2002, **2**, 1176–1177.
- 46 M. Uzelac, I. Borilovic, M. Amores, T. Cadenbach, A. R. Kennedy, G. Aromí and E. Hevia, *Chem. Eur. J.*, 2016, **22**, 4843–4854.
- 47 R. E. Mulvey, *Chem. Commun.*, 2001, 1049–1056.
- 48 A. R. Kennedy, R. E. Mulvey, C. L. Raston, B. A. Roberts and R. B. Rowlings, *Chem. Commun.*, 1999, **2**, 353–354.
- 49 G. C. Forbes, A. R. Kennedy, R. E. Mulvey, R. B. Rowlings, W. Clegg, S. T. Liddle and C. C. Wilson, *Chem. Commun.*, 2000, **2**, 1759–1760.
- 50 A. R. Kennedy, J. Klett, R. E. Mulvey, S. Newton and D. S. Wright, *Chem. Commun.*, 2008, **7345**, 308–310.
- 51 G. E. Coates, J. A. Heslop, M. E. Redwood and D. Ridley, *J. Chem. Soc. A Inorganic, Phys. Theor.*, 1968, **5**, 1118.
- 52 M. M. Sung, C. G. Kim, J. Kim and Y. Kim, *Chem. Mater.*, 2002, **14**, 826–831.
- 53 C. A. Moreno, D. L. Hughes and M. Bochmann, *Polyhedron*, 2007, **26**, 2523–2526.
- 54 S. Heitz, Y. Aksu, C. Merschjann and M. Driess, *Chem. Mater.*, 2010, **22**, 1376–1385.
- 55 J. Francos, P. C. Gros, A. R. Kennedy and C. T. O’Hara, *Organometallics*, 2015, **34**, 2550–2557.
- 56 C. Yeardley, A. R. Kennedy, P. C. Gros, S. Touchet, M. Fairley, R. McLellan, A. J. Martínez-Martínez and C. T. O’Hara, *Dalton Trans.*, 2020, **49**, 5257–5263.
- 57 R. Neufeld and D. Stalke, *Chem. Sci.*, 2015, **6**, 3354–3364.

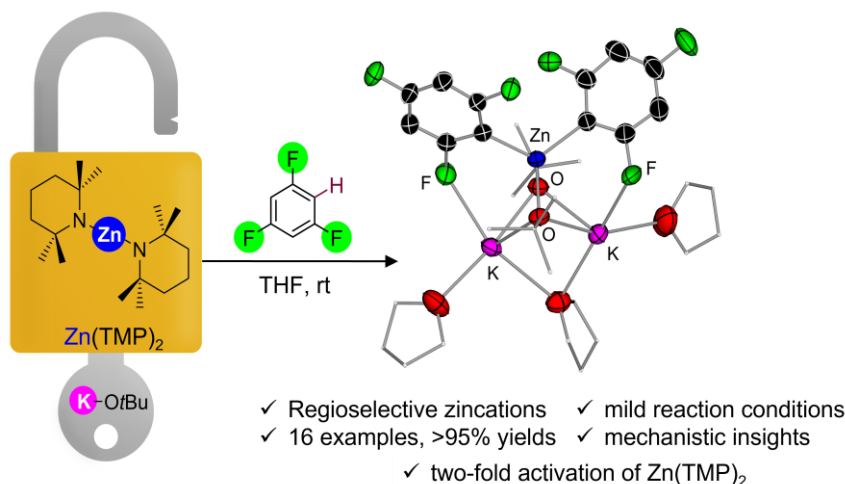


- 58 M. Fairley, L. Davin, A. Hernán-Gómez, J. García-Álvarez, C. T. O'Hara and E. Hevia, *Chem. Sci.*, 2019, **10**, 5821–5831.

## Chapter 4: Alkali-Metal-Alkoxide Powered Zincation of Fluoroarenes Employing Zinc Bis-Amide Zn(TMP)<sub>2</sub>

This chapter is adapted from a publication in a peer reviewed journal:

*Alkali-metal-alkoxide powered zincation of fluoroarenes employing zinc bis-amide Zn(TMP)<sub>2</sub>*, N. R. Judge and E. Hevia, *Angew. Chem. Int. Ed.*, **2023**, 62, e202303099.



Contributing authors to the manuscript and their role:

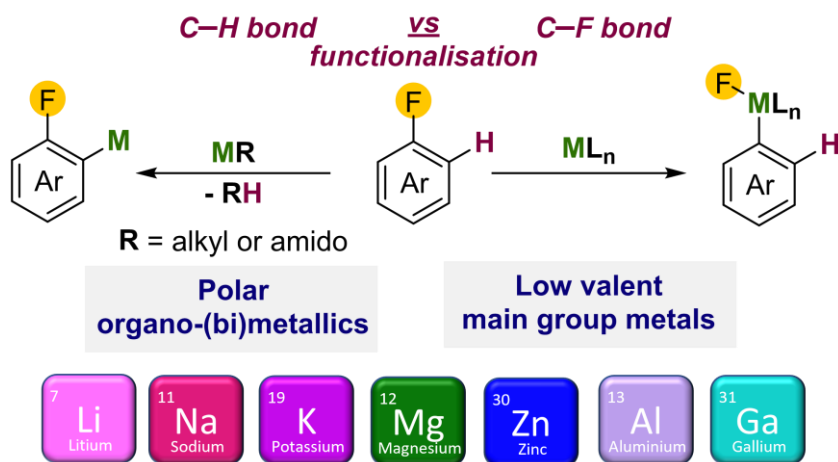
Neil Judge: Designed and performed all experimental work, analysed and processed all data, wrote the first draft of the manuscript and the supporting information.

Eva Hevia: Principal Investigator, conceived the project, secured the funding, directed the work, and revised the final version of the manuscript.

The introduction to this Chapter is adapted from a publication in a peer reviewed journal:

*Main Group Metal Strategies for C–H and C–F Bond Functionalisation of Fluoroarenes.*

N. R. Judge, A. Logallo and E. Hevia, *Chem Sci*, **2023**, 14, 11617. (Perspective Article)



Contributing authors to the manuscript and their role:

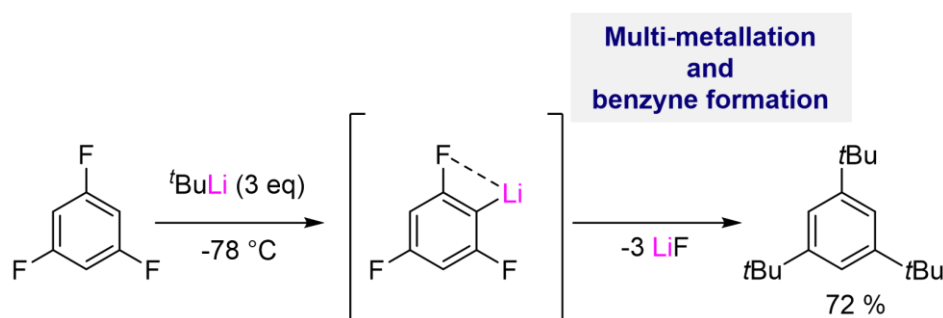
Neil Judge: Wrote the first draft of the manuscript specifically focussing on main group metal strategies for C–H functionalisation of fluoroarenes.

Alessandra Logallo: Wrote the first draft of the manuscript specifically focussing on main group metal strategies for C–F functionalisation of fluoroarenes.

Eva Hevia: Principal Investigator, edited and revised the final version of the manuscript with contributions from all authors.

## 4.1 Introduction

Fluoroarenes are recurrent structural building blocks present in a variety of agrochemicals and active pharmaceutical ingredients.<sup>1–3</sup> The special nature of fluorine can provide organic compounds with enhanced metabolic stability, bioavailability, lipophilicity and binding affinity among other properties.<sup>4,5</sup> Despite their synthetic relevance and the fact that fluorine is the most abundant halogen in the Earth's crust, fluoroarenes are rarely found in nature.<sup>6</sup> Thus, the development of methods for the regioselective functionalisation of the C–H bonds in these molecules is highly relevant in synthesis to access value added polyfunctionalised fluoroarenes. Classical approaches include the use of *s*-block organometallics, typically alkyl lithium reagents, for deprotonative metalation or nucleophilic aromatic substitutions of fluoroarenes.<sup>7,8</sup> However the highly polar nature of these reagents and the fragility of the relevant metalated intermediates imposes important drawbacks, including limited functional group tolerance and selectivity, requiring in many cases the use of strict reaction conditions.<sup>8</sup> The complexity of these reactions is illustrated by Schlosser's seminal study on the lithiation of 1,3,5-trifluorobenzene,<sup>8</sup> where the initial metalation of this substrate by *t*BuLi at -78 °C leads to multiple hydrogen/lithium interconversions, along with benzyne formation, triggering a cascade C-F to C-C bond process giving 1,3,5-tri(*tert*-butyl)benzene.

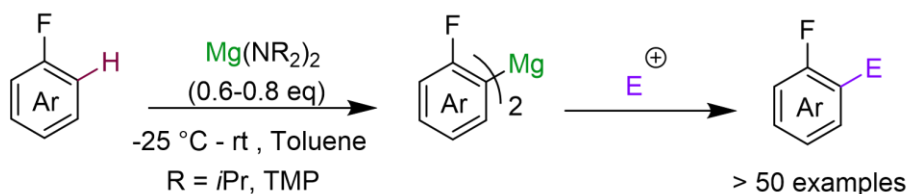


**Scheme 1.** Challenges in the deprotonative metalation of fluoroarenes using organolithium reagents.

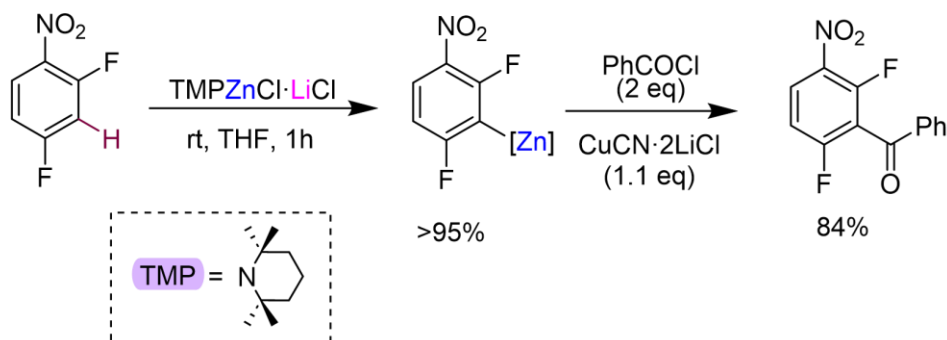
To address these limitations, alternative metalating reagents have been developed using non-nucleophilic bases containing bulky basic amide groups in combination with less

electropositive metals (e.g., Mg, Zn). Seminal advances in this field include Knochel's work who has recently described the use of magnesium amides  $Mg(NR_2)_2$  ( $NR_2 = NiPr_2$ , TMP; TMP= 2,2,6,6-tetramethylpiperidide) for the regioselective C–H magnesiation of a wide range of substituted fluoroarenes producing *bis*-aryl magnesium intermediates  $Mg(Ar^F)_2$  (Scheme 2a).<sup>9,10</sup> This methodology boasts an impressive substrate scope (including perfluoroarenes and fluoropyridines) and tolerates sensitive functional groups such as ester, amide and azide functionalities. Remarkably, most of these reactions can be carried out at room temperature in toluene solutions. While no trapping or characterisation of the metalated intermediates has been reported, their electrophilic interception has been extensively studied, demonstrating the excellent versatility of this approach to furnish highly functionalised fluoroarenes. The same group has also developed highly chemoselective LiCl-powered Zn bases containing TMP groups, namely  $TMPZnCl \cdot LiCl$  and  $TMP_2Zn \cdot 2MgCl_2 \cdot 2LiCl$ .<sup>11,12</sup> These mild and efficient Zn bases can successfully promote direct Zn–H exchanges of fluoroarenes bearing extremely sensitive functional groups such as nitro moieties (as shown for 2,4-difluoronitrobenzene in Scheme 2b).<sup>11,13</sup> The zincated intermediates can participate directly in Negishi cross-couplings or undergo transmetalation with Cu salts which enables the formation of the relevant arylation products in high yields (Scheme 2b). While from a mechanistic perspective the constitution of the organometallic intermediates involved in these reactions remains blurred, work assessing the constitution of Turbo Hauser bases  $(NR_2)MgCl \cdot LiCl$  and  $TMPZnBr \cdot LiBr$  has revealed the involvement of kinetically activated lithium magnesiate and zincate species respectively.<sup>14–16</sup>

## a) Mg bis(amides)



## b) LiCl-powered Zn-TMP bases



**Scheme 2.** Magnesium and zinc amide bases for regioselective C-H metalation of fluoroarenes.

While, as mentioned above, direct lithiation of fluoroarenes can be challenging Mulvey and Hevia have shown that when using the utility amide LiTMP in combination with an organometallic trap such as Al(TMP)*i*Bu<sub>2</sub> or Ga(CH<sub>2</sub>SiMe<sub>3</sub>)<sub>3</sub>, it is possible to stabilise and structurally define the relevant metalated intermediates (Figure 1).<sup>17</sup> This approach also known in the literature as *Trans-Metal-Trapping (TMT)* relies on the steric incompatibility between the metalating reagent (LiTMP) and the organometallic trap which precludes their co-complexation to form an ate complex. Instead, operating in tandem, these bimetallic mixtures exploit the strong basicity of the lithium amide with the stronger carbophilic character of the trapping agent (which traps and stabilizes the incipient anion generated via metalation) to enable the functionalisation of aromatic substrates with high selectivity under mild reaction conditions.<sup>18,19</sup> *TMT* studies using a LiTMP/Al(TMP)*i*Bu<sub>2</sub> combination towards 3-fluoroanisole furnished aluminated product [2-{(iBu)<sub>2</sub>Al(μ-TMP)Li·THF}-3-fluoroanisyl] (Figure 1). However, the aluminated product was found to decompose at room temperature eliminating LiAlF(TMP)*i*Bu<sub>2</sub> with concomitant formation of (3-methoxyphenyl)-2,2,6,6-tetramethylpiperidine as a by-product resulting from the interception of the relevant benzyne species with the amine TMP(H) (present in solution from the initial lithiation reaction) (Figure 1). Thus, even the use of less electropositive main group metals, when compared to Li, can induce benzyne formation. Contrastingly, when the same approach is employed using Ga(CH<sub>2</sub>SiMe<sub>3</sub>)<sub>3</sub> as a metal trap, more robust intermediates can be obtained as shown in Figure 1 for the gallation of fluorobenzene which furnishes [2-Ga(CH<sub>2</sub>SiMe<sub>3</sub>)<sub>3</sub>-1-F-C<sub>6</sub>H<sub>4</sub>·Li(PMDTA)]. While the metalation reaction needs to be performed at -78 °C, is stable

in solution at room temperature and it can engage in further functionalisation reactions as for example Pd-catalysed arylation reaction. The greater stability of the lithium gallate vs the lithium aluminate has been attributed to the more fluorophilic character of Al vs Ga.

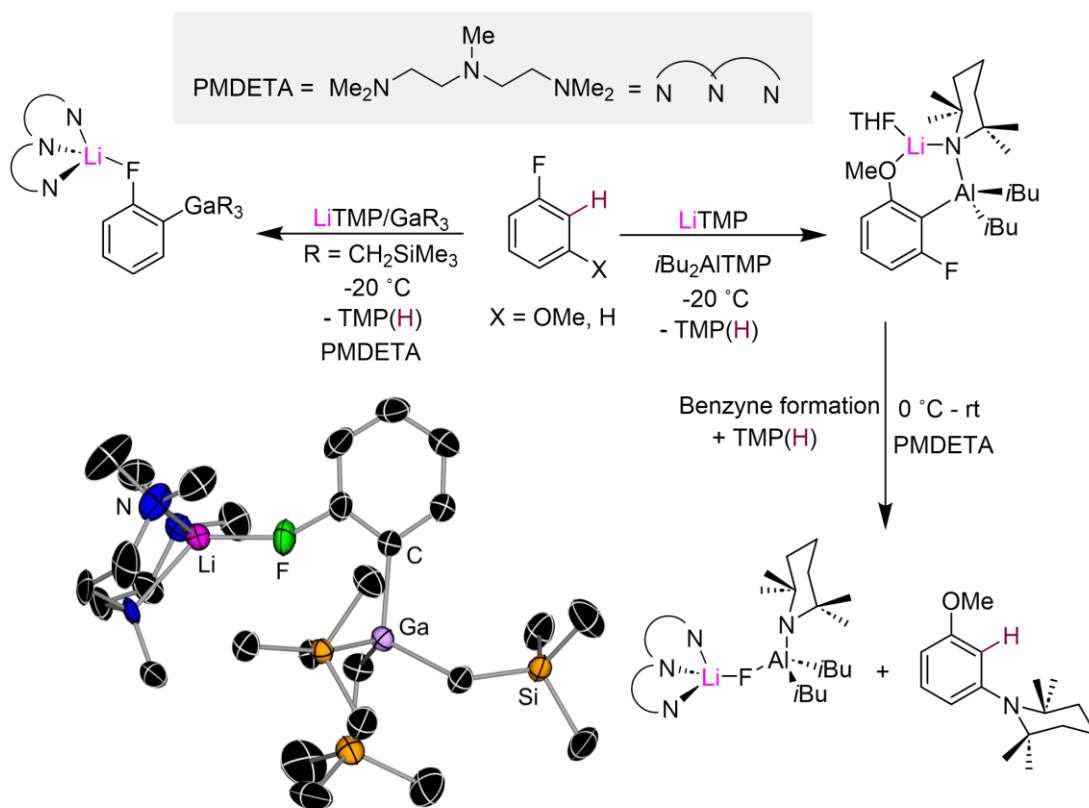
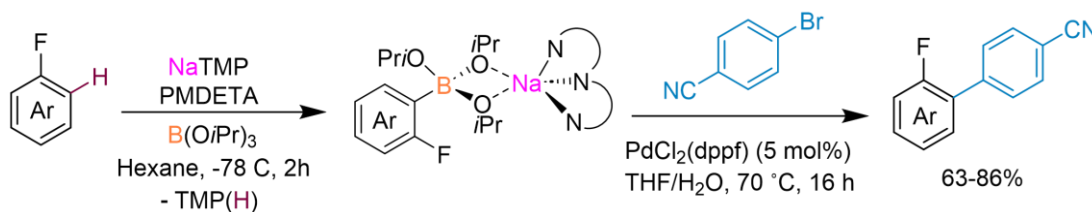


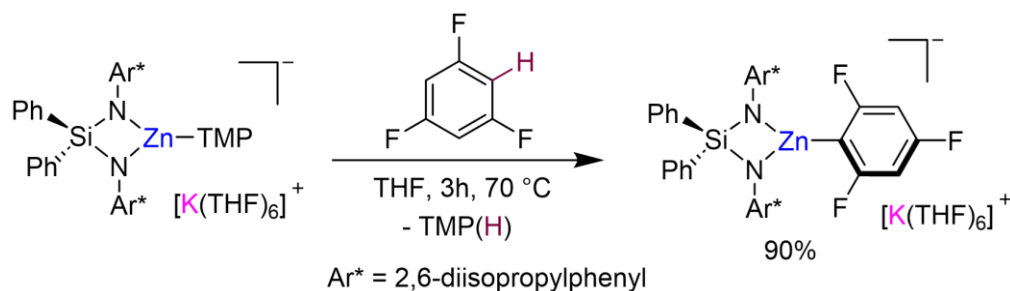
**Figure 1.** Contrasting Al vs Ga *Trans-Metal-Trapping* (TMT) outcomes on reactions with fluoroarenes. Molecular structure of 2-Ga(CH<sub>2</sub>SiMe<sub>3</sub>)<sub>3</sub>-1-F-C<sub>6</sub>H<sub>4</sub>-Li(PMDETA) resulting from the reaction of fluorobenzene with equimolar amounts of LiTMP/Ga(CH<sub>2</sub>SiMe<sub>3</sub>)<sub>3</sub>/PMDETA in hexane.

Related metalation strategies have been developed using NaTMP/PMDETA/B(OiPr)<sub>3</sub> combinations, which tolerate fluoroarenes such as fluorobenzene, 4-fluoroanisole and 4-fluorotoluene.<sup>20</sup> Reactions need to be carried out at  $-78\text{ }^\circ\text{C}$ , and the presence of PMDETA is crucial in order to de-aggregate the sodium amide and enhance its solubility and kinetic reactivity. For these substrates, regioselective *ortho*-sodiation to the fluorine substituent is observed followed by fast trapping with B(OiPr)<sub>3</sub> furnishing sodium borates [(PMDETA)NaB(Ar<sup>F</sup>)(OiPr)<sub>3</sub>] (Scheme 3). These intermediates are stable at room temperature and can be directly used in Pd catalysed Suzuki-Miyaura cross-couplings to give the relevant bis(aryl) products in good yields.



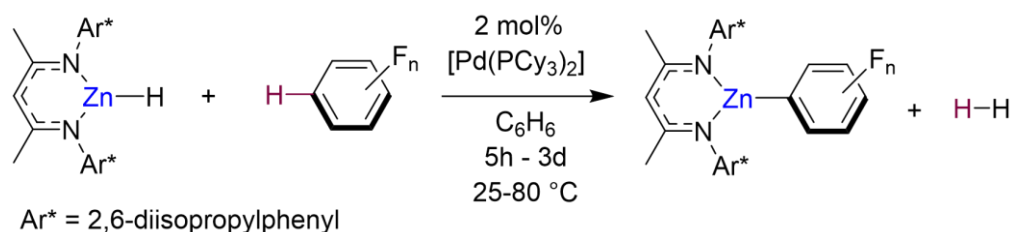
**Scheme 3.** Sodium-mediated deprotonative C-H borylation of fluoroarenes using NaTMP/PMDETA/B(OiPr)<sub>3</sub> with subsequent Suzuki-Miyaura cross-coupling

Other bimetallic systems which have shown exciting potential for fluoroarene metalation are potassium zincates. Combining a bulky silylbis(amide)  $\{\text{Ph}_2\text{Si}(\text{NAr}^*)_2\}^{2-}$  ( $\text{Ar}^* = 2,6\text{-diisopropylphenyl}$ ) and a reactive one-coordinate TMP ligand, our group has developed a K/Zn heteroleptic base  $[\{\text{Ph}_2\text{Si}(\text{NAr}^*)_2\text{Zn}(\text{TMP})\}^- \{\text{K}(\text{THF})_6\}^+]$  (Scheme 4) for regioselective zincation of fluoroarenes.<sup>21</sup> This special ligand set allows for the trapping and characterisation of the organometallic intermediate from these Zn-H exchange processes as shown in Scheme 4 for the formation of  $[\{\text{Ph}_2\text{Si}(\text{NAr}^*)_2\text{Zn}(\text{C}_6\text{H}_2\text{F}_3)\}^- \{\text{K}(\text{THF})_6\}^+]$  which can be isolated in a 90% yield by reacting equimolar amounts of the TMP based potassium zincate and 1,3,5-trifluorobenzene for 3h at 70 °C in THF. This approach can be extended to a wide range of fluoroarenes including those containing extremely sensitive NO<sub>2</sub> groups with reaction conditions varying from -40 °C to 70 °C, depending on the degree of activation of the substrate (in terms of p*K*<sub>a</sub> values). In this regard when fluorobenzene was employed, sluggish reactivity was observed (17% after 24h at 70 °C). Preliminary reactivity studies have also shown that these intermediates can undergo Pd-catalysed C–C bond forming processes with bromoarenes. It should be noted that Zn(TMP)<sub>2</sub> on its own fails to metalate these substrates and that when ultrasensitive nitro-fluoroarenes were reacted with the related potassium zincate [(PMDETA)KZn(TMP)Et<sub>2</sub>], previously reported by Mulvey,<sup>22</sup> a complex mixture of decomposition products was observed. These findings suggest that key for the success of this approach is the combination of a sterically demanding *bis*(amide) supporting ligand, which provides stability to the fragile fluoroaryl fragments in the metalated intermediates; and a terminal, kinetically ate-activated TMP basic site on Zn, which enables direct zincation of the fluoroarene.



**Scheme 4.** Reaction of TMP based potassium zincate with 1,3,5-trifluorobenzene supported by bulky silyl amide ligand forming  $[\{\text{Ph}_2\text{Si}(\text{NAr}^*)_2\text{Zn}(\text{C}_6\text{H}_2\text{F}_3)\}^- \{\text{K}(\text{THF})_6\}^+]$ .

Crimmin has recently developed an elegant method for the C–H bond zincation of fluoroarenes using Pd catalysis.<sup>23</sup> Combining monomeric zinc hydride [(DippNacnac)ZnH]<sup>24</sup> with catalytic amounts of [Pd(PCy<sub>3</sub>)<sub>2</sub>] the chemo- and regioselective transformation of C–H bonds to C–Zn bonds in a wide range of fluoroarenes has been achieved furnishing Zn aryl intermediates [(DippNacnac)ZnAr<sup>F</sup>] (Scheme 5) with the concomitant elimination of dihydrogen as a by-product. Regarding the substrate scope of this Zn/Pd approach, activated substrates with high fluorine content react under milder conditions and can tolerate halogen, trifluoromethyl and methoxy functional groups. However, lowering the fluorine content led to sluggish reactivity, for example the C–H zincation of fluorobenzene afforded less than 30% product after 3 days at 80 °C. Insightful mechanistic studies combining kinetic investigations with DFT calculations and the trapping of key reaction intermediates, revealed that these transformations involved the formation of heterobimetallic Pd/Zn species, and it is underpinned by special cooperation between the two distinct metal partners. Whilst not discussed thoroughly in this catalytic cycle, the authors attribute the primary role of the β-diketiminato ligand to provide kinetic stability to the reactive intermediates in the catalysis and the Zn hydride complex itself. Hence, the ligand-metal cooperativity is of paramount importance to the C–H zincation of the fluoroarenes along with the bimetallic cooperativity observed between Zn and Pd.



**Scheme 5.** C–H bond zincation of fluoroarenes via β-diketiminato supported Zn-hydride catalysed by [Pd(PCy<sub>3</sub>)<sub>2</sub>]

Chapters 2 and 3 highlighted the profound activating effects varying amounts of alkali metal alkoxides can have on dialkyl magnesium or zinc reagents and their reactivity towards metal-halogen exchange reactions via the formation of reactive mixed-metal/mixed-ligand aggregates.<sup>25–29</sup> Opening new ground in this field, this Chapter, we investigate the activating effects of alkali-metal alkoxides when combined with the zinc bis-amide, Zn(TMP)<sub>2</sub> focusing on the metalation of fluoroarenes.<sup>30</sup> Finding numerous applications as a mild metalating agent for the deprotonation of relatively acidic organic substrates such as ketones and esters,<sup>31–34</sup> it should be noted that this commercially available zinc amide (as a 0.5 M solution in toluene) has shown little promise for zincation of less activated substrates such as arenes.<sup>35</sup> Here, we reveal its true potential by reporting its first applications for regioselective zincation of



fluoroarenes. As mentioned previously, these substrates were chosen for their synthetic relevance, as they are present in a multitude of biologically active and pharmaceutical compounds,<sup>2,4,36</sup> but also for their sensitivity to highly polar organometallic reagents.<sup>8,37</sup>

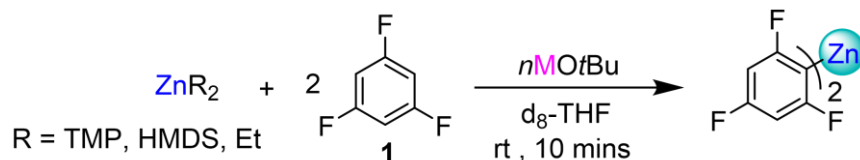
## **4.2 Aims**

Taking inspiration from the archetypal Lochmann-Schlosser superbases mixtures, we pondered if the addition of KO<sup>t</sup>Bu to Zn(TMP)<sub>2</sub> would kinetically activate the Zn-N bonds enabling deprotonation of sensitive fluoroarene substrates via the formation of mixed-metal mixed-ligand aggregates. The aims of this Chapter were to probe this activation of Zn(TMP)<sub>2</sub> through detailed reactivity profiles, spectroscopic and crystallographic studies.

## 4.3 Results and Discussion

### 4.3.1 Zincate screening towards metalation of 1,3,5-trifluorobenzene

We started our investigation using 1,3,5-trifluorobenzene (**1a**) as a model substrate (calculated  $pK_a = 31.5$ ),<sup>38</sup> finding that Zn(TMP)<sub>2</sub> in THF is completely inert towards **1a**, even under refluxing



conditions (entry 1, Table 1). Addition of one equivalent of LiOtBu led to a noticeable increase in reactivity to a 42% conversion (entry 2) to a zincated species in just 10 minutes at room temperature. A revealing alkali metal effect was noted when moving to the heavier alkali metal congeners with addition of one equivalent of NaOtBu giving a 69% conversion of **1a** (entry 3). Most remarkably, the addition of KOtBu to Zn(TMP)<sub>2</sub> led to the full zincation of two equivalents of **1a** at room temperature in just 10 minutes (entry 4) with concomitant formation of two equivalents of TMP(H) proving both TMP groups are active towards metalation. <sup>1</sup>H NMR monitoring of this reaction indicated that while quantitative metalation of **1a** is seen, a mixture of at least four species containing Zn-C<sub>6</sub>H<sub>2</sub>F<sub>3</sub> fragments is present in solution. Attempts to unequivocally ascertain the constitution of the different species present in this mixture were infructuous (*vide infra*). Related to these findings, it should be noted that our previous research probing the constitution of *s*Bu<sub>2</sub>Mg in the presence of equimolar amounts of lithium alkoxides has also established the presence of complex equilibria, with different bimetallic complexes coexisting in solution (see section 2.3.3 in Chapter 2).<sup>28</sup> Table 1. Screening of Zn-H exchange capabilities of different zinc bases towards 1,3,5-trifluorobenzene.

Entry	Base	Conversion <sup>[a]</sup> (%)
1	Zn(TMP) <sub>2</sub>	0 <sup>[b]</sup>
2	Zn(TMP) <sub>2</sub> + LiOtBu	42 <sup>[c]</sup>
3	Zn(TMP) <sub>2</sub> + NaOtBu	69 <sup>[c]</sup>
4	Zn(TMP) <sub>2</sub> + KOtBu	99 <sup>[c]</sup>
5	Zn(TMP) <sub>2</sub> + 2KOtBu	99 <sup>[d]</sup>
6	TMPZnCl·LiCl	13 <sup>[e]</sup>
7	Zn(HMDS) <sub>2</sub> + 2KOtBu	46
8	ZnEt <sub>2</sub> + 2KOtBu	43

[a] Conversions determined by <sup>1</sup>H NMR monitoring using hexamethylbenzene as internal standard [b] Reaction refluxed for 2h [c] Multiple metalated species observed in solution [d] Single metalated species **2a** observed in solution [e] Conversion determined after 1h at room temperature.

Interestingly, on using 2 equivalents of KOtBu, full conversion of **1** was also achieved (entry 5), but on this occasion a single organometallic complex [(THF)<sub>3</sub>K<sub>2</sub>Zn(Ar)<sub>2</sub>(OtBu)<sub>2</sub>]

(**2a**) (Ar = C<sub>6</sub>H<sub>2</sub>F<sub>3</sub>) was observed (*vide infra*). In order to avoid the presence of different organometallic species in solution, we opted for the use of Zn(TMP)<sub>2</sub> with two equivalents of KO<sup>t</sup>Bu as the optimal bimetallic combination for this study. We also rationalized that forming higher-order (so called because of its 2:1 K:Zn ratio) zincate **2a** could be beneficial for forward reactivity with electrophiles.<sup>39-41</sup> Assessing solvent effects, full conversion is also achieved using d<sub>8</sub>-toluene although on this occasion the metalation product precipitates as a white solid, therefore THF was chosen as the preferred solvent. No decrease in conversion of **1** is observed when using a 0.5 M solution of Zn(TMP)<sub>2</sub> in toluene. Using Knochel's Turbo zinc reagent TMPZnCl·LiCl which has previously been employed for arene metalations, afforded only a 13% conversion of **1** in 1h at room temperature (entry 6).<sup>42</sup> Lastly, replacing Zn(TMP)<sub>2</sub> with Zn(HMDS)<sub>2</sub> [HMDS = N(SiMe<sub>3</sub>)<sub>2</sub>, entry 7] or ZnEt<sub>2</sub> (entry 8) gave significantly lower conversions of **1** (46% and 43% respectively). Rapid zincation of **1** with this bimetallic combination under extremely mild reaction conditions contrasts with previous studies on the zincation of fluoroarenes previously discussed in **Section 4.1** in this *Chapter* that require the use of sterically demanding ligands, higher temperatures, longer reaction times and in some cases the use of Pd catalysis.<sup>21,23</sup> For example, using the TMP-based potassium zincate supported by a bulky bis(amide) ligand {Ph<sub>2</sub>Si(NAr\*)<sub>2</sub>}<sup>2-</sup>(Ar\*= 2,6-diisopropylphenyl) (Scheme 4), we reported zincation of 1,3,5-trifluorobenzene (**1a**) required 3h at refluxing temperatures in THF or three days at room temperature.<sup>21</sup>

### 4.3.2 Investigating the role of KO<sup>t</sup>Bu towards the activation of Zn(TMP)<sub>2</sub>

Intrigued by these findings, we next looked at the constitution of the metalation product and the active base in this reaction in order to gain a better understanding of the potassium alkoxide's role in activating Zn(TMP)<sub>2</sub> towards deprotonation reactions. <sup>1</sup>H NMR monitoring showed that reaction of a 2:1 mixture of KO<sup>t</sup>Bu and Zn(TMP)<sub>2</sub> with 2 equivalents of 1,3,5-trifluorobenzene yielded **2a** quantitatively (Figure 2) and concomitant formation of TMP(H). X-ray crystallographic studies established the bimetallic higher order (2:1 K:Zn ratio) constitution of **2a**.<sup>39,43</sup> Adopting a bent K1···Zn1···K2 geometry [65.945(16)°], the central zinc centre binds to two *ortho*-C of two fluoroaryl groups occupying the position previously filled by a H atom and completes its tetrahedral coordination by binding to two O alkoxide atoms. In contrast, each K coordinates to the two alkoxide bridges and forms a K···F contact with one F atom *ortho* to the zincated C atom (Figure 2). Coordinative saturation of K is achieved by two THF molecules, one of which acts as a bridge between two K centers. While this coordination mode is rare, Strohmman recently proposed that for Lochmann-Schlosser superbases mixtures, the THF bridge could shift between the K centers providing a coordination site for substrates.<sup>44</sup>

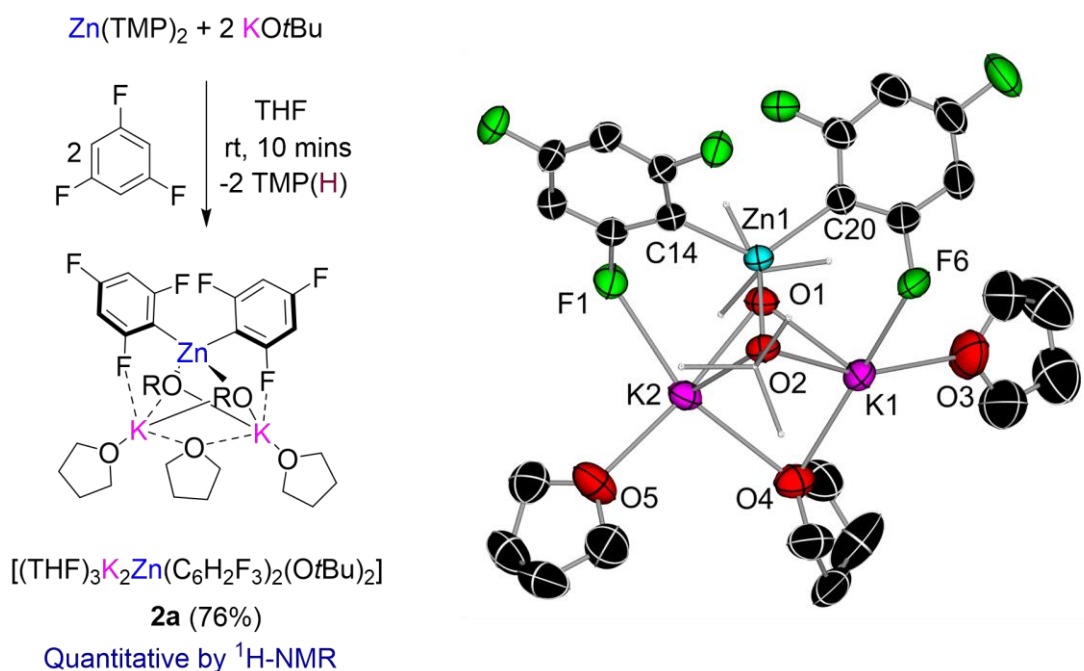


**Figure 2.** a) Zincation of 1,3,5-trifluorobenzene via  $\text{Zn(TMP)}_2/2\text{KOtBu}$  mixture to form higher order zincate  $(\text{THF})_3\text{K}_2\text{Zn}(\text{C}_6\text{H}_2\text{F}_3)_2(\text{OtBu})_2$  (**2a**). Molecular structure of **2a** with displacement ellipsoids at 50% probability, H atoms omitted and alkoxide C atoms drawn as wire frames for clarity

<sup>1</sup>H-DOSY analysis in *d*<sub>8</sub>-THF supports that the mixed-metal/mixed-ligand constitution of compound **2a** observed in the solid state is retained in solution as the metalated fluoroaryl fragments  $\text{Zn}(\text{C}_6\text{H}_2\text{F}_3)_2$  and alkoxide fragments *OtBu* display similar diffusion coefficients ( $D = 4.62 \times 10^{-10} \text{ m}^2\text{s}^{-1}$  and  $D = 4.69 \times 10^{-10} \text{ m}^2\text{s}^{-1}$  respectively) (Figure 3). Moreover, compound **2a** is remarkably stable in *d*<sub>8</sub>-THF since no benzyne formation was observed, though such decomposition reactions are common for these hypersensitive fluoroaryls once metalated as discussed above in the introduction to this chapter (section 4.1).<sup>8</sup> Compound **2a** exhibits two distinct signals at -84.2 ppm and 121.2 ppm in the <sup>19</sup>F{<sup>1</sup>H} NMR spectrum which differ significantly to the singlet observed for the starting material **1a** (-108.6 ppm).

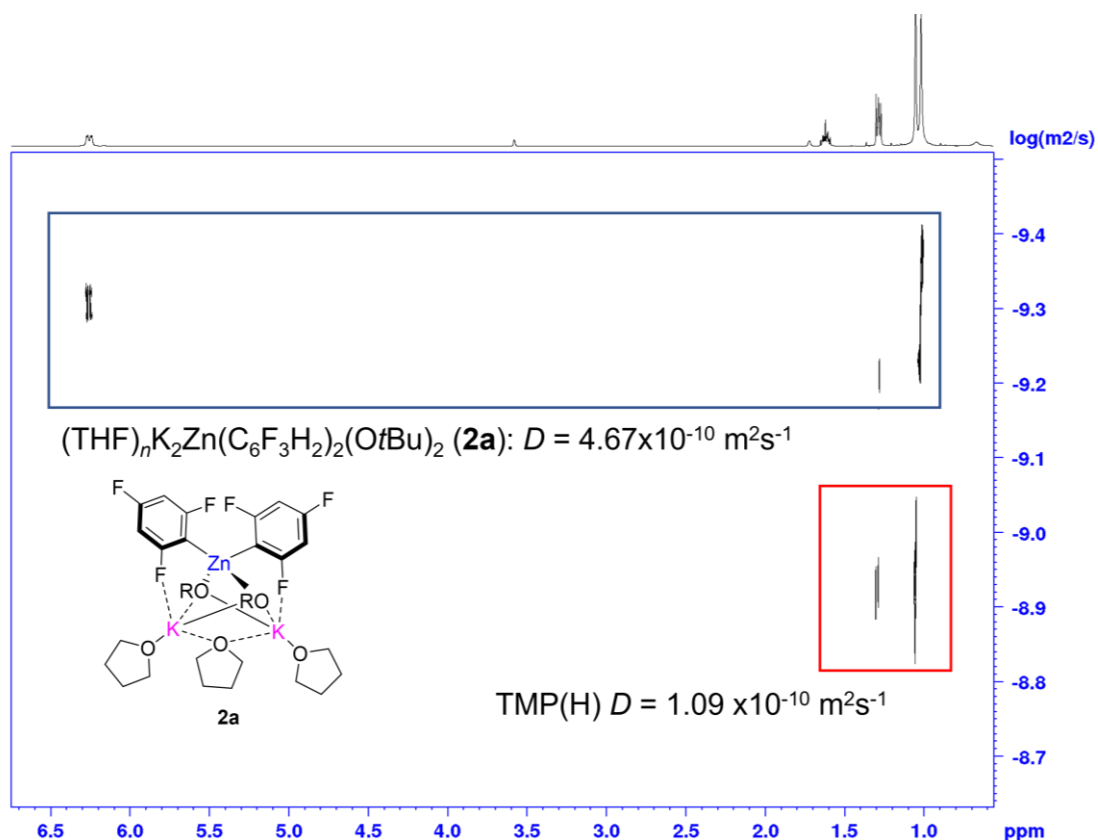


**Figure 3.** <sup>1</sup>H-DOSY NMR in d<sub>8</sub>-THF of the *in-situ* formation of [(THF)<sub>3</sub>K<sub>2</sub>Zn(C<sub>6</sub>F<sub>3</sub>H<sub>2</sub>)<sub>2</sub>(OtBu)<sub>2</sub>] (**2a**) with concomitant formation of TMP(H)

We next evaluated the constitution of this bimetallic combination by performing the reaction of 2 equivalents of KO*t*Bu with Zn(TMP)<sub>2</sub> in hexane in the presence of tridentate donor PMDETA (N,N,N',N'',N''-pentamethyldiethylenetriamine) in an effort to uncover the active base in this transformation. Despite the use of two equivalents of KO*t*Bu employed, this reaction led to the formation of the lower order (1K:1Zn) potassium zincate [(PMDETA)KZn(TMP)<sub>2</sub>(OtBu)] (**3**) as a crystalline solid in a 54 % yield (Figure 4). Its molecular structure consists of one potassium alkoxide unit co-complexed with Zn(TMP)<sub>2</sub> where one TMP and the *tert*-butoxide group bridge between the K and Zn atoms while the remaining TMP resides terminally on Zn. PMDETA then satisfies the coordination sphere of K resulting in a structural motif previously seen in other lower order zincates.<sup>45-49</sup>

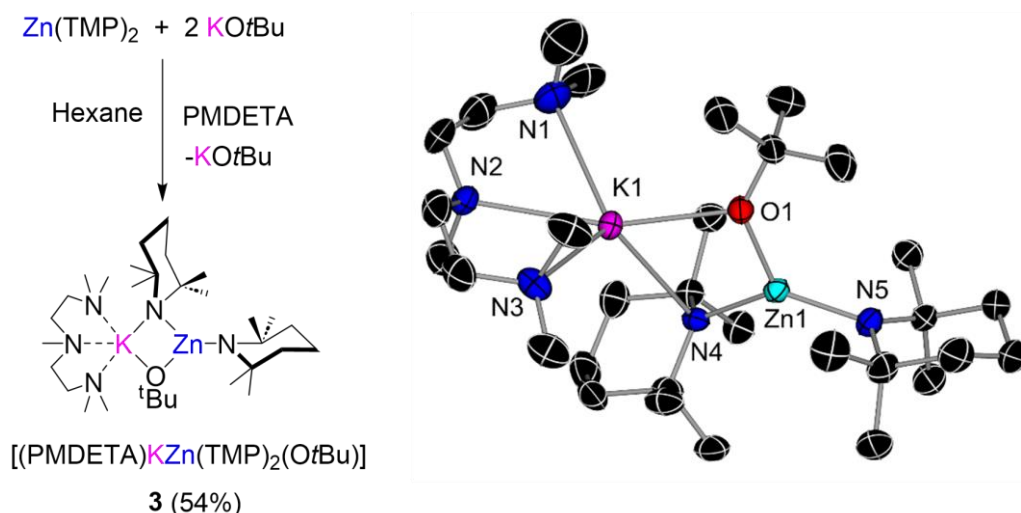


**Figure 4.** Formation of lower order potassium zincate (PMDETA)KZn(TMP)<sub>2</sub>OtBu (**3**) via co-complexation of Zn(TMP)<sub>2</sub> and KOtBu. Molecular structures of **3** with displacement ellipsoids at 50% probability with H atoms omitted for clarity

NMR spectroscopic studies suggest that this bimetallic motif is retained in d<sub>8</sub>-THF solutions with the exception of PMDETA being presumably replaced by the coordinating deuterated solvent. Studies assessing the co-complexation of a second equivalent of KOtBu support that in THF solution this reaction does not occur as shown in Figure 4 whereupon addition of a second equivalent of KOtBu the chemical shift of the *t*Bu fragment in the <sup>1</sup>H NMR spectra does not shift from a standard of KOtBu in d<sub>8</sub>-THF. Moreover, the <sup>1</sup>H NMR profile of potassium zincate **3** is also unaltered by the presence of a second equivalent of alkoxide and the same can also be said for the <sup>13</sup>C NMR spectra (Figure 5). Unfortunately, <sup>1</sup>H-DOSY NMR studies of a 1:2 mixture of Zn(TMP)<sub>2</sub> and KOtBu were inconclusive in confirming if (THF)<sub>x</sub>KZn(TMP)<sub>2</sub>(OtBu) (**3**) and KOtBu remain as independent species in solution as both exhibit similar diffusion coefficients in d<sub>8</sub>-THF ( $D = 7.55 \times 10^{-10} \text{ m}^2\text{s}^{-1}$  (THF)<sub>x</sub>KZn(TMP)<sub>2</sub>(OtBu) and  $D = 7.00 \times 10^{-10} \text{ m}^2\text{s}^{-1}$ , KOtBu). <sup>1</sup>H-DOSY NMR of a standard of KOtBu displayed a diffusion coefficient of  $7.73 \times 10^{-10} \text{ m}^2\text{s}^{-1}$  which with an error of 12% suggests it exists in d<sub>8</sub>-THF as a tetrasolvated dimer calculated from the diffusion coefficients established from the <sup>1</sup>H DOSY NMR spectrum using Stalke's external calibration curve (ECC) method against the normalised diffusion coefficient for the internal reference tetraphenyl naphthalene.<sup>50</sup> However, based on the solution and solid-state studies on the 1:2 mixture of Zn(TMP)<sub>2</sub> and KOtBu it was concluded that KOtBu does not co-complex with **3** in solution to form a higher order zincate. This is not surprising considering the high steric demands of the TMP groups and aligns well with previous findings assessing the coordination ability of Zn(TMP)<sub>2</sub> which fails to form adducts with donors such as pyrimidine or undergo co-complexation with Li(TMP).<sup>51,52</sup> In fact, a search of the CSD revealed that **3** is the first structurally defined alkali-metal zincate resulting from co-complexation of Zn(TMP)<sub>2</sub> with another organometallic species.

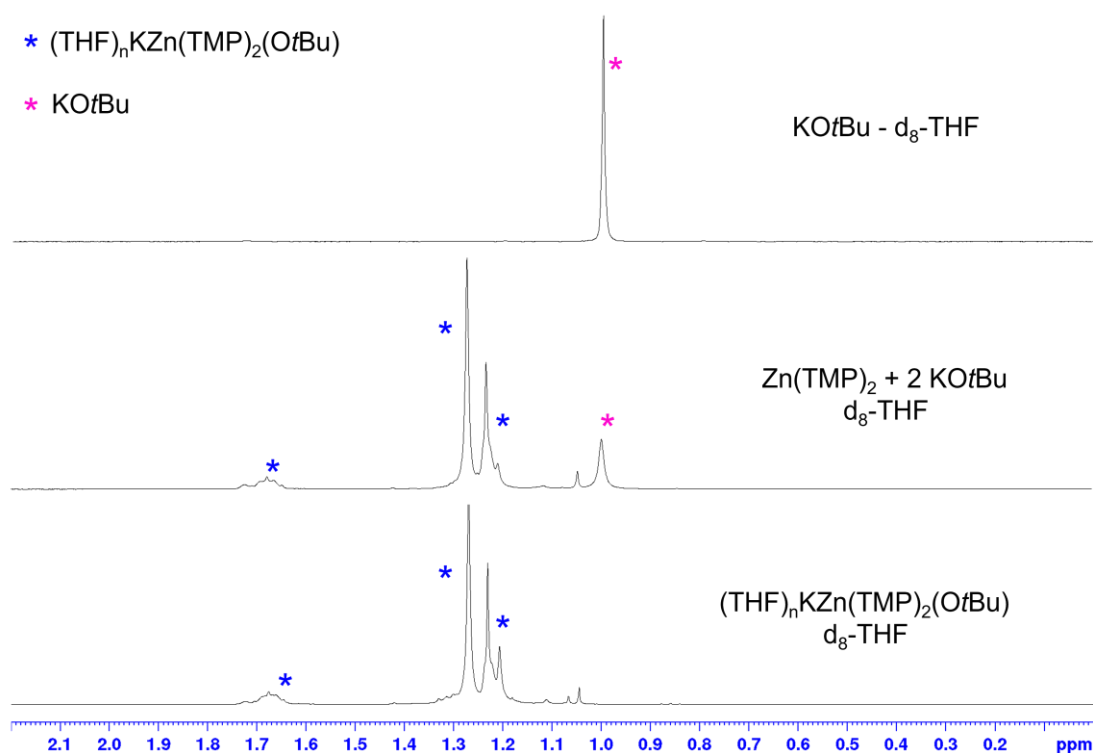
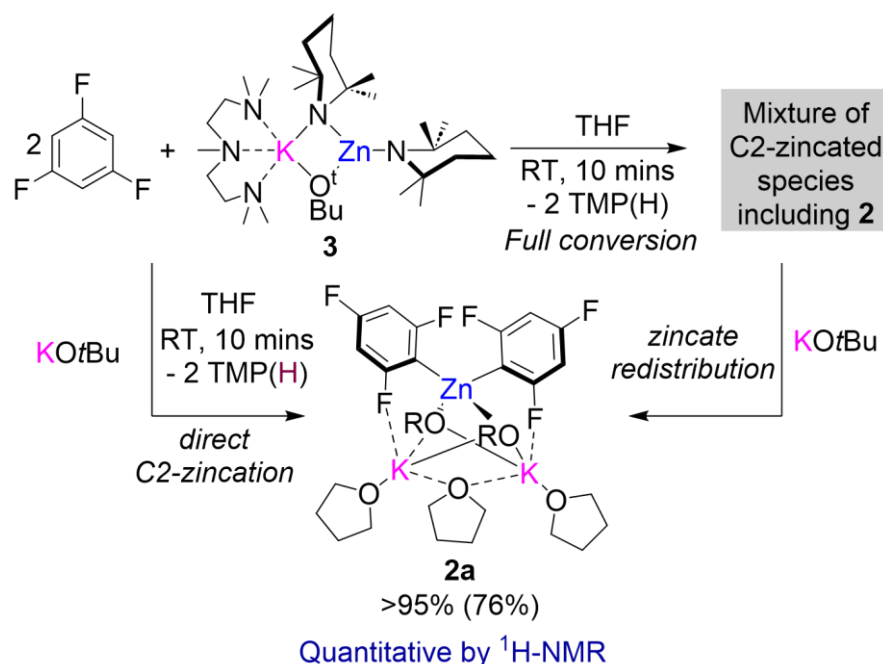


**Figure 5.** Stacked  $^1H$  NMR spectra of 1:1 mixture of  $Zn(TMP)_2$  and KOtBu (bottom), 1:2 mixture of  $Zn(TMP)_2$  and KOtBu (middle) and KOtBu (top) in  $d_8$ -THF.

To assess the role of the second KOtBu equivalent on the formation of higher order zincate **2a** we looked at the metalation of two equivalents of 1,3,5-trifluorobenzene **1a** with lower order zincate **3**. In agreement with our observations in Table 1, entry 4,  $^1H$  and  $^{19}F$  NMR reaction monitoring indicated the formation of up to four different organometallic species containing metalated aryl fragments with the full conversion of **1a** and concomitant liberation of two equivalents of TMP(H) (Scheme 6). One of these species can be assigned to higher order zincate **2a** which can actually be crystallized from this reaction mixture as a minor product. Unfortunately, the other zincated products could not be identified although the disproportionation to a potassiated aryl species can be ruled out as no decomposition and/or benzyne formation with concomitant KF elimination is observed. However, as mentioned above, the complexity of this reaction mixture can be simplified by the addition of a second equivalent of KOtBu (pre or post metalation) affording higher order potassium zincate **2a** as the sole zincated intermediate (Scheme 6). These findings provide another enlightening example of the complexity of using group 1 metal alkoxides as additives to other organometallics which may not only have an activating effect but can also instigate ligand redistribution processes, affecting the speciation of the organometallic product(s).



**Scheme 6.** Role of second equivalent of KOtBu in metalation of two equivalents of 1,3,5-trifluorobenzene **1** with lower-order potassium zincate **3**.

### 4.3.3 Expanding the substrate scope of fluoroarene metalation

Encouraged by the extremely fast and efficient zincation of 1,3,5-trifluorobenzene **1a**, at room temperature using the Zn(TMP)<sub>2</sub>/2KOtBu combination we then looked to expand the substrate scope of this approach (Figure 6). Considering the thermal stability of **2a**, reactions were carried out in THF and the zincated products were isolated as pure white solids by precipitation with hexane. Both polyfluorinated fluoroarenes 1,2,4,5-tetrafluorobenzene and 1,2,3,4,5-pentafluorobenzene were zincated to give higher-order potassium zincates **2b** and **2c** in 10 minutes at room temperature. Remarkably despite the fragility of these sensitive fluoroaryls, **2b** and **2c** are stable at room temperature without observing any apparent decomposition after several hours in THF-d<sub>8</sub> solutions. This thermal stability contrasts with previous zincation studies by Mulvey and Uchiyama where the products of *ortho*-zincation of chloro- and bromo arenes using lithium zincates can undergo rapid LiCl or LiBr elimination forming benzyne intermediates.<sup>53–55</sup> Significantly less activated substrates such as fluorobenzene and 1-fluoronaphthalene are also quantitatively zincated in 24h at room temperature to give products **2d** and **2e**. This is striking as previous approaches using alternative zincating reagents mentioned above fail to metalate these substrates in reasonable yields even when harsh reaction conditions are employed.<sup>21,23</sup> Bromo and chloro *para*-substituted arenes are zincated easily in 1h to give zincates **2f** and **2g**. *Ortho*, *meta*, and *para* fluorotoluene can be regioselectively zincated *ortho* to the fluorine substituent to give products **2h–2j** avoiding any competing lateral metalation of the methyl substituent as reported for 2-fluorotoluene using the aforementioned LiNK superbases, which favors the benzylic metalation



product.<sup>56</sup> Reactivity studies with 2- and 4-fluoroanisole revealed that acidifying effects take prevalence over coordination effects, thus favoring quantitative zincation at the *ortho*-position to the F substituent furnishing **2k** and **2l** (Figure 6). This preferred regioselectivity has been previously noted using Lochman-Schlosser superbases although reactions need to be performed at -78 °C.<sup>57</sup> The same preference on regioselectivity was observed for 2-(4-fluorophenyl)-4,4-dimethyl-4,5-dihydroxazole where oxazoline bearing zincate **2m** was formed in a 93% yield with regioselective zincation occurring *ortho* to the fluoro substituent (*vide infra*). Knochel recently reported the metalation of this substrate using magnesium-bis-diisopropylamide (Mg(NiPr<sub>2</sub>)<sub>2</sub>), which occurs preferentially *ortho* to the oxazoline unit, a substituent typically regarded as a very strong *ortho*-directing group in DoM chemistry.<sup>10</sup> Olefinic moieties are also tolerated as a functional group as shown by the efficient zincation of 4-fluorostyrene in 3h furnishing **2n**. While attempts to promote regioselective zincation of fluoropyridines at room temperature proved fruitless forming intractable black solids which could not be analyzed, pyridine is tolerated as a remote functional group under these conditions as shown by the quantitative metalation of 2-(2,4-difluorophenyl)pyridine yielding zincate **2o**. Unfortunately attempts to extend the substrate scope to fluoroarenes bearing extremely sensitive functional groups such as nitro (e.g 4-fluoronitrobenzene) or cyano (4-fluorobenzonitrile) groups resulted in decomposition of the resulting zincate forming intractable mixtures even at cryogenic temperatures.

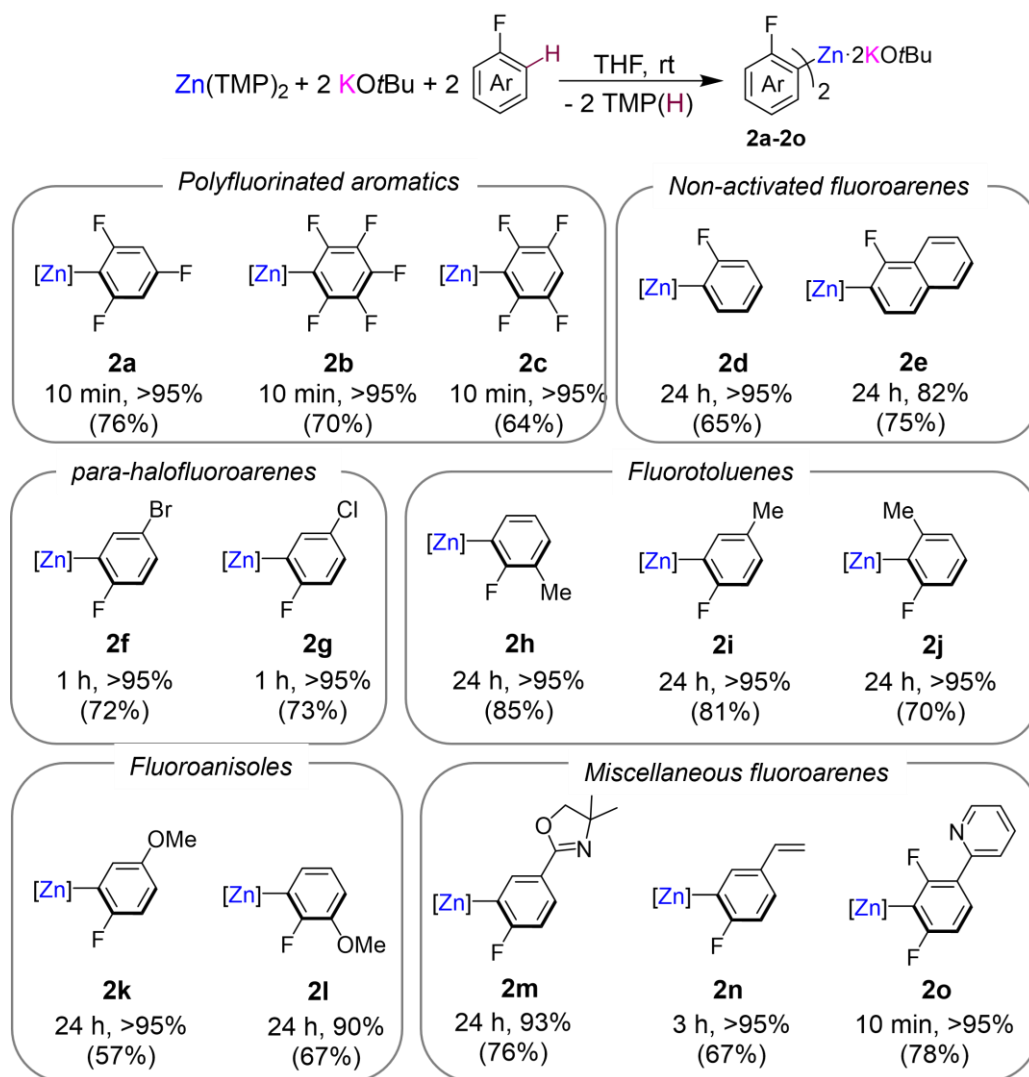


**Figure 6.** Scope of the C-H zincation of fluoroarenes using 2:1 mixture of KOtBu/Zn(TMP)<sub>2</sub>. NMR yields for [K<sub>2</sub>ZnAr<sub>2</sub>(OtBu)<sub>2</sub>] (**2a-2o**) determined by <sup>1</sup>H NMR spectroscopy using hexamethylbenzene as an internal standard and isolated crystalline yields shown in brackets.

As described above, the zincation of these fluoroarenes occurs regioselectively *ortho* to the fluorine moiety which was confirmed by the structural elucidation of the molecular structures of **2k** and **2m**. These structures display almost identical structural motifs to that described for **2a** with K preferentially interacting with the *ortho*-F to the C which has undergone zincation (Figure 7). This is highlighted by examining the average of the key bond distances in potassium zincates **2a**, **2k** and **2m** (Table 2) in which the three metalated intermediates display similar Zn-C, Zn-O, K-O and K-F. The distances of the K...F interactions are slightly longer (2.742 Å) in **2a** when compared to that of **2k** (2.674 Å) and **2m** (2.631 Å). No interaction is observed between the alkali metal and the *ortho* directing methoxy or oxazoline groups providing evidence that acidifying effects prevail over coordination effects. Typically, coordination effects dominate in non-coordinating solvents where the alkali metal can satisfy its coordination sphere via interactions with the *ortho* directing functional group<sup>58,59</sup> however the zincation of 4-fluoroanisole persisted regioselectively *ortho* to the

fluorine atom even when the reaction was carried out in hexane in the absence of a Lewis donor (i.e. THF).

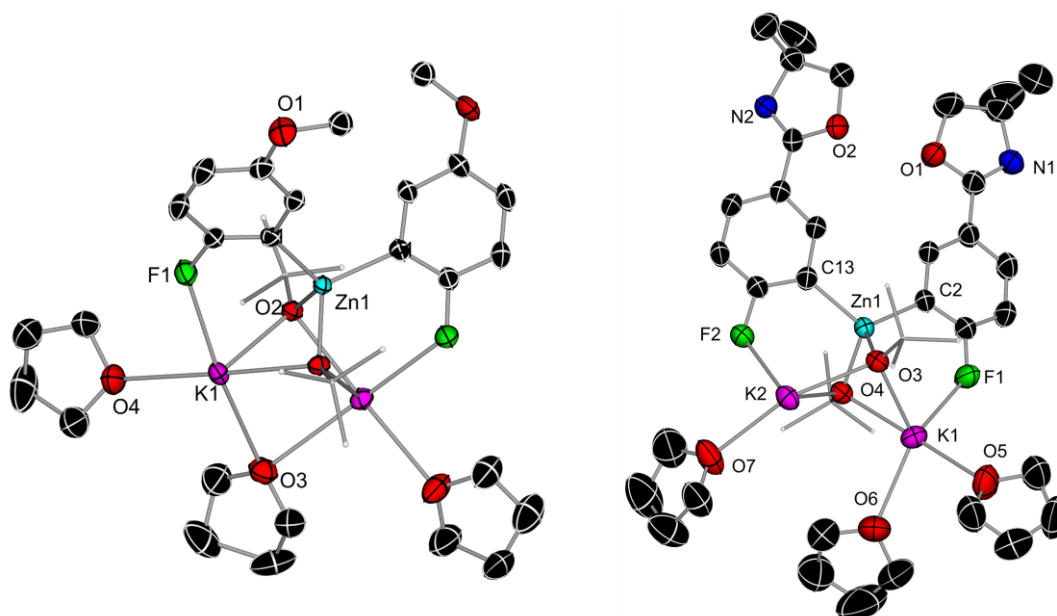


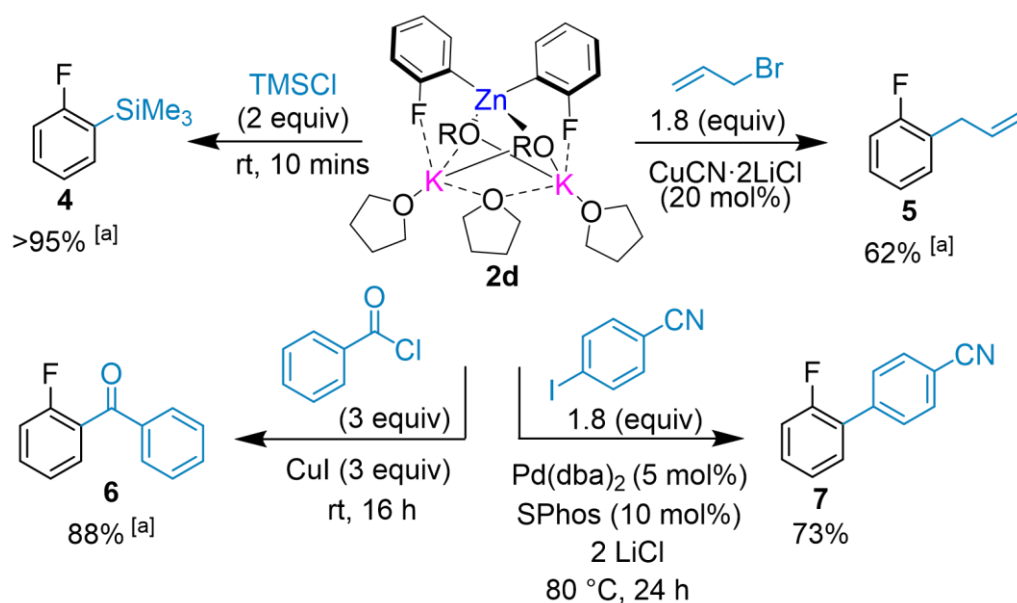
**Figure 7.** (LHS) Molecular structure of zincate **2k** with displacement ellipsoids at 50% probability, H atoms omitted and alkoxide C atoms drawn as wire frames for clarity; (RHS) Molecular structure of zincate **2m** with displacement ellipsoids at 50% probability, H atoms omitted and alkoxide C atoms drawn as wire frames for clarity.

**Table 2.** Selected average bond distances for potassium zincates **2a**, **2k** and **2m**.

Average bond distances (Å)	<b>2a</b>	<b>2k</b>	<b>2m</b>
Zn-C	2.076	2.055	2.072
Zn-O	2.013	2.016	2.020
K-O	2.625	2.647	2.655
K-F	2.742	2.674	2.631

#### 4.3.4 Further functionalisation of potassium zincate intermediates

Despite the enhanced stability of these zincated intermediates, they show good reactivity towards electrophilic interception. Thus, using potassium zincate **2d**, resulting from *ortho*-zincation of fluorobenzene (Scheme 7), Reaction with equimolar amounts of TMSCl afforded silylated species **4** in a quantitative yield. **2d** was found to participate in a copper catalysed allylation using allyl bromide to give allylated product **5** in a 62% yield. Similarly, a copper-catalysed arylation using benzoyl chloride gave 2-fluorobenzophenone **6** in an 88% yield. Finally, **2d** undergoes the classical Pd catalysed Negishi cross-coupling reaction with 4-iodobenzonitrile to give *bis*-aryl compound **7** in a 73% yield displaying the synthetic utility of these higher order zincated fluoroaryl intermediates.



**Scheme 7.** Electrophilic interception studies of zincate **2d** prepared in-situ via zincation of 2 equivalents of fluorobenzene with a 2:1 mixture of KO*t*Bu/Zn(TMP)<sub>2</sub>. <sup>[a]</sup> NMR yields determined by <sup>1</sup>H NMR spectroscopic data using hexamethylbenzene as internal standard.

#### 4.3.5 Extension to the zincation of non-activated arenes

Confirming the strong metalating power of this mixed potassium/zinc bimetallic combination, we also noted that a 2:1 mixture of KO*t*Bu/Zn(TMP)<sub>2</sub> left to stir at room temperature in toluene caused the solution to turn bright orange (see Figure 12, **Section 4.5.5**) in a characteristic trait for benzylic metalation of the arene.<sup>60</sup> Indeed, a crop of crystals grown from the solution revealed the formation of [(THF)<sub>2</sub>K<sub>2</sub>Zn(Bz)<sub>2</sub>(O*t*Bu)<sub>2</sub>]<sub>∞</sub> (Bz = CH<sub>2</sub>Ph) (**8**) in a 65% isolated yield (Figure 8). X-ray crystallographic analysis revealed the formation of a polymeric higher-order potassium zincate resulting from lateral metalation of two equivalents of toluene and liberation of 2 equivalents of TMP(H). The central Zn atom bonds to two benzylic carbon anions and to two *tert*-butoxide anions which bridge to the two potassium atoms present. The two potassium centers connect by two bridging alkoxide groups and a bridging THF molecule. K1 completes its coordination sphere binding to a terminal THF and  $\pi$ -engaging in an  $\eta^{-4}$  fashion with the aromatic groups of one of the benzyl anions. Similar  $\pi$ -interactions are observed between K2 and a benzyl group of a neighboring unit propagating the two-dimensional polymeric structure of **8** (see Figure 13, **Section 4.5.5**).<sup>61</sup> <sup>1</sup>H and <sup>13</sup>C NMR studies support that the bimetallic constitution of **8** is retained in solution, displaying a distinct signal at 1.67 ppm for the CH<sub>2</sub> group in the <sup>1</sup>H NMR spectrum. Potassium zincate **8** can react efficiently with the Weinreb amide N-methoxy-N-methylbenzamide to give 1,2-diphenylethanone **9** in an 85% yield (Figure 8). This efficiency under extremely mild reaction conditions contrasts with the inertness of both monometallic components KO*t*Bu and



previously discussed Zn/Pd bimetallic system however the reaction requires to be refluxed at 100 °C for 5 days under static vacuum using benzene as a solvent.<sup>23</sup> The facile zincation of benzene using the Zn(TMP)<sub>2</sub>/2KO*t*Bu combination forming potassium zincate **10** is more akin to Mulvey's report using sodium dialkyl-amidozincate [(TMEDA)NaZn(TMP)(*t*Bu)<sub>2</sub>] which reacts with benzene through one of its alkyl substituents forming [(TMEDA)NaZn(TMP)(*t*Bu)(C<sub>6</sub>H<sub>5</sub>)] although this method requires the pre-synthesis of *t*Bu<sub>2</sub>Zn and NaTMP to form the bimetallic base.<sup>46</sup>

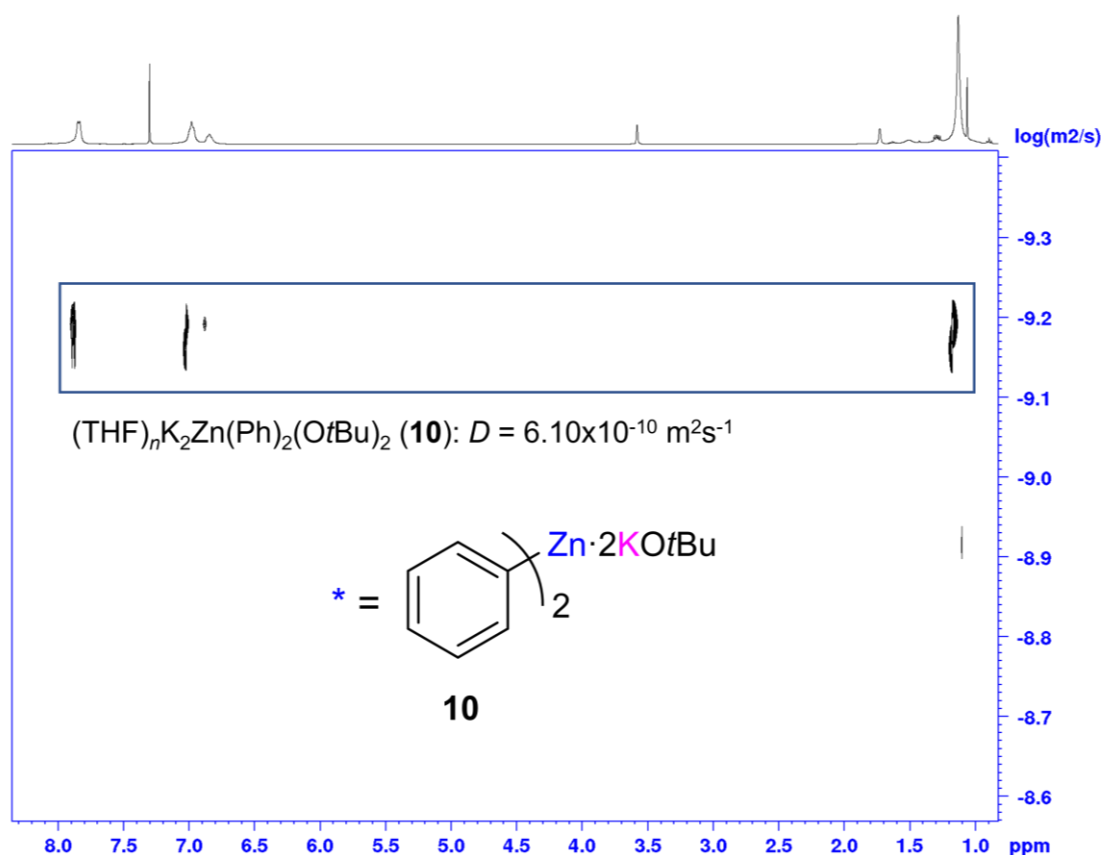


Figure 9 <sup>1</sup>H-DOSY NMR spectra of K<sub>2</sub>Zn(Ph)<sub>2</sub>(O*t*Bu)<sub>2</sub> **10** in d<sub>8</sub>-THF

#### 4.3.6 Formation of sodium zincates using a Zn(TMP)<sub>2</sub>/NaO*t*Bu combination

Early studies exploring the kinetic activation of Zn(TMP)<sub>2</sub> with alkali metal alkoxides began with NaO*t*Bu, before discovering the superiority of the heavier potassium congener. Reaction of 2 equivalents of NaO*t*Bu with Zn(TMP)<sub>2</sub> in hexane in the presence of bidentate donor TMEDA (N,N,N',N'-tetramethylethylenediamine) led to the formation of lower order sodium zincate [(TMEDA)NaZn(TMP)<sub>2</sub>(O*t*Bu)] (**11**) (Figure 10) as a crystalline solid in a 50% yield. This is essentially an identical structure to that of lower order potassium zincate [(PMDETA)KZn(TMP)<sub>2</sub>(O*t*Bu)] (**3**) (Figure 4) however in the case of the Na congener the bidentate donor TMEDA is sufficient to satisfy the coordination sphere of the smaller alkali metal. Like with K, an excess of NaO*t*Bu does not facilitate the formation of a higher order

mixed-metal/mixed-ligand aggregate due to the large steric demands of the bulky amido TMP groups around Zn. No notable change is observed in the chemical shifts of the TMP and alkoxide fragments in the <sup>1</sup>H and <sup>13</sup>C NMR spectra when comparing [(PMDETA)KZn(TMP)<sub>2</sub>(OtBu)] (**3**) with its Na congener [(TMEDA)NaZn(TMP)<sub>2</sub>(OtBu)] (**11**).

The Zn(TMP)<sub>2</sub>/2NaOtBu combination proved sufficient to quantitatively zincate two equivalents of 1,3,5-trifluorobenzene at room temperature in THF in 30 minutes and in the presence of two equivalents of TMEDA furnished higher order sodium zincate (TMEDA)(THF)Na<sub>2</sub>Zn(C<sub>6</sub>F<sub>3</sub>H<sub>2</sub>)<sub>2</sub>(OtBu)<sub>2</sub> (**12**) (Figure 10) with concomitant formation of two equivalents of TMP(H). Despite using two equivalents of TMEDA only Na1 is capped by the bidentate donor whereas Na2 is coordinated to a single THF molecule giving rise to this unusual unsymmetrical donor system. Sodium zincate **12** is analogous to its heavier potassium zincate congener [(THF)<sub>3</sub>K<sub>2</sub>Zn(C<sub>6</sub>F<sub>3</sub>H<sub>2</sub>)<sub>2</sub>(OtBu)<sub>2</sub>] **2a** (Figure 2). Naturally, a smaller alkali metal leads to shorter alkali metal contacts with the bridging O atoms in the alkoxide and with the fluorine atoms in the fluoroaryl unit. The average bond distances of the Na...F contacts in **12** is 2.389 Å opposed to 2.742 Å for the K...F contacts in potassium zincate **2a**. Similarly, the average bond distances of the Na...O contacts in **12** is 2.296 Å whereas slightly longer distances are observed for the potassium congener **2a** at 2.625 Å. No appreciable change is observed for the Zn-C and Zn-O bonds on moving from potassium zincate **2a** to sodium zincate **12**.

Zincation of two equivalents of 4-fluoroanisole using the Zn(TMP)<sub>2</sub>/2NaOtBu mixture is achieved in THF stirring for 48 h at room temperature with regioselective zincation occurring *ortho* to the fluorine atom in the substrate which was confirmed by X-ray crystallography revealing [(TMEDA)(THF)Na<sub>2</sub>Zn(*p*-OMe-C<sub>6</sub>H<sub>3</sub>F)<sub>2</sub>(OtBu)<sub>2</sub>] (**13**) (Figure 10) in a 38% crystalline yield. The regioselectivity falls in line with the formation of potassium zincate **2k** from C-H zincation of 4-fluoroanisole with the Zn(TMP)<sub>2</sub>/2KOtBu combination (Figure 6). The molecular structures of **2k** and **13** differ only by their donor system where in **13** one Na is coordinated by TMEDA and the other a single molecule of THF, as similarly observed in sodium zincate **12**. Whilst these findings also demonstrate that NaOtBu can kinetically activate the Zn-N bonds in Zn(TMP)<sub>2</sub>, via the formation of the mixed amido/alkoxy zincate [(TMEDA)NaZn(TMP)<sub>2</sub>(OtBu)] (**11**), its efficiency to promote these zincations is diminished when compared to the potassium system requiring longer reaction times to reach full conversion in the deprotonation of fluoroarenes. This caveat to the sodium system is exacerbated when turning to the zincation of non-activated arenes such as toluene where, as described previously, no reaction with toluene is observed even under refluxing conditions using Zn(TMP)<sub>2</sub>/2NaOtBu.

With a slightly less reactive base in hand we thought to test its reactivity towards substrates in which the potassium zincate system seems too aggressive (for example 4-fluoronitrobenzene). However, the same problems persisted with intractable mixtures forming via decomposition of the resulting metalated intermediates and the same can be said for the lithium congeners employing  $LiOtBu$  therefore it can be deduced that altering the alkali metal afforded no increased functional group tolerance.

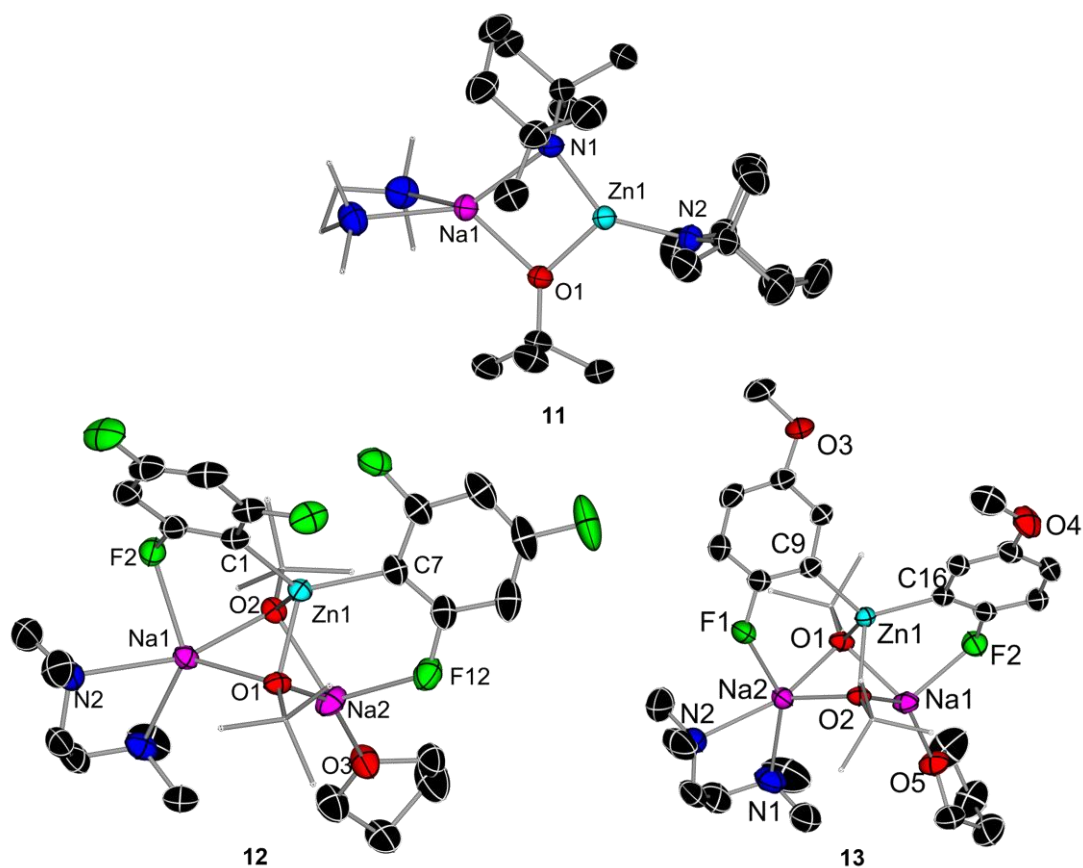


**Figure 10.** Molecular structures of zincates  $(TMEDA)NaZn(TMP)_2OtBu$  **11** (TOP),  $(TMEDA)(THF)Na_2Zn(C_6F_3H_2)_2(OtBu)_2$  **12** (BOTTOM, LHS) and  $(TMEDA)(THF)Na_2Zn(p-OMe-C_6H_3F_2)_2(OtBu)_2$  **13** (BOTTOM, RHS) with displacement ellipsoids at 50% probability, H atoms omitted and alkoxide C atoms drawn as wire frames for clarity in **12** and **13**.

#### 4.4 Conclusions

To conclude, combining the commercially available reagents  $Zn(TMP)_2$  and  $KOtBu$  led to a profound enhancement in the reactivity of the former towards fluoroarene deprotonation reactions via the formation of a novel mixed amido/alkoxy potassium zincate. Detailed structural and NMR spectroscopic studies established that whilst one equivalent of  $KOtBu$  was sufficient in kinetically activating both basic TMP groups on  $Zn(TMP)_2$  towards



deprotonation reactions, although an additional equivalent of alkoxide was required to provide stabilization of the metalated intermediates via the formation of higher order zincates. This highlights another example where the equivalency of the alkali metal alkoxide used can alter the nature of the reactive intermediates and whilst the synthetic utility of Zn(TMP)<sub>2</sub> has been enhanced, this work also highlights the hidden complexity on the nature of the organometallic intermediates involved. It also underlines the importance of alkali-metal effects when using alkali metal alkoxides as additives in deprotonative metalation reactions, with the K system outperforming its lighter Li and Na congeners. The potential of this bimetallic combination to promote the zincation of non-activated substrates has been initially demonstrated for toluene and benzene, forming higher order potassium zincate intermediates, which provided the inspiration to further explore the use of this Zn(TMP)<sub>2</sub>/KOtBu combination for the deprotonation of non-activated arenes (*vide infra*, Chapter 5).

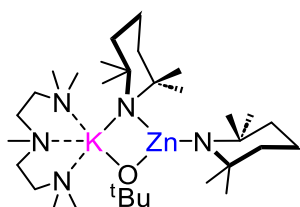
## 4.5 Experimental

Zn(TMP)<sub>2</sub> was synthesised according to an adapted literature procedure (see Chapter 7).<sup>33</sup> 2-(4-fluorophenyl)-4,4-dimethyl-4,5-dihydrooxazole was synthesised according to literature procedures.<sup>10</sup> All other reagents purchased from commercial suppliers and used as received.

A link is provided below for the Electronic Supporting Information (ESI) from the peer reviewed article on which this experimental section is based:

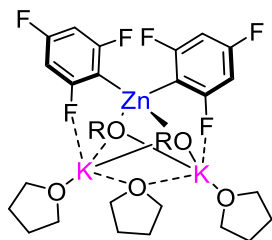
[downloadSupplement \(wiley.com\)](#)

### 4.5.1 Synthesis of [(PMDETA)KZn(TMP)<sub>2</sub>O*t*Bu] (3)



To an argon flushed Schlenk flask, Zn(TMP)<sub>2</sub> (350 mg, 1 mmol) and KO*t*Bu (110 mg, 1 mmol) were suspended in hexane (5 mL). To this suspension was added PMDETA (0.21 mL, 1 mmol) and with gentle heating afforded a pale-yellow solution. The solution was then stored at -30 °C overnight affording a colourless crop of crystals – compound **3**. Yield 340 mg, 54%. Anal. Calcd. for C<sub>31</sub>H<sub>68</sub>KN<sub>5</sub>OZn C, 58.97; H, 10.86; N, 11.09. Found: C, 58.84; H, 10.86; N, 11.19. <sup>1</sup>H-NMR (300.1 MHz, D<sub>8</sub>-THF, **298 K**): δ / ppm = 2.36 (m, 8H, 2 x (CH<sub>2</sub>)<sub>2</sub>, PMDETA), 2.19 (s, 3H, NMe, PMDETA), 2.15 (s, 12H, 2 x NMe<sub>2</sub>, PMDETA), 1.68 (m, 4H, 2 x γ-CH<sub>2</sub>, TMP), 1.27 (s, 24 H, 8 x CH<sub>3</sub>, 2x TMP), 1.23 (s, 9H, CH<sub>3</sub>, *Ot*Bu) & (m, 8H, β-CH<sub>2</sub>, 2 x TMP) overlapping. <sup>13</sup>C{<sup>1</sup>H}-NMR (101 MHz, D<sub>8</sub>-THF, **298 K**): δ / ppm = 69.5 (s, C<sub>q</sub>-O, *Ot*Bu), 53.8 (s, C<sub>q</sub>-N, 2 x TMP), 42.2 (s, β-CH<sub>2</sub>, 2 x TMP), 36.1 (s, CH<sub>3</sub>, *Ot*Bu), 35.7 (s, CH<sub>3</sub>, 2x TMP), 20.6 (s, γ-CH<sub>2</sub>, 2 x TMP).

### 4.5.2 Synthesis of (THF)<sub>3</sub>K<sub>2</sub>Zn(C<sub>6</sub>F<sub>3</sub>H<sub>2</sub>)<sub>2</sub>(*Ot*Bu)<sub>2</sub> **2a**



To an argon flushed Schlenk flask, Zn(TMP)<sub>2</sub> (180 mg, 0.5 mmol) and KO*t*Bu (110 mg, 1 mmol) were dissolved in THF (5 mL). To this solution was added 1,3,5-trifluorobenzene (**1a**) (0.1 mL, 1 mmol) and stirred at room temperature for 30 mins. All solvent was removed in vacuo, and the resulting white solid was suspended in hexane (5 mL). Gentle heating and addition of THF afforded a pale-yellow solution. The solution was then stored at -30 °C overnight affording a colourless crop of crystals – compound **2a**. Yield 210 mg, 76%. Anal. Calcd. for C<sub>24</sub>H<sub>30</sub>F<sub>6</sub>K<sub>2</sub>O<sub>3</sub>Zn (1 THF molecule coordinated) C, 46.19; H, 4.85; C<sub>20</sub>H<sub>22</sub>F<sub>6</sub>K<sub>2</sub>O<sub>2</sub>Zn (no THF molecules), C, 43.52; H, 4.02. Found: C, 44.46; H, 4.46. NMR and Elemental analysis consistent with an average between 0 and 1 THF molecules

coordinated to K after drying under vacuum. <sup>1</sup>H-NMR (300.1 MHz, D<sub>8</sub>-THF, 298 K): δ / ppm = 6.30 (m, 4H, Ar-H), 3.66 (THF), 1.81 (THF) 1.06 (s, 18H, CH<sub>3</sub>, 2 x OtBu). <sup>19</sup>F{<sup>1</sup>H}-NMR (D<sub>8</sub>-THF, 298 K): δ / ppm = -84.16 (s, 2F), -121.2 (s, 1F). <sup>13</sup>C{<sup>1</sup>H}-NMR (101 MHz, D<sub>8</sub>-THF, 298 K): δ / ppm = 170.0 (ddd, J = 223.3 Hz, 37.6 Hz, 15.1 Hz, 2 x C-F), 161.5 (d, J = 236.6 Hz, 2 x C-F), 131.6 (t, J = 82.1, 2 x C<sub>q</sub>-Zn), 96.4 (ddd, J = 67 Hz, 43.6 Hz, 5 Hz, 2 x C-H), 67.3 (s, C<sub>q</sub>-O, 2 x OtBu), 67.2 (s, O-CH<sub>2</sub>, THF), 34.3 (s, CH<sub>3</sub>, 2 x OtBu), 25.4 (s, CH<sub>2</sub>, THF).

### 4.5.3 Synthesis of higher order potassium zincates (THF)<sub>3</sub>K<sub>2</sub>Zn(Ar)<sub>2</sub>(OtBu)<sub>2</sub> **2b-2o**

*General Procedure* To an argon flushed Schlenk flask, Zn(TMP)<sub>2</sub> (1 eq) and KOtBu (2 eq) were dissolved in THF (5 mL). To this solution was added the desired fluoroarene (2 eq) at room temperature and allowed to stir for the allotted time. All solvent removed under vacuum and the resulting white solid suspended in hexane (10 mL). Potassium zincates **2b-2o** isolated as white solids via cannula filtration and washed with hexane (4 x 10 mL) (to remove TMP(H) and any unreacted fluoroarene) then dried under vacuum and stored in the glovebox.

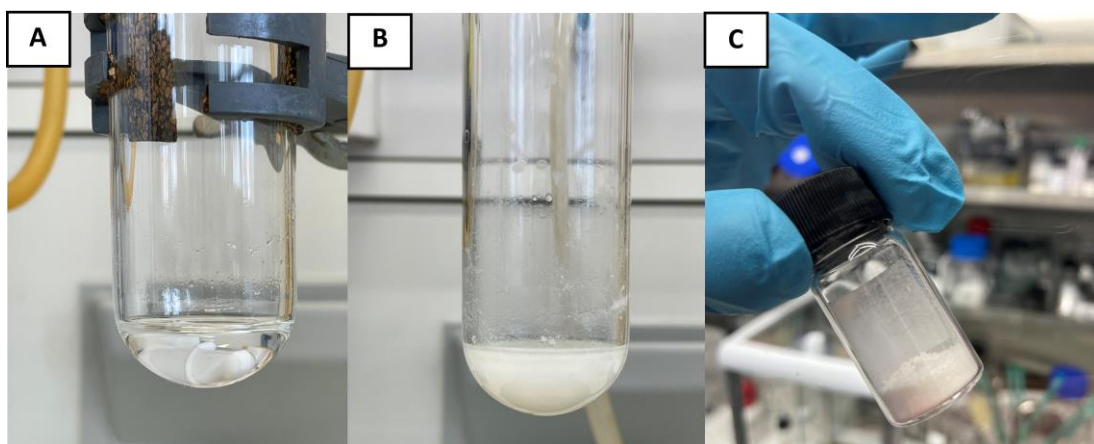


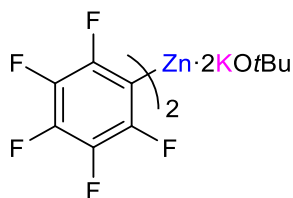
**Figure 11.** Example synthesis of higher order zincates **2a-o**. A: clear solution of **2a** in THF formed in-situ via deprotonation of 2 e.q of 1,3,5-trifluorobenzene with Zn(TMP)<sub>2</sub>/2KOtBu. B: suspension of **2a** after precipitation in hexane (THF removed under vacuum and solvent switched to hexane). C: isolated white solid of **2a** stored in the glovebox isolated via excessive washing with hexane, cannula filtration and dried under vacuum on the Schlenk line.

#### *General Procedure – NMR yield determination*

In an argon flushed J Young's NMR tube fluoroarene (0.2 mmol) and hexamethylbenzene (approx. 5.4 mg) was dissolved in d<sub>8</sub>-THF (0.5 mL). <sup>1</sup>H NMR recorded. To this solution was added Zn(TMP)<sub>2</sub> (0.1 mmol, 35 mg) and KOtBu (0.2 mmol, 22 mg). <sup>1</sup>H NMR recorded overtime and yield of zincated intermediate calculated using hexamethylbenzene as an internal standard\*.

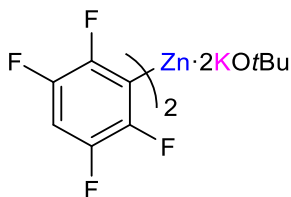
\* Yield calculated based on a “t = 0” of hexamethylbenzene and fluoroarene to standardise the hexamethylbenzene peak via integration. TMS used as internal standard for 3-fluorotoluene and 2-fluorotoluene.

#### Synthesis of K<sub>2</sub>Zn(C<sub>6</sub>F<sub>5</sub>)<sub>2</sub>(OtBu)<sub>2</sub> **2b**



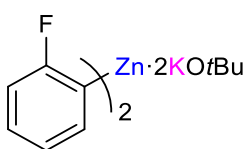
According to the general procedure, zincate **2b** was synthesised via reaction of 1,2,3,4,5-pentafluorobenzene (**1b**) (2 mmol, 0.22 mL) with Zn(TMP)<sub>2</sub> (1 mmol, 350 mg) and KOtBu (2 mmol, 220 mg) in THF (5 mL) at room temperature in 10 minutes. **2b** isolated as a white solid (550 mg, 70%). Anal. Calcd. for C<sub>28</sub>H<sub>34</sub>F<sub>10</sub>K<sub>2</sub>O<sub>4</sub>Zn (2 THF molecules coordinated) C, 43.78; H, 4.46. Found: C, 42.77; H, 4.46. <sup>1</sup>H-NMR (300.1 MHz, D<sub>8</sub>-THF, 298 K): δ / ppm = 3.50 (THF), 1.66 (THF), 0.91 (s, 18H, CH<sub>3</sub>, 2 x OtBu). <sup>19</sup>F{<sup>1</sup>H}-NMR (D<sub>8</sub>-THF, 298 K): δ / ppm = -115.85 (d, J = 26.58 Hz, 4F), -164.4 (t, J = 19.93 Hz, 4F), -164.97 (t, J = 21.75, 2F). <sup>13</sup>C{<sup>1</sup>H}-NMR (101 MHz, D<sub>8</sub>-THF, 298 K): δ / ppm = 68.2 (s, C<sub>q</sub>-O, 2 x OtBu), 68.0 (O-CH<sub>2</sub>, THF), 35.0 (s, CH<sub>3</sub>, 2 x OtBu), 26.2 (CH<sub>2</sub>, THF).

#### Synthesis of K<sub>2</sub>Zn(C<sub>6</sub>F<sub>4</sub>)<sub>2</sub>(OtBu)<sub>2</sub> **2c**



According to the general procedure, zincate **2c** was synthesised via reaction of 1,2,4,5-tetrafluorobenzene (**1c**) (2 mmol, 0.22 mL) with Zn(TMP)<sub>2</sub> (1 mmol, 350 mg) and KOtBu (2 mmol, 220 mg) in THF (5 mL) at room temperature in 10 minutes. **2c** isolated as a white solid (420 mg, 64%). Anal. Calcd. for C<sub>20</sub>H<sub>20</sub>F<sub>8</sub>K<sub>2</sub>O<sub>2</sub>Zn (0 THF molecules coordinated) C, 40.86; H, 3.43. Found: C, 41.06; H, 3.78. <sup>1</sup>H-NMR (300.1 MHz, D<sub>8</sub>-THF, 298 K): δ / ppm = 6.64 (m, 2H, 2 x Ar-H), 1.02 (s, 18H, CH<sub>3</sub>, 2 x OtBu). <sup>19</sup>F{<sup>1</sup>H}-NMR (D<sub>8</sub>-THF, 298 K): δ / ppm = -117.6 (dd, J = 36.16 Hz, 19.85 Hz, 4F), -143.94 (dd, J = 36.19 Hz, 19.35 Hz, 4F). <sup>13</sup>C{<sup>1</sup>H}-NMR (101 MHz, D<sub>8</sub>-THF, 298 K): δ / ppm = 101.4 (m, 2 x C-H), 68.1 (s, C<sub>q</sub>-O, 2 x OtBu), 35.0 (s, CH<sub>3</sub>, 2 x OtBu).

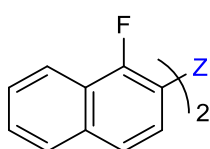
#### Synthesis of K<sub>2</sub>Zn(C<sub>6</sub>H<sub>4</sub>F)<sub>2</sub>(OtBu)<sub>2</sub> **2d**



According to the general procedure, zincate **2d** was synthesised via reaction of fluorobenzene (**1d**) (2 mmol, 0.19 mL) with Zn(TMP)<sub>2</sub> (1 mmol, 350 mg) and KOtBu (2 mmol, 220 mg) in THF (5 mL) at room temperature for 24 hours. **2d** isolated as a white solid (310 mg, 65%). Anal. Calcd. for C<sub>20</sub>H<sub>26</sub>F<sub>2</sub>K<sub>2</sub>O<sub>2</sub>Zn (0 THF molecules coordinated) C, 50.05; H, 5.46. Found: C, 51.11; H, 5.67. As per the <sup>1</sup>H spectra a residual amount of THF is coordinated to K which could account for a slightly higher C content observed in the elemental analysis. <sup>1</sup>H-NMR (300.1 MHz, D<sub>8</sub>-THF, 298 K): δ / ppm = 7.76-7.72 (m, 2H, 2 x Ar-H), 6.86-6.78 (m, 2H, 2 x

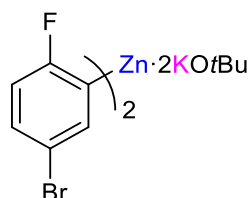
Ar-H), 6.65-6.60 (m, 2H, 2 x Ar-H), 1.00 (s, 18H, CH<sub>3</sub>, 2 x OtBu). <sup>19</sup>F{<sup>1</sup>H}-NMR (**D**<sub>8</sub>-THF, **298 K**): δ / ppm = -90.4 (s, 2F). <sup>13</sup>C{<sup>1</sup>H}-NMR (101 MHz, **D**<sub>8</sub>-THF, **298 K**): δ / ppm = 171.6 (d, J = 210 Hz, 2 x C<sub>q</sub>-F), 153.2 (d, J = 80 Hz, 2 x C<sub>q</sub>-Zn), 143.7 (d, J = 33 Hz, 2 x C-H), 124.8 (d, J = 10 Hz, 2 x C-H), 122.7 (s, 2 x C-H), 111.0 (d, J = 40 Hz, 2 x C-H), 68.0 (s, C<sub>q</sub>-O, 2 x OtBu), 35.4 (s, CH<sub>3</sub>, 2 x OtBu).

#### Synthesis of K<sub>2</sub>Zn(C<sub>10</sub>H<sub>6</sub>F)<sub>2</sub>(OtBu)<sub>2</sub> **2e**

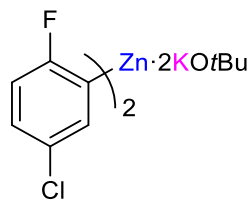


According to the general procedure, zincate **2e** was synthesised via reaction of 1-fluoronaphthalene (**1e**) (2 mmol, 0.26 mL) with Zn(TMP)<sub>2</sub> (1 mmol, 350 mg) and KOtBu (2 mmol, 220 mg) in THF (5 mL) at room temperature for 24 hours. **2e** isolated as a white solid (520 mg, 72%). Anal. Calcd. for C<sub>32</sub>H<sub>38</sub>F<sub>2</sub>K<sub>2</sub>O<sub>3</sub>Zn (1 THF molecule coordinated) C, 58.93; H, 5.87. Found: C, 58.35; H, 5.86. <sup>1</sup>H-NMR (300.1 MHz, **D**<sub>8</sub>-THF, **298 K**): δ / ppm = 8.00-7.96 (m, 2H, 2 x Ar-H), 7.91-7.86 (m, 2H, 2 x Ar-H), 7.71-7.68 (m, 2H, 2 x Ar-H), 7.36-7.19 (m, 6H, 6 x Ar-H), 3.62 (THF), 1.77 (THF), 1.00 (s, 18H, CH<sub>3</sub>, 2 x OtBu). <sup>19</sup>F{<sup>1</sup>H}-NMR (**D**<sub>8</sub>-THF, **298 K**): δ / ppm = -104.2 (s, 2F). <sup>13</sup>C{<sup>1</sup>H}-NMR (101 MHz, **D**<sub>8</sub>-THF, **298 K**): δ / ppm = 164.5 (d, J = 218 Hz, 2 x C<sub>q</sub>-F), 147.2 (d, J = 78 Hz, 2 x C<sub>q</sub>-Zn), 141.1 (d, J = 33 Hz, 2 x C-H), 134.0 (d, J = 5 Hz, 2 x C-H), 126.7 (d, J = 5 Hz, 2 x C-H), 123.3 (s, 2 x C<sub>q</sub>), 123.0 (d, J = 41 Hz, 2 x C-H), 123.0 (s, 2 x C<sub>q</sub>), 120.5 (d, J = 3 Hz, 2 x C-H), 119.3 (d, J = 3 Hz, 2 x C-H), 67.3 (s, C<sub>q</sub>-O, 2 x OtBu), 67.2 (s, O-CH<sub>2</sub>, THF), 34.7 (s, CH<sub>3</sub>, 2 x OtBu), 25.4 (s, CH<sub>2</sub>, THF).

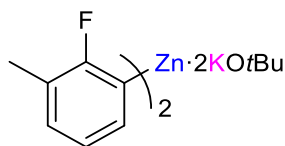
#### Synthesis of K<sub>2</sub>Zn(C<sub>6</sub>H<sub>3</sub>FBr)<sub>2</sub>(OtBu)<sub>2</sub> **2f**



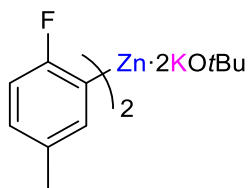
According to the general procedure, zincate **2f** was synthesised via reaction of 1-fluoro-4-bromobenzene (**1f**) (2 mmol, 0.22 mL) with Zn(TMP)<sub>2</sub> (1 mmol, 350 mg) and KOtBu (2 mmol, 220 mg) in THF (5 mL) at room temperature in 1 hour. **2f** isolated as a white solid (520 mg, 72%). Anal. Calcd. for C<sub>24</sub>H<sub>32</sub>F<sub>2</sub>Br<sub>2</sub>K<sub>2</sub>O<sub>3</sub>Zn (1 THF molecule coordinated) C, 40.61; H, 4.54. Found: C, 40.27; H, 4.33. <sup>1</sup>H-NMR (300.1 MHz, **D**<sub>8</sub>-THF, **298 K**): δ / ppm = 7.79-7.78 (m, 2H, 2 x Ar-H), 7.00-6.95 (m, 2H, 2 x Ar-H), 6.62-6.58 (m, 2H, 2 x Ar-H), 3.62 (THF), 1.77 (THF), 1.00 (s, 18H, CH<sub>3</sub>, 2 x OtBu). <sup>19</sup>F{<sup>1</sup>H}-NMR (**D**<sub>8</sub>-THF, **298 K**): δ / ppm = -94.4 (s, 2F). <sup>13</sup>C{<sup>1</sup>H}-NMR (101 MHz, **D**<sub>8</sub>-THF, **298 K**): δ / ppm = 169.3 (d, J = 217 Hz, 2 x C<sub>q</sub>-F), 157.5 (d, J = 79 Hz, 2 x C<sub>q</sub>-Zn), 144.1 (d, J = 31 Hz, 2 x C-H), 127.0 (d, J = 9 Hz, 2 x C-H), 117.1 (d, J = 3 Hz, 2 x C<sub>q</sub>-Br), 113.6 (d, J = 42 Hz, 2 x C-H), 67.2 (s, O-CH<sub>2</sub>, THF), 67.0 (s, C<sub>q</sub>-O, 2 x OtBu), 34.6 (s, CH<sub>3</sub>, 2 x OtBu), 25.4 (s, CH<sub>2</sub>, THF).

Synthesis of K<sub>2</sub>Zn(C<sub>6</sub>H<sub>3</sub>ClBr)<sub>2</sub>(OtBu)<sub>2</sub> **2g**

According to the general procedure, zincate **2g** was synthesised via reaction of 1-fluoro-4-chlorobenzene (**1g**) (2 mmol, 0.21 mL) with Zn(TMP)<sub>2</sub> (1 mmol, 350 mg) and KOtBu (2 mmol, 220 mg) in THF (5 mL) at room temperature in 1 hour. **2g** isolated as a white solid (450 mg, 73%). Anal. Calcd. for C<sub>24</sub>H<sub>32</sub>F<sub>2</sub>Cl<sub>2</sub>K<sub>2</sub>O<sub>3</sub>Zn (1 THF molecule coordinated) C, 46.42; H, 5.19. Found: C, 45.30; H, 5.21. (As per the <sup>1</sup>H NMR spectra the THF integration averages at slightly less than one full molecule of THF and can account for the slightly lower C content than expected for the elemental analysis). <sup>1</sup>H-NMR (300.1 MHz, D<sub>8</sub>-THF, 298 K): δ / ppm = 7.64-7.63 (m, 2H, 2 x Ar-H), 6.86-6.80 (m, 2H, 2 x Ar-H), 6.66-6.61 (m, 2H, 2 x Ar-H), 3.61 (THF), 1.77 (THF), 1.00 (s, 18H, CH<sub>3</sub>, 2 x OtBu). <sup>19</sup>F{<sup>1</sup>H}-NMR (D<sub>8</sub>-THF, 298 K): δ / ppm = -94.8 (s, 2F). <sup>13</sup>C{<sup>1</sup>H}-NMR (101 MHz, D<sub>8</sub>-THF, 298 K): δ / ppm = 169.6 (d, J = 216 Hz, 2 x C<sub>q</sub>-F), 157.2 (d, J = 84 Hz, 2 x C<sub>q</sub>-Zn), 141.9 (d, J = 31 Hz, 2 x C-H), 128.7 (d, J = 3 Hz, 2 x C<sub>q</sub>-Cl), 124.8 (d, J = 9 Hz, 2 x C-H), 113.6 (d, J = 42 Hz, 2 x C-H), 68.0 (s, O-CH<sub>2</sub>, THF), 67.8 (s, C<sub>q</sub>-O, 2 x OtBu), 35.3 (s, CH<sub>3</sub>, 2 x OtBu), 26.1 (s, CH<sub>2</sub>, THF).

Synthesis of K<sub>2</sub>Zn(o-Me-C<sub>6</sub>H<sub>3</sub>F)<sub>2</sub>(OtBu)<sub>2</sub> **2h**

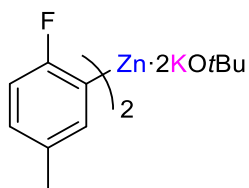
According to the general procedure, zincate **2h** was synthesised via reaction of 2-fluorotoluene (**1h**) (2 mmol, 0.22 mL) with Zn(TMP)<sub>2</sub> (1 mmol, 350 mg) and KOtBu (2 mmol, 220 mg) in THF (5 mL) at room temperature in 24 hours. **2g** isolated as a white solid (430 mg, 85%). Anal. Calcd. for C<sub>22</sub>H<sub>30</sub>F<sub>2</sub>K<sub>2</sub>OZn (O THF molecules coordinated) C, 52.01; H, 5.95. Found: C, 52.69; H, 6.17. (Residual amounts of 2-fluorotoluene that cannot be removed and coordinated THF observed in <sup>1</sup>H NMR spectra). <sup>1</sup>H-NMR (300.1 MHz, D<sub>8</sub>-THF, 298 K): δ / ppm = 7.53-7.51 (m, 2H, 2 x Ar-H), 7.53-7.51 (m, 2H, 2 x Ar-H), 6.70-6.66 (m, 4H, 4 x Ar-H), 2.16 (s, 6H, 2 x CH<sub>3</sub>), 1.00 (s, 18H, CH<sub>3</sub>, 2 x OtBu). <sup>19</sup>F{<sup>1</sup>H}-NMR (D<sub>8</sub>-THF, 298 K): δ / ppm = -95.5 (s, 2F). <sup>13</sup>C{<sup>1</sup>H}-NMR (101 MHz, D<sub>8</sub>-THF, 298 K): δ / ppm = 170.1 (d, J = 213 Hz, 2 x C<sub>q</sub>-F), 152.5 (d, J = 82 Hz, 2 x C<sub>q</sub>-Zn), 141.5 (d, J = 35 Hz, 2 x C-H), 126.6 (d, J = 5 Hz, 2 x C-H), 122.8 (s, 2 x C-H), 120.1 (d, J = 33 Hz, 2 x C<sub>q</sub>), 68.0 (s, C<sub>q</sub>-O, 2 x OtBu), 35.4 (s, CH<sub>3</sub>, 2 x OtBu), 15.9 (d, J = 2 Hz, 2 x Me).

Synthesis of K<sub>2</sub>Zn(p-Me-C<sub>6</sub>H<sub>3</sub>F)<sub>2</sub>(OtBu)<sub>2</sub> **2i**

According to the general procedure, zincate **2i** was synthesised via reaction of 4-fluorotoluene (**1i**) (2 mmol, 0.22 mL) with Zn(TMP)<sub>2</sub> (1 mmol, 350 mg) and KOtBu (2 mmol, 220 mg) in THF (5 mL) at room temperature in 24 hours. **2i** isolated as a white solid (410 mg, 81%). Anal. Calcd. for C<sub>22</sub>H<sub>30</sub>F<sub>2</sub>K<sub>2</sub>OZn (O THF molecules coordinated) C, 52.01; H, 5.95. Found: C, 52.92; H, 6.25. (Residual amounts of 4-fluorotoluene that cannot be removed observed in

<sup>1</sup>H NMR spectra). **<sup>1</sup>H-NMR (300.1 MHz, D<sub>8</sub>-THF, 298 K):**  $\delta$  / ppm = 7.57 (br. s, 2H, 2 x Ar-H), 6.66-6.60 (m, 2H, 2 x Ar-H), 6.53-6.48 (m, 2H, 2 x Ar-H), 2.19 (s, 6H, 2 x CH<sub>3</sub>), 1.00 (s, 18H, CH<sub>3</sub>, 2 x OtBu). **<sup>19</sup>F{<sup>1</sup>H}-NMR (D<sub>8</sub>-THF, 298 K):**  $\delta$  / ppm = -96.2 (s, 2F). **<sup>13</sup>C{<sup>1</sup>H}-NMR (101 MHz, D<sub>8</sub>-THF, 298 K):**  $\delta$  / ppm = 170.1 (d, J = 216 Hz, 2 x C<sub>q</sub>-F), 152.9 (d, J = 76 Hz, 2 x C<sub>q</sub>-Zn), 144.4 (d, J = 32 Hz, 2 x C-H), 130.3 (d, J = 2 Hz, 2 x C-H), 125.4 (s, 2 x C-H), 111.4 (d, J = 40 Hz, 2 x C<sub>q</sub>), 68.0 (s, C<sub>q</sub>-O, 2 x OtBu), 35.4 (s, CH<sub>3</sub>, 2 x OtBu), 20.9 (d, J = 3 Hz, 2 x Me).

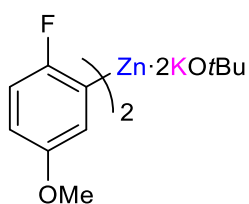
#### Synthesis of K<sub>2</sub>Zn(*m*-Me-C<sub>6</sub>H<sub>3</sub>F)<sub>2</sub>(OtBu)<sub>2</sub> **2j**



According to the general procedure, zincate **2j** was synthesised via reaction of 3-fluorotoluene (**1j**) (2 mmol, 0.22 mL) with Zn(TMP)<sub>2</sub> (1 mmol, 350 mg) and KOtBu (2 mmol, 220 mg) in THF (5 mL) at room temperature in 24 hours. **2j** isolated as a white solid (380 mg, 70%).

Anal. Calcd. for C<sub>22</sub>H<sub>30</sub>F<sub>2</sub>K<sub>2</sub>OZn (O THF molecules coordinated) C, 52.01; H, 5.95. Found: C, 48.46; H, 5.84. (Small amounts of 3-fluorotoluene and residual TMP(H) that cannot be removed observed in <sup>1</sup>H NMR and <sup>19</sup>F NMR spectra and possibly accounts for the unsatisfactory elemental analysis). **<sup>1</sup>H-NMR (300.1 MHz, D<sub>8</sub>-THF, 298 K):**  $\delta$  / ppm = 7.58-7.56 (m, 2H, 2 x Ar-H), 6.63-6.61 (m, 2H, 2 x Ar-H), 6.47-6.45 (m, 2H, 2 x Ar-H), 2.19 (s, 6H, 2 x CH<sub>3</sub>), 1.00 (s, 18H, CH<sub>3</sub>, 2 x OtBu). **<sup>19</sup>F{<sup>1</sup>H}-NMR (D<sub>8</sub>-THF, 298 K):**  $\delta$  / ppm = -92.0 (s, 2F). **<sup>13</sup>C{<sup>1</sup>H}-NMR (101 MHz, D<sub>8</sub>-THF, 298 K):**  $\delta$  / ppm = 171.5 (d, J = 213 Hz, 2 x C<sub>q</sub>-F), 148.7 (d, J = 71 Hz, 2 x C<sub>q</sub>-Zn), 143.6 (d, J = 32 Hz, 2 x C-H), 133.8 (d, J = 7 Hz, 2 x C-H), 123.7 (s, 2 x C-H), 112.7 (d, J = 39 Hz, 2 x C<sub>q</sub>), 35.6 (s, CH<sub>3</sub>, 2 x OtBu), 21.2 (s, 2 x Me).

#### Synthesis of K<sub>2</sub>Zn(*p*-OMe-C<sub>6</sub>H<sub>3</sub>F)<sub>2</sub>(OtBu)<sub>2</sub> **2k**

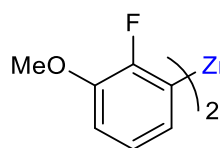


According to the general procedure, zincate **2k** was synthesised via reaction of 4-fluoroanisole (**1k**) (2 mmol, 0.23 mL) with Zn(TMP)<sub>2</sub> (1 mmol, 350 mg) and KOtBu (2 mmol, 220 mg) in THF (5 mL) at room temperature in 24 hours. **2k** isolated as a white solid (420 mg, 57%). Anal. Calcd. for C<sub>22</sub>H<sub>30</sub>F<sub>2</sub>K<sub>2</sub>O<sub>4</sub>Zn (2 THF molecules coordinated) C, 52.66; H, 6.78. Found: C, 52.99; H, 7.11. A portion of this isolated zincate

can be recrystallised from a hexane/THF mixture to give a crop of block like crystals which were analysed by x-ray crystallography to reveal the molecular structure of higher order zincate (THF)<sub>3</sub>K<sub>2</sub>Zn(*p*-OMe-C<sub>6</sub>H<sub>3</sub>F)<sub>2</sub>(OtBu)<sub>2</sub> **2k** (Figure 5). **<sup>1</sup>H-NMR (300.1 MHz, D<sub>8</sub>-THF, 298 K):**  $\delta$  / ppm = 7.34-7.33 (m, 2H, 2 x Ar-H), 6.56-6.51 (m, 2H, 2 x Ar-H), 6.37-6.32 (m, 2H, 2 x Ar-H), 3.66 (THF), 3.63 (s, 6H, 2 x OMe), 1.76 (THF), 1.00 (s, 18H, CH<sub>3</sub>, 2 x OtBu). **<sup>19</sup>F{<sup>1</sup>H}-NMR (D<sub>8</sub>-THF, 298 K):**  $\delta$  / ppm = -101.9 (s, 2F). **<sup>13</sup>C{<sup>1</sup>H}-NMR (101 MHz, D<sub>8</sub>-THF, 298 K):**  $\delta$  / ppm = 166.0 (d, J = 208 Hz, 2 x C<sub>q</sub>-F), 155.6 (s, 2 x C<sub>q</sub>-O), 126.7 (d, J = 33

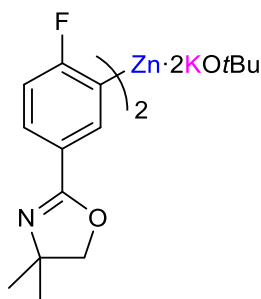
Hz, 2 x C-H), 111.9 (d, J = 43 Hz, 2 x C-H), 110.8 (d, J = 10 Hz, 2 x C-H), 68.0 (THF), 67.8 (s, C<sub>q</sub>-O, 2 x OtBu), 55.3 (s, CH<sub>3</sub>, 2 x OMe), 35.4 (s, CH<sub>3</sub>, 2 x OtBu), 26.1 (THF).

#### Synthesis of K<sub>2</sub>Zn(*o*-OMe-C<sub>6</sub>H<sub>3</sub>F)<sub>2</sub>(OtBu)<sub>2</sub> **2l**



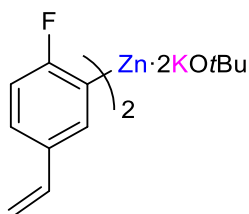
According to the general procedure, zincate **2l** was synthesised via reaction of 2-fluoroanisole (**1l**) (2 mmol, 0.23 mL) with Zn(TMP)<sub>2</sub> (1 mmol, 350 mg) and KOtBu (2 mmol, 220 mg) in THF (5 mL) at room temperature in 24 hours. **2l** isolated as a white solid (360 mg, 67%). Anal. Calcd. for C<sub>22</sub>H<sub>30</sub>F<sub>2</sub>K<sub>2</sub>O<sub>2</sub>Zn (residual THF molecules coordinated) C, 48.93; H, 5.60. Found: C, 48.01; H, 5.82. (Small amounts of 2-fluoroanisole that cannot be removed observed in <sup>1</sup>H NMR and <sup>19</sup>F NMR spectra and residual coordinated THF can account for the slightly low value found for C in the elemental analysis). **<sup>1</sup>H-NMR (300.1 MHz, D<sub>8</sub>-THF, 298 K):** δ / ppm = 7.27 (d, J= 7 Hz, 2H, 2 x Ar-H), 6.73 (t, J= 8 Hz, 2H, 2 x Ar-H), 6.56-6.50 (m, 2H, 2 x Ar-H), 3.71 (s, 6H, 2 x OMe), 1.00 (s, 18H, CH<sub>3</sub>, 2 x OtBu). **<sup>19</sup>F{<sup>1</sup>H}-NMR (D<sub>8</sub>-THF, 298 K):** δ / ppm = -113.1 (s, 2F). **<sup>13</sup>C{<sup>1</sup>H}-NMR (101 MHz, D<sub>8</sub>-THF, 298 K):** δ / ppm = 159.6 (d, J = 209 Hz, 2 x C<sub>q</sub>-F), 154.6 (d, J = 73 Hz, 2 x C<sub>q</sub>-Zn), 146.4 (d, J = 25 Hz, 2 x C<sub>q</sub>-O), 135.0 (d, J = 30 Hz, 2 x C-H), 122.7 (s, 2 x C-H), 109.0 (s, 2 x C-H), 68.0 (s, C<sub>q</sub>-O, 2 x OtBu), 55.4 (s, CH<sub>3</sub>, 2 x OMe), 35.4 (s, CH<sub>3</sub>, 2 x OtBu).

#### Synthesis of K<sub>2</sub>Zn(Ar)<sub>2</sub>(OtBu)<sub>2</sub> **2m**

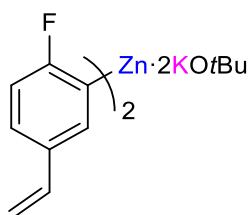


According to the general procedure, zincate **2m** was synthesised via reaction of 2-(4-fluorophenyl)-4,4-dimethyl-4,5-dihydrooxazole (**1m**) (2 mmol, 386 mg) with Zn(TMP)<sub>2</sub> (1 mmol, 350 mg) and KOtBu (2 mmol, 220 mg) in THF (5 mL) at room temperature in 12 hours. **2m** isolated as a white solid (510 mg, 67%). Anal. Calcd. for C<sub>34</sub>H<sub>48</sub>F<sub>2</sub>K<sub>2</sub>O<sub>5</sub>Zn (1 THF molecule coordinated) C, 54.72; H, 6.48. Found: C, 54.52; H, 6.62. A portion of this isolated zincate can be recrystallised from a hexane/THF mixture to give a crop of block like crystals which were analysed by x-ray crystallography to reveal the molecular structure of higher order zincate (THF)<sub>3</sub>K<sub>2</sub>Zn(Ar)<sub>2</sub>(OtBu)<sub>2</sub> **2m** (Figure 5). **<sup>1</sup>H-NMR (300.1 MHz, D<sub>8</sub>-THF, 298 K):** δ / ppm = 8.40 (s, 2H, 2 x C-H), 7.60-7.54 (m, 2H, 2 x C-H), 6.67-6.62 (m, 2H, 2 x C-H), 3.93 (s, 4H, 2 x O-CH<sub>2</sub>), 3.61 (THF), 1.77 (THF), 1.25 (s, 12H, 4 x CH<sub>3</sub>), 1.00 (s, 18H, CH<sub>3</sub>, 2 x OtBu). **<sup>19</sup>F{<sup>1</sup>H}-NMR (D<sub>8</sub>-THF, 298 K):** δ / ppm = -86.9 (s, 2F). **<sup>13</sup>C{<sup>1</sup>H}-NMR (101 MHz, D<sub>8</sub>-THF, 298 K):** δ / ppm = 173.4 (d, J = 216 Hz, 2 x C<sub>q</sub>-F), 163.6 (s, 2 x C<sub>q</sub>), 153.0 (d, J = 80 Hz, 2 x C<sub>q</sub>-Zn), 143.9 (d, J = 37 Hz, 2 x C-H), 126.8 (d, J = 9 Hz, 2 x C-H), 123.4 (s, 2 x C<sub>q</sub>), 111.8 (d, J= 40 Hz, 2 x C-H), 79.0 (s, 2 x O-CH<sub>2</sub>), 68.0 (s, THF), 67.6 (s, C<sub>q</sub>-O, 2 x OtBu), 35.4 (s, CH<sub>3</sub>, 2 x OtBu), 28.8 (s, 4 x CH<sub>3</sub>), 26.2 (THF).

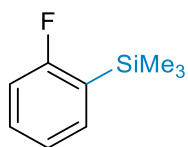


Synthesis of K<sub>2</sub>Zn(p-F-C<sub>6</sub>H<sub>4</sub>-CH=CH<sub>2</sub>)<sub>2</sub>(OtBu)<sub>2</sub> **2n**

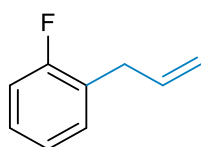
According to the general procedure, zincate **2n** was synthesised via reaction of 4-fluorostyrene (**1n**) (2 mmol, 0.24 mL) with Zn(TMP)<sub>2</sub> (1 mmol, 350 mg) and KOtBu (2 mmol, 220 mg) in THF (5 mL) at room temperature in 3 hours. **2n** isolated as a white solid (380 mg, 72%). Anal. Calcd. for C<sub>24</sub>H<sub>30</sub>F<sub>2</sub>K<sub>2</sub>O<sub>2</sub>Zn (0 THF molecules coordinated) C, 54.18; H, 5.68. Found: C, 54.14; H, 5.89. <sup>1</sup>H-NMR (300.1 MHz, D<sub>8</sub>-THF, 298 K): δ / ppm = 7.88 (m, 2H, 2 x Ar-H), 7.00-6.96 (m, 2H, 2 x Ar-H), 6.69-6.58 (m, 4H, 2 x Ar-H & 2 x C-H overlapping), 5.49 (dd, J = 17 Hz, 2 Hz, 2 x C-H), 5.49 (dd, J = 17 Hz, 2 Hz, 2 x C-H), 4.87 (dd, J = 10 Hz, 2 Hz, 2 x C-H), 1.00 (s, 18H, CH<sub>3</sub>, 2 x OtBu). <sup>19</sup>F{<sup>1</sup>H}-NMR (D<sub>8</sub>-THF, 298 K): δ / ppm = -94.4 (s, 2F). <sup>13</sup>C{<sup>1</sup>H}-NMR (101 MHz, D<sub>8</sub>-THF, 298 K): δ / ppm = 172.0 (d, J = 219 Hz, 2 x C<sub>q</sub>-F), 153.0 (d, J = 80 Hz, 2 x C<sub>q</sub>-Zn), 142.6 (d, J = 33 Hz, 2 x C-H), 139.5 (s, 2 x CH<sub>2</sub>), 132.0 (d, J = 2 Hz, 2 x C<sub>q</sub>), 123.2 (d, J = 8 Hz, 2 x C-H), 112.0 (d, J = 40 Hz, 2 x C-H), 109.0 (s, 2 x C-H), 68.0 (s, C<sub>q</sub>-O, 2 x OtBu), 35.4 (s, CH<sub>3</sub>, 2 x OtBu).

Synthesis of K<sub>2</sub>Zn(Ar)<sub>2</sub>(OtBu)<sub>2</sub> **2o**

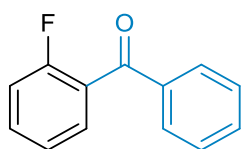
According to the general procedure, zincate **2o** was synthesised via reaction of 2-(2,4-difluorophenyl)pyridine (**1o**) (2 mmol, 0.30 mL) with Zn(TMP)<sub>2</sub> (1 mmol, 350 mg) and KOtBu (2 mmol, 220 mg) in THF (5 mL) at room temperature in 10 minutes. **2o** isolated as a white solid (520 mg, 78%). Anal. Calcd. for C<sub>30</sub>H<sub>30</sub>F<sub>4</sub>K<sub>2</sub>O<sub>2</sub>N<sub>2</sub>Zn (0 THF molecules coordinated) C, 53.77; H, 4.51; N, 4.18 Found: C, 53.74; H, 4.78; N, 4.18. <sup>1</sup>H-NMR (300.1 MHz, D<sub>8</sub>-THF, 298 K): δ / ppm = 8.55 (d, J = 4Hz, 2H, 2 x Ar-H), 7.81 (d, J = 8 Hz, 2H, 2 x Ar-H), 7.67-7.53 (m, 4H, 4 x Ar-H), 7.06-7.01 (m, 2 x Ar-H), 6.62 (q, J = 4 Hz, 2 x Ar-H), 1.09 (s, 18H, CH<sub>3</sub>, 2 x OtBu). <sup>19</sup>F{<sup>1</sup>H}-NMR (D<sub>8</sub>-THF, 298 K): δ / ppm = -86.0 (s, 2F), -86.3 (s, 2F). <sup>13</sup>C{<sup>1</sup>H}-NMR (101 MHz, D<sub>8</sub>-THF, 298 K): δ / ppm = 171.8 (dd, J = 226 Hz, 34 Hz, 2 x C-F), 168.6 (dd, J = 229 Hz, 32 Hz, 2 x C-F), 157.3 (s, 2 x C-H), 149.6 (s, 2 x C-H), 138.5 (t, J = 77 Hz, 2 x C<sub>q</sub>-Zn), 135.7 (s, 2 x C-H), 128.7 (d, J = 9 Hz, 2 x C<sub>q</sub>), 124.8 (d, J = 14 Hz, 2 x C-H), 122.2 (d, J = 27 Hz, 2 x C<sub>q</sub>), 120.9 (s, 2 x C-H), 109.5 (d, J = 36 Hz, 2 x C-H), 68.18 (s, C<sub>q</sub>-O, 2 x OtBu), 35.2 (s, CH<sub>3</sub>, 2 x OtBu).

4.5.4 Electrophilic quenches of potassium zincate **2d**Synthesis of 2-fluorophenyl)trimethylsilane **4**

In an argon flushed J. Youngs NMR tube, 2 equivalents of fluorobenzene (0.2 mmol, 19  $\mu$ L) and hexamethylbenzene (5.4 mg) were dissolved in 5 mL of d<sub>8</sub>-THF. T=0 <sup>1</sup>H-NMR recorded. To this solution was added Zn(TMP)<sub>2</sub> (0.1 mmol, 35 mg) and 2 equivalents of KO<sup>t</sup>Bu (0.2 mmol, 22 mg). After 24 h at room temperature, 2 equivalents of TMSCl (0.2 mmol, 26  $\mu$ L) were added instantly forming the desired silylated species **4** in a quantitative yield. Yield determined using hexamethylbenzene as an internal standard. NMR consistent with literature reports. <sup>64</sup> <sup>1</sup>H-NMR (300.1 MHz, D<sub>8</sub>-THF, 298 K):  $\delta$  / ppm = 7.52-7.50 (m, 1H, Ar-H), 7.09-7.04 (m, 1H, Ar-H), 6.97-6.94 (m, 1H, Ar-H), 6.82-6.77 (m, 1H, Ar-H), 0.09 (s, 9H, 3 x CH<sub>3</sub>). <sup>19</sup>F{<sup>1</sup>H}-NMR (D<sub>8</sub>-THF, 298 K):  $\delta$  / ppm = -84.3 (s, 1F).

Synthesis of 1-Allyl-2-fluorobenzene **5**

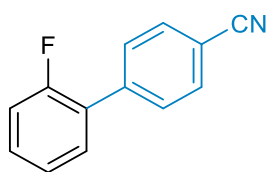
In an argon flushed Schlenk flask, 2 equivalents of fluorobenzene (1 mmol, 94  $\mu$ L) and hexamethylbenzene (10 mol%) were dissolved in 5 mL of THF. To this solution was added Zn(TMP)<sub>2</sub> (0.5 mmol, 180 mg) and 2 equivalents of KO<sup>t</sup>Bu (1 mmol, 110 mg). After 24 h at room temperature, forming **2d in-situ**, CuCN·2LiCl (20 mol %) was added along with 2 equivalents allyl bromide (1 mmol, 86  $\mu$ L) and stirred for 16 h at room temperature. Reaction quenched with NH<sub>4</sub>Cl (10 mL), organics extracted with EtOAc (3 x 10 mL), washed with brine (1 x 10 mL), dried over MgSO<sub>4</sub> and filtered. Aliquot taken, all solvent removed, and NMR analysis carried out in CDCl<sub>3</sub> confirming the formation of 1-Allyl-2-fluorobenzene **5** in a 62% yield. Yield determined using hexamethylbenzene as an internal standard. NMR consistent with literature reports. <sup>65</sup> <sup>1</sup>H-NMR (300.1 MHz, CDCl<sub>3</sub>, 298 K):  $\delta$  / ppm = 7.21-7.00 (m, 4H, 4 x Ar-H), 6.04-5.88 (m, 1H, 1 x C-H), 5.09-5.04 (m, 2H, 1 x CH<sub>2</sub>), 3.40 (d, J = 2 Hz, 2H, 1 x CH<sub>2</sub>). <sup>19</sup>F{<sup>1</sup>H}-NMR (CDCl<sub>3</sub>, 298 K):  $\delta$  / ppm = -118.8 (s, 1F).

Synthesis of 2-fluoroacetophenone **6**

In an argon flushed Schlenk flask, 2 equivalents of fluorobenzene (1 mmol, 94  $\mu$ L) and hexamethylbenzene (10 mol%) were dissolved in 5 mL of THF. To this solution was added Zn(TMP)<sub>2</sub> (0.5 mmol, 180 mg) and 2 equivalents of KO<sup>t</sup>Bu (1 mmol, 110 mg). After 24 h at room temperature, forming **2d in-situ**, CuI (3 e.q, 571 mg) was added along with 3 equivalents of benzoyl chloride (3 e.q, 0.35 mL) and stirred for 16 h at room temperature. Reaction quenched with NH<sub>4</sub>Cl (10 mL), organics extracted with EtOAc (3 x 10 mL), washed with brine (1 x 10 mL), dried over MgSO<sub>4</sub> and filtered. Aliquot taken, all solvent removed, and NMR analysis

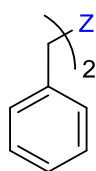
carried out in CDCl<sub>3</sub> confirming the formation of 2-fluoroacetophenone **6** in an 87% yield. Yield determined using hexamethylbenzene as an internal standard. NMR consistent with literature reports.<sup>66</sup> **Note:** By-products present due to the excess of benzoyl chloride used so remaining aromatic signals of **6** overlapping with said by-products. The two signals reported below are clean with no overlapping signals and match the literature values for 2-fluoroacetophenone and were used to calculate the yield. <sup>19</sup>F NMR spectra identical to that reported for **6** and shows a clean signal at -111.0 ppm. <sup>1</sup>H-NMR (300.1 MHz, CDCl<sub>3</sub>, 298 K): δ / ppm = 7.84 (d, J = 8Hz, 2H, 2 x Ar-H), 7.16 (t, J = 9 Hz, 1H, 1 x Ar-H). <sup>19</sup>F{<sup>1</sup>H}-NMR (CDCl<sub>3</sub>, 298 K): δ / ppm = -111.0 (s, 1F).

#### Synthesis of 2'-fluoro-[1,1'-biphenyl]-4-carbonitrile **7**



In an argon flushed Schlenk flask, 2 equivalents of fluorobenzene (1 mmol, 94 μL) was dissolved in 5 mL of THF and to this solution was added Zn(TMP)<sub>2</sub> (0.5 mmol, 180 mg) and 2 equivalents of KO<sup>t</sup>Bu (1 mmol, 110 mg). After 24 h at room temperature, forming **2d in-situ**, this solution was transferred to an argon flushed ampoule charged with Pd(dba)<sub>2</sub> (5 mol%), SPhos (10 mol%), LiCl (2 e.q, 1 mmol) and 4-iodobenzonitrile (1.8 e.q, 458 mg). Reaction refluxed for 24h. Reaction quenched with NH<sub>4</sub>Cl (10 mL), organics extracted with EtOAc (3 x 10 mL), washed with brine (1 x 10 mL), dried over MgSO<sub>4</sub> and filtered. Purified via silica column chromatography (Hexane:EtOAc 100:0 to 90:10) to produce **7** as a colourless oil (122 mg, 75%). Spectroscopic data is an identical match for those previously reported.<sup>20</sup> <sup>1</sup>H-NMR (300.1 MHz, CDCl<sub>3</sub>, 298 K): δ / ppm = 7.70 – 7.57 (m, 2H, Ar-H), 7.61 – 7.56 (m, 2H, Ar-H), 7.46 – 7.34 (m, 2H, Ar-H), 7.20 – 7.07 (m, 2H, Ar-H). <sup>19</sup>F{<sup>1</sup>H}-NMR (CDCl<sub>3</sub>, 298 K): δ / ppm = -117.5 (s, 1F).

#### 4.5.5 Synthesis of 8 (THF)<sub>2</sub>K<sub>2</sub>Zn(Bz)<sub>2</sub>(O<sup>t</sup>Bu)<sub>2</sub> (Bz = CH<sub>2</sub>Ph) (toluene zincation)



In an argon flushed Schlenk flask, Zn(TMP)<sub>2</sub> (1 mmol, 350 mg) and KO<sup>t</sup>Bu (2 mmol, 220 mg) were suspended in toluene (5 mL) at room temperature and left to stir for 24h at room temperature resulting in an orange suspension. All solvent removed and the resulting white solid was washed with hexane (5 x 10 mL). All solvent removed and zincate **8** isolated as a white solid (400 mg, 65 %). Anal. Calcd. for C<sub>22</sub>H<sub>32</sub>K<sub>2</sub>O<sub>2</sub>Zn. C, 55.97; H, 6.83 Found: C, 55.97; H, 7.4. A portion of this isolated zincate can be recrystallised from a hexane/THF mixture to give a crop of block like crystals which were analysed by x-ray crystallography to reveal the molecular structure of higher order zincate (THF)<sub>2</sub>K<sub>2</sub>Zn(Bz)<sub>2</sub>(O<sup>t</sup>Bu)<sub>2</sub> (Bz = CH<sub>2</sub>Ph) **8** (Figure 6). <sup>1</sup>H-NMR (300.1 MHz, D<sub>8</sub>-THF, 298 K): δ / ppm = 6.84-6.77 (m, 8H, 8 x Ar-H), 6.25 (br.

s, 2H, 2 x Ar-H), 3.6 (THF), 1.77 (THF), 1.65 (s, 4H, 2 x CH<sub>2</sub>-Zn), 1.12 (s, 18H, CH<sub>3</sub>, 2 x *Ot*Bu). Residual toluene signals present. <sup>13</sup>C{<sup>1</sup>H}-NMR (101 MHz, D<sub>8</sub>-THF, 298 K): δ / ppm = 159.1 (s, 2 x C<sub>q</sub>), 127.7 (s, 2 x C-H), 123.9 (s, 2 x C-H), 114.7 (s, 2 x C-H), 68.0 (THF), 35.5 (s, CH<sub>3</sub>, 2 x *Ot*Bu), 30.8 (s, 2 x CH<sub>2</sub>-Zn), 26.2 (THF).

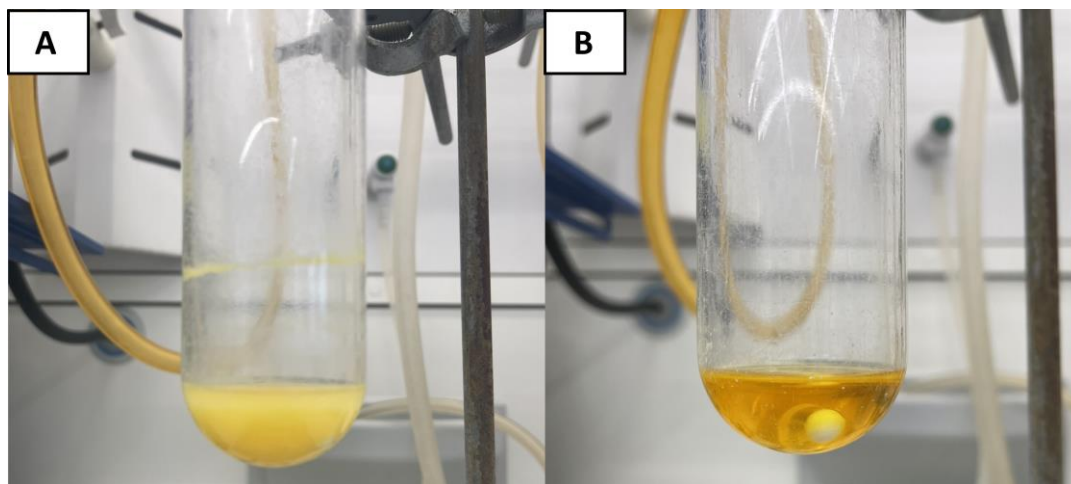


**Figure 12.** Synthesis of K<sub>2</sub>Zn(Bz)<sub>2</sub>(*Ot*Bu)<sub>2</sub> **8** (Bz = CH<sub>2</sub>Ph). A: Suspension of **8** in toluene displaying a light orange/yellow colour characteristic of benzylic metalation. B: Solution of **8** in THF displaying an orange colour characteristic of benzylic metalation.

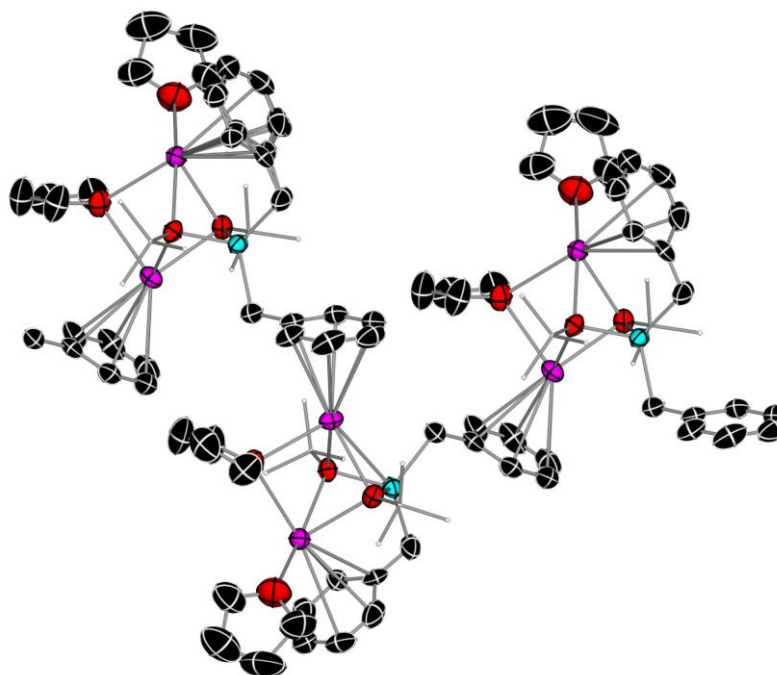
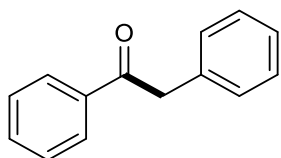


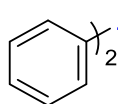
**Figure 13.** 2D polymeric fragment of **8** with displacement ellipsoids at 50% probability, all H atoms omitted and with C atoms in the alkoxide substituent drawn as wire frames for clarity. K...π interactions connect the monomeric units of **8** engaging in an h-6 fashion to a neighbouring arene moiety.

### 4.5.6 Synthesis of 1,2-diphenylethanone **9** via arylation of **8**



In an argon flushed Schlenk flask, Zn(TMP)<sub>2</sub> (1 mmol, 350 mg) and KO<sub>t</sub>Bu (2 mmol, 220 mg) were suspended in toluene (5 mL) at room temperature and left to stir for 24h at room temperature resulting in an orange suspension. All solvent removed under vacuum and the resulting solid dissolved in THF (5 mL). N-Methoxy-N-methylbenzamide (1.8 mmol, 0.27 mL) was subsequently added via syringe immediately forming a colourless solution which was stirred at ambient temperature for 2 hours. The reaction was quenched with H<sub>2</sub>O and extracted from aq. NH<sub>4</sub>Cl with EtOAc. The organics were collected, dried over MgSO<sub>4</sub> and concentrated in vacuo. Purified via silica column chromatography (Hexane:EtOAc 100:0 to 90:10) to produce **9** as a white crystalline solid (300 mg, 85%). NMR consistent with literature reports.<sup>67</sup> **<sup>1</sup>H-NMR (300.1 MHz, D<sub>8</sub>-THF, 298 K):** δ / ppm = 8.04 – 8.00 (m, 2H), 7.56 (tt, J = 7.3, 2.2 Hz, 1H), 7.51 – 7.38 (m, 2H), 7.38 – 7.24 (m, 5H), 4.29 (s, 2H).

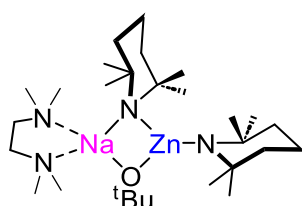
### 4.5.7 Synthesis of [K<sub>2</sub>Zn(Ph)<sub>2</sub>(OtBu)<sub>2</sub>] **10** (benzene zincation)



In an argon flushed Schlenk flask, Zn(TMP)<sub>2</sub> (1 mmol, 350 mg) and KO<sub>t</sub>Bu (2 mmol, 220 mg) were suspended in benzene (5 mL) at room temperature and left to stir for 24h. All solvent removed under vacuum and the resulting white solid washed with hexane (5 x 10 mL). All solvent removed under vacuum to afford K<sub>2</sub>Zn(Ph)<sub>2</sub>(OtBu)<sub>2</sub> **10** (400 mg, 91%). **<sup>1</sup>H-NMR (300.1 MHz, D<sub>8</sub>-THF, 298 K):** δ / ppm = 7.84 (br. m, 4H, 4 x Ar-H), 6.97 (br. m, 4H, 4 x Ar-H), 6.84 (br. m, 2H, 2 x Ar-H), 1.13 (s, 18H, CH<sub>3</sub>, 2 x OtBu). **<sup>13</sup>C{<sup>1</sup>H}-NMR (101 MHz, D<sub>8</sub>-THF, 298 K):** δ / ppm = 172.0 (s, 2 x C<sub>q</sub>-Zn), 140.9 (s, 2 x C-H), 126.0 (s, 2 x C-H), 123.4 (s, 2 x C<sub>q</sub>-Zn), 67.7 (s, C<sub>q</sub>-O, 2 x OtBu), 36.2 (s, CH<sub>3</sub>, 2 x OtBu). <sup>1</sup>H-DOSY NMR spectroscopic studies indicate the formation of a single molecular potassium zincate entity (THF)<sub>2</sub>K<sub>2</sub>Zn(Ph)<sub>2</sub>(OtBu)<sub>2</sub> **10** based on the independent diffusion coefficients of the chemical shifts in the <sup>1</sup>H NMR spectra representing the aryl moiety and the alkoxide fragment. (THF)<sub>n</sub>K<sub>2</sub>Zn(Ph)<sub>2</sub>(OtBu)<sub>2</sub> (**10**): *D* = 6.1x10<sup>-10</sup> m<sup>2</sup>s<sup>-1</sup>.

### 4.5.8 Synthesis of sodium zincates **11**, **12** and **13**

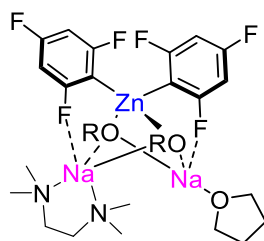
#### Synthesis of [(TMEDA)NaZn(TMP)<sub>2</sub>(OtBu)] **11**



To an argon flushed Schlenk flask, Zn(TMP)<sub>2</sub> (350 mg, 1 mmol) and NaOtBu (96 mg, 1 mmol) were suspended in hexane (5 mL). To this suspension was added TMEDA (0.15 mL, 1 mmol) and with gentle heating afforded a pale-yellow solution. The solution

was then stored at -30 °C overnight affording a colourless crop of crystals – compound **11**. Yield 350 mg, 60%. <sup>1</sup>H-NMR (300.1 MHz, D<sub>8</sub>-THF, 298 K): δ / ppm = 2.30 (s, 4H, 2 x CH<sub>2</sub>, TMEDA), 2.19 (s, 12H, 4 x NMe, TMEDA), 1.67 (m, 4H, 2 x γ-CH<sub>2</sub>, TMP), 1.32 (m, 8H, β-CH<sub>2</sub>, 2 x TMP) 1.22 (s, 24 H, 8 x CH<sub>3</sub>, 2x TMP), 1.03 (s, 9H, CH<sub>3</sub>, OtBu). <sup>13</sup>C{<sup>1</sup>H}-NMR (101 MHz, D<sub>8</sub>-THF, 298 K): δ / ppm = 66.3 (s, C<sub>q</sub>-O, OtBu), 58.7 (s, C<sub>q</sub>-N, 2 x TMP), 46.0 (s, β-CH<sub>2</sub>, 2 x TMP), 36.1 (s, CH<sub>3</sub>, OtBu), 39.8 (s, CH<sub>3</sub>, 2x TMP), 19.7 (s, γ-CH<sub>2</sub>, 2 x TMP).

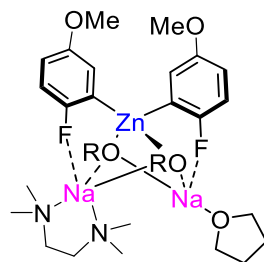
#### Synthesis of (TMEDA)(THF)Na<sub>2</sub>Zn(C<sub>6</sub>F<sub>3</sub>H<sub>2</sub>)<sub>2</sub>(OtBu)<sub>2</sub> **12**



To an argon flushed Schlenk flask, Zn(TMP)<sub>2</sub> (350 mg, 1 mmol) and NaOtBu (192 mg, 2 mmol) were dissolved in THF (5 mL). To this solution was added 1,3,5-trifluorobenzene (0.2 mL, 2 mmol) and stirred at room temperature for 2 hours. All solvent was removed in vacuo, and the resulting white solid was suspended in hexane (5 mL).

Gentle heating with the addition of TMEDA (0.3 mL, 2 mmol) and toluene afforded a pale-yellow solution. The solution was then stored at -30 °C overnight affording a colourless crop of crystals – compound **12**. Yield 100 mg, 14%. <sup>1</sup>H-NMR (300.1 MHz, D<sub>8</sub>-THF, 298 K): δ / ppm = 6.32-6.20 (2 x m, 4H, Ar-H), 2.24 (s, 4H, 2 x CH<sub>2</sub>, TMEDA), 2.09 (s, 12H, 4 x NMe, TMEDA), 1.03 (s, 9H, CH<sub>3</sub>, OtBu), 0.96 (s, 9H, CH<sub>3</sub>, OtBu). <sup>19</sup>F{<sup>1</sup>H}-NMR (D<sub>8</sub>-THF, 298 K): δ / ppm = -86.1 (s, 2F), -88.1 (s, 2F), -119.2 (s, 1F), -119.5 (s, 1F).

#### Synthesis of (TMEDA)(THF)Na<sub>2</sub>Zn(p-OMe-C<sub>6</sub>H<sub>3</sub>F)<sub>2</sub>(OtBu)<sub>2</sub> **13**



To an argon flushed Schlenk flask, Zn(TMP)<sub>2</sub> (180 mg, 0.5 mmol) and NaOtBu (96 mg, 1 mmol) were dissolved in THF (5 mL). To this solution was added 4-fluoroanisole (0.11 mL, 1 mmol) and stirred at room temperature for 2 hours. All solvent was removed in vacuo, and the resulting white solid was suspended in hexane (5 mL). Gentle heating with the addition of TMEDA (0.15 mL, 1 mmol) and toluene

afforded a pale-yellow solution. The solution was then stored at -30 °C overnight affording a colourless crop of crystals – compound **13**. Yield 150 mg, 38%.



## 4.6 References

- 1 S. Purser, P. R. Moore, S. Swallow and V. Gouverneur, *Chem. Soc. Rev.*, 2008, **37**, 320–330.
- 2 J. Wang, M. Sánchez-Roselló, J. L. Aceña, C. Del Pozo, A. E. Sorochinsky, S. Fustero, V. A. Soloshonok and H. Liu, *Chem. Rev.*, 2014, **114**, 2432–2506.
- 3 O. Eisenstein, J. Milani and R. N. Perutz, *Chem. Rev.*, 2017, **117**, 8710–8753.
- 4 K. Müller, C. Faeh and F. Diederich, *Science*, 2007, **317**, 1881–1886.
- 5 W. K. Hagmann, *J. Med. Chem.*, 2008, **51**, 4359–4369.
- 6 X. H. Xu, G. M. Yao, Y. M. Li, J. H. Lu, C. J. Lin, X. Wang and C. H. Kong, *J. Nat. Prod.*, 2003, **66**, 285–288.
- 7 R. D. Howells and H. Gilman, *Tetrahedron Lett.*, 1974, **15**, 1319–1320.
- 8 M. Schlosser, L. Guio and F. Leroux, *J. Am. Chem. Soc.*, 2001, **123**, 3822–3823.
- 9 A. Hess, N. Alandini, H. C. Guelen, J. P. Prohaska and P. Knochel, *Chem. Commun.*, 2022, **58**, 8774–8777.
- 10 A. Hess, N. Alandini, Y. C. Guersoy and P. Knochel, *Angew. Chem. Int. Ed.*, , DOI:10.1002/anie.202206176.
- 11 M. Mosrin and P. Knochel, *Org. Lett.*, 2009, **11**, 1837–1840.
- 12 B. Haag, M. Mosrin, H. Ila, V. Malakhov and P. Knochel, *Angew. Chem. Int. Ed.*, 2011, **50**, 9794–9824.
- 13 S. H. Wunderlich and P. Knochel, *Angew. Chem. Int. Ed.*, 2007, **46**, 7685–7688.
- 14 P. García-Álvarez, D. V. Graham, E. Hevia, A. R. Kennedy, J. Klett, R. E. Mulvey, C. T. O’Hara and S. Weatherstone, *Angew. Chemie*, 2008, **120**, 8199–8201.
- 15 R. Neufeld, T. L. Teuteberg, R. Herbst-Irmer, R. A. Mata and D. Stalke, *J. Am. Chem. Soc.*, 2016, **138**, 4796–4806.
- 16 A. Kremsmair, A. S. Sunagatullina, L. J. Bole, P. Mastropierro, S. Graßl, H. R. Wilke, E. Godineau, E. Hevia and P. Knochel, *Angew. Chem. Int. Ed.*, 2022, **61**, 3–9.
- 17 R. McLellan, M. Uzelac, A. R. Kennedy, E. Hevia and R. E. Mulvey, *Angew. Chem. Int. Ed.*, 2017, **56**, 9566–9570.
- 18 M. Uzelac and R. E. Mulvey, *Chem. Eur. J.*, 2018, **24**, 7786–7793.



- 19 M. Uzelac, A. R. Kennedy and E. Hevia, *Inorg. Chem.*, 2017, **56**, 8615–8626.
- 20 L. J. Bole, A. Tortajada and E. Hevia, *Angew. Chemie*, ,  
DOI:10.1002/ange.202204262.
- 21 P. Mastropierro, A. R. Kennedy and E. Hevia, *Chem. Commun.*, 2022, **58**, 5292–5295.
- 22 W. Clegg, S. H. Dale, D. V. Graham, R. W. Harrington, E. Hevia, L. M. Hogg, A. R. Kennedy and R. E. Mulvey, *Chem. Commun.*, 2007, 1641–1643.
- 23 M. Garçon, N. W. Mun, A. J. P. White and M. R. Crimmin, *Angew. Chem. Int. Ed.*, 2021, **60**, 6145–6153.
- 24 J. Spielmann, D. Piesik, B. Wittkamp, G. Jansen and S. Harder, *Chem. Commun.*, 2009, 3455–3456.
- 25 M. Balkenhohl, D. S. Ziegler, A. Desaintjean, L. J. Bole, A. R. Kennedy, E. Hevia and P. Knochel, *Angew. Chem. Int. Ed.*, 2019, **58**, 12898–12902.
- 26 D. S. Ziegler, K. Karaghiosoff and P. Knochel, *Angew. Chem. Int. Ed.*, 2018, **57**, 6701–6704.
- 27 A. Desaintjean, T. Haupt, L. J. Bole, N. R. Judge, E. Hevia and P. Knochel, *Angew. Chem. Int. Ed.*, 2021, **60**, 1513–1518.
- 28 L. J. Bole, N. R. Judge and E. Hevia, *Angew. Chem. Int. Ed.*, 2021, **60**, 7626–7631.
- 29 N. R. Judge, L. J. Bole and E. Hevia, *Chem. – A Eur. J.*, 2022, **28**, 1–8.
- 30 T. X. Gentner and R. E. Mulvey, *Angew. Chem. Int. Ed.*, 2021, **60**, 9247–9262.
- 31 M. L. Hlavinka and J. R. Hagadorn, *Organometallics*, 2007, **26**, 4105–4108.
- 32 D. R. Armstrong, A. M. Drummond, L. Balloch, D. V. Graham, E. Hevia and A. R. Kennedy, *Organometallics*, 2008, **27**, 5860–5866.
- 33 D. Huang, D. Olivieri, Y. Sun, P. Zhang and T. R. Newhouse, *J. Am. Chem. Soc.*, 2019, **141**, 16249–16254.
- 34 P. Zhang, J. Wang, Z. R. Robertson and T. R. Newhouse, *Angew. Chem. Int. Ed.*, ,  
DOI:10.1002/anie.202200602.
- 35 F. H. Lutter, L. Grokenberger, L. A. Perego, D. Broggini, S. Lemaire, S. Wagschal and P. Knochel, *Nat. Commun.*, 2020, **11**, 1–8.
- 36 T. Ahrens, J. Kohlmann, M. Ahrens and T. Braun, *Chem. Rev.*, 2015, **115**, 931–972.

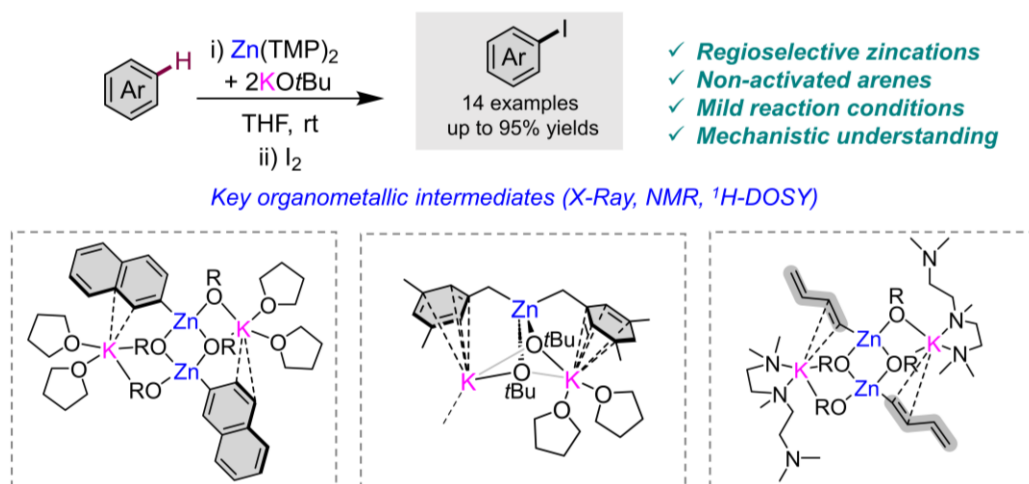
- 37 L. Gupta, A. C. Hoepker, K. J. Singh, D. B. Collum and C. U. V, *J. Org. Chem.*, 2009, **74**, 2231–2233.
- 38 K. Shen, Y. Fu, J. N. Li, L. Liu and Q. X. Guo, *Tetrahedron*, 2007, **63**, 1568–1576.
- 39 M. Uchiyama, M. Koike, M. Kameda, Y. Kondo and T. Sakamoto, *J. Am. Chem. Soc.*, 1996, **118**, 8733–8734.
- 40 M. Dell’Aera, F. M. Perna, P. Vitale, A. Altomare, A. Palmieri, L. C. H. Maddock, L. J. Bole, A. R. Kennedy, E. Hevia and V. Capriati, *Chem. Eur. J.*, 2020, **26**, 8742–8748.
- 41 L. C. McCann and M. G. Organ, *Angew. Chemie*, 2014, **126**, 4475–4478.
- 42 T. Bresser, M. Mosrin, G. Monzon and P. Knochel, *J. Org. Chem.*, 2010, **75**, 4686–4695.
- 43 D. T. Hurd, *J. Org. Chem.*, 1948, **13**, 711–713.
- 44 L. Brieger, T. Schrimpf, R. Scheel, C. Unkelbach and C. Strohmann, *Chem. – A Eur. J.*, , DOI:10.1002/chem.202202660.
- 45 H. R. L. Barley, W. Clegg, S. H. Dale, E. Hevia, G. W. Honeyman, A. R. Kennedy and R. E. Mulvey, *Angew. Chem. Int. Ed.*, 2005, **44**, 6018–6021.
- 46 P. C. Andrikopoulos, D. R. Armstrong, H. R. L. Barley, W. Clegg, S. H. Dale, E. Hevia, G. W. Honeyman, A. R. Kennedy and R. E. Mulvey, *J. Am. Chem. Soc.*, 2005, **127**, 6184–6185.
- 47 R. E. Mulvey, *Acc. Chem. Res.*, 2009, **42**, 743–755.
- 48 R. E. Mulvey, F. Mongin, M. Uchiyama and Y. Kondo, *Angew. Chem. Int. Ed.*, 2007, **46**, 3802–3824.
- 49 S. D. Robertson, M. Uzelac and R. E. Mulvey, *Chem. Rev.*, 2019, **119**, 8332–8405.
- 50 R. Neufeld and D. Stalke, *Chem. Sci.*, 2015, **6**, 3354–3364.
- 51 A. A. Kremsmair, A. S. Sunagatullina, J. Leonie, P. Mastropierro, S. Graßl, H. R. Wilke, E. Godineau, E. Hevia and P. Knochel, , DOI:10.1002/anie.202210491.
- 52 P. García-Úlvarez, R. E. Mulvey and J. A. Parkinson, *Angew. Chem. Int. Ed.*, 2011, **50**, 9668–9671.
- 53 M. Uchiyama, T. Miyoshi, Y. Kajihara, T. Sakamoto, Y. Otani, T. Ohwada and Y. Kondo, *J. Am. Chem. Soc.*, 2002, **124**, 8514–8515.

- 54 M. Uchiyama, Y. Kobayashi, T. Furuyama, S. Nakamura, Y. Kajihara, T. Miyoshi, T. Sakamoto, Y. Kondo and K. Morokuma, *J. Am. Chem. Soc.*, 2008, **130**, 472–480.
- 55 D. R. Armstrong, L. Balloch, W. Clegg, S. H. Dale, P. García-Álvarez, E. Hevia, L. M. Hogg, A. R. Kennedy, R. E. Mulvey and C. T. O'Hara, *Angew. Chem. Int. Ed.*, 2009, **48**, 8675–8678.
- 56 P. Fleming and D. F. O Shea, *J. Am. Chem. Soc.*, 2011, **133**, 1698–1701.
- 57 G. Katsoulos, S. Takagishi and M. Schlosser, *Synlett*, 1991, **1991**, 731–732.
- 58 V. Snieckus, *Chem. Rev.*, 1990, **90**, 879–933.
- 59 A. J. Martínez-Martínez, A. R. Kennedy, R. E. Mulvey and C. T. O'Hara, *Science*, 2014, **346**, 834–837.
- 60 T. Tatic, S. Hermann, M. John, A. Loquet, A. Lange and D. Stalke, *Angew. Chem. Int. Ed.*, 2011, **50**, 6666–6669.
- 61 W. Clegg, G. C. Forbes, A. R. Kennedy, R. E. Mulvey and S. T. Liddle, *Chem. Commun.*, 2003, **3**, 406–407.
- 62 T. X. Gentner, A. R. Kennedy, E. Hevia and R. E. Mulvey, *ChemCatChem*, 2021, **13**, 2371–2378.
- 63 D. B. Pardue, S. J. Gustafson, R. A. Periana, D. H. Ess and T. R. Cundari, *Comput. Theor. Chem.*, 2013, **1019**, 85–93.
- 64 E. Masson and M. Schlosser, *European J. Org. Chem.*, 2005, 4401–4405.
- 65 J. Albarrán-Velo, V. Gotor-Fernández and I. Lavandera, *Adv. Synth. Catal.*, 2021, **363**, 4096–4108.
- 66 X. Zhu, C. Liu, Y. Liu, H. Yang and H. Fu, *Chem. Commun.*, 2020, **56**, 12443–12446.
- 67 D. Anderson, A. Tortajada and E. Hevia, *Angew. Chemie*, 2023, e**202218498**, 1–10.

## Chapter 5: Zincation of Non-Activated Arenes with an Alkoxide Powered Zn(TMP)<sub>2</sub> Base

This Chapter was adapted from a manuscript prepared for publication:

“Combining Two Relatively Weak Bases (Zn(TMP)<sub>2</sub> and KOtBu) for the Regioselective Metalation of Non-Activated Arenes and Heteroarenes”, N. R. Judge and E. Hevia, *Chem. Sci.*, **2024**, Accepted Manuscript. DOI: <https://doi.org/10.1039/D4SC03892D>



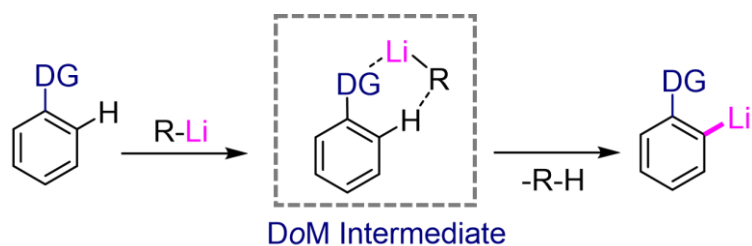
Contributing authors to the manuscript and their role:

Neil Judge: Designed and performed all experimental work, analysed and processed all data, wrote the first draft of the manuscript and the supporting information.

Eva Hevia: Principal Investigator, conceived the project, secured the funding, directed the work, and wrote the final version of the manuscript with contributions from all authors.

### 5.1 Introduction

Directed-*ortho* metalation (DoM) constitutes one of the most powerful and widely used methodology in synthesis for the regioselective functionalisation of aromatic rings.<sup>1,2</sup> The regioselectivity and efficiency of such deprotonations is favoured by the presence of directing functional groups *ortho*-located to the C-H bond that undergoes metalation.<sup>3,4</sup> A dual activating effect has been noted. Electron withdrawing directing groups (DGs) enhance the acidity of their vicinal *ortho*-H's but, in addition, the DG provides a coordination site for the metalating reagent which directs the *ortho*-regioselectivity of the process (Scheme 1).<sup>5-7</sup>



**Scheme 1.** Proposed mechanism of Directed *ortho* Metalation (DoM)

Contrasting the regioselective metalation of non-activated arenes lacking a directing group is significantly more challenging, frequently requiring the use of harsh reaction conditions and strong bases which often lead to low conversions and poor regioselectivities. This can be nicely illustrated for naphthalene, which possesses two equally non-activated sites for metalation with similar acidities in terms of pK<sub>a</sub> values (43.4 and 43.8 for C1 and C2 sites respectively).<sup>8</sup> Employing *n*BuLi, Gilman has reported low conversions (up to 20%) of a mixture of C1- and C2-lithiated isomers in a 2.5:1 ratio respectively.<sup>3</sup> The difficulties in controlling the selectivity in this reaction was further emphasised by Schlosser when employing a threefold excess of the bimetallic LICKOR, *n*BuLi·KO*t*Bu, superbasic combination which led to a complex mixture of twelve different isomers of mono- and di-metalation in an overall moderate yield (53%).<sup>9</sup>

Breaking new ground in this field, seminal work by Mulvey has demonstrated that using sodium zincate [(TMEDA)NaZn(TMP)*t*Bu<sub>2</sub>] as a bimetallic base made up by the combination of NaTMP (TMP= 2,2,6,6-tetramethylpiperidide) with Zn*t*Bu<sub>2</sub> allows for the direct C2 zincation of one equivalent of naphthalene forming [(TMEDA)NaZn(2-C<sub>10</sub>H<sub>7</sub>)(TMP)(*t*Bu)] under mild reaction conditions in a 50% yield.<sup>10</sup> Although, an iodine quench of an *in-situ* mixture shows this alkali-metal mediated zincation (AMMZn) of naphthalene is almost quantitative with an 83% yield of 2-iodonaphthalene observed (Figure 1). It's important to note that despite the molecular structure of this zincated intermediate containing a TMP group, suggesting alkyl basicity, subsequent theoretical studies by Uchiyama<sup>11</sup> and experimental studies by Hevia<sup>12</sup> demonstrated these type of dialkyl(amido)zincates actually exhibit amido basicity. An initial deprotonation of the arene by a reactive TMP group is followed by a subsequent deprotonation of the liberated TMP(H) in solution, re-incorporating the TMP anion back into the structure.

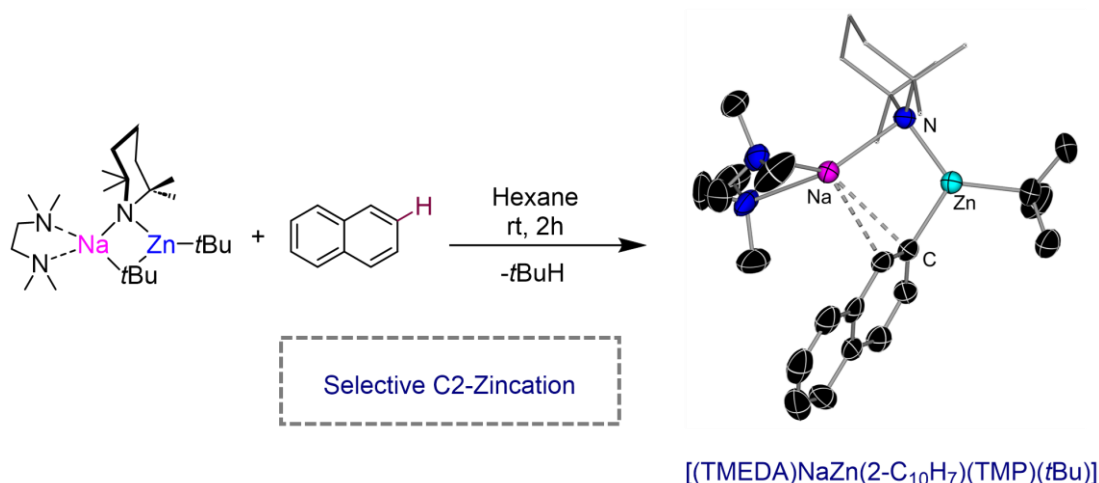


**Figure 1.** Selective C2 metalation of naphthalene using sodium zincate [(TMEDA)NaZn(TMP)*t*Bu<sub>2</sub>]<sup>10</sup>

O'Hara has subsequently developed an elegant bimetallic system for the selective dimagnesiumation of non-activated arenes using sodium magnesiate [Na<sub>4</sub>Mg<sub>2</sub>(TMP)<sub>6</sub>*n*Bu<sub>2</sub>] prepared by combining a 2:1 mixture of NaTMP and *n*Bu<sub>2</sub>Mg.<sup>2,13,14</sup> This base was found to effect the deprotonation of arenes via its alkyl substituents, in a templated manner, forming large macrocyclic structures in the solid state comprised of a multi-atom cationic skeleton of alternating metal and nitrogen atoms, centred around the deprotonated arene core. For example, **Scheme 2** showcases the molecular structure of {[Na<sub>4</sub>Mg<sub>2</sub>(TMP)<sub>6</sub>]<sub>2</sub>(1,4-biphenylene-di-ide)}, achieved from the unusual 1,4-dimagnesiumation of biphenylene by the aforementioned sodium magnesiate.<sup>14</sup> This striking arrangement of atoms around the 1,4-dimetallated arene is labelled as an *inverse crown complex*— so called because of its inverse topological arrangement to conventional crown ethers.<sup>15</sup> A similar 1,4- substitution pattern is also observed for the dimagnesiumation of naphthalene. Exploiting the power of this templated metalation, O'Hara extended this methodology to an array of non-activated arenes accessing a range of 1,4- and 3,5- dimagnesiumated products which could be subsequently quenched with iodine giving access to previously inaccessible multi-iodoarenes.

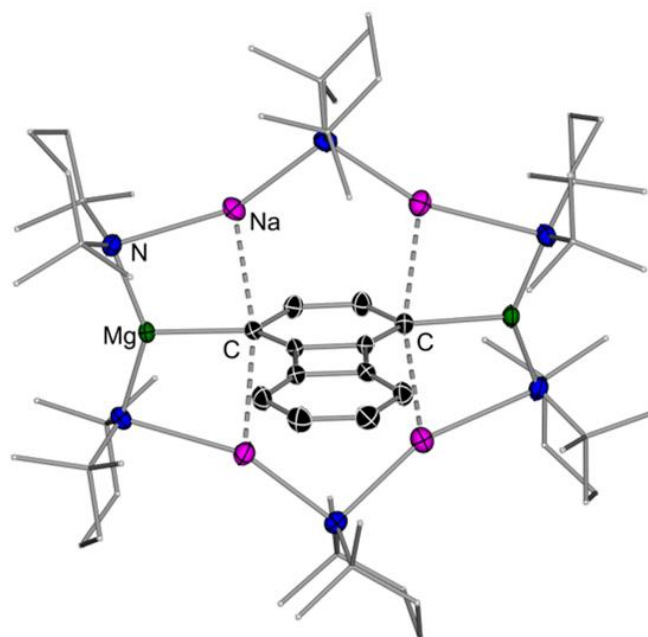


**Figure 2.** Molecular structure of {[Na<sub>4</sub>Mg<sub>2</sub>(TMP)<sub>6</sub>]<sub>2</sub>(1,4-biphenylene-di-ide)}

The above processes are described as sodium-mediated-metalations, with sodium being proposed to play a prominent role in coordinating naphthalene via pi-electrostatic interactions, favouring the low polarity metalation effected by Zn or Mg. However, recent studies from our group have also shown the potential of NaTMP as a monometallic base, in combination with the Lewis donor PMDETA and B(O*i*Pr)<sub>3</sub> as an *in situ* electrophilic partner to promote the regioselective and high yielding C2 borylation of naphthalene furnishing a sodium boronate species that can be subsequently used for Suzuki-Miyaura coupling reactions (see *Chapter 4, Scheme 3*).<sup>16</sup>

## 5.2 Aims

Having previously highlighted, in *Chapter 4*, the ability of Zn(TMP)<sub>2</sub>/2KO*t*Bu combinations to carry out the zincation of toluene and benzene under mild conditions, this *Chapter* aims to expand the synthetic potential of this mixed amido/alkoxy zincate for the regioselective zincation of non-activated substrates. Given its powerful reactivity, focus is also placed on the zincation of a range of sensitive heterocyclic molecules. Through isolation and characterisation of the metalated intermediates we aim to provide mechanistic detail into the mode of operation behind this potassium zincate and its ability to induce complex speciation upon reaction with aromatic substrates.

## 5.3 Results and Discussion

### 5.3.1 Reaction Optimisation for Regioselective Zincation of Naphthalene

We began our studies using naphthalene **1** as a model substrate assessing the selectivity and extent of metalation via an iodine quench after reaction with different bases in THF (Table 1). Unsurprisingly, Zn(TMP)<sub>2</sub> completely fails to promote any metalation of **1** in the absence of alkoxide additives with complete recovery of naphthalene observed even under refluxing conditions (entry 1). In stark contrast, the addition of one equivalent (entry 2) or two equivalents (entry 3) of KO<sup>*t*</sup>Bu led to the quantitative and selective C2-zincation of two equivalents of naphthalene in just two hours at room temperature as confirmed by electrophilic interception with iodine forming 2-iodonaphthalene **2a** in a 95% yield. As previously mentioned, the zincation of toluene and benzene using this system required the arene to be used as a solvent for quantitative zincation after 24h yet with naphthalene stoichiometric quantities can be used where both TMP groups are reactive towards Zn-H exchange in the C2 position. A dramatic alkali metal effect is observed using the lighter alkali metal tert-butoxide congeners, LiO<sup>*t*</sup>Bu (entry 4) or NaO<sup>*t*</sup>Bu (entry 5) which completely shuts down the reactivity of the bimetallic mixture towards **1** where no zincation is observed. This aligns well with recent studies by Mulvey which highlight the difference in reactivities between lithium and sodium and the heavier alkali metals in which the different degrees of metal cation- $\pi$  interactions have thought to be a key factor.<sup>17</sup> The softer and larger K centres in this case can be conceptualised as built in Lewis acidic centres which can  $\pi$ -engage with the naphthalene ring activating the substrate towards C-H zincation. Pardue has previously probed the benzylic deprotonation of toluene by alkali metal amides via DFT calculations concluding that the aforementioned cation- $\pi$  interactions facilitate the C-H bond scission finding where heaviest alkali metal Cs amide offers the lowest energy barrier for this transformation.<sup>18</sup> The importance of these K- $\pi$  interactions for successful zincation of naphthalene is demonstrated in entry 6 where the same reaction is carried out in the presence of two equivalents of 18-crown-6, which can sequester the K cations,<sup>19</sup> forming a solvent separated ion pair, coordinatively saturating the potassium centres and most likely precluding precoordination of the substrate, shutting down the zincation process. Using monometallic potassium amide KTMP also failed to promote the metalation of naphthalene in THF at room temperature (entry 7) highlighting the importance of a bimetallic system for this transformation.



**Table 1.** Screening of naphthalene (**1**) C2-zincation by different Zn(TMP)<sub>2</sub>/*n*AMOtBu combinations and subsequent iodine quench forming 2-iodonaphthalene (**2a**).

$\text{Zn(TMP)}_2 + n\text{AMOtBu} + 2$ 
 $\xrightarrow[\text{- 2 TMP(H)}]{\text{i) THF, rt, 2h; ii) I}_2 \text{ (5 e.q)}}$

$\text{AM} = \text{Li, Na, K}$ 
**1**
**2a**

Entry	Base	Yield <sup>[a]</sup> (%)
1	Zn(TMP) <sub>2</sub>	0 <sup>[b]</sup>
2	<b>Zn(TMP)<sub>2</sub> + KOtBu</b>	<b>&gt;95</b>
3	<b>Zn(TMP)<sub>2</sub> + 2KOtBu</b>	<b>&gt;95 (89)<sup>[c]</sup></b>
4	Zn(TMP) <sub>2</sub> + LiOtBu	0
5	Zn(TMP) <sub>2</sub> + NaOtBu	0
6	Zn(TMP) <sub>2</sub> + KOtBu + 2 (18-Crown-6)	0
7	KTMP	0
8	LiTMP + KOtBu	<5%
9	LiTMP + Zn(TMP) <sub>2</sub>	<5%
10	Zn(TMP) <sub>2</sub> ·2MgCl <sub>2</sub> ·2LiCl	<5%

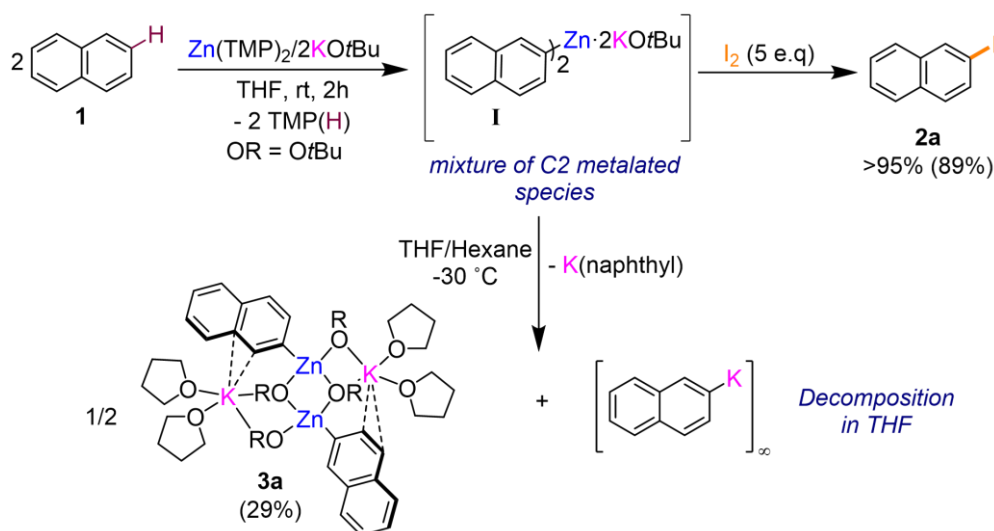
[a] Conversions determined by <sup>1</sup>H NMR using hexamethylbenzene as internal standard [b] Reaction refluxed for 2h [c] Isolated yield.

Interestingly it should also be noted that under these conditions other bimetallic bases which have previously show great promised for arene or benzylic metalation also fail to metalate naphthalene to any appreciable extent. This includes the LiNK reagent<sup>20</sup> (entry 8), Mongin's tandem LiTMP + Zn(TMP)<sub>2</sub> combination<sup>21</sup> (entry 9) and Knochel's powerful Turbo Hauser Zinc reagent Zn(TMP)<sub>2</sub>·2MgCl<sub>2</sub>·2LiCl<sup>22</sup> (entry 10). Highlighting the striking ability of our Zn(TMP)<sub>2</sub>/2KOtBu to deliver a regioselective C2 zincation of naphthalene after two hours at room temperature. The alkali metal effect observed in Table 1 is quite remarkable given the complete inactivity of the lighter alkali metal alkoxide congeners NaOtBu and LiOtBu. As discussed in *Chapter 4* both the Li and NaOtBu can activate Zn(TMP)<sub>2</sub> towards the deprotonation of 1,3,5-trifluorobenzene (see *Chapter 4*, Table 1) although reaction times are longer when compared with KOtBu. <sup>1</sup>H-DOSY NMR in d<sub>8</sub>-THF suggests, in both cases, the formation of a mixed amido/alkoxy zincate of the form (THF)<sub>x</sub>AMZn(TMP)<sub>2</sub>OtBu (AM = Li, Na) which in the case of Na has been structurally authenticated using PMDETA as a Lewis donor [(PMDETA)NaZn(TMP)<sub>2</sub>OtBu] (see *Chapter 4*, section 4.3.6). Hence the lack of reactivity observed cannot be attributed to unsuccessful co-complexation of the single metal components. These findings offer further support to the key role on the pre-coordination of the arene substrate to potassium via π-interactions is imperative to induce the zincation of the non-activated arenes. In line with our previous studies outlined in *Chapter 4*, only one equivalent of KOtBu is required to kinetically activate the Zn-N bonds in Zn(TMP)<sub>2</sub> towards the zincation

of naphthalene (Table 1, entry 2) although the use of two equivalents of alkoxide is preferred to favour the formation of more reactive higher order potassium zincates.

### 5.3.2 Solid and Solution State Complexity in the Zincation of Non-Activated Arenes

Based on our previous studies on the zincations of fluoroarenes (see *Chapter 4, section 4.3.2*), we assumed the formation of a higher order potassium zincate [K<sub>2</sub>Zn(Ar)<sub>2</sub>(OtBu)<sub>2</sub>] (**I**) (Scheme 2) as the metalated intermediate in the reaction between naphthalene and our favoured KZn(TMP)<sub>2</sub>(OtBu) + KOtBu (shortened to Zn(TMP)<sub>2</sub>/2KOtBu throughout) combination. Taking a closer look at this reaction, NMR spectroscopic studies in d<sub>8</sub>-THF of the reaction mixture showed the presence in solution of at least two different metalated naphthalenide species, indicating the formation of a more complex mixture of products than when fluoroarenes were employed (which form higher order potassium zincates of the form [K<sub>2</sub>Zn(Ar)<sub>2</sub>(OtBu)<sub>2</sub>], see *Chapter 4, Section 4.3.2*). Although the exact constitution of these aggregates could not be established by NMR methods, an iodine quench of this mixture affords the formation of 2-iodonaphthalene **2a** in an 89% isolated yield (Scheme 2) confirming the C2 regioselectivity of the metalation. Curiously, crystallisation attempts before electrophilic interception afforded the repeated isolation of a lower order potassium zincate [(THF)<sub>2</sub>KZn(2-C<sub>10</sub>H<sub>7</sub>)(OtBu)<sub>2</sub>]<sub>2</sub> (**3a**) in a 29% crystalline yield, which was characterised by X-Ray crystallography (Scheme 2 and Figure 3). Likely a product of a redistribution process, from a putative higher order intermediate [K<sub>2</sub>Zn(Ar)<sub>2</sub>(OtBu)<sub>2</sub>] (**I**), it seems the rational formation of **3a** would proceed with the concomitant formation of potassium naphthalenide as the corresponding disproportionation partner (Scheme 2). We previously reported a similar type of disproportionation of a lower order mixed aryl/alkoxy lithium magnesiate [LiMg(Ar)<sub>2</sub>(dmem)] (Ar = *o*-OMe-C<sub>6</sub>H<sub>4</sub>) into [ArMg(dmem)] and a potassium aryl moiety, although both products are monometallic in this case (see *Section 3.3.3*, in *Chapter 3*).<sup>23</sup> It should be noted that attempts to rationally access **3a** using [KZn(TMP)(OtBu)<sub>2</sub>] (prepared *in-situ* by treating [KZn(TMP)<sub>2</sub>(OtBu)] with one equivalent of *t*BuOH), showing that this potassium zincate cannot metalate naphthalene under the same conditions. Moreover, comparing the <sup>1</sup>H and <sup>13</sup>C NMR spectra of an isolated sample of **3a** with those obtained from the reaction mixture when naphthalene is treated with the Zn(TMP)<sub>2</sub>/KOtBu combination, it can be concluded that **3a** is not present amongst the C2 zincated species initially formed in the reaction mixture, offering further support to its formation being due to a redistribution process upon crystallisation. It should be noted that a mixture of C2 metalated species is also present using a 1:1 mixture of Zn(TMP)<sub>2</sub> and KOtBu, forming KZn(TMP)<sub>2</sub>(OtBu) as the base, and similar yields of **2a** are obtained from an iodine quench of this mixture.



**Scheme 2.** Proposed formation of potassium zincate  $[(\text{THF})_2\text{KZn}(2\text{-C}_{10}\text{H}_7)(\text{OrBu})_2]_2$  (**3a**) via deprotonation of two equivalents of naphthalene (**1**) and subsequent disproportionation of a putative higher order intermediate (**I**) with concomitant formation of potassium naphthalenide

Analysis of the filtrate after isolating crystalline **3a** confirmed the presence of TMP(H) and free naphthalene. The presence of naphthalene can be attributed to the decomposition of the proposed potassium aryl product of the redistribution process which generates **3a**, potassium naphthalenide, which can be expected to rapidly decompose in THF.<sup>24</sup> <sup>1</sup>H-NMR monitoring of the stability of a related potassium aryl, phenyl potassium (KPh), in *d*<sub>8</sub>-THF resulted in rapid decomposition of the potassium species releasing benzene as the by-product. Hence, a similar outcome would be expected for the stability of naphthalenide in THF. Given the thermal stability of the zincated products  $[\text{K}_2\text{Zn}(\text{Ar})_2(\text{OrBu})_2]$  discussed in *Chapter 4*, it is unlikely this presence of naphthalene results from the decomposition of a zincated naphthalenide unit as seen in **3a**. Thus, our working hypothesis is that lower order potassium zincate **3a** forms, as a crystallisation effect, in parallel with a potassium naphthalenide unit which subsequently decomposes in THF.

Potassium zincate **3a** was characterised by X-Ray crystallography (Figure 3). Featuring a centrosymmetric four-membered  $\{\text{ZnOZnO}\}$  unit **3a** exhibits a dimeric ladder motif in the solid state comprised of outer K-O rungs (K1-O1, 2.535 (3) Å) and inner Zn-O (Zn1-O2, 2.049 (2) Å) rungs. Completing the structure along the ladder edge, alkoxide groups bridge the K and Zn atoms and coordinative saturation of the K atoms is achieved by two THF molecules. A C2 metalated naphthalenide moiety resides terminal on Zn (Zn1-C9, 2.028(4) Å) completing the structure and confirming the regioselectivity of the metalation. Both K atoms form electrostatic  $\pi$ -interactions with two C atoms in the arene fragment. This structure can also be envisaged as two dinuclear  $\{\text{ZnOKO}\}$  rings which combine laterally via their Zn-O edges to generate this tetranuclear ladder. **3a** boasts a distinct C<sub>q</sub>-Zn signal at  $\delta = 163.0$  ppm in the <sup>13</sup>C NMR spectra which is in line with a similar chemical shift,  $\delta = 169.0$  ppm, that was

reported by Mulvey for the same signal in the aforementioned sodium zincate [(TMEDA)NaZn(2-C<sub>10</sub>H<sub>7</sub>)(TMP)(*t*Bu)] (Figure 1).<sup>10</sup> Indicative of C2 substituted naphthalene derivatives, **3a** exhibits a sharp singlet at 8.15 ppm in the <sup>1</sup>H NMR for the C<sub>1</sub>-H signal.

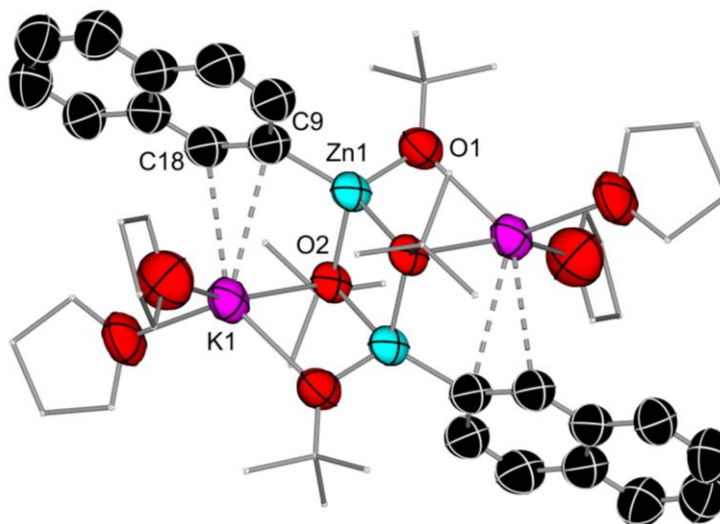


**Figure 3.** Molecular structure of [(THF)<sub>2</sub>KZn(2-C<sub>10</sub>H<sub>7</sub>)(*O**t*Bu)<sub>2</sub>]<sub>2</sub> (**3a**) with displacement ellipsoids at 50% probability, all H atoms omitted and with C atoms in the alkoxide substituent and THF molecules drawn as wire frames for clarity.

As previously discussed in *Chapter 4*, reaction of Zn(TMP)<sub>2</sub>/2KO*t*Bu in neat benzene afforded the formation of higher order potassium zincate [K<sub>2</sub>Zn(C<sub>6</sub>H<sub>5</sub>)<sub>2</sub>(*O**t*Bu)<sub>2</sub>] (**II**) (Figure 4), confirmed by <sup>1</sup>H, <sup>13</sup>C NMR and <sup>1</sup>H-DOSY NMR, which can be isolated in an almost quantitative yield as a white solid and is stable in d<sub>8</sub>-THF (see *Chapter 4*, **section 4.3.5**). However, taking [K<sub>2</sub>Zn(C<sub>6</sub>H<sub>5</sub>)<sub>2</sub>(*O**t*Bu)<sub>2</sub>] (**II**) in a hexane/THF mixture resulted in the elucidation of an almost identical metalated intermediate to **3a** forming dimeric [(THF)<sub>2</sub>KZn(C<sub>6</sub>H<sub>5</sub>)(*O**t*Bu)<sub>2</sub>]<sub>2</sub> (**3b**) in the solid state, confirmed by X-Ray crystallography, undergoing the same redistribution pathway observed with naphthalene (Figure 4). Whilst only isolated in a 23% crystalline yield, analysis of the filtrate of **3b** confirmed the presence of remnant [K<sub>2</sub>Zn(C<sub>6</sub>H<sub>5</sub>)<sub>2</sub>(*O**t*Bu)<sub>2</sub>] (**II**), that has not undergone full redistribution, and a substantial portion of benzene (from decomposition of KPh with THF). **3b** displays similar <sup>1</sup>H and <sup>13</sup>C NMR spectra to that previously reported for phenyl containing alkali-metal zincates such as [LiZnPh<sub>3</sub>]; with a distinct 2:2:1 ratio of aromatic signals, for the *ortho*, *meta* and *para*-H atoms at 7.89, 7.00 and 6.89 ppm respectively, of the zincated phenyl group and a characteristic signal at δ = 165 ppm in the <sup>13</sup>C NMR spectra for the *ipso* C<sub>q</sub>-Zn bond. Inspection of the molecular structure of **3b** (Figure 4) reveals an identical dimeric ladder motif to that found in **3a** (Figure 3) with similar Zn-C bond distances between the Zn centres and the terminal arene moieties in both structures: **3a**, Zn1-C9, 2.028(4) Å) and **3b** Zn1-C1, 2.033(15) Å).

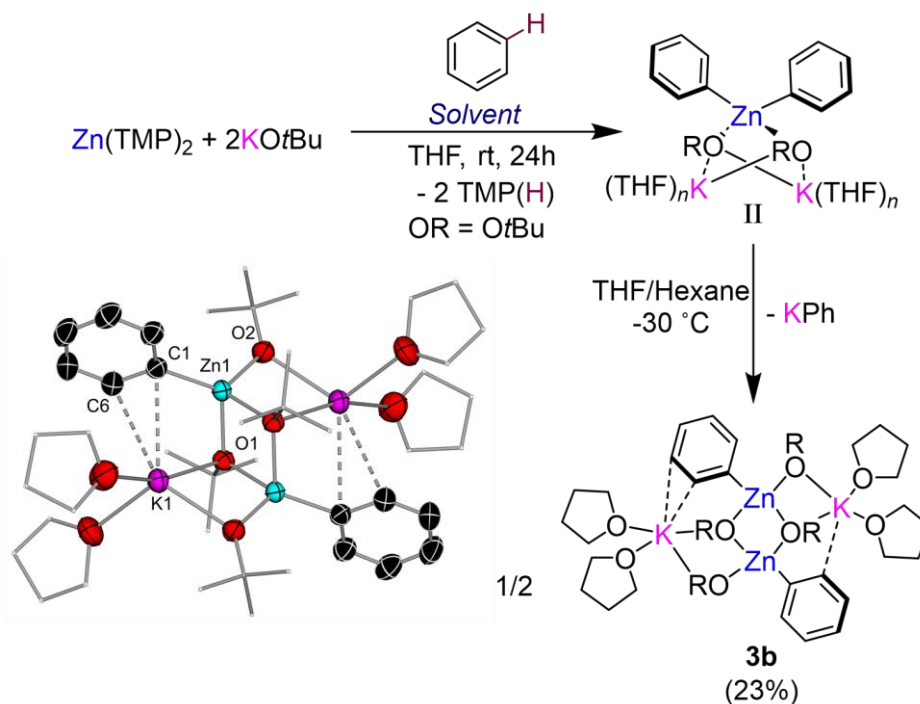


**Figure 4.** Formation of lower order potassium zincate **3b** via disproportionation of higher order potassium zincate **II**. Molecular structure of [(THF)<sub>2</sub>KZn(C<sub>6</sub>H<sub>5</sub>)(OtBu)<sub>2</sub>]<sub>2</sub> (**3b**) with displacement ellipsoids at 50% probability, all H atoms omitted and with C atoms in the alkoxide substituent and THF molecules drawn as wire frames for clarity

Comparison of the molecular structures of **3a** and **3b** with those of higher order potassium zincates [(THF)<sub>3</sub>K<sub>2</sub>Zn(Ar)<sub>2</sub>(OtBu)<sub>2</sub>] (Ar = fluoroaryl) (see Figure 2, Chapter 4) accessed from the deprotonation of two equivalents of a fluoroarene with Zn(TMP)<sub>2</sub>/2KOtBu, it seems apparent that the electrostatic K⋯F interactions contribute to the stability of these structures in the solid state. In the absence of an anchoring fluoro substituent, higher order zincates such as **(I)** (Scheme 2) are not stable in the solid state, hence redistribution of the organometallic products ensues forming dimeric lower order potassium zincates **3a** and **3b** in the solid state.

### 5.3.3 Regioselective Iodinations of Non-Activated Arenes via Alkoxide Mediated Zincations

Despite the complex solution and structural behaviour demonstrated for the zincation of naphthalene (**1**) by our Zn(TMP)<sub>2</sub>/2KOtBu mixture, treatment of the reaction mixture with an excess of iodine (5 equivalents) affords 2-iodonaphthalene (**2a**) in an 89% isolated yield (Figure 5) (quantitative by <sup>1</sup>H-NMR spectroscopy using an internal standard). As pointed out in the introduction to this Chapter, the regioselective metalation of naphthalene using conventional polar organometallic reagents, such as *n*BuLi or the LIC-KOR superbase, is challenging resulting in a mixture of products in poor yields. However, in this case, using commercially available starting materials Zn(TMP)<sub>2</sub> and KOtBu a facile C2 zincation of naphthalene is achieved under mild conditions (room temperature, 2h). Quantitative formation

of iodobenzene **2b** is achieved using longer reaction times to allow for the complete zincation of benzene which is used as a solvent in this case. Interestingly, a 50% yield of 2-iodoanthracene **2c** (42% isolated yield) could be obtained via the zincation of two equivalents of anthracene at room temperature after 2 hours. Direct deprotonative metalation and functionalisation of anthracene is extremely scarce and to the best of our knowledge the only example is from our group in which the arene is treated with the aforementioned NaTMP/B(OiPr)<sub>3</sub> combination and a subsequent Suzuki cross-coupling of the borylated product gave a 35% yield of the relevant *bis*-aryl compound.<sup>16</sup> Extension to other  $\pi$ -extended systems, such as pyrene, proved futile forming deep coloured NMR silent<sup>25</sup> solutions indicative of single electron transfer (SET) processes.<sup>26</sup> This perhaps explains the moderate yield of 2-iodoanthracene **2c** which also forms a deep orange solution upon reaction with Zn(TMP)<sub>2</sub>/2KO*t*Bu and treatment with iodine (which can behave as an oxidant)<sup>27</sup> leads to a 50% recovery of anthracene, suggesting a competing SET process. Compared with naphthalene, anthracene possesses a higher reduction potential presenting a more facile SET process which helps to explain why this competing reaction is not observed for arenes with lower reduction potentials.<sup>28</sup> Although KO*t*Bu is known to induce SET processes,<sup>29</sup> control reactions show the alkoxide alone is not capable of promoting these transformations.

Turning our attention to the antiaromatic compound biphenylene, out with the regioselective 1,4-dimagnesiumation reported from O'Hara (see **Figure 2**), synthetic protocols for the metalation of this arene are rare. The C1-lithiation is achieved using an excess of *t*BuLi (2.5 equivalents) however the reaction requires to be held at cryogenic temperatures for three days to achieve good yields.<sup>30</sup> Contrastingly, when two equivalents of biphenylene are reacted with Zn(TMP)<sub>2</sub>/2KO*t*Bu in THF at room temperature, a quantitative C1 zincation is achieved after 24h forming 1-iodobiphenylene **2d** in a 71% isolated yield after an iodine quench. In line with typical DoM type reactivity, Zn(TMP)<sub>2</sub>/2KO*t*Bu reacts smoothly with two equivalents of 2-methoxynaphthalene affording a 62% yield of 3-iodo-2-methoxynaphthalene **2e**, post electrophilic interception. Treatment of a mixture of Zn(TMP)<sub>2</sub>/2KO*t*Bu that had been left to stir at room temperature for 24h in neat trimethyl(phenyl)silane with iodine afforded a mixture of the corresponding *meta* and *para* substituted iodoarenes **2g** (1:1.5 *m:p* ratio respectively) in an overall 62% yield (Figure 5). The steric bulk of the silyl group precludes a regioselective *ortho* zincation leading to a mixture of isomers, although this is common for this substrate. Unfortunately, attempts to zincate quinoline were unsuccessful observing decomposition when carrying out the reaction at room temperature which is in line with our previous studies observing similar decomposition upon reactions with fluoropyridines or sensitive diazines (see **Chapter 4, section 4.3.3**). Zn(TMP)<sub>2</sub>/2KO*t*Bu failed to metalate other non-activated arenes such diphenylacetylene, 9-methylanthracene or 1,3,5-triphenylbenzene demonstrating some limitations of this combination.

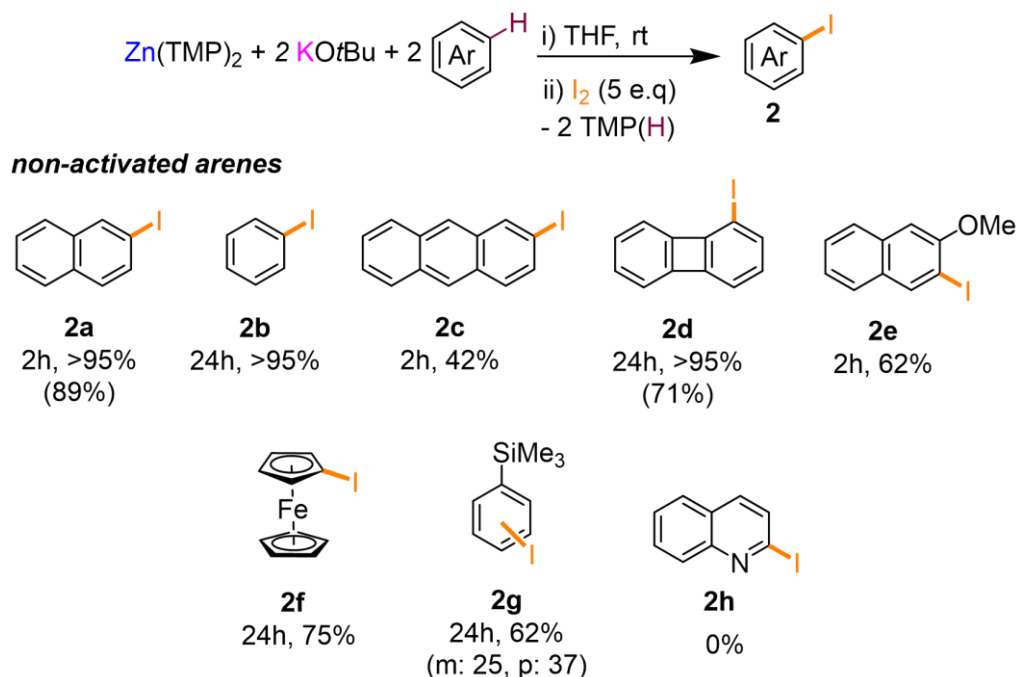


**Figure 5.** Scope of the C-H zincation and subsequent iodination of non-activated arenes using a 2:1 mixture of KO $t$ Bu/Zn(TMP)<sub>2</sub>. NMR yields for iodoarenes (**2a-2h**) determined by <sup>1</sup>H NMR spectroscopy using hexamethylbenzene as an internal standard and isolated yields shown in brackets.

The selective mono-metalation of ferrocene is challenging due to the propensity of the mono-metalated fragment to undergo a second metalation, a concept well known for the lithiation of ferrocene.<sup>31</sup> Mulvey and Hevia have demonstrated that alkali-metal zincates can deliver selective metalations of ferrocene and its derivatives including mono-zincation and even revealed the structure of a tetra-zincated ferrocene intermediate.<sup>32-35</sup> In line with these findings, 1-iodoferrocene **2f** can be isolated in a 75% yield after deprotonation of ferrocene with Zn(TMP)<sub>2</sub>/2KO $t$ Bu for 24h followed by iodination (Figure 5). However, trace amounts (<5%) of 1,1-diiodoferrocene were observed in the reaction mixture. Attempts to structurally characterise the metalated intermediate of this reaction, afforded the isolation of the alkoxide free lower order zincate [(THF)<sub>3</sub>KZn(Fc)<sub>3</sub>] (Fc = 1-ferrocenyl) (**4**) (Figure 6) in a poor crystalline yield of 18%. The central Zn centre lies in a distorted trigonal planar arrangement comprising three mono-zincated 1-ferrocenyl ligands. Two of these ferrocenyl ligands are deprotonated via their top Cp rings (Zn1-C2 and Zn1-C21) whereas the remaining ferrocenyl ligand is zincated on its bottom ring (Zn1-C11). The K atom lies above two of the ferrocenyl moieties of which it exhibits electrostatic  $\pi$  interactions in an  $\eta$ -<sup>2</sup> fashion holding the structure together as a contacted ion pair (CIP) potassium zincate. The K atoms find coordinative saturation from three THF molecules completing the structure. This structure closely resembles that of solvent separated ion pair (SSIP) [Li(THF)<sub>4</sub>]<sup>+</sup>[Zn(Fc)<sub>3</sub>]<sup>-</sup>, reported by Hevia and Mulvey, resulting from the deprotonation of ferrocene via lithium zincate [(TMEDA)LiZn(TMP)( $n$ Bu)<sub>2</sub>] and subsequent redistribution of the resulting product.

Similarly, **4** likely forms as a crystallisation effect via the redistribution of *in-situ* generated mixed ferrocenyl/alkoxy potassium zincates. Due to time constraints the exact mechanism of this redistribution has not been investigated thoroughly. Nevertheless, the structural authentication of **4** confirmed the regioselectivity of the ferrocene zincation by our Zn(TMP)<sub>2</sub>/2KOtBu mixture. Both **4** and [Li(THF)<sub>4</sub>]<sup>+</sup>[Zn(Fc)<sub>3</sub>]<sup>-</sup> display similar distinct C<sub>q</sub>-Zn signals at  $\delta = 86.5$  and 86.7 ppm in the <sup>13</sup>C NMR spectra respectively.

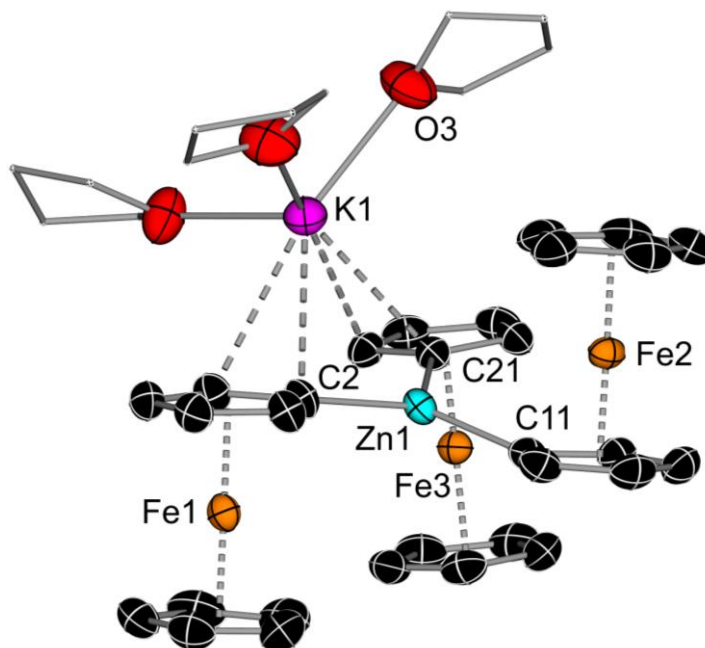


**Figure 6.** Molecular structure of [(THF)<sub>3</sub>KZn(Fc)<sub>3</sub>] (Fc = 1-ferrocenyl) (**4**) with displacement ellipsoids at 50% probability, all H atoms omitted and with C atoms in the THF molecules drawn as wire frames for clarity

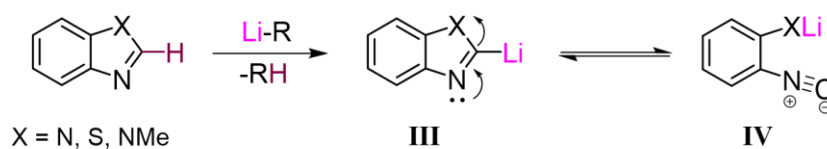
### 5.3.4 Investigations into the Zincation of 5-Membered Fused Heterocycles

Given the poor reactivity observed of our Zn(TMP)<sub>2</sub>/2KOtBu system towards sensitive heterocycles such as quinoline (*vide supra*), we explored the use of this base as a means to zincate a range of 5-membered fused heterocycles, attempting to expand the substrate scope (*vide infra*). Hetero-aromatic compounds, such as 1,3-azoles, are precious structural units in many biologically active pharmaceutical and agricultural compounds as well as a number of natural products.<sup>36–38</sup> The most commonly used synthetic methodology to functionalise these heterocycles to incorporate them into more complex organic frameworks is deprotonative metalation.<sup>39</sup> In general, metalation is achieved at the most acidic C2 site<sup>8</sup> of such heterocycles typically using conventional organolithium reagents at cryogenic temperatures.<sup>39</sup> However, such metalated 1,3-azoles (**III**) (Scheme 3a) are known to be unstable even under cryogenic conditions and are often in equilibrium with their cyano

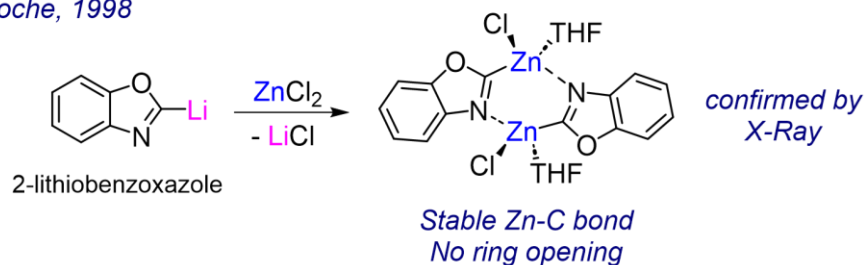


tautomers (**IV**) via a ring opening mechanism.<sup>40</sup> Thus, treatment of 2-lithio azoles with an electrophile (even at -78 °C) can often lead to a mixture of C2 and C4 substituted products (resulting from the reaction of the ring-opened enolate **IV** with the electrophile followed by its cyclization).<sup>40</sup> NMR spectroscopic and X-ray crystallographic studies have shown that metalated thiazoles and imidazoles tend to be more stable than oxazoles with the equilibrium lying toward the cyclic isomer (**III**).<sup>41</sup> Boche demonstrated the benefit of employing a less electropositive metal in these reactions by adding stoichiometric amounts of ZnCl<sub>2</sub> to 2-lithiobenzoxazole which led to the immediate cyclisation of the acyclic ring opened isomer forming 2-ZnCl-benzoxazole. This zincated heterocycle was characterised X-ray crystallography and theoretical calculations indicate formation of this isomer is thermodynamically more favourable than its acyclic congener.<sup>41</sup>

a) *Lithiation of 1,3-azoles*



b) *Boche, 1998*



**Scheme 3.** a) Equilibrium between C2-lithiated 1,3-azoles (**III**) and their ring opened isomers (**IV**) b) Formation of [2-ZnCl-benzoxazole] via 2-lithiobenzoxazole and ZnCl<sub>2</sub>

Hence, the use of less polar monometallic magnesium bases<sup>42</sup> or more sophisticated heterobimetallic magnesiates<sup>43</sup> and zincates<sup>22,44</sup> has allowed for the deprotonation and functionalisation of such heterocycles at room temperature. Particularly relevant to our studies is Mongin's bimetallic Li/Zn system combining 3 equivalents of LiTMP with (TMEDA)ZnCl<sub>2</sub> in THF. Initial reports suggested the formation of a lithium zincate [(TMEDA)LiZn(TMP)<sub>3</sub>] which is capable of chemoselectively functionalising many aromatic molecules in an improved manner compared to their monometallic counterparts, implying synergistic behaviour. However, detailed NMR spectroscopic studies by Mulvey, including <sup>1</sup>H-DOSY NMR, indicated the formation of a LiTMP·2LiCl adduct and Zn(TMP)<sub>2</sub> in d<sub>8</sub>-THF solutions have suggested that the formation of a *tris*-TMP lithium zincate is unlikely.<sup>45</sup> The current proposed *modus operandi* of this mixed metal base is a two-step tandem reaction involving an initial lithiation followed by stabilisation with a Zn species.<sup>46</sup> Mongin has used this mixture to carry out formal zincations and subsequent functionalisation of 5 membered heterocycles in varying

yields (17-73%) under mild conditions (room temperature, 2 hours).<sup>44</sup> However, this is not an entirely atom economical reaction as a three-fold excess of TMP is used with respect to the substrate.

It's important to note that in terms of pK<sub>a</sub> the 5-membered fused heterocyclic substrates (pK<sub>a</sub> range of approximately 24-38) discussed herein are significantly more activated than the non-activated substrates discussed in Figure 5. Thus, treatment of two equivalents of 1,3-benzoxazole with a 2:1 mixture of KO<sup>t</sup>Bu/Zn(TMP)<sub>2</sub> followed by iodination after 20 minutes at room temperature afforded the quantitative formation of 2-iodobenzoxazole (**5a**) (Figure 7). This methodology was successfully extended to the regioselective zincation of 1,3-benzothiazole, benzothiophene, benzofuran, 1-methylbenzo-imidazole, 1-methyl-1,2,4-triazole and caffeine forming the corresponding iodoarenes (**5b-5g**), after an electrophilic quench, in excellent yields from 81-96% (Figure 7). Compared to Mongin's tandem Li/Zn system, both TMP groups are active towards deprotonation of the heterocyclic substrates in this case, due to the formation of a reactive potassium zincate [KZn(TMP)<sub>2</sub>(O<sup>t</sup>Bu)].

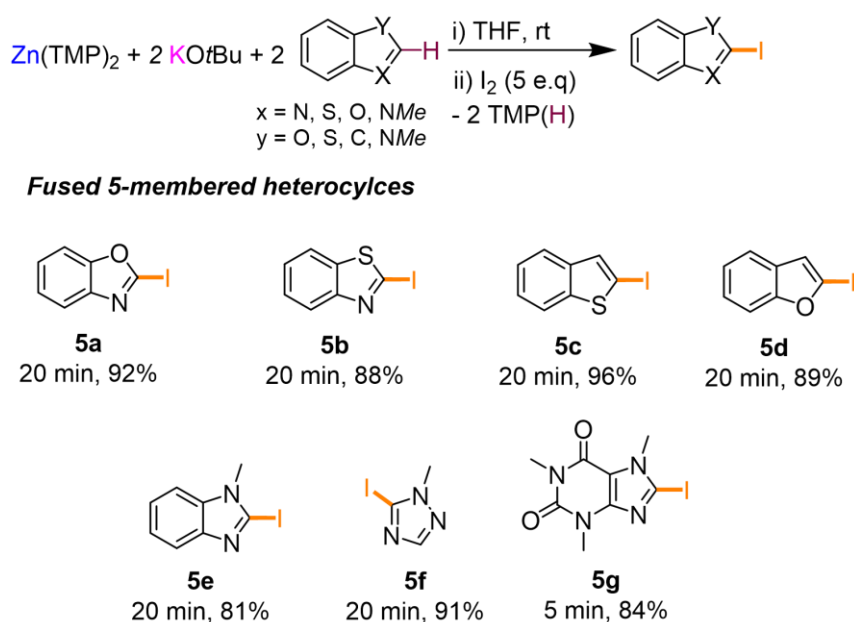


**Figure 7.** Scope of the C-H zincation and subsequent iodination of 5 membered fused heterocycles using a 2:1 mixture of KO<sup>t</sup>Bu/Zn(TMP)<sub>2</sub>. Isolated yields of iodoarenes (**5a-5g**).

Given the substrate dependence on the nature of the metalated products observed using Zn(TMP)<sub>2</sub>/2KO<sup>t</sup>Bu as a base, we looked to probe the constitution of the reaction with 1,3-benzoxazole prior to electrophilic interception. A crop of crystals from the reaction between two equivalents of 1,3-benzoxazole and Zn(TMP)<sub>2</sub>/2KO<sup>t</sup>Bu, analysed by X-ray crystallography and NMR spectroscopy, revealed the formation of lower order potassium zincate [(THF)<sub>2</sub>KZn(2-benzoxazolyl)(O<sup>t</sup>Bu)<sub>2</sub>] (**6**) (Figure 8a) in a 24% crystalline yield. This structure resembles an almost identical motif to that observed for **3a** and **3b** (Scheme 2). However, in this case <sup>1</sup>H-NMR monitoring of this reaction in d<sub>8</sub>-THF reveals the formation of

two distinct products: one which is assigned to potassium zincate **6** and one in which the aromatic signals closely resemble that of a ring opened benzoxazole fragment (Scheme 8c). Given our proposed mechanism for the formation of metalated products such as **6** which occurs with formation of a potassium aryl moiety, the second product observed by NMR was putatively assigned as the potassium phenolate **7** resulting from the ring opening of a 2-potassio-benzoxazole fragment. Independent synthesis of **7** was achieved via the deprotonation of 1,3-benzoxazole with potassium alkyl  $\text{K}(\text{CH}_2\text{SiMe}_3)$  and  $^1\text{H-NMR}$  suggested the presence of this acyclic product in the parent reaction mixture (Figure 8b and c). Despite the 1:1 mixture between potassium zincate **6** and potassium phenolate **7** in solution, treatment of this mixture with iodine affords the quantitative formation of 2-iodobenzoxazole **5a** (Figure 7) suggesting the electrophile reacts faster with zincate **6** than with **7** driving the equilibrium towards the C2 substituted isomer. Concomitant formation of **7** represents concrete evidence for the formation of potassium aryl moieties as the disproportionation partners to metalated intermediates **3a-b** and **6**.

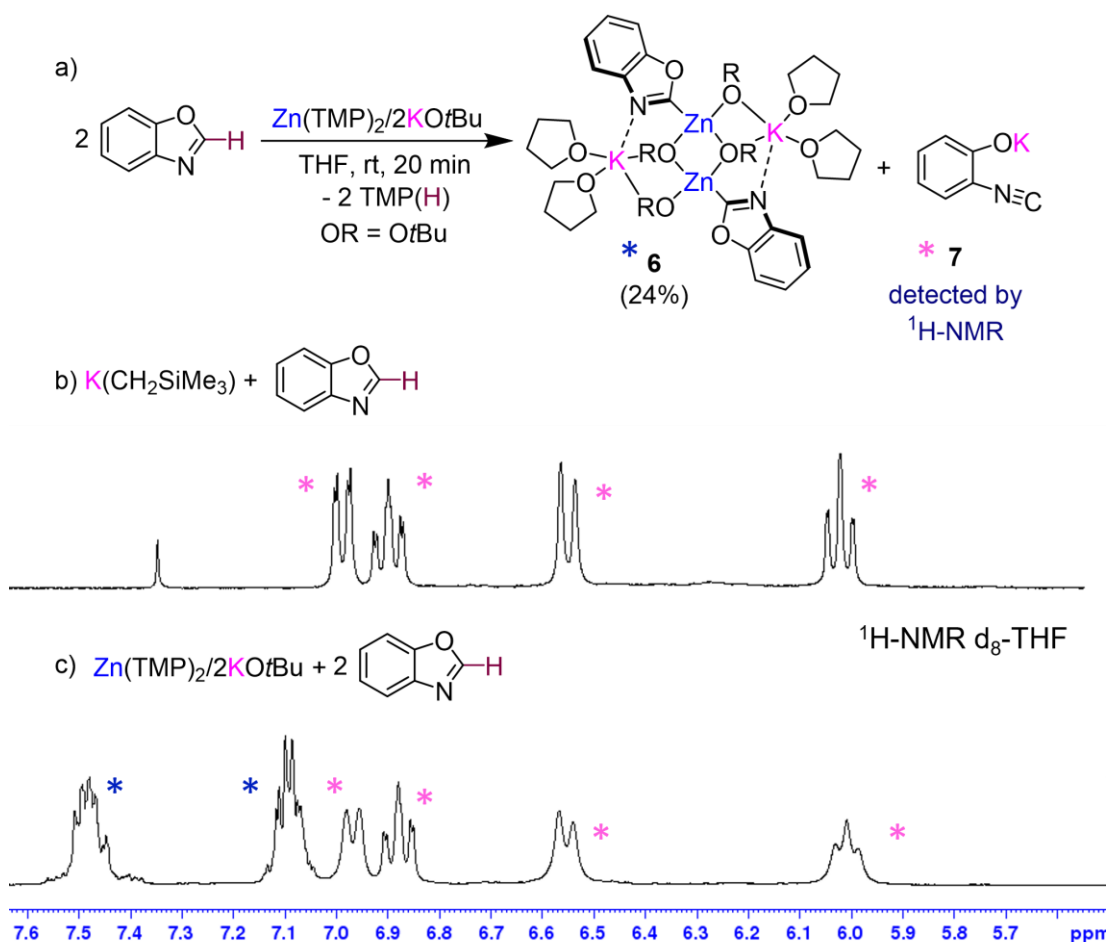


**Figure 8.** a) C-H zincation of 1,3-benzoxazole forming  $[(\text{THF})_2\text{KZn}(2\text{-benzoxazolyl})(\text{OtBu})_2]$  (**6**) with concomitant formation of potassium phenolate (**7**) b)  $^1\text{H-NMR}$  spectra of **7** in  $d_8\text{-THF}$  c) *in-situ*  $^1\text{H-NMR}$  spectra of the reaction between  $\text{Zn}(\text{TMP})_2/2\text{KOtBu}$  and two equivalents of 1,3-benzoxazole

The molecular structure of potassium zincate [(THF)<sub>2</sub>KZn(2-benzoxazolyl)(OtBu)<sub>2</sub>]<sub>2</sub> (**6**) was established by X-Ray crystallography (Figure 9). Featuring an identical central ladder motif to that of **3a** and **3b** (Figure 3 and 4), the structure of **6** differs mainly in the interactions between the metalated substrate molecule and the K atoms within the structure. A dative interaction between the N atom in the C2-zincated benzoxazole unit to the K atom on the end of the ladder rungs forms a striking 5 membered {KNCZNO} ring. The Zn1-C1 distance of 2.007(3) Å in **6** is similar to those reported for the Zn-C bonds in other zincated benzoxazole structures.<sup>41</sup> **6** also features a very distinct downfield C<sub>q</sub>-Zn signal at 198 ppm in the <sup>13</sup>C-NMR spectra.

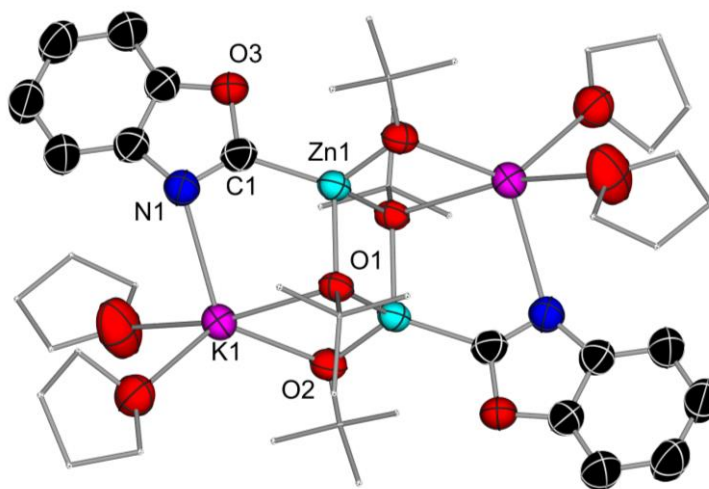
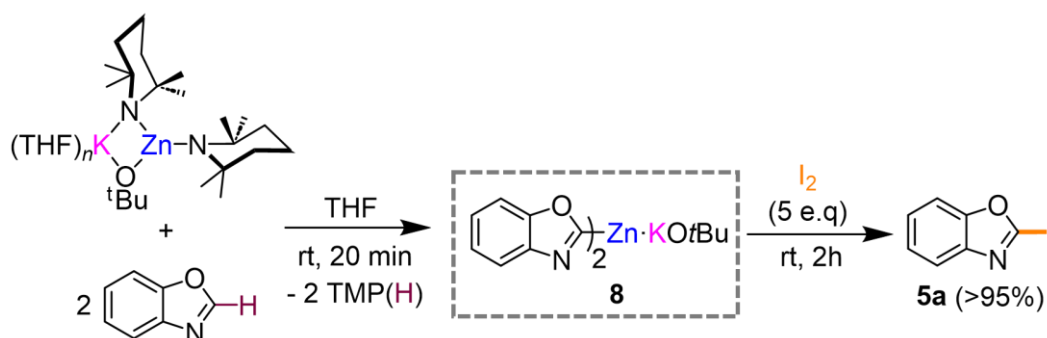


**Figure 9.** Molecular structure of [(THF)<sub>2</sub>KZn(2-benzoxazolyl)(OtBu)<sub>2</sub>]<sub>2</sub> (**6**) with displacement ellipsoids at 50% probability, all H atoms omitted and with C atoms in the alkoxide and THF molecules drawn as wire frames for clarity

Interestingly, using just one equivalent of KOtBu in combination with Zn(TMP)<sub>2</sub> (forming bimetallic base [KZn(TMP)<sub>2</sub>(OtBu)] *in-situ*, see Chapter 4 for its structure and full characterisation) precludes the formation of any ring opening product and NMR spectroscopy indicates the complete consumption of two equivalents of 1,3-benzoxazole likely forming a C2-zincated intermediate putatively assigned as [(THF)<sub>x</sub>KZn(2-benzoxazolyl)<sub>2</sub>(OtBu)] (**8**) (Scheme 4). <sup>1</sup>H-NMR monitoring of this reaction shows that the addition of [KZn(TMP)<sub>2</sub>(OtBu)] to a solution of two equivalents of 1,3-benzoxazole results in the complete disappearance of the downfield C(2)-H signal at 8.3 ppm with concomitant formation of two equivalents of TMP(H). Similar to the <sup>1</sup>H-NMR spectra of **6**, [(THF)<sub>x</sub>KZn(2-benzoxazolyl)<sub>2</sub>(OtBu)] (**8**) displays two multiplets at 7.5 ppm and 7.1 ppm which are distinctively different to the signals of the ring opened product **7**. Treatment of this mixture with iodine also affords the quantitative formation of 2-iodobenzoxazole **5a**. This is yet another example where simply changing the stoichiometry of the alkoxide additive used has a profound effect on the metalated intermediates formed in C-H zincations using Zn(TMP)<sub>2</sub>/*n*KOtBu (*n* = 1 or 2). However, it's important to note that using the more robust S

containing heterocycle, 1,3-benzothiazole, no ring opening products were observed using a 2:1 ratio of KO<sup>t</sup>Bu/Zn(TMP)<sub>2</sub>.



**Scheme 4.** Reaction of a 1:1 mixture of Zn(TMP)<sub>2</sub> and KO<sup>t</sup>Bu with two equivalents of 1,3-benzoxazole forming putative lower order potassium zincate **8** with subsequent formation of 2-iodobenzoxazole **5a** in a quantitative yield determined by <sup>1</sup>H-NMR using hexamethylbenzene as internal standard

### 5.3.5 Cleave and Capture Chemistry using Zn(TMP)<sub>2</sub>/2KO<sup>t</sup>Bu

Leaving a solution of Zn(TMP)<sub>2</sub>/2KO<sup>t</sup>Bu in d<sub>8</sub>-THF to stand at room temperature for 3 days was accompanied with a dramatic colour change from colourless to an intense bright purple solution. <sup>1</sup>H-NMR analysis of this solution indicated that all Zn-TMP signals had been converted to TMP(D), indicating a possible deprotonative metalation reaction between the zinc base and the THF solvent. Intrigued by this potential C-sp<sup>3</sup> metalation, our Zn(TMP)<sub>2</sub>/2KO<sup>t</sup>Bu combination was left to stir in protic THF over the course of three days giving a deep purple/black solution with a black deposit appearing on the Teflon stirrer bar. A work-up of this reaction in hexane with the addition of Lewis donor PMDETA afforded a colourless crop of crystals which was analysed by a combination of NMR spectroscopy and X-ray crystallography revealing potassium zincate [(PMDETA)KZn(C<sub>4</sub>H<sub>5</sub>)(O<sup>t</sup>Bu)<sub>2</sub>]<sub>2</sub> (**9**) (Figure 10) formed in a 37% crystalline yield. The molecular structure of **9** (Figure 10b) closely resembles the dimeric ladder motif described for potassium zincates **3a-b** (Figure 3 and 4) and **6** (Figure 9) however in this case an unexpected *s-trans*-1,3-butadiene (C<sub>4</sub>H<sub>5</sub><sup>-</sup>) fragment resides terminally on the Zn centre. Bond lengths within this chain (C18-C19, 1.351(3) Å; C19-C20, 1.467(3) Å; C20-C21, 1.315(3) Å) denote a localized double-bond, single bond, double bond pattern consistent with that in the parent diene.<sup>47</sup> The C<sub>4</sub> chain is connected to Zn through a Zn1-C18 σ bond (2.00(15) Å) and interacts with the K atom through π-type contacts via two of its C atoms (C18 and C19). The K atoms in **9** are then capped by two N donor atoms in PMDETA whilst the third N atom of the Lewis donor lies pendant.

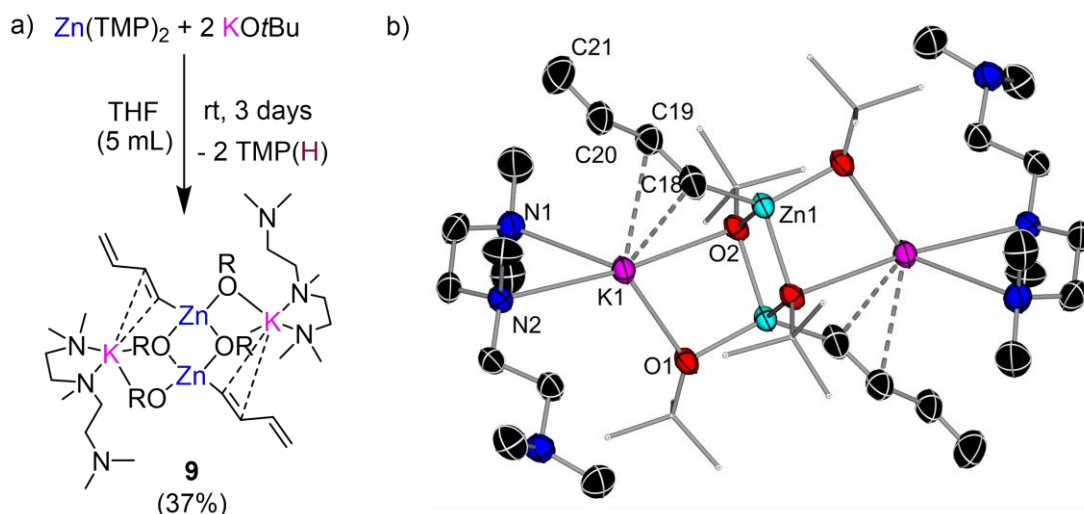
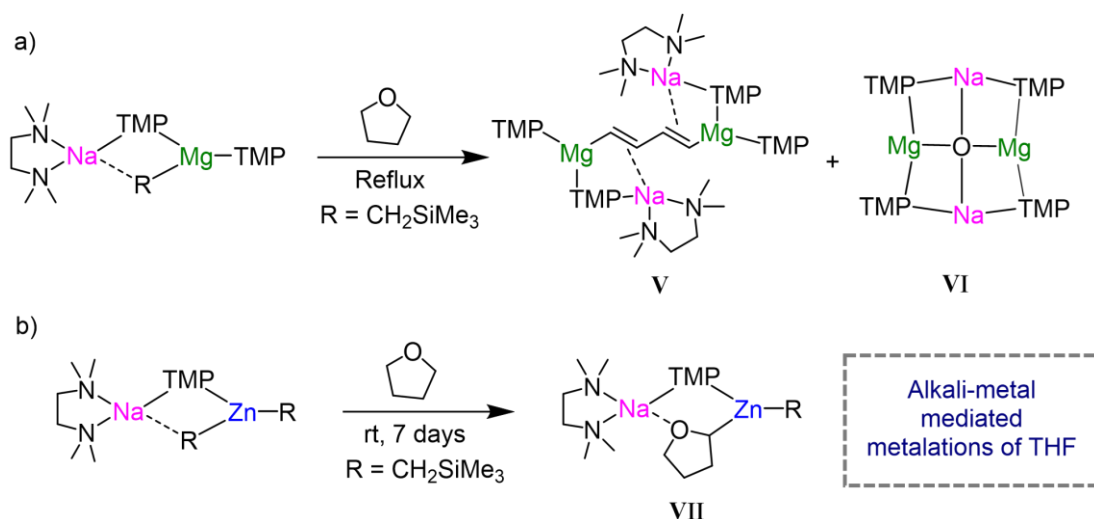


**Figure 10.** a) Reaction of  $\text{Zn}(\text{TMP})_2/2\text{KO}t\text{Bu}$  with excess THF forming  $[(\text{PMDETA})\text{KZn}(\text{C}_4\text{H}_5)(\text{O}t\text{Bu})_2]_2$  (**9**) b) Molecular structure of **9** with displacement ellipsoids at 50% probability, all H atoms omitted and with C atoms in the alkoxide fragment drawn as wire frames for clarity

This type of metalated butadiene fragment, formed as a result of a dramatic decomposition of THF in the presence of a strong base, has been previously reported by Mulvey in the form of a di-magnesiated 1,3-butadiene species (**V**) formed from the treatment of sodium magnesiate  $[(\text{TMEDA})\text{NaMg}(\text{TMP})_2\text{R}]$  ( $\text{R} = \text{CH}_2\text{SiMe}_3$ ) with one equivalent of THF in hexane (Scheme 5a).<sup>48</sup> In this case, the decapitated O atom from THF is trapped as an oxo dianion ( $\text{O}^{2-}$ ) within a mixed Na/Mg TMP inverse crown ether (**VI**). To quote Mulvey this reaction represents “chemical carnage” in which two C-O bonds and four C-H bonds are cleaved, completely destroying the heterocyclic THF molecule. A putative mechanism for the formation of (**V**) was proposed by the authors involving an initial  $\alpha, \alpha'$  magnesiation of THF leading to a build up of charge either side of the oxygen heteroatom which is subsequently expelled as an oxide inverse crown (**VI**). Subsequent intramolecular rearrangement of the C<sub>4</sub> chain and a two-fold deprotonation of the resulting butadiene fragment complete the proposed reaction sequence. Although the mechanism could not be fully disclosed for this transformation, carrying out the reaction with d<sub>8</sub>-THF and subsequent D<sup>2</sup>-NMR analysis unequivocally proved the butadiene fragment belonged to the parent THF molecule. Using a related sodium zincate, Mulvey also reported the  $\alpha$ -zincation of THF this time keeping the heterocycle intact forming heteroleptic sodium zincate  $[(\text{TMEDA})\text{NaZn}(\text{C}_5\text{H}_9\text{O})(\text{TMP})(\text{R})]$  ( $\text{R} = \text{CH}_2\text{SiMe}_3$ ) (**VII**) (Scheme 5b).



**Scheme 5.** a) Formation of dimagnesiated 1,3-butadiene **V** and inverse crown ether complex **VI** from reaction of  $[(\text{TMEDA})\text{NaMg}(\text{TMP})_2\text{R}]$  ( $\text{R} = \text{CH}_2\text{SiMe}_3$ ) with THF b)  $\alpha$ -zincation of THF forming sodium zincate **VII**

We propose that the formation of **9** could occur through an initial  $\alpha$ -zincation of THF, however attempts to intercept such a species have been unsuccessful so far. The mechanism in which this proposed metalated intermediate is then transformed into **9** remains unclear and is likely highly complex. The intense bright purple solution formed in this reaction is also highly indicative of a radical type process and Maercker cites many examples where radical species are involved in the cleavage of ethers using organo alkali-metal compounds.<sup>49</sup> On this note, the fate of the oxygen heteroatom remains a mystery at this stage and no inverse crown ether type complexes such as **VI** have been isolated from the reaction mixture indicating a different reaction mechanism for this transformation to that reported by Mulvey for the formation of dimagnesiated 1,3-butadiene **V**. Despite the surrounding unanswered questions around this seemingly chaotic reaction, it highlights the metalating power of the mixed amido/alkoxy  $\text{Zn}(\text{TMP})_2/\text{KO}t\text{Bu}$  system able to effect a challenging C-sp<sup>3</sup> metalation of a relatively inert C-H bond in THF.

Finally, we investigated the reaction between  $\text{Zn}(\text{TMP})_2/2\text{KO}t\text{Bu}$  and the sulphur containing cousin of THF, tetrahydrothiophene (THT). Simply changing the heteroatom on the saturated five membered ring led to the isolation of a remarkably different decomposition product forming dimeric lower order potassium zincate  $[(\text{PMDETA})\text{KZn}(\text{SMe})_2(\text{O}t\text{Bu})]_2$  (**10**) (Figure 11) after allowing a mixture of  $\text{Zn}(\text{TMP})_2/2\text{KO}t\text{Bu}$  to stir in excess THT for a week at room temperature. A close inspection of the molecular structure of **10** reveals a central Zn centre bonded to two methylene sulphide ( $\text{S-CH}_3$ ) groups ( $\text{Zn1-S1}$ , 2.3108(9) Å;  $\text{Zn1-S2}$ , 2.3003(9) Å) formed from what appears to be a complete destruction of the aliphatic THT ring. Exhibiting an incomplete double cubane motif, with a missing vertex in each cube, **10** closely resembles the structure described for mixed alkyl/alkoxy magnesiate of the form  $[\text{AMMgR}_2(\text{dmem})]$  ( $\text{AM} = \text{Na}, \text{K}$ ,  $\text{dmem} = \text{O}(\text{CH}_2)_2\text{NMe}(\text{CH}_2)_2\text{NMe}_2$ ) (see **Figure 4**, Chapter

2). **10** can also be described as inverse crowns,<sup>15,50–52</sup> comprising a cationic octagonal  $\{(KSZnS)\}_2^{2+}$  ring which hosts two alkoxide anions in its core. The K atom attains hexacoordination by the three N donor atoms in PMDETA, completing the structure.

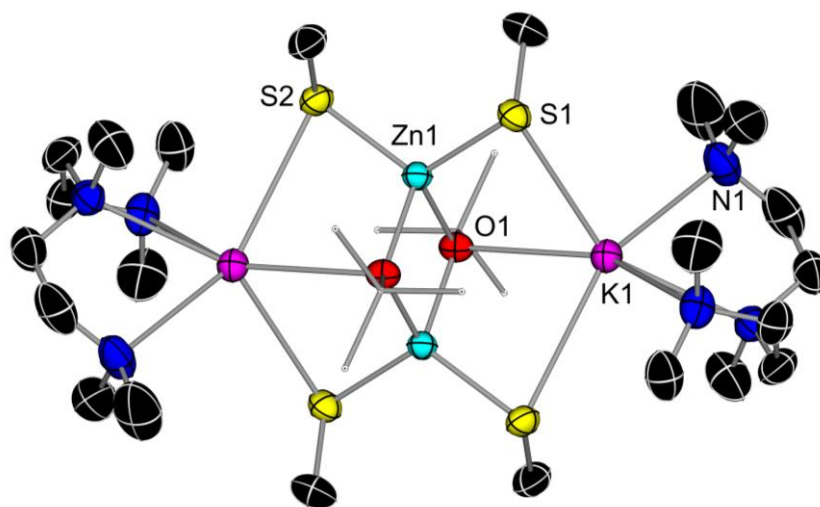


**Figure 11.** Molecular structure of [(PMDETA)KZn(SMe)<sub>2</sub>(OtBu)]<sub>2</sub> (**10**) with displacement ellipsoids at 50% probability, all H atoms omitted and with C atoms in the alkoxide fragment drawn as wire frames for clarity

Given the presence of TMP(H) in the filtrate of crystalline **10**, our current thinking is that an initial  $\alpha$ -zincation of THT takes place however we are unsure of the type of cleave and capture mechanism that generates the expulsion of two methylene sulphide groups. Due to time constraints, we have not been able to elucidate such a mechanism or rigorously monitor this reaction. Glass and Liu previously reported that metalation of THT was possible using the LIC-KOR superbases, although the Li/K metalated intermediate decomposed completely to a thioenolate and ethene at 5°C.<sup>53</sup> Mulvey has since used the aforementioned TMP based magnesiate [(TMEDA)NaMg(TMP)<sub>2</sub>R] (R = CH<sub>2</sub>SiMe<sub>3</sub>) and a related aluminate to sequester these sensitive anions, structurally characterising the metalated intermediates of the form [(TMEDA)NaMg(TMP)<sub>2</sub>(SC<sub>4</sub>H<sub>7</sub>)] keeping the saturated heterocycle intact.<sup>54,55</sup> Interestingly, in the case of Mg the authors report a decomposition over time to dimagnesiated 1,3-butadiene species **V** (Scheme 5a) confirming an identical decomposition product to that observed with the O-analogue THF. Given the similarities between our mono-zincated butadiene complex **9** and **V**, it is surprising to see that reaction of THT with Zn(TMP)<sub>2</sub>/2KOtBu does not follow a similar reaction pathway to that observed with THF. Thus, the formation of **10** represents an unprecedented decomposition pathway for a metalated THT molecule adding to the complexity observed when employing our mixed amido/alkoxy zincate system Zn(TMP)<sub>2</sub>/2KOtBu.



## 5.4 Conclusions and Future Work

Building upon our previous work outlined in *Chapter 4*, we have further demonstrated the dramatic activation of Zn(TMP)<sub>2</sub> mediated by KO<sup>t</sup>Bu through the formation of a mixed amido/alkoxy zincate. Kinetic activation of both TMP groups on Zn has allowed for the atom economical and regioselective zincation of non-activated arenes such as naphthalene, ferrocene and benzene under mild conditions. A quite drastic alkali-metal effect was observed within these reactions, specifically with the metalation of naphthalene, where switching to the lighter AM-OR congeners Li and NaO<sup>t</sup>Bu completely shuts down the metalation of the arene. Our current hypothesis is that the softer, larger K atom interacts more favourably via  $\pi$  interactions with the arene substrate acting as a built in Lewis acid priming the arene for metalation. Additionally, the use of an alkali-metal sequestering agent, 18-crown-6, results in a loss of metalating power of this base highlighting the need for bimetallic cooperativity in the form of a contacted ion-pair (CIP) where simple “ate” activation of zinc is not sufficient to deliver the metalation of naphthalene. NMR spectroscopic and X-Ray crystallographic analysis of the metalated intermediates of these reactions added a new layer of complexity within these mixed-metal/mixed-ligand systems which are able to eliminate potassium aryl moieties from the resulting reaction mixture forming lower order potassium zincates as their disproportionation partner, where in the case of 1,3-benzoxazole this could be unequivocally demonstrated. The complex behaviour of these metalated intermediates must be taken into consideration when considering the further functionalisation and synthetic utility of these reactions. Although THF is the choice of solvent for metalations with our Zn(TMP)<sub>2</sub>/2KO<sup>t</sup>Bu combination to ensure solubility of the metalated intermediates, this powerful mixed-metal base was shown to react with the THF solvent itself resulting in a complete destruction of the aliphatic heterocycle revealing an unusual zincated butadiene fragment.

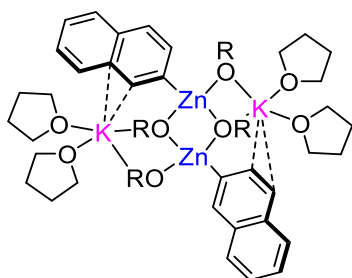
Regarding future work within this *Chapter*, work is currently ongoing to expand the substrate scope to other non-activated arenes whilst also exploring the opportunities of dimetalations, which we have observed in trace amounts for ferrocene. A more thorough and robust investigation into the  $\alpha$ -C-sp<sup>3</sup> metalations proposed as the initial step in the decomposition reactions observed with THF and THT is required. Attempts will be made to try and uncover the seemingly complex mechanisms of these reactions, which could potentially involve radical species, by trying to intercept any intermediates pre-ring opening of heterocycles and attempt to monitor this decomposition pathway closer.

## 5.4 Experimental

Zn(TMP)<sub>2</sub> was synthesised according to an adapted literature procedure (see Chapter 7).<sup>56</sup> Reduced yields of iodination products were noticed when using iodine which was stored under air for long periods of time. Therefore sublimed iodine was bought from Acros Organics then subsequently stored in a desiccator under argon. All other reagents purchased from commercial suppliers and used as received.

### 5.5.1 Synthesis of Organometallic Compounds 3a-b, 4, 6, 7, 9 and 10

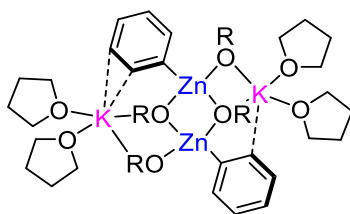
#### [(THF)<sub>2</sub>KZn(2-C<sub>10</sub>H<sub>7</sub>)(OtBu)<sub>2</sub>]<sub>2</sub> (3a)



To an argon flushed Schlenk flask, Zn(TMP)<sub>2</sub> (350 mg, 1 mmol), KOtBu (220 mg, 2 mmol) and naphthalene (260 mg, 2 mmol) were dissolved in THF (5 mL). This solution was allowed to stir at room temperature for 2 hours affording a bright yellow solution. The solvent was reduced to approximately 0.5 mL and hexane was layered on top of the THF solution. The solution was then stored at

-30 °C for 4 days affording a colourless crop of crystals – compound **3a**. Yield 300 mg, 29%. **<sup>1</sup>H-NMR (300.1 MHz, D<sub>8</sub>-THF, 298 K):** δ / ppm = 8.15 (s, 1H, Ar-H), 7.91 (d, J = 7.32 Hz, 1H, Ar-H), 7.60 (t, J = 8.75 Hz, 2H, Ar-H), 7.49 (d, J = 7.3 Hz, 1H, Ar-H), 7.18 (m, 2H, Ar-H), 1.22 (s, 18H, 2 x OtBu). **<sup>13</sup>C{<sup>1</sup>H}-NMR (101 MHz, D<sub>8</sub>-THF, 298 K):** δ / ppm = 163.0 (s, C<sub>q</sub>-Zn), 138.6 (s, Ar, C-H), 134.4 (s, Ar, C-H), 134.3 (s, Ar, C-H), 132.9 (s, Ar, C-H), 127.8 (s, Ar, C-H), 127.7 (s, Ar, C-H), 124.4 (s, Ar, C-H), 124.0 (s, Ar, C-H), 123.3 (s, Ar, C-H), 35.5 (s, CH<sub>3</sub>, 2 x OtBu).

#### Synthesis of [(THF)<sub>2</sub>KZn(C<sub>6</sub>H<sub>5</sub>)(OtBu)<sub>2</sub>]<sub>2</sub> (3b)



To an argon flushed Schlenk flask, Zn(TMP)<sub>2</sub> (180 mg, 0.5 mmol), KOtBu (110 mg, 1 mmol) were dissolved in benzene (5 mL) and left to stir at room temperature for 24 hours. All solvent was removed under vacuum and the resulting white solid was suspended in hexane (5 mL). THF was dripped into

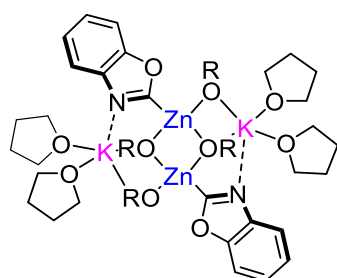
solution until a pale-yellow solution was formed. The solution was then stored at -30 °C overnight affording a colourless crop of crystals – compound **3b**. Yield 110 mg, 29%. Anal. Calcd. for C<sub>36</sub>H<sub>64</sub>K<sub>2</sub>O<sub>6</sub>Zn<sub>2</sub> (2 THF molecules coordinated) C, 53.92; H, 8.05. Found: C, 53.55; H, 7.49. **<sup>1</sup>H-NMR (300.1 MHz, D<sub>8</sub>-THF, 298 K):** δ / ppm = 7.81 (br. m, 2H, Ar-H), 7.00 (t, J = 7.85 Hz, 2H, Ar-H), 6.89 (m, 1H, Ar-H), 3.61 (THF), 1.77 (THF), 1.30 (s, 9H, OtBu) 1.06 (s, 9H, OtBu). **<sup>13</sup>C{<sup>1</sup>H}-NMR (101 MHz, D<sub>8</sub>-THF, 298 K):** δ / ppm = 165.7 (s, C<sub>q</sub>-Zn), 140.4

(s, Ar, C-H), 126.9 (s, Ar, C-H), 124.9 (s, Ar, C-H), 68.5 (br. s, 2 x C<sub>q</sub>, 2 x OtBu), 68.0 (THF), 37.0 (s, CH<sub>3</sub>, OtBu), 35.8 (s, CH<sub>3</sub>, OtBu), 26.1 (THF).

#### Synthesis of [(THF)<sub>3</sub>KZn(Fc)] (Fc = 1-ferrocenyl) (**4**)

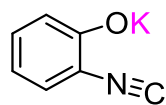
To an argon flushed Schlenk flask, Zn(TMP)<sub>2</sub> (180 mg, 0.5 mmol), KOtBu (110 mg, 1 mmol) were dissolved in THF (5 mL) and to this solution was added ferrocene (190 mg, 1 mmol) giving a bright orange solution which was stirred for 24 hours. After this time, solvent was reduced to half volume under vacuum and hexane (2 mL) layered on top of the THF solution. The solution was then stored at -30 °C overnight affording crop of orange crystals – compound **4**. Yield 80 mg, 18%. Anal. Calcd. for C<sub>42</sub>H<sub>51</sub>Fe<sub>3</sub>KO<sub>3</sub>Zn (3 THF molecules coordinated) C, 57.59; H, 5.87. Found: C, 57.54; H, 5.81. <sup>1</sup>H-NMR (300.1 MHz, D<sub>8</sub>-THF, 298 K): δ / ppm = 4.14 (br. m, 12H; overlapping CH<sub>β</sub> and CH<sub>γ</sub>, C<sub>5</sub>H<sub>4</sub>, 3 x Fc), 4.03 (br. s, 15H, C<sub>5</sub>H<sub>5</sub>, 3 x Fc) 3.56 (br. s, THF), 1.73 (br. s, THF). <sup>13</sup>C{<sup>1</sup>H}-NMR (101 MHz, D<sub>8</sub>-THF, 298 K): δ / ppm = 86.5 (s, 3 x C<sub>q</sub>-Zn, Fc), 78.9 (s, 3 x C<sub>β</sub>, Fc), 69.9 (s, 3 x C<sub>γ</sub>, Fc), 68.2 (THF), 67.3 (C<sub>5</sub>H<sub>5</sub>, 3 x Fc), 26.4 (THF).

#### Synthesis of [(THF)<sub>2</sub>KZn(2-benzoxazolyl)(OtBu)<sub>2</sub>]<sub>2</sub> (**6**)



To an argon flushed Schlenk flask, Zn(TMP)<sub>2</sub> (350 mg, 1 mmol), KOtBu (220 mg, 2 mmol) and 1,3-benzoxazole (240 mg, 2 mmol) were dissolved in THF (5 mL) giving a red solution. After 20 mins stirring at room temperature solvent half volume under vacuum and hexane (2 mL) layered on top of the THF solution. The solution was then stored at -30 °C overnight affording crop of colourless crystals – compound **6**. Yield 250 mg, 24%. Anal. Calcd. for C<sub>34</sub>H<sub>52</sub>N<sub>2</sub>K<sub>2</sub>O<sub>7</sub>Zn<sub>2</sub> (1 THF molecule coordinated) C, 50.43; H, 6.47. Found: C, 49.66; H, 6.49. <sup>1</sup>H-NMR (300.1 MHz, D<sub>8</sub>-THF, 298 K): δ / ppm = 7.49 (m, 2H, Ar-H), 7.10 (m, 2H, Ar-H), 3.61 (THF), 1.76 (THF), 1.30 (2 x s overlapping, s, 18H, 2 x OtBu). <sup>13</sup>C{<sup>1</sup>H}-NMR (101 MHz, D<sub>8</sub>-THF, 298 K): δ / ppm = 197.9 (s, C<sub>q</sub>-Zn), 153.1 (s, Ar, C-H), 143.0 (s, Ar, C-H), 122.8 (s, Ar, C-H), 122.2 (s, Ar, C-H), 118.4 (s, Ar, C-H), 110.4 (s, Ar, C-H), 70.1 (s, C<sub>q</sub>, OtBu), 68.8 (s, C<sub>q</sub>, OtBu), 68.0 (THF), 35.6 (s, CH<sub>3</sub>, OtBu), 34.1 (s, CH<sub>3</sub>, OtBu), 26.2 (THF).

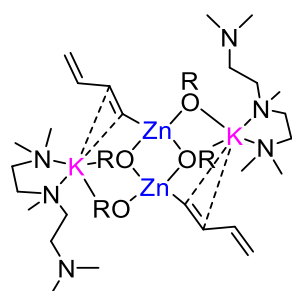
#### Synthesis of potassium 2-isocyanophenolate (**7**)



To an argon flushed Schlenk flask, 1,3-benzoxazole (0.5 mmol, 60 mg) was dissolved in benzene (2.5 mL) and cooled to 0 °C. K(CH<sub>2</sub>SiMe<sub>3</sub>) (0.5 mmol, 63mg) was then added via a solid addition tube giving a red/brownish suspension. After 10 mins, all solvent was removed, and the resulting solid was dried under vacuum affording a red/brown solid – compound **7**. Yield 75 mg, 48%. <sup>1</sup>H-NMR (300.1 MHz,

**D<sub>8</sub>-THF, 298 K):**  $\delta$  / ppm = 6.94 (dd,  $J$  = 7.70 Hz, 1.85 Hz, 1H, Ar-H), 6.85 (td,  $J$  = 7.76 Hz, 1.91, 1H, Ar-H), 6.50 (d,  $J$  = 8.30 Hz, 1H, Ar-H), 5.98 (td,  $J$  = 7.54 Hz, 1.15 Hz, 1H, Ar-H). **<sup>13</sup>C{<sup>1</sup>H}-NMR (101 MHz, D<sub>8</sub>-THF, 298 K):**  $\delta$  / ppm = 168.8 (s, Ar, C-H), 163.8 (s, Ar, C<sub>q</sub>, C-H), 130.7 (s, Ar, C-H), 128.8 (s, Ar, C<sub>q</sub>-H), 121.3 (s, Ar, C-H), 117.4 (s, CN), 108.5 (s, Ar, C-H). NMR spectroscopy fits well with those reported for lithium 2-isocyanophenolate.<sup>43</sup>

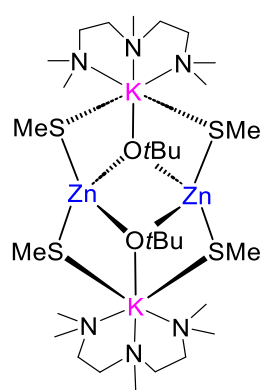
#### Synthesis of [(PMDETA)KZn(C<sub>4</sub>H<sub>5</sub>)(OtBu)<sub>2</sub>]<sub>2</sub> (**9**)



To an argon flushed Schlenk flask, Zn(TMP)<sub>2</sub> (350 mg, 1 mmol) and KOtBu (220 mg, 2 mmol) were allowed to stir in THF (5 mL) for 3 days at room temperature giving a deep purple/black solution. All solvent removed and the resulting oil was reconstituted in hexane (5 mL) giving a wispy suspension. PMDETA (0.42 mL, 2 mmol) was then added to give a pale-yellow solution. The solution was then stored at -30 °C overnight affording crop of colourless

crystals – compound **9**. Yield 350 mg, 37%. **<sup>1</sup>H-NMR (300.1 MHz, D<sub>8</sub>-THF, 298 K):**  $\delta$  / ppm = 6.68 (2 x overlapping m, 2H), 6.23 (m, 2H), 4.73 (dd,  $J$  = 17.08 Hz, 2.27 Hz, 1H), 4.54 (dd,  $J$  = 10 Hz, 2.5 Hz, 1H), 2.35 (m, 8H, 2 x (CH<sub>2</sub>)<sub>2</sub>, PMDETA), 2.18 (s, 3H, NMe, PMDETA), 2.14 (s, 12H, 2 x NMe<sub>2</sub>, PMDETA), 12.5 (s, 9H, OtBu), 1.15 (s, 9H, OtBu). **<sup>13</sup>C{<sup>1</sup>H}-NMR (101 MHz, D<sub>8</sub>-THF, 298 K):**  $\delta$  / ppm = 164.2 (s, Zn-C=CH), 146.3 (s, CH=CH), 143.7 (s, CH<sub>2</sub>), 107.5 (s, CH=CH), 58.7 (s, CH<sub>2</sub>-PMDETA), 57.3 (s, CH<sub>2</sub>-PMDETA), 46.0 (s, CH<sub>3</sub>-PMDETA), 46.0 (s, CH<sub>3</sub>-PMDETA), 35.4 (s, CH<sub>3</sub>, OtBu), 33.8 (s, CH<sub>3</sub>, OtBu).

#### Synthesis of [(PMDETA)KZn(SCH<sub>3</sub>)<sub>2</sub>(OtBu)]<sub>2</sub> (**10**)



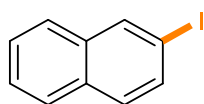
To an argon flushed Schlenk flask, Zn(TMP)<sub>2</sub> (350 mg, 1 mmol) and KOtBu (220 mg, 2 mmol) were allowed to stir in THT (5 mL) for 5 days at room temperature. All solvent removed and the resulting oil was reconstituted in hexane (5 mL) giving a wispy suspension. PMDETA (0.42 mL, 2 mmol) was then added to give a pale-yellow solution. The solution was then stored at -30 °C overnight affording crop of colourless crystals – compound **10**. **<sup>1</sup>H-NMR (300.1 MHz, D<sub>8</sub>-THF, 298 K):**  $\delta$  / ppm = 2.35 (m, 8H, 2 x (CH<sub>2</sub>)<sub>2</sub>, PMDETA), 2.18 (s, 3H, NMe, PMDETA), 2.14 (s, 12H, 2 x NMe<sub>2</sub>, PMDETA), 1.95 (s, 6H, 2 x CH<sub>3</sub>, SMe), 1.19 (s, 9H, OtBu).

## 5.5.2 Synthesis of Iodoarenes Compounds 2a-g and 5a-f

### General Procedure

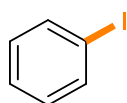
In an argon flushed Schlenk flask, Zn(TMP)<sub>2</sub> (1 e.q) and KO<sup>t</sup>Bu (2 e.q) were dissolved in THF (5 mL). To this solution was added the desired substrate (2 e.q) at room temperature and allowed to stir for the allotted time. Sublimed I<sub>2</sub> (5 e.q) was then added to the solution and then stirred overnight. Reaction mixture quenched with Na<sub>2</sub>S<sub>2</sub>O<sub>3</sub> (10 mL), organics extracted with EtOAc (3 x 10 mL), washed with brine (1 x 10 mL), dried over MgSO<sub>4</sub> and filtered. Crude reaction mixtures purified as stated or yield determined using hexamethylbenzene (10 mol%) as an internal standard unless otherwise stated.

### Synthesis of 2-iodonaphthalene 2a



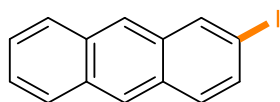
**2a** was synthesised according to the general procedure using sublimed naphthalene (2 mmol, 260 mg) stirring the reaction at room temperature for 2 hours giving a bright yellow solution before quenching with iodine (5 e.q). The resulting mixture was concentrated and purified by filtration through a plug of silica gel using hexane as eluent to yield 2-iodonaphthalene **2a** (450 mg, 89%) as an off-white solid. Spectroscopic data is an identical match for those previously reported.<sup>57</sup> **<sup>1</sup>H-NMR (300.1 MHz, CDCl<sub>3</sub>, 298 K):** δ / ppm = 8.24 (s, 1H), 7.81-7.78 (m, 1H), 7.74-7.71 (m, 2H), 7.58 (d, J = 8.5 Hz, 1H), 7.51-7.49 (m, 2H) ppm. **<sup>13</sup>C{<sup>1</sup>H}-NMR (101 MHz, CDCl<sub>3</sub>, 298 K):** δ / ppm = 136.7, 135.1, 134.5, 132.2, 129.6, 128.0, 126.9, 126.8, 126.6, 91.6 ppm.

### Synthesis of 2-iodonaphthalene 2b



Higher order potassium zincate **II** was prepared as described in *Chapter 4, section 4.5.7*. A portion of **II** (0.04 mmol) and hexamethylbenzene (10 mol%) were dissolved in d<sub>8</sub>-THF and to this solution was added I<sub>2</sub> (5 e.q, 0.15 mmol, 40 mg) giving a deep black solution. After 2 hours at room temperature <sup>1</sup>H-NMR spectroscopy confirmed a quantitative (>95%) conversion to iodobenzene **2b**. **<sup>1</sup>H-NMR (300.1 MHz, d<sub>8</sub>-THF, 298 K):** δ / ppm = 7.68 (d, J = 7.85, 2H, Ar-H), 7.32 (m, 1H, Ar-H), 7.10 (t, J = 8.35, 2H, Ar-H).

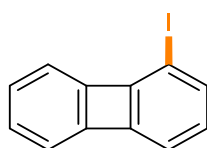
### Synthesis of 2-iodoanthracene 2c



**2c** was synthesised according to the general procedure using anthracene (2 e.q, 0.5 mmol, 90 mg) stirring the reaction at room temperature for 2 hours giving a deep orange solution. Reaction then

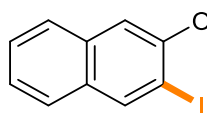
quenched with iodine and left to stir overnight. Crude reaction mixture purified by Kugelrohr distillation to give 2-iodoanthracene **2c** as a white crystalline solid (62 mg, 42% yield). NMR spectroscopic data consistent with literature reports.<sup>58</sup> **<sup>1</sup>H-NMR (300.1 MHz, CDCl<sub>3</sub>, 298 K):**  $\delta$  / ppm = 8.42 (s, 1H, Ar-H), 8.38 (s, 1H, Ar-H), 8.29 (s, 1H, Ar-H), 8.01-7.97 (m, 2H, Ar-H), 7.74 (d, 1H, J = 9Hz, Ar-H), 7.65 (dd, 1H, J = 9 Hz, 2 Hz, Ar-H), 7.49 (m, 2H, Ar-H). **<sup>13</sup>C{<sup>1</sup>H}-NMR (101 MHz, CDCl<sub>3</sub>, 298 K):**  $\delta$  / ppm = 137.0 (s, C<sub>Ar-H</sub>), 133.8 (s, C<sub>Ar-H</sub>), 133.1 (s, C<sub>q</sub>), 132.1 (s, C<sub>q</sub>), 132.0 (s, C<sub>q</sub>), 130.1 (s, C<sub>q</sub>), 129.8 (s, C<sub>Ar-H</sub>), 128.4 (s, C<sub>Ar-H</sub>), 128.3 (s, C<sub>Ar-H</sub>), 126.7 (s, C<sub>Ar-H</sub>), 126.1 (s, C<sub>Ar-H</sub>), 126.0 (s, C<sub>Ar-H</sub>), 125.3 (s, C<sub>Ar-H</sub>), 91.3 (s, C<sub>q-I</sub>).

#### Synthesis of 1-iodobiphenylene **2d**

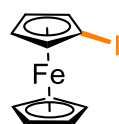


**2d** was synthesised according to the general procedure using biphenylene (2 e.q, 0.5 mmol, 76 mg) stirring the reaction at room temperature for 24 hours giving a pale orange solution before quenching with iodine. The resulting mixture was concentrated and purified by filtration by column chromatography using hexane as eluent to yield 1-iodobiphenylene **2d** (100 mg, 71%) as a yellow oil. **<sup>1</sup>H-NMR (300.1 MHz, CDCl<sub>3</sub>, 298 K):**  $\delta$  / ppm = 6.95 (d, J = 8.32 Hz, 1H, Ar-H), 6.82 (m, 2H, 3 x Ar-H), 6.65 (m, 1H, Ar-H), 6.56 (d, J = 7.06, 1H, Ar-H), 6.46 (m, 1H, Ar-H). **<sup>13</sup>C{<sup>1</sup>H}-NMR (101 MHz, CDCl<sub>3</sub>, 298 K):**  $\delta$  / ppm = 156.8 (s, C<sub>q</sub>, Ar), 152.9 (s, C<sub>q</sub>, Ar), 151.2 (s, C<sub>q</sub>, Ar), 149.7 (s, C<sub>q</sub>, Ar), 136.3 (s, C<sub>q</sub>, C-H), 129.8 (s, Ar, C-H), 129.3 (s, Ar, C-H), 128.7 (s, Ar, C-H), 117.9 (s, Ar, C-H), 116.6 (s, Ar, C-H), 80.8 (s, Ar, C<sub>q-I</sub>). **HRMS (EI, 70 eV)** m/z: calc. for C<sub>12</sub>H<sub>7</sub>I 277.9587; found: 277.9590.

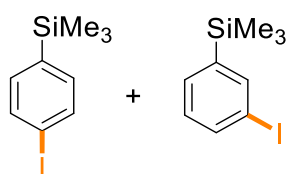
#### Synthesis of 3-iodo-2-methoxynaphthalene **2e**



**2e** was synthesised according to the general procedure using 2-methoxynaphthalene (2 e.q, 79 mg, 0.5 mmol) stirring the reaction at room temperature for 3 hours giving a pale-yellow solution before quenching with iodine. Crude reaction mixture purified by column chromatography (distilled pentane, using fine silica gel, 0.015-0.04 mm) affording of 3-iodo-2-methoxynaphthalene **2e** as a white solid (175 mg, 62%). NMR spectroscopic data consistent with literature reports.<sup>59</sup> **<sup>1</sup>H-NMR (300.1 MHz, CDCl<sub>3</sub>, 298 K):**  $\delta$  / ppm = 8.33 (s, 1H, Ar-H), 7.73-7.66 (m, 1H, Ar-H), 7.64 (m, 1H, Ar-H), 7.50 (t, J = 7.37 Hz, 1H, Ar-H), 7.35 (t, J = 7.62, 1H, Ar-H), 3.99 (s, 3H, OMe). **<sup>13</sup>C{<sup>1</sup>H}-NMR (101 MHz, CDCl<sub>3</sub>, 298 K):**  $\delta$  / ppm = 155.2 (s, C<sub>q</sub>), 139.3 (s, C<sub>Ar-H</sub>), 134.4 (s, C<sub>q</sub>), 130.5 (s, C<sub>q</sub>), 127.0 (s, C<sub>Ar-H</sub>), 126.7 (s, C<sub>Ar-H</sub>), 126.6 (s, C<sub>Ar-H</sub>), 124.4 (s, C<sub>Ar-H</sub>), 105.6 (s, C<sub>Ar-H</sub>), 88.2 (s, Ar, C<sub>q-I</sub>), 55.5 (s, OMe<sub>3</sub>).

Synthesis of 1-iodoferrocene **2f**

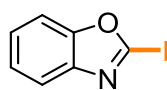
**2f** was synthesised according to the general procedure using ferrocene (2 e.q, 93 mg, 0.5 mmol) stirring the reaction at room temperature for 24 hours giving a bright orange solution before quenching with iodine. Crude reaction mixture purified by column chromatography (hexane 100%) affording 1-iodoferrocene **2f** as an orange oil (235 mg, 75%). NMR spectroscopic data consistent with literature reports.<sup>60</sup> Traces amounts of 1,1'-diiodoferrocene present in crude NMR (<5%).<sup>61</sup> **<sup>1</sup>H-NMR (300.1 MHz, CDCl<sub>3</sub>, 298 K):**  $\delta$  / ppm = 4.41 (t,  $J$  = 1.80 Hz, 2H, C<sub>5</sub>H<sub>4</sub>,  $\beta$ H's), 4.18 (s, 5H, C<sub>5</sub>H<sub>5</sub>), 4.15 (m, 2H, C<sub>5</sub>H<sub>4</sub>,  $\gamma$ H's). **<sup>13</sup>C{<sup>1</sup>H}-NMR (101 MHz, CDCl<sub>3</sub>, 298 K):**  $\delta$  / ppm = 74.6 (s, 2 x C<sub>Cp-I</sub>), 71.2 (s, 5 x C<sub>Cp</sub>), 68.9 (s, 2 x C<sub>Cp-I</sub>), 39.9 (s, C<sub>q-I</sub>).

Iodination of 3-iodo and 4-iodo-trimethyl(phenyl)silane **2g**

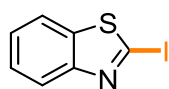
Reaction carried out following the general procedure using 5 mL trimethyl(phenyl)silane stirring the reaction for 24 hours at room temperature giving a greyish solution before quenching with iodine. Yield was determined using hexamethylbenzene (10 mol%) as an internal standard affording a mixture of 3-iodo-trimethyl(phenyl)silane (25%) and 4-iodo-trimethyl(phenyl)silane (37%).

3-iodo-trimethyl(phenyl)silane, **<sup>1</sup>H-NMR (300.1 MHz, CDCl<sub>3</sub>, 298 K):**  $\delta$  / ppm = 7.81 (s, 1H, Ar-H), 7.70 (m, 1H, Ar-H), 7.47 (dt,  $J$  = 7.2 Hz, 1H, Ar-H), 7.10 (t,  $J$  = 7.61, 1H, Ar-H), 0.28 (s, 9H, SiMe<sub>3</sub>). Spectroscopic data is an identical match for those previously reported.<sup>62</sup>

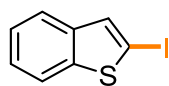
4-iodo-trimethyl(phenyl)silane, **<sup>1</sup>H-NMR (300.1 MHz, CDCl<sub>3</sub>, 298 K):**  $\delta$  / ppm = 7.68 (d,  $J$  = 8.13 Hz, 2H, Ar-H), 7.24 (d,  $J$  = 8.12 Hz, 2H, Ar-H).<sup>63</sup>

Synthesis of 2-iodobenzoxazole **5a**

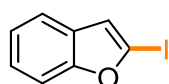
**5a** was synthesised according to the general procedure using 1,3-benzoxazole (2 e.q, 120 mg, 1 mmol) stirring the reaction at room temperature for 20 mins giving a bright red solution before quenching with iodine. Crude reaction mixture purified by column chromatography (hexane/EtOAc, 90:10) affording 2-iodobenzoxazole **5a** as a yellow powder (225 mg, 92%). Note that upon standing **5a** rapidly turns to a brownish powder. NMR spectroscopic data consistent with literature reports.<sup>44</sup> **<sup>1</sup>H-NMR (300.1 MHz, CDCl<sub>3</sub>, 298 K):**  $\delta$  / ppm = 7.73-7.69 (m, 1H, Ar-H), 7.57-7.53 (m, 1H, Ar-H), 7.33-7.30 (m, 2H, Ar-H). **<sup>13</sup>C{<sup>1</sup>H}-NMR (101 MHz, CDCl<sub>3</sub>, 298 K):**  $\delta$  / ppm = 154.2 (s, C<sub>q</sub>), 142.8 (s, C<sub>q</sub>), 125.4 (s, C<sub>Ar-H</sub>), 124.8 (s, C<sub>Ar-H</sub>), 119.4 (s, C<sub>Ar-H</sub>), 110.2 (s, C<sub>Ar-H</sub>), 108.2 (s, 2 x C<sub>Cp-I</sub>).

Synthesis of 2-iodobenzothiazole **5b**

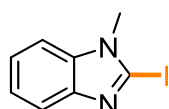
**5b** was synthesised according to the general procedure using 1,3-benzothiazole (2 e.q, 110  $\mu$ L, 1 mmol) stirring the reaction at room temperature for 20 mins giving a yellow solution before quenching with iodine. Crude reaction mixture purified by column chromatography (hexane/EtOAc, 80:20) affording 2-iodobenzothiazole **5b** as a yellow powder (230 mg, 88%). NMR spectroscopic data consistent with literature reports.<sup>44</sup> **<sup>1</sup>H-NMR (300.1 MHz, CDCl<sub>3</sub>, 298 K):**  $\delta$  / ppm = 8.03 (dd,  $J$  = 8.32 Hz, 1.73 Hz, 1H, Ar-H), 7.85 (dd,  $J$  = 7.63 Hz,  $J$  = 1.72, 1H, Ar-H), 7.46-7.35 (m, 2H, Ar-H). **<sup>13</sup>C{<sup>1</sup>H}-NMR (101 MHz, CDCl<sub>3</sub>, 298 K):**  $\delta$  / ppm = 154.4 (s, C<sub>q</sub>), 139.3 (s, C<sub>q</sub>), 126.5 (s, C<sub>Ar-H</sub>), 125.7 (s, C<sub>Ar-H</sub>), 122.7 (s, C<sub>Ar-H</sub>), 120.5 (s, C<sub>Ar-H</sub>), 105.8 (s, C<sub>q-I</sub>).

Synthesis of 2-iodobenzothiophene **5c**

**5c** was synthesised according to the general procedure using benzothiophene (2 e.q, 134 mg, 1 mmol) stirring the reaction at room temperature for 20 mins giving a yellow solution before quenching with iodine. Crude reaction mixture purified by column chromatography (hexane 100%) affording 2-iodobenzothiophene **5c** as a light-yellow powder (250 mg, 96%). NMR spectroscopic data consistent with literature reports<sup>44</sup> **<sup>1</sup>H-NMR (300.1 MHz, CDCl<sub>3</sub>, 298 K):**  $\delta$  / ppm = 7.78-7.70 (m, 2H, Ar-H), 7.54 (s, 1H, Ar-H), 7.31-7.21 (m, 2H, Ar-H). **<sup>13</sup>C{<sup>1</sup>H}-NMR (101 MHz, CDCl<sub>3</sub>, 298 K):**  $\delta$  / ppm = 144.5 (s, C<sub>q</sub>), 140.9 (s, C<sub>q</sub>), 133.9 (s, C<sub>Ar-H</sub>), 124.6 (s, C<sub>Ar-H</sub>), 124.5 (s, C<sub>Ar-H</sub>), 122.4 (s, C<sub>Ar-H</sub>), 121.4 (s, C<sub>Ar-H</sub>), 78.5 (s, C<sub>q-I</sub>).

Synthesis of 2-iodobenzofuran **5d**

**5d** was synthesised according to the general procedure using benzofuran (2 e.q, 110  $\mu$ L, 1 mmol) stirring the reaction at room temperature for 20 mins giving a yellow solution before quenching with iodine. Crude reaction mixture purified by column chromatography (hexane 100%) yield of 2-iodobenzofuran **5d** as a yellow oil (185 mg, 81%). NMR spectroscopic data consistent with literature reports.<sup>44</sup> **<sup>1</sup>H-NMR (300.1 MHz, CDCl<sub>3</sub>, 298 K):**  $\delta$  / ppm = 7.53-7.46 (m, 2H, Ar-H), 7.23-7.20 (m, 2H, Ar-H), 6.96 (d,  $J$  = 0.81 Hz, 1H, Ar-H). **<sup>13</sup>C{<sup>1</sup>H}-NMR (101 MHz, CDCl<sub>3</sub>, 298 K):**  $\delta$  / ppm = 158.4 (s, C<sub>q</sub>), 129.4 (s, C<sub>q</sub>), 124.4 (s, C<sub>Ar-H</sub>), 123.3 (s, C<sub>Ar-H</sub>), 119.8 (s, C<sub>Ar-H</sub>), 117.4 (s, C<sub>Ar-H</sub>), 110.9 (s, C<sub>Ar-H</sub>), 95.9 (s C<sub>q-I</sub>).

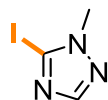
Synthesis of 2-iodo-1-methylbenzimidazole **5e**

**5e** was synthesised according to the general procedure using 1-methylbenzimidazole (2 e.q, 132 mg, 1 mmol) stirring the reaction at room temperature for 20 mins giving a yellow solution before quenching with iodine. Crude reaction mixture purified by column chromatography (EtOAc, 100%) affording



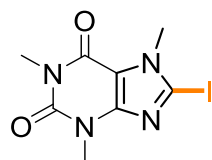
2-iodo-1-methylbenzimidazole **2m** as a yellow powder (210 mg, 81%). NMR spectroscopic data consistent with literature reports.<sup>64</sup> **<sup>1</sup>H-NMR (300.1 MHz, CDCl<sub>3</sub>, 298 K):**  $\delta$  / ppm = 7.64-7.60 (m, 1H, Ar-H), 7.25-7.22 (m, 1H, Ar-H), 7.18-7.11 (m, 2H, Ar-H), 3.67 (s, 3H, NMe). **<sup>13</sup>C{<sup>1</sup>H}-NMR (101 MHz, CDCl<sub>3</sub>, 298 K):**  $\delta$  / ppm = 145.6 (s, C<sub>q</sub>), 136.4 (s, C<sub>q</sub>), 123.2 (s, C<sub>Ar</sub>-H), 122.3 (s, C<sub>Ar</sub>-H), 119.3 (s, C<sub>Ar</sub>-H), 109.5 (s, C<sub>Ar</sub>-H), 104.4 (s, C<sub>q</sub>-I), 33.8 (s, NMe).<sup>65</sup>

#### Synthesis of 5-iodo-1-methyl-1,2,4-triazole **5f**



**5f** was synthesised according to the general procedure using 1-methyl-1,2,4-triazole (2 e.q, 57  $\mu$ L, 1 mmol) stirring the reaction at room temperature for 20 mins giving a yellow solution before quenching with iodine. Crude reaction mixture purified by column chromatography (hexane/EtOAc 40:60 to 60:40) affording 5-iodo-1-methyl-1,2,4-triazole **5f** as an off-white solid (190 mg, 91%). **<sup>1</sup>H-NMR (300.1 MHz, CDCl<sub>3</sub>, 298 K):**  $\delta$  / ppm = 7.88 (s, 1H, Ar-H), 3.90 (s, 3H, NMe). **<sup>13</sup>C{<sup>1</sup>H}-NMR (101 MHz, CDCl<sub>3</sub>, 298 K):**  $\delta$  / ppm = 154.3 (s, C<sub>Ar</sub>-H), 100.2 (s, C<sub>q</sub>-I), 38.0 (s, NMe).

#### Synthesis of iodocaffeine **5g**



**5g** was synthesised according to the general procedure using caffeine (2 e.q, 194 mg, 1 mmol) stirring the reaction at room temperature for 10 mins giving a white suspension before quenching with iodine. Crude reaction mixture filtered through a plug of silica gel and washed with DCM affording iodocaffeine **5g** as a white solid (270 mg, 84%). **<sup>1</sup>H-NMR (300.1 MHz, CDCl<sub>3</sub>, 298 K):**  $\delta$  / ppm = 3.94 (s, CH<sub>3</sub>, NMe), 3.55 (s, CH<sub>3</sub>, NMe), 3.38 (s, CH<sub>3</sub>, NMe). **<sup>13</sup>C{<sup>1</sup>H}-NMR (101 MHz, CDCl<sub>3</sub>, 298 K):**  $\delta$  / ppm = 154.3 (s, C<sub>q</sub>), 151.4 (s, C<sub>q</sub>), 149.7 (s, C<sub>q</sub>), 110.9 (s, C<sub>q</sub>), 101.2 (s, C<sub>q</sub>-I), 36.3 (s, CH<sub>3</sub>, NMe), 29.9 (s, CH<sub>3</sub>, NMe), 28.2 (s, CH<sub>3</sub>, NMe).

### 5.5.3 Selected crystallographic parameters for compounds 3a-b, 4, 6, 9 and 10

**Table 2.** Selected crystallographic parameters for compound **3a**

Compound Number	<b>3a</b>
Empirical formula	C <sub>52</sub> H <sub>82</sub> K <sub>2</sub> O <sub>8</sub> Zn <sub>2</sub>
Formula weight	1044.11
Temperature/K	173.01(10)
Crystal system	monoclinic
Space group	I2/a
a/Å	18.2697(3)
b/Å	17.0018(3)
c/Å	20.8902(3)
α/°	90
β/°	112.7772(18)
γ/°	90
Volume/Å <sup>3</sup>	5982.84(18)
Z	4
ρ <sub>calc</sub> /cm <sup>3</sup>	1.159
μ/mm <sup>-1</sup>	2.577
F(000)	2224
Crystal size/mm <sup>3</sup>	0.131 × 0.069 × 0.067
Radiation	Cu Kα (λ = 1.54184)
2θ range for data collection/°	6.934 to 142.53
Index ranges	-22 ≤ h ≤ 22, -20 ≤ k ≤ 20, -25 ≤ l ≤ 21
Reflections collected	59420
Independent reflections	5794 [R <sub>int</sub> = 0.0602, R <sub>sigma</sub> = 0.0256]
Data/restraints/parameters	5794/115/295
Goodness-of-fit on F <sup>2</sup>	1.062
Final R indexes [I ≥ 2σ (I)]	R <sub>1</sub> = 0.0625, wR <sub>2</sub> = 0.1977
Final R indexes [all data]	R <sub>1</sub> = 0.0691, wR <sub>2</sub> = 0.2066
Largest diff. peak/hole / e Å <sup>-3</sup>	0.75/-0.48

**Table 3.** Selected crystallographic parameters for compound **3b**

Compound Number	<b>3b</b>
Empirical formula	C <sub>44</sub> H <sub>78</sub> K <sub>2</sub> O <sub>8</sub> Zn <sub>2</sub>
Formula weight	944
Temperature/K	173.00(10)
Crystal system	monoclinic
Space group	P2 <sub>1</sub> /n
a/Å	12.74441(7)
b/Å	14.35189(9)
c/Å	14.07101(7)
α/°	90
β/°	94.0280(5)
γ/°	90
Volume/Å <sup>3</sup>	2567.32(2)
Z	2
ρ <sub>calc</sub> /cm <sup>3</sup>	1.221
μ/mm <sup>-1</sup>	2.946
F(000)	1008
Crystal size/mm <sup>3</sup>	0.317 × 0.266 × 0.186
Radiation	Cu Kα (λ = 1.54184)
2θ range for data collection/°	8.812 to 140.918
Index ranges	-15 ≤ h ≤ 15, -17 ≤ k ≤ 17, -16 ≤ l ≤ 17
Reflections collected	50337
Independent reflections	4926 [R <sub>int</sub> = 0.0323, R <sub>sigma</sub> = 0.0134]
Data/restraints/parameters	4926/18/315
Goodness-of-fit on F <sup>2</sup>	1.049
Final R indexes [I ≥ 2σ (I)]	R <sub>1</sub> = 0.0286, wR <sub>2</sub> = 0.0784
Final R indexes [all data]	R <sub>1</sub> = 0.0290, wR <sub>2</sub> = 0.0788
Largest diff. peak/hole / e Å <sup>-3</sup>	0.32/-0.26

**Table 4.** Selected crystallographic parameters for compound **4**

Compound Number	<b>4</b>
Empirical formula	C <sub>42</sub> H <sub>51</sub> Fe <sub>3</sub> KO <sub>3</sub> Zn
Formula weight	875.84
Temperature/K	173.00(10)
Crystal system	triclinic
Space group	P-1
a/Å	10.50392(13)
b/Å	11.90732(16)
c/Å	15.56204(19)
α/°	80.6515(11)
β/°	87.6971(10)
γ/°	88.7201(10)
Volume/Å <sup>3</sup>	1918.75(4)
Z	2
ρ <sub>calc</sub> /cm <sup>3</sup>	1.516
μ/mm <sup>-1</sup>	1.875
F(000)	908
Crystal size/mm <sup>3</sup>	0.19 × 0.139 × 0.126
Radiation	Mo Kα (λ = 0.71073)
2θ range for data collection/°	4.62 to 61.016
Index ranges	-15 ≤ h ≤ 15, -17 ≤ k ≤ 17, -22 ≤ l ≤ 22
Reflections collected	116343
Independent reflections	11691 [R <sub>int</sub> = 0.0355, R <sub>sigma</sub> = 0.0190]
Data/restraints/parameters	11691/173/562
Goodness-of-fit on F <sup>2</sup>	1.068
Final R indexes [I ≥ 2σ (I)]	R <sub>1</sub> = 0.0294, wR <sub>2</sub> = 0.0724
Final R indexes [all data]	R <sub>1</sub> = 0.0384, wR <sub>2</sub> = 0.0756
Largest diff. peak/hole / e Å <sup>-3</sup>	0.82/-0.22

**Table 5.** Selected crystallographic parameters for compound **6**

Compound Number	<b>6</b>
Empirical formula	C <sub>46</sub> H <sub>76</sub> K <sub>2</sub> N <sub>2</sub> O <sub>10</sub> Zn <sub>2</sub>
Formula weight	1026.02
Temperature/K	100.0(2)
Crystal system	orthorhombic
Space group	Pbca
a/Å	18.3733(3)
b/Å	15.7455(3)
c/Å	18.5165(3)
α/°	90
β/°	90
γ/°	90
Volume/Å <sup>3</sup>	5356.74(16)
Z	4
ρ <sub>calc</sub> /cm <sup>3</sup>	1.272
μ/mm <sup>-1</sup>	2.909
F(000)	2176
Crystal size/mm <sup>3</sup>	0.252 × 0.234 × 0.197
Radiation	Cu Kα (λ = 1.54184)
2θ range for data collection/°	8.804 to 149.008
Index ranges	-17 ≤ h ≤ 22, -19 ≤ k ≤ 19, -23 ≤ l ≤ 23
Reflections collected	50695
Independent reflections	5474 [R <sub>int</sub> = 0.0375, R <sub>sigma</sub> = 0.0176]
Data/restraints/parameters	5474/48/306
Goodness-of-fit on F <sup>2</sup>	1.077
Final R indexes [I ≥ 2σ (I)]	R <sub>1</sub> = 0.0473, wR <sub>2</sub> = 0.1317
Final R indexes [all data]	R <sub>1</sub> = 0.0525, wR <sub>2</sub> = 0.1367
Largest diff. peak/hole / e Å <sup>-3</sup>	0.52/-0.65

**Table 6.** Selected crystallographic parameters for compound **9**

Compound number	<b>9</b>
Empirical formula	C <sub>42</sub> H <sub>92</sub> K <sub>2</sub> N <sub>6</sub> O <sub>4</sub> Zn <sub>2</sub>
Formula weight	954.15
Temperature/K	173.01(10)
Crystal system	triclinic
Space group	P-1
a/Å	10.92429(16)
b/Å	11.04872(16)
c/Å	13.15156(19)
α/°	112.4692(14)
β/°	92.8879(12)
γ/°	107.7984(13)
Volume/Å <sup>3</sup>	1371.22(4)
Z	1
ρ <sub>calc</sub> /cm <sup>3</sup>	1.155
μ/mm <sup>-1</sup>	2.733
F(000)	516
Crystal size/mm <sup>3</sup>	0.236 × 0.183 × 0.122
Radiation	Cu Kα (λ = 1.54184)
2θ range for data collection/°	7.41 to 135.808
Index ranges	-13 ≤ h ≤ 13, -13 ≤ k ≤ 13, -15 ≤ l ≤ 15
Reflections collected	51627
Independent reflections	4979 [R <sub>int</sub> = 0.0224, R <sub>sigma</sub> = 0.0086]
Data/restraints/parameters	4979/5/443
Goodness-of-fit on F <sup>2</sup>	1.074
Final R indexes [I ≥ 2σ (I)]	R <sub>1</sub> = 0.0213, wR <sub>2</sub> = 0.0562
Final R indexes [all data]	R <sub>1</sub> = 0.0215, wR <sub>2</sub> = 0.0564
Largest diff. peak/hole / e Å <sup>-3</sup>	0.38/-0.38

**Table 7.** Selected crystallographic parameters for compound **10**

Compound number	<b>10</b>
Empirical formula	C <sub>30</sub> H <sub>76</sub> N <sub>6</sub> O <sub>2</sub> S <sub>4</sub> K <sub>2</sub> Zn <sub>2</sub>
Formula weight	890.14
Temperature/K	173.00(10)
Crystal system	orthorhombic
Space group	Pbca
a/Å	17.7814(3)
b/Å	13.0360(3)
c/Å	20.4259(3)
α/°	90
β/°	90
γ/°	90
Volume/Å <sup>3</sup>	4734.70(15)
Z	4
ρ <sub>calc</sub> /cm <sup>3</sup>	1.249
μ/mm <sup>-1</sup>	1.396
F(000)	1904
Crystal size/mm <sup>3</sup>	0.137 × 0.088 × 0.067
Radiation	Mo Kα (λ = 0.71073)
2θ range for data collection/°	4.358 to 61.016
Index ranges	-25 ≤ h ≤ 25, -18 ≤ k ≤ 18, -29 ≤ l ≤ 29
Reflections collected	210271
Independent reflections	7230 [R <sub>int</sub> = 0.1192, R <sub>sigma</sub> = 0.0368]
Data/restraints/parameters	7230/6/218
Goodness-of-fit on F <sup>2</sup>	1.126
Final R indexes [I ≥ 2σ (I)]	R <sub>1</sub> = 0.0545, wR <sub>2</sub> = 0.1147
Final R indexes [all data]	R <sub>1</sub> = 0.0899, wR <sub>2</sub> = 0.1285
Largest diff. peak/hole / e Å <sup>-3</sup>	0.41/-0.31





## 5.6 References

- 1 M. Schlosser, *Organometallics in Synthesis*, Wiley, 2013.
- 2 A. J. Martínez-Martínez, A. R. Kennedy, R. E. Mulvey and C. T. O'Hara, *Science*, 2014, **346**, 834–837.
- 3 R. L. Bebb and H. Gilman, *J. Am. Chem. Soc.*, 1939, **61**, 106–109.
- 4 G. Wittig, U. Pockels and H. Dröge, *Berichte der Dtsch. Chem. Gesellschaft*, 1938, **71**, 1903–1912.
- 5 V. Snieckus, *Chem. Rev.*, 1990, **90**, 879–933.
- 6 P. Beak and V. Snieckus, *Acc. Chem. Res.*, 1982, **15**, 306–312.
- 7 M. C. Whisler, S. MacNeil, V. Snieckus and P. Beak, *Angew. Chem. Int. Ed.*, 2004, **43**, 2206–2225.
- 8 K. Shen, Y. Fu, J. N. Li, L. Liu and Q. X. Guo, *Tetrahedron*, 2007, **63**, 1568–1576.
- 9 M. Schlosser, H. C. Jung and S. Takagishi, *Tetrahedron*, 1990, **46**, 5633–5648.
- 10 W. Clegg, S. H. Dale, E. Hevia, L. M. Hogg, G. W. Honeyman, R. E. Mulvey and C. T. O'Hara, *Angew. Chem. Int. Ed.*, 2006, **45**, 6548–6550.
- 11 Y. Kondo, J. V. Morey, J. C. Morgan, H. Naka, D. Nobuto, P. R. Raithby, M. Uchiyama and A. E. H. Wheatley, *J. Am. Chem. Soc.*, 2007, **129**, 12734–12738.
- 12 W. Clegg, B. Conway, E. Hevia, M. D. McCall, L. Russo and R. E. Mulvey, *J. Am. Chem. Soc.*, 2009, **131**, 2375–2384.
- 13 A. J. Martínez-Martínez, D. R. Armstrong, B. Conway, B. J. Fleming, J. Klett, A. R. Kennedy, R. E. Mulvey, S. D. Robertson and C. T. O'Hara, *Chem. Sci.*, 2014, **5**, 771–781.
- 14 A. J. Martínez-Martínez, S. Justice, B. J. Fleming, A. R. Kennedy, I. D. H. Oswald and C. T. O'Hara, *Sci. Adv.*, 2017, **3**, 1–9.
- 15 R. E. Mulvey, *Chem. Commun.*, 2001, 1049–1056.
- 16 L. J. Bole, A. Tortajada and E. Hevia, *Angew. Chem. Int. Ed.*, , DOI:10.1002/anie.202204262.
- 17 T. X. Gentner and R. E. Mulvey, *Angew. Chem. Int. Ed.*, 2021, **60**, 9247–9262.
- 18 D. B. Pardue, S. J. Gustafson, R. A. Periana, D. H. Ess and T. R. Cundari, *Comput. Theor. Chem.*, 2013, **1019**, 85–93.

- 19 M. Fairley, L. Davin, A. Hernán-Gómez, J. García-Álvarez, C. T. O'Hara and E. Hevia, *Chem. Sci.*, 2019, **10**, 5821–5831.
- 20 P. Fleming and D. F. Oshea, *J. Am. Chem. Soc.*, 2011, **133**, 1698–1701.
- 21 A. Seggio, F. Chevallier, M. Vaultier, F. Mongin, D. Rennes, S. De Beaulieu, R. Cedex and R. V April, 2007, 6602–6605.
- 22 S. H. Wunderlich and P. Knochel, *Angew. Chem. Int. Ed.*, 2007, **46**, 7685–7688.
- 23 N. R. Judge, L. J. Bole and E. Hevia, *Chem. – A Eur. J.*, 2022, **28**, 1–8.
- 24 M. Schlosser and S. Strunk, *Tetrahedron Lett.*, 1984, **25**, 741–744.
- 25 D. Shimizu and A. Osuka, *Chem. Sci.*, 2018, **9**, 1408–1423.
- 26 A. Shiozuka, K. Sekine and Y. Kuninobu, *Synth.*, 2022, **54**, 2330–2339.
- 27 S. Samanta and S. Mondal, *Asian J. Org. Chem.*, 2021, **10**, 2503–2520.
- 28 K. Seto, T. Nakayama and B. Uno, *J. Phys. Chem. B*, 2013, **117**, 10834–10845.
- 29 E. C. Ashby, A. B. Goel and R. N. DePriest, *J. Org. Chem.*, 1981, **46**, 2429–2431.
- 30 R. Beck and S. A. Johnson, *Chem. Commun.*, 2011, **47**, 9233–9235.
- 31 M. D. Rausch and D. J. Ciappenelli, *J. Organomet. Chem.*, 1967, **10**, 127–136.
- 32 H. R. L. Barley, W. Clegg, S. H. Dale, E. Hevia, G. W. Honeyman, A. R. Kennedy and R. E. Mulvey, *Angew. Chem. Int. Ed.*, 2005, **44**, 6018–6021.
- 33 W. Clegg, B. Conway, P. García-Álvarez, A. R. Kennedy, J. Klett, R. E. Mulvey and L. Russo, *Dalton Trans.*, 2010, **39**, 62–65.
- 34 L. E. Lemmerz, R. McLellan, N. R. Judge, A. R. Kennedy, S. A. Orr, M. Uzelac, E. Hevia, S. D. Robertson, J. Okuda and R. E. Mulvey, *Chem. Eur. J.*, 2018, **24**, 9940–9948.
- 35 E. Hevia, A. R. Kennedy and M. D. McCall, *J. Chem. Soc. Dalt. Trans.*, 2012, **41**, 98–103.
- 36 A. T. Balaban, D. C. Oniciu and A. R. Katritzky, *Chem. Rev.*, 2004, **104**, 2777–2812.
- 37 A. R. Looker, B. J. Littler, T. A. Blythe, J. R. Snoonian, G. K. Ansell, A. D. Jones, P. Nyce, M. Chen and B. J. Neubert, *Org. Process Res. Dev.*, 2008, **12**, 666–673.
- 38 R. S. Compagnone and H. Rapoport, *J. Org. Chem.*, 1986, **51**, 1713–1719.
- 39 R. Chinchilla, C. Nájera and M. Yus, *Chem. Rev.*, 2004, **104**, 2667–2722.

- 40 J. C. Hodges, W. C. Patt and C. J. Connolly, *J. Org. Chem.*, 1991, **56**, 449–452.
- 41 G. Boche, F. Bosold, H. Hermann, M. Marsch, K. Harms and J. C. W. Lohrenz, 1998, 814–817.
- 42 B. D. Kenney, M. Breslav, R. Chang, R. Glaser, B. D. Harris, C. A. Maryanoff, J. Mills, A. Roessler, B. Segmuller and F. J. Villani, *J. Org. Chem.*, 2007, **72**, 9798–9801.
- 43 O. Bayh, H. Awad, F. Mongin, C. Hoarau, F. Trécourt, G. Quéguiner, F. Marsais, F. Blanco, B. Abarca and R. Ballesteros, *Tetrahedron*, 2005, **61**, 4779–4784.
- 44 J. M. L’Helgoual’ch, A. Seggio, F. Chevallier, M. Yonehara, E. Jeanneau, M. Uchiyama and F. Mongin, *J. Org. Chem.*, 2008, **73**, 177–183.
- 45 P. García-Úlvarez, R. E. Mulvey and J. A. Parkinson, *Angew. Chem. Int. Ed.*, 2011, **50**, 9668–9671.
- 46 S. D. Robertson, M. Uzelac and R. E. Mulvey, *Chem. Rev.*, 2019, **119**, 8332–8405.
- 47 W. Caminati, G. Grassi and A. Bauder, *Chem. Phys. Lett.*, 1988, **148**, 13–16.
- 48 R. E. Mulvey, V. L. Blair, W. Clegg, A. R. Kennedy, J. Klett and L. Russo, *Nat. Chem.*, 2010, **2**, 588–591.
- 49 A. Maercker, *Angew. Chemie Int. Ed. English*, 1987, **26**, 972–989.
- 50 A. R. Kennedy, R. E. Mulvey, C. L. Raston, B. A. Roberts and R. B. Rowlings, *Chem. Commun.*, 1999, **2**, 353–354.
- 51 G. C. Forbes, A. R. Kennedy, R. E. Mulvey, R. B. Rowlings, W. Clegg, S. T. Liddle and C. C. Wilson, *Chem. Commun.*, 2000, **2**, 1759–1760.
- 52 A. R. Kennedy, J. Klett, R. E. Mulvey, S. Newton and D. S. Wright, *Chem. Commun.*, 2008, **7345**, 308–310.
- 53 Y. Liu and R. S. Glass, *Tetrahedron Lett.*, 1997, **38**, 8615–8618.
- 54 E. Crosbie, P. García-Álvarez, A. R. Kennedy, J. Klett, R. E. Mulvey and S. D. Robertson, *Angew. Chem. Int. Ed.*, 2010, **49**, 9388–9391.
- 55 V. L. Blair, A. R. Kennedy, R. E. Mulvey and C. T. O’Hara, *Chem. Eur. J.*, 2010, **16**, 8600–8604.
- 56 D. Huang, D. Olivieri, Y. Sun, P. Zhang and T. R. Newhouse, *J. Am. Chem. Soc.*, 2019, **141**, 16249–16254.

- 57 Y. Gu and R. Martín, *Angew. Chem. Int. Ed.*, 2017, **56**, 3187–3190.
- 58 P. C. Meltzer, P. Blundell, H. Huang, S. Liu, Y. F. Yong and B. K. Madras, *Bioorganic Med. Chem.*, 2000, **8**, 581–590.
- 59 Z. Wu, F. Wei, B. Wan and Y. Zhang, *J. Am. Chem. Soc.*, 2021, **143**, 4524–4530.
- 60 J. C. Goeltz and C. P. Kubiak, *Organometallics*, 2011, **30**, 3908–3910.
- 61 M. S. Inkpen, S. Du, M. Driver, T. Albrecht and N. J. Long, *Dalton Trans.*, 2013, **42**, 2813–2816.
- 62 N. H. Chang, X. C. Chen, H. Nonobe, Y. Okuda, H. Mori, K. Nakajima and Y. Nishihara, *Org. Lett.*, 2013, **15**, 3558–3561.
- 63 E. B. Stephens, K. E. Kinsey, J. F. Davis and J. M. Tour, *Macromolecules*, 1993, **26**, 3519–3532.
- 64 J. Bergman and L. Venemalm, *J. Org. Chem.*, 1992, **57**, 2495–2497.
- 65 Q. Shi, S. Zhang, J. Zhang, V. F. Oswald, A. Amassian, S. R. Marder and S. B. Blakey, *J. Am. Chem. Soc.*, 2016, **138**, 3946–3949.

## Chapter 6 - Conclusions and Outlook

Drawing to a close, this *Thesis* attempted to advance the applications and understanding of using alkali-metal alkoxides as additives to activate organomagnesium and organozinc reagents towards arene functionalisation, focusing on two cornerstone transformations in organic chemistry: metal/halogen exchange and deprotonative metalation. Shedding light on the constitution of the organometallic intermediates, we have uncovered a variety of novel mixed-metal/mixed-ligand complexes which have been characterised by a combination of spectroscopic and crystallographic studies. This work has also highlighted the complex solution chemistry of some of these heterobimetallic combinations. The results discussed within this *Thesis* have revealed the close interplay between the metals in these bimetallic reagents resulting in synergistic behaviour whilst showcasing how subtle changes to the alkali metal or the nature of the alkoxide ligand can have drastic effects on the reactivity and constitution of the resulting bimetallic reagents and their metalated intermediates.

**Chapter 2** centred around uncovering the true constitution of the mixed alkyl/alkoxide (alkoxide = 2-ethylhexanolate) lithium magnesiate reagent involved in Mg/Br exchange. Prompted by the crystallographic characterisation of two entirely different intermediary products of Mg/Br exchange, namely  $[\text{LiMgAr}_2(\text{OR}')_2]$  ( $\text{Ar} = o\text{-OMe-C}_6\text{H}_4$ ) (**1a**) and  $[\text{Li}_2\text{Mg}(\text{Ar})_4]$  (**2a**) from the reactions with 2- and 4-bromoanisole respectively, we could reveal the true constitution of this powerful exchange reagent. Coupled with detailed spectroscopic studies, a novel bimetallic Schlenk type equilibrium was established where  $\text{LiMg}_s\text{Bu}_2(\text{OR}')$  (**I**), formed from co-complexation of  $s\text{Bu}_2\text{Mg}$  and  $\text{LiOR}'$ , was found to be in equilibrium with a higher order tetraalkyl lithium magnesiate  $\text{Li}_2\text{Mg}_s\text{Bu}_4$  (**II**) and neutral magnesium alkoxide  $\text{Mg}(\text{OR}')_2$  (**III**). Exposing the active species within this complex mixture, experiments involving equilibrium manipulation to test reactivity showed **I** to be completely inactive towards exchange, pointing towards the reaction taking place via the more reactive tetraalkyl species, **II**. Confirming **II** as the genuine exchange reagent, NMR spectroscopic experiments showed that *ortho*-substituted tetra(aryl)magnesiate intermediates (e.g.  $\text{Li}_2\text{MgAr}_4$  ( $\text{Ar} = o\text{-OMe-C}_6\text{H}_4$ ) (**6**)) can co-complex with  $\text{Mg}(\text{OR}')_2$  (**II**), explaining the formation of alkoxide containing intermediates such as **1a**. Many of the themes discussed in this Chapter set the tone for subsequent studies in the *Thesis*.

Building on the work detailed in **Chapter 2**, we then focused our attention on systematically examining the alkali metal and alkoxide effects in similar Mg/Br exchange reactions. **Chapter 3** details the formation of a series of mixed alkyl/alkoxy magnesiates  $[\text{MMg}(\text{CH}_2\text{SiMe}_3)_2(\text{dmem})_2]$  ( $\text{M} = \text{Li}$ , **4**;  $\text{Na}$ , **5**;  $\text{K}$ , **6**) employing a chelating alkoxide ligand with intramolecular donating properties. Reactivity studies with 2-bromoanisole revealed a

clear alkali-metal effect with the larger K congener performing best in Mg/Br exchange, consistent with the alkali-metal playing an important role in mediating this process. An alkali-metal effect was also apparent in determining the constitution of these mixed-metal/mixed/ligand reagents where isolation of sodium and potassium magnesiates  $[\text{MMg}(\text{CH}_2\text{SiMe}_3)_2(\text{OR}')_2]$  (M= Na, **9**; K, **10**) employing the previously mentioned long chain alkoxide (R' = 2-ethylhexyl) is successful whereas the Li congener participates in a similar bimetallic Schlenk equilibrium as reported in **Chapter 2**. Uncovering a new element of complexity, simply changing the nature of alkoxide ligand had a drastic effect on the constitution of the metalated intermediates formed, while the long aliphatic alkoxide OR' bimetallic intermediate  $[\text{KMgAr}_2(\text{OR}')_2]$  (**12**) is stable in arene solutions, employing dmem led to the formation of the single metal species  $[\text{MgAr}(\text{dmem})_2]$  (**8**) with concomitant precipitation of  $[\text{KAr}]_n$ .

To quote Robinson, “the TMP ligand has contributed to the renaissance of metalation chemistry involving organozincate compounds”.<sup>1</sup> Thus, **Chapter 4** introduced the use of KO $t$ Bu to activate the mild zinc *bis*-amide reagent  $\text{Zn}(\text{TMP})_2$  towards deprotonative metalation reactions through the formation of a novel mixed amido/alkoxy zincate species  $[(\text{PMDETA})\text{KZn}(\text{TMP})_2\text{O}t\text{Bu}]$  (**3**). Whilst this species could promote the rapid and regioselective zincation of a wide range of sensitive fluoroarenes, the addition of a second equivalent of KO $t$ Bu was necessary to prevent ligand redistribution giving rise to a series of *bis*-aryl potassium zincates (**2a-o**). Crystallographic characterisation of these intermediates demonstrated that both TMP groups on Zn were active towards Zn-H exchange and the resulting products underwent successful further functionalisation through electrophilic interception reactions, including Negishi cross-coupling reactions. This  $\text{Zn}(\text{TMP})_2/2\text{KO}t\text{Bu}$  exhibited significantly enhanced reactivity compared to commonly used zincating reagents such as Knochel’s turbo-Hauser zinc base  $\text{TMPZnCl}\cdot\text{LiCl}$ . Showcasing the enhanced metalating power of this bimetallic combination, zincation of toluene and even benzene at room temperature can be accomplished when these arenes are used as solvents. This special combination can be conceptualised as a Zn-TMP version of the widely used LIC-KOR and LiNK superbasic combinations, giving it a colloquial catchy name in our lab as the ZiNK base. It should be noted that both single-metal components of this combination,  $\text{Zn}(\text{TMP})_2$  and KO $t$ Bu are commercially available, allowing for its straightforward preparation in THF.

**Chapter 5** focused on deploying our ZiNK base for the regioselective zincations of more challenging non-activated arenes such as naphthalene, biphenylene and ferrocene under mild conditions, confirmed by an iodine quench revealing iodoarenes (**2**). A dramatic alkali-metal effect was observed for these reactions where using the lighter AM-OR congeners Li and NaO $t$ Bu completely shut down the metalating capabilities of  $\text{Zn}(\text{TMP})_2$ . In the case of

naphthalene and benzene, a new type of metalated intermediate for these reactions was discovered in the form of lower order potassium zincates  $[(\text{THF})_2\text{KZn}(\text{Ar})(\text{OtBu})_2]_2$  (**3a-b**) adding further complexity to these systems. Putatively presumed to form through the redistribution of a higher order potassium zincate intermediate, forming **3a-b** along with expulsion of a potassium aryl unit. This peculiar redistribution process could be authenticated through the isolation of  $[(\text{THF})_2\text{KZn}(2\text{-benzoxazolyl})(\text{OtBu})_2]_2$  (**6**), from the reaction of two equivalents of 1,3-benzoxazole with  $\text{Zn}(\text{TMP})_2/2\text{KOtBu}$ , which occurs with concomitant formation of potassium phenolate (**7**) formed from the ring opening of a transient potassium aryl species. This *Chapter* is concluded by unmasking the unusual decomposition pathways of aliphatic heterocycles THF and THT through “cleave and capture” chemistry, where  $\text{Zn}(\text{TMP})_2/2\text{KOtBu}$  appears to carry out initial C-sp<sup>3</sup>  $\alpha$ -metalations of these solvents forming unstable products which subsequently decompose, ripping apart the heterocycles.

To conclude, this *Thesis* has illuminated the profound activating effects of alkali-metal alkoxides on organomagnesium and organozinc species for key organometallic transformations. Detailed spectroscopic and crystallographic studies helped in unravelling the intricate relationships between the individual components of these mixtures. The comprehensive exploration of these activating effects provides valuable insights into designing more efficient and selective synthetic methodologies using alkali-metal alkoxide additives, with implications for the advancement of diverse fields such as organic synthesis and perhaps lays the blueprint to upgrade these systems to catalytic protocols which require powerful metalating agents. Indeed, alkali-metal magnesiates and zincates have found recent applications in catalytic transformations where the alkali-metal can act as a built-in Lewis acid to maximise substrate/catalyst interaction.<sup>2-4</sup> The reactivity of the mixed-metal/mixed-ligand species discussed within this *Thesis* appear to be inextricably linked to the nature of the alkoxide used, therefore it would be interesting to investigate the use of different alkoxide ligands in combination with  $\text{Zn}(\text{TMP})_2$  attempting to tune the reactivity of these systems perhaps tolerating substrates containing more sensitive functional groups (e.g.  $\text{NO}_2$ ,  $\text{CN}$ ). Moreover, the use of a long chain alkoxide ligand could potentially allow for reactions to be carried out in hydrocarbon solvents minimising the risk of side reactions/decomposition with ethereal solvents. Given the greater reactivity of  $\text{Mg}(\text{TMP})_2$  compared to its Zn congener,<sup>5</sup> the combination of the magnesium *bis*-amide with suitable alkoxide ligands presents an opportunity for an even more powerful metalating reagent than  $\text{Zn}(\text{TMP})_2/2\text{KOtBu}$ . It's clear there is scope to further develop the synthetic utility of this chemistry using alkali-metal alkoxide additives to activate other organometallic reagents and it's hoped this *Thesis* provides a platform for such investigations.





## Chapter 7 – General Experimental Techniques and Procedures

### 7.1 Schlenk Techniques

Working with polar organometallic reagents can be very challenging due to their extreme sensitivities to air and moisture. Accordingly, the handling of these compounds requires working under an inert argon atmosphere to eliminate any air and moisture from the system. As a result, all of the manipulative chemistry was carried out using a high vacuum Schlenk line – a widely used piece of apparatus developed by Wilhelm Schlenk.<sup>6,7</sup>



**Figure 1.** Typical Schlenk-line set up

The Schlenk line shown in Figure 1 is comprised of a vacuum manifold connected to a vacuum pump and an inert gas manifold which is connected to a gas inlet and gas outlet (in the form of an oil bubbler/Dreschel) so as to avoid pressure build-up within the system. The vacuum manifold is connected to the pump through a liquid nitrogen cooled ( $-196\text{ }^{\circ}\text{C}$ ) solvent trap in order to condense any volatiles from reaction mixtures. There are also ten J. Youngs valve taps which allow application of either inert gas or vacuum to attached glassware (namely, Schlenk flasks) at five separate stations.

Before a procedure could be commenced, all glassware has to be entirely clean and dried at  $175\text{ }^{\circ}\text{C}$  overnight. In order to maintain an air-tight seal, all ground-glass joints must

be sealed with Dow-Corning grease (or similar) – J. Young’s valve taps can also be used so as to remain grease-free. The vessel can then be attached to the Schlenk line and placed under vacuum for 15 minutes. After this, the equipment is then filled with argon, and the entire process is repeated another two times before synthetic procedures can be commenced.

## 7.2 Glovebox

Whilst all manipulative chemistry can be conducted on the Schlenk line, the majority of preparative chemistry was carried out in an MBraun LabStar argon-filled glovebox containing two antechambers. Each of the antechambers (or ‘ports’) have one inner and one outer door, allowing for transfer of materials into the inert-gas main body of the glovebox without the possibility of air compromising the argon atmosphere. All chemicals and glassware can be safely transferred into the glovebox via one of the two antechambers by three vacuum/argon flushing cycles – small port = 3 x 5 minutes under vacuum, large port = 3 x 15 minutes under vacuum. The main chamber of the glovebox is comprised of a gas recirculation and purification system, allowing for minimal presence of oxygen and moisture.

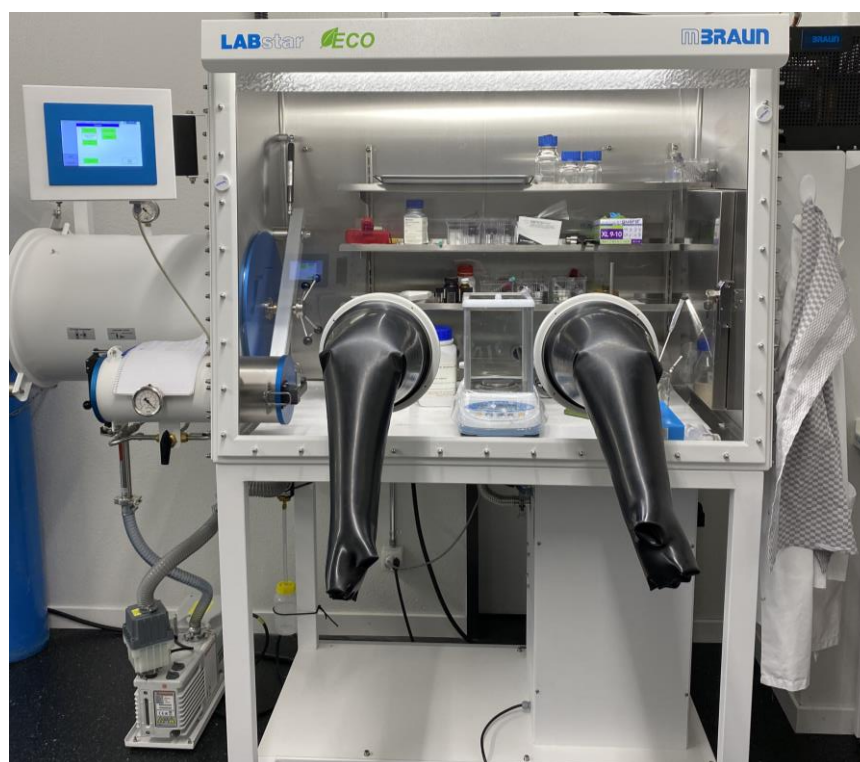


Figure 2. MBraun LabStar glovebox

### 7.3 Solvent Purification

Hexane, toluene, diethyl ether (Et<sub>2</sub>O), benzene and pentane solvents were de-gassed using an MBraun Solvent Purification System (SPS). The SPS consists of a vacuum pump and dry nitrogen supply, allowing for collection of solvent under inert atmosphere. The reaction flask, containing activated 4 Å molecular sieves, is first prepared under argon on the Schlenk line via vacuum/argon cycles. The final vacuum cycle is held – this negative pressure is what allows for solvent collection into the vessel. Upon dispensing, the solvent is de-oxygenated with nitrogen gas and pulled from the reservoir through a drying column, into the collection flask. These solvents are continuously stored over 4 Å molecular sieves to ensure dryness. The molecular sieves are typically changed after two solvents cycles.

Tetrahydrofuran (THF) and 1,4-dioxane were both dried over sodium wire and then stored over 4 Å molecular sieves during use to ensure dryness. Distillation over sodium with a benzophenone ketyl radical anion indicator is a highly common and effective procedure used for removing any dissolved water from solvents. The sodium metal prompts benzophenone to undergo a one electron reduction forming the ketyl radical anion which can react with any traces of oxygen and water. When this radical is actively working, an intense blue colour is observed in the solvent meaning that it is dry and safe to use in these types of organometallic reactions.

### 7.4 Reagent Purification

All reagents used in this this were purchased from Sigma Aldrich, Alfa Aesar, Fluorochem or Acros Organics. Where appropriate, reagents were distilled over CaH<sub>2</sub> to remove any residual moisture and then stored over 4 Å molecular sieves in a J. Young's tap flask under inert atmosphere to maintain dryness.

### 7.5 Standardisation of Organometallic Reagents

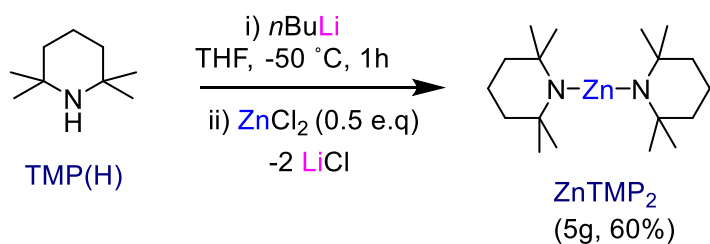
Grignard, diorganozinc and diorganomagnesium reagents were standardised against a THF solution of a defined amount of iodine to determine the exact concentration – this method was developed by Knochel.<sup>8</sup> Addition of the organometallic reagent to the iodine/THF solution containing LiCl was performed until a visible brown to colourless colour change of the solution persisted. From the volume of reagent used it was possible to determine the concentration of the reagent.

Organolithium reagents were standardised against L(-)-menthol in THF with 2,2'-bipyridine as an indicator. In a dried round-bottomed flask, 200 mg (1.3 mmol) of L(-)-menthol

and 5 mg of 2,2'-bipyridine were prepared under argon and dissolved in 7 mL of THF. The organolithium reagent (e.g. *n*BuLi) was then added dropwise until the intense dark red colour persisted. The colour is a result of alkylation of 2,2'-bipyridine by excess alkyllithium.

## 7.6 Synthesis of Zn(TMP)<sub>2</sub>

The following procedure is an adapted protocol from one previously described in the literature.<sup>9</sup>



In a large (250 mL) argon-flushed Schlenk flask, *n*BuLi (31.5 mL, 1.6 M in hexanes, 50 mmol) was suspended in THF (40 mL) at -50 °C. TMP(H) (8.5 mL, 50 mmol) was then added slowly forming a pale-yellow solution which was stirred at this temperature for 1 hour. To the resulting light-yellow suspension was added ZnCl<sub>2</sub><sup>a</sup> (3.4 g, 25 mmol) via a solid addition tube, at -50 °C, which was vigorously stirred at this temperature for 20 minutes before allowing the mixture to warm to room temperature and stirring for a further 2 hours (minimum). All solvent was removed under vacuum, using an external cold trap, and the resulting solid was suspended in hexane (50 mL) and stirred for 30 minutes. The mixture was then filtered via cannula filtration (can also filter through celite/glass wool) and the resulting solid (LiCl) was washed with hexane (20 mL). All solvent was then removed under vacuum using an external cold trap affording a light yellow solid (typical crude yields of approximately 8g, >90% yield).<sup>b</sup> The crude yellow solid was then transferred into a clean, dry large Schlenk flask and sublimed at 70-75 °C at approximately 0.08 mbar affording Zn(TMP)<sub>2</sub> as a white crystalline solid (typical yields of approx. 5g, 60% yield). **<sup>1</sup>H-NMR (300.1 MHz, D<sub>8</sub>-THF, 298 K):** δ / ppm = 1.72-1.64 (m, 4H, 2 x γ-CH<sub>2</sub>, TMP), 1.32 (t, J = 6.34 Hz, 2 x β-CH<sub>2</sub>, TMP), 1.22 (s, 24H, 8 x CH<sub>3</sub>, 2x TMP). **<sup>13</sup>C{<sup>1</sup>H}-NMR (101 MHz, D<sub>8</sub>-THF, 298 K):** δ / ppm 53.3 (s, C<sub>q</sub>-N, 2 x TMP), 39.8 (s, β-CH<sub>2</sub>, 2 x TMP), 36.8 (s, CH<sub>3</sub>, 2x TMP), 19.7 (s, γ-CH<sub>2</sub>, 2 x TMP). **Notes:** [a] ZnCl<sub>2</sub> flame dried under vacuum prior to use and stored in glovebox. [b] If a yellow oil persists at this stage, carefully freezing the oil in liquid nitrogen will solidify the oil which continues to stay as a solid when warming to room temperature and can be manipulated in the glovebox before sublimation. (This problem persists due to salt impurities or excess TMP(H) in the reaction mixture).

## 7.7 Analytical Procedures

All NMR experiments were carried out using Bruker AV3, AV400 and DPX 300 MHz spectrometers. Experiments were recorded at:  $^1\text{H}$  = 400.1 or 300.1 MHz,  $^{13}\text{C}$  = 100.6 or 75.5 MHz,  $^{19}\text{F}$  = 376.5 MHz and  $^7\text{Li}$  = 116.6 MHz. All 1D and 2D spectra were processed using Topspin software. Abbreviations for NMR splitting patterns are quoted as follows: singlet (s), doublet (d), triplet (t), quartet (q), quintet (quin), septet (sept), broad signal (br).

GC spectra were obtained using an Agilent Technologies 7890A GC System, Agilent Technologies 5975C Inert XL EI/CI MSD with Triple-Axis Detector, Agilent Technologies 7693 Autosampler and Restek GC Column (30 m, 0.25 mm i.d., 0.25  $\mu\text{m}$ ).

Elemental analyses (C, H and N) were conducted with a Perkin Elmer 2400 Analyser or a Flash 2000 Organic Elemental Analyser (Thermo Scientific). Samples were prepared in the glovebox under argon atmosphere and sealed in an air-tight container prior to analyses. All results were obtained in triplicate to ensure consistency. HRMS data was obtained using a Bruker UltrafleXtreme MALDI TOF/TOF.

Single crystal X-ray diffraction (Universität Bern) measurements were made on a *RIGAKU Synergy S* area-detector diffractometer using mirror optics monochromated Cu  $K\alpha$  radiation ( $\lambda = 1.54184 \text{ \AA}$ ). Data reduction was performed using the *CrysAlisPro* program. The intensities were corrected for Lorentz and polarization effects, and an absorption correction based on the multi-scan method using SCALE3 ABSPACK in *CrysAlisPro* was applied. The structures were solved by direct methods using *SHELXT*,<sup>10</sup> Refinement of the structure was carried out on  $F^2$  using full-matrix least-squares procedures, which minimized the function  $\sum w(F_o^2 - F_c^2)^2$ . The weighting scheme was based on counting statistics and included a factor to downweight the intense reflections. All calculations were performed using the *SHELXL-2014/7*<sup>11</sup> program in OLEX2<sup>12</sup> which revealed the positions of all non-hydrogen atoms of the title compound. All non-hydrogen atoms were refined anisotropically. H-atoms were assigned in geometrically calculated positions and refined using a riding model where each H-atom was assigned a fixed isotropic displacement parameter with a value equal to 1.2Ueq of its parent atom (1.5 Ueq for methyl groups).

## 7.8 References

- 1 Y. Wang, Y. Xie, M. Y. Abraham, R. J. Gilliard, P. Wei, C. F. Campana, H. F. Schaefer, P. V. R. Schleyer and G. H. Robinson, *Angew. Chem. Int. Ed.*, 2012, **51**, 10173–10176.
- 2 J. M. Gil-Negrete and E. Hevia, *Chem. Sci.*, 2021, 1982–1992.
- 3 T. X. Gentner, A. R. Kennedy, E. Hevia and R. E. Mulvey, *ChemCatChem*, 2021, **13**, 2371–2378.
- 4 T. X. Gentner and R. E. Mulvey, *Angew. Chem. Int. Ed.*, 2021, **60**, 9247–9262.
- 5 F. H. Lutter, L. Grokenberger, L. A. Perego, D. Broggini, S. Lemaire, S. Wagschal and P. Knochel, *Nat. Commun.*, 2020, **11**, 1–8.
- 6 T. T. Tidwell, *Angew. Chem. Int. Ed.*, 2001, **40**, 331–337.
- 7 A. M. Borys, *Organometallics*, , DOI:10.1021/acs.organomet.2c00535.
- 8 A. Krasovskiy and P. Knochel, *Synthesis (Stuttg.)*, 2006, 890–891.
- 9 D. Huang, D. Olivieri, Y. Sun, P. Zhang and T. R. Newhouse, *J. Am. Chem. Soc.*, 2019, **141**, 16249–16254.
- 10 G. M. Sheldrick, *Acta Crystallogr. Sect. A Found. Crystallogr.*, 2015, **71**, 3–8.
- 11 G. M. Sheldrick, *Acta Crystallogr. Sect. C Struct. Chem.*, 2015, **71**, 3–8.
- 12 O. V. Dolomanov, L. J. Bourhis, R. J. Gildea, J. A. K. Howard and H. Puschmann, *J. Appl. Crystallogr.*, 2009, **42**, 339–341.

